

Exploring Reactor Design to Harness Reactive Intermediates

Tom McBride

This thesis is submitted for the degree of Doctor of
Philosophy (PhD) at Cardiff University



July 2021

Summary

This thesis explores the design and engineering of flow reactors to facilitate synthetic organic transformations. The designs of these flow reactors are focussed on manipulating and controlling reactive intermediates *in situ* and enabling the facile use of acetylene gas; acyl ketenes; and biphasic systems, as useful synthetic tools.

Initially, this thesis explores the use of generating acetylene gas *in situ* without the use of a resident gas cylinder from commercially available calcium carbide. The calcium carbide is formulated into an applicable flow reagent for the safe generation of acetylene gas in a continuous manner. Acetylene gas is intercepted via various organic transformations thus constructing telescoped flow systems. The aim to generate and harness acetylene gas *in situ* via intricate design of reactor has been met and successfully explored.

Secondly, utilising flow's excellent ability of thermal control, the thermolysis of an acyl ketene precursor is explored. In this section, a flow reactor is designed to thermally decompose an acyl ketene precursor thus liberate an acyl ketene *in situ*. This highly reactive intermediate is explored and intercepted with various ketene traps yielding β -keto esters/amides and functionalised novel coumarins. Post-functionalisation of the synthesised β -keto ester feedstocks are further explored by the Biginelli reaction catalysed by pyridinium triflates in neat microwave conditions. Therefore, a tandem flow-microwave processing system is designed to work towards the synthesis of a compound library.

Finally, flow reactor design is explored to synthesise Civetone, a natural musk fragrance, in continuous flow via a Dieckmann macrocyclisation. This transformation is commonly biphasic (liquid-solid reaction mixture) and can therefore cause blockages in flow processing. The use of Continuously Stirred Tank Reactors (CSTRs) are explored to facilitate the difficult handling of a biphasic flow reaction and promote the macrocyclisation (and scale up) towards the synthesis of natural product, Civetone, via 'mimicked' dropwise addition in flow.

The chapters of this thesis primarily focus on how a flow reactor can be constructed to enable and harness highly reactive intermediates and explore the chemical space of these transformations.

Related publications

Some of the work presented in this thesis has been submitted for publication in the following papers:

1) Manganese-Catalyzed Electrochemical Deconstructive Chlorination of Cycloalkanols via Alkoxy Radicals*

B. D. W. Allen, M. D. Hareram, A. C. Seastram, T. McBride, T. Wirth, D. L. Browne and L. C. Morrill, *Org. Lett.*, 2019, **21**, 9241–9246. (10.1021/acs.orglett.9b03652)

2) Exploring the Generation and Use of Acylketenes with Continuous Flow processing

R. Galaverna, T. McBride, J. C. Pastre and D. L. Browne, *React. Chem. Eng.*, 2019, **4**, 1559–1564. (10.1039/c9re00072k)

3) Formation and Utility of Reactive Ketene Intermediates Under Continuous Flow Conditions

H. R. Smallman, J. A. Leitch, T. McBride, S. V. Ley, D. L. Browne, *Tetrahedron*, (submitted) (10.1016/j.tet.2021.132305)

Acknowledgments

This thesis and my overall PhD experience would not be possible without the support of the people around me, and I would like to express my gratitude herein.

Firstly, I would like to thank all the great scientists who have collaborated with me. Renan Galaverna, Imke Reuther and Yaoyu Ding provided vital results with respect to the acyl ketenes project and were excellent co-workers. I also owe thanks to Idriss Curbet for his results in the Civetone project that we closely collaborated on. A special thanks must go to Dr. Duncan Browne for his continuous input into my research project and providing me with many development opportunities. He has taught me some valuable life lesson that I'll take forward with me in my continued development. I'd like to also thank the EPSRC for funding this research project.

When I first joined the research world, I was greeted by three fantastic people, Joey, James, and Chrissi. These individuals welcomed me, taught me more than I can say, and were great life friends to gain. A special mention to Roddy Stark, your wit and friendship supported me greatly throughout the PhD and cannot say thanks enough! Will, you and I have gone through this together and I want to thank you for supporting me and being an excellent lab mate and friend. I would like to thank the members of the DLB and LCM group, pub trips and lab work will never be forgotten!

I'd like to say thank you to Andy, for listening to my furious ramblings and being a fantastic Overwatch buddy. Alex, thanks for making both the lab and home a fun, relaxed place to be and your cool-headedness is something I aspire to be. I like to especially thank Jenna for an amazing new friendship and helping me through the last stages of my PhD, I really appreciate it.

Jenny, I cannot thank you enough for the 8 years of dealing with me. You are such patience and supportive friend, and I would not have got through this all without your silly, infectious humour, and life enlightenments we have shared!

To my parents, your continuous support has and will never go unnoticed. Thanks to dad for the late night logical debriefs and thanks mum for the countless phone calls that got me through my week. My sister, Holly, is my rock and a conversation with you always inspired me to stay strong and be the best I can. I could not thank you enough for being in my life.

Finally, Jessica, meeting you made everything better and this thesis would not be where it is today without your support! From the bottom of my heart, thank you and cannot wait to explore the next chapter with you.

Abbreviations

AI	artificial intelligence
API	active pharmaceutical ingredient
[bmim][BF ₄]	1-butyl-3-methyl-imidazolium tetrafluoroborate
BPR	back-pressure regulator
CASP	computer-aided synthesis planning
CDI	1,1'-carbonyldiimidazole
CRD	Cambridge Reactor Design
CSTR	continuously stirred tank reactor
DCE	dichloroethane
DCM	dichloromethane
DHPMs	dihydropyrimidinones
DIBAL	diisobutylaluminum (hydride)
DMF	dimethylformamide
DMPSi	poly(dimethylsilane) (-Pd/Al ₂ O ₃)
DMSO	dimethyl sulfoxide
E _{1CB}	unimolecular conjugate-base elimination
Et ₃ N	triethyl amine
GC-MS	gas-chromatography mass-spectrometry
HDA	hetero-Diels-Alder
HEX	hexane
HPLC	high pressure liquid chromatography
HRMS	high-resolution mass-spectrometry
ID	internal diameter
IPA	isopropyl alcohol
IR	infrared
KHMDS	potassium bis(trimethylsilyl)amide
LDA	lithium diisopropylamide
LiHMDS	lithium bis(trimethylsilyl)amide
MeTHF	2-methyl tetrahydrofuran
MFC	mass flow controller
MJOD	multijet oscillating disk (reactor)
MOF	metal organic framework

MS	molecular sieves
MW	microwave
NaHMDS	sodium bis(trimethylsilyl)amide
NBS	<i>N</i> -bromosuccinimide
NCS	<i>N</i> -chlorosuccinimide
NiT	needle-in-tube
NMR	nuclear magnetic resonance
PAO	poly- α -olefin synthetic oil
PDC	pyridinium dichromate (Cornforth reagent)
PEEK	polyether ether ketone
PFA	perfluoroalkoxy (tubing)
PS	polymer support
PTFE	polytetrafluoroethylene
RBF	round bottom flask
RCM	ring-closing metathesis
RME	reaction mass efficiency
RPM	rotations per minute
RT	room temperature (rt)
SM	starting material
STY	space-time-yield
TBAB	tetrabutylammonium bromide
TBME	<i>tert</i> -butylmethyl ether
TFAA	trifluoroacetic anhydride
THF	tetrahydrofuran
TLC	thin layer chromatography
TMD	2,2,6-trimethyl-4 <i>H</i> -1,3-dioxin-4-one
TMS	trimethylsilane
TOF	time of flight
TSEMO	Thompson sampling efficient multi-objective (algorithm)
USP	United States pharmacopeia
WiT	wire-in-tube

Table of Contents

1	Introduction.....	1
1.1	General introduction to flow chemistry.....	2
1.2	Reactor design enabling organic reactions.....	2
1.2.1	Single Transformation Systems.....	4
1.2.2	Telescoped Systems.....	8
1.2.3	Intelligent data-rich systems.....	13
1.3	Conclusion.....	19
1.4	Thesis outlook.....	20
1.5	References.....	21
2	Designing a Reactor to Generate and Use Acetylene Gas.....	25
2.1	Introduction.....	26
2.1.1	Reactive gases in flow – with a resident gas cylinder.....	26
2.1.2	Reactive gases in flow – without a resident gas cylinder.....	29
2.1.3	Solid gas storage matrix - calcium carbide.....	30
2.2	Project Aims and Objectives.....	33
2.3	Results and Discussion.....	34
2.3.1	Calcium carbide.....	34
2.3.2	Creating the acetylene generator.....	34
2.3.3	Quantifying the acetylene generator.....	39
2.3.4	Application of the acetylene generating module - Cycloadditions.....	42
2.3.5	Application of the acetylene generating module – Lithium acetylide.....	47
2.4	Conclusions and outlook.....	57
2.5	References.....	59
3	Designing a Reactor to Thermally Generate and Intercept Acyl Ketenes.....	62
3.1	Introduction.....	63
3.1.1	Thermal control in flow.....	63
3.1.2	Acyl ketenes.....	65

3.2.3	Harnessing acyl ketenes in flow.....	68
3.2	Aims and Objectives	70
3.3	Results and Discussion	71
3.2.1	Discovery and reactivity of the acyl ketene	71
3.2.2	Exploring various ketene traps.....	73
3.2.3	Post-functionalisation reaction – Biginelli	82
3.4	Conclusions and outlook.....	93
3.5	References	95
4	Designing a Reactor for the Continuous Production of Civetone.....	99
4.1	Introduction	100
4.1.1	Civetone	100
4.1.2	Designing flow reactors to facilitate the metathesis reaction	106
4.1.3	Designing flow reactors to facilitate solid forming reactions	108
4.2	Background and Aims of Project	110
4.3	Results and Discussion	112
4.3.1	Dieckmann cyclisation – batch conditions.....	112
4.3.2	Designing a flow reactor for the Dieckmann cyclisation	113
4.3.3	Chemical optimisation in the <i>f</i> Reactor.....	119
4.4	Conclusions and outlook.....	124
4.5	References	126
5	Experimental	128
5.1	General Methods	129
5.2	Acetylene experimental.....	130
5.3	Acyl ketene experimental.....	136
5.4	Civetone experimental	148
5.5	References	152

1 Introduction

1	Introduction.....	1
1.1	General introduction to flow chemistry	2
1.2	Reactor design enabling organic reactions.....	2
1.2.1	Single Transformation Systems	4
1.2.2	Telescoped Systems	8
1.2.3	Intelligent data-rich systems	13
1.3	Conclusion.....	19
1.4	Thesis outlook	20
1.5	References	21

1.1 General introduction to flow chemistry

This introduction will explore the literature and highlight a selection of examples that demonstrate how careful reactor design has enabled the implementation of synthetic chemistry under continuous flow process. Throughout this thesis, a set of common symbols will be used to depict various components of flow equipment (Figure 1).

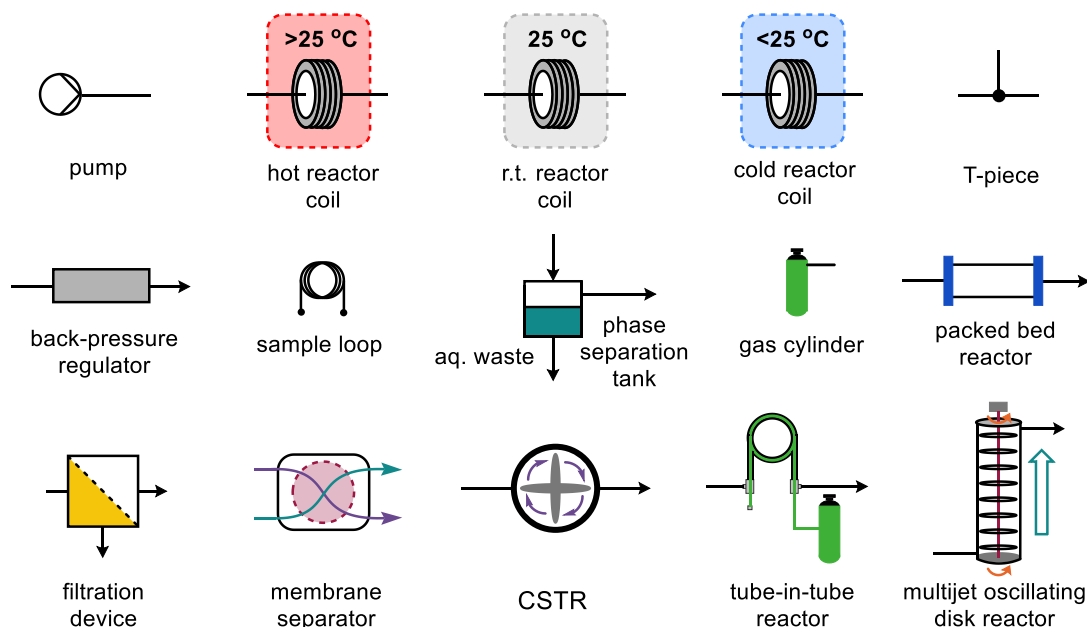


Figure 1 - Common flow scheme symbols – 3rd row of symbols are uncommon flow reactor components

The first two rows of symbols are in general circulation throughout the flow chemistry community; however, the third row illustrates more complex reactors used in flow chemistry which will be explored and detailed further in this introduction (Figure 1).

1.2 Reactor design enabling organic reactions

Flow chemistry for organic synthesis is an enabling technology that, initially, had been used to overcome batch chemistry limitations, such as scaling up and integrated telescoped transformations. However, (in the not-so-distant future) it seems that flow is transitioning into a technique for automation using unique reactor design and machine learning to support organic chemists with rapid screening and repetitive tasks. The development of reactor design has enabled the use of difficult gaseous reagents to be harnessed and analysed in flow; multiphasic reactions to process successfully without blockages; and coupling multiple synthetic tools together such as, electro-flow/microwave-flow/photo-flow.¹⁻⁹ An overarching goal that drives the development of flow chemistry reactors is to overcome the limitations and challenges of classical synthesis techniques. To this extent, it is common to see in the literature how various

flow techniques can deliver improvements compared to batch counterparts, which is why this area of research has seen a rapid growth in development of complex flow systems in relatively short order. The theme of this thesis is to explore how creative reactor design has overcome batch limitations or created simplicity and ease for the organic chemist. This introduction will aim to broadly illustrate the journey of reactor design from streamlining multiple chemistry transformations to innovative couplings of technologies ending on the future of automation and programmable chemical vending machines.¹⁰ Flow chemistry has been around for many decades, most commonly in the petrochemical industry, and this thesis is documenting the miniaturisation of these industrial scale techniques. When reactor design and engineering is discussed, great inspiration is taken from these already established industrial practices, and we, as organic chemists, are taking this equipment and miniaturising them for 'meso-scale' flow synthesis.

Research in flow chemistry has evolved to explore various reactor design for multiple purposes. Depending on the desired system, different design considerations must be incorporated; the more complex the system, the more design considerations there tend to be. This introduction will explore different reactor designs and how they are appropriate for the required chemistry in continuous flow (Figure 2).

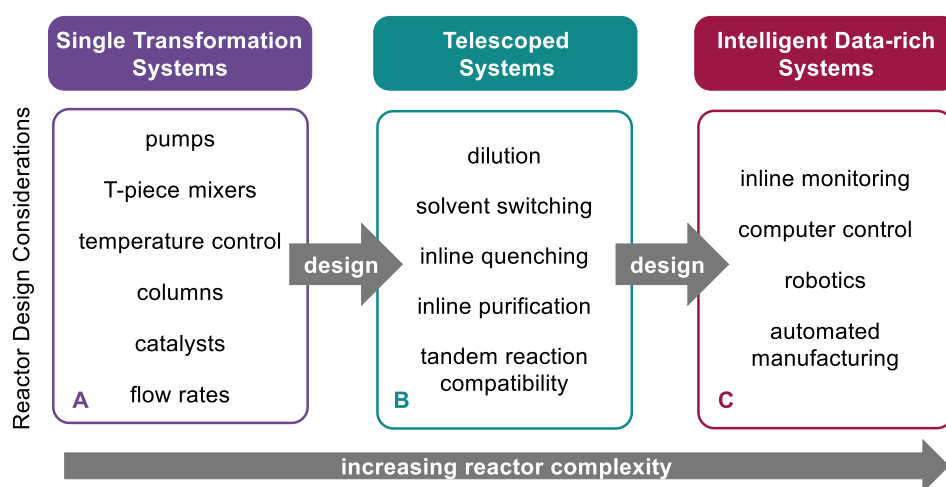


Figure 2 - Reactor design considerations for various flow systems

Single transformation systems are most likened to batch conditions where it is commonplace to translate batch transformations into a continuous process for scale up or greater parameter control. These synthetic parameters, such as temperature, equivalence, and mixing, are all fundamental to a reaction's success. However, translating this chemistry into flow most often requires some careful reactor design considerations such as: type of pumps used; use of flow columns; catalytic systems; exotherms; and circumventing blockages (Figure 2, A). To integrate downstream

processing (workup/purification) or multi-step synthetic transformations, additional consideration must be made to successfully handle a more complex reactor system (Figure 2, B). Solvent compatibility, biphasic mixtures, and tandem reaction compatibility are all additional factors that must be included when considering design of the continuous reactor. Finally, to create a data-rich intelligent flow system requires the integration of in-line analysis to monitor the reaction and programmable software to process the data allowing the system to learn and adapt. This increases the complexity of the flow system further as all previous considerations and parameters discussed, must also be included (Figure 2, C).

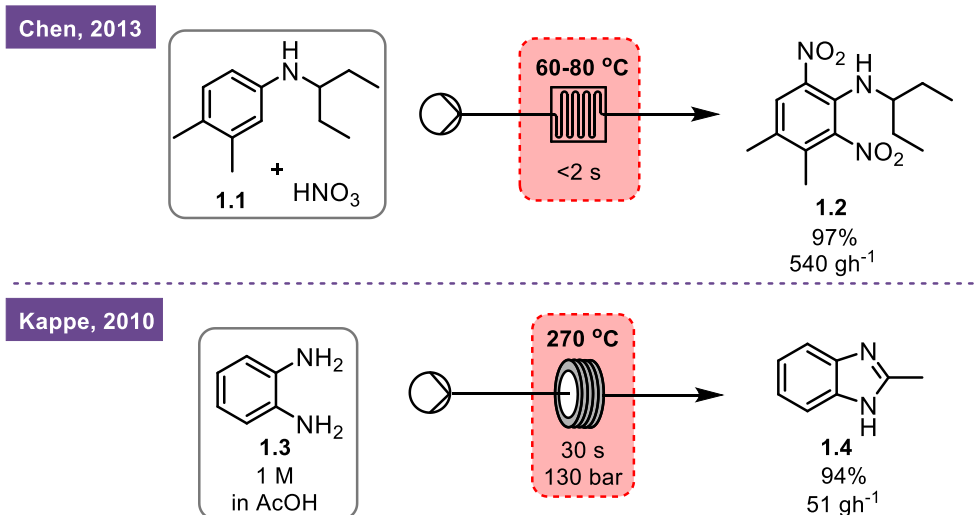
Flow chemistry can facilitate chemical transformations and can be engineered to overcome limitations that arise in both batch and flow. This introduction will explore how scientists have overcome these limitations via innovative reactor design.

1.2.1 Single Transformation Systems

Perhaps the simplest reactor design to implement a flow process is that of a single pump and coil process. Indeed, such a setup has been reported many times in the literature, whereby reagents are carried in solvent via pumps through tubular reactor coils. Two different reagent streams can be mixed, either within the reaction zone or pre-mixed via a T-piece, which brings both reagent streams together. Reactor coils can vary in length (and therefore reaction time) and due to the high surface area-to-volume ratio an external heating/cooling source can efficiently influence the conditions within the tubular reactor.¹¹ These are all important considerations when designing a flow system for a single chemical transformation. In some systems, additional equipment is required to facilitate chemistry to occur in continuous flow. This may include: flow columns, catalyst bed reactors, gas handling flow equipment, passive/active mixers, and back-pressure regulators. There are numerous examples of researchers using the above equipment to perform single transformation chemistry.¹²⁻²²

Thermal control

Precise thermal control of flow systems has been hailed as one of the excellent attributes of flow chemistry and has been utilised over the past 10 years (Scheme 1).



Scheme 1 – Thermal control of flow systems to manage dangerous conditions

In 2013, Chen and co-workers performed a dinitration reaction on compound **1.1** using a 16-channel microreactor. At a high flow rate, excellent mass and heat transfer was achieved which created great mixing and precise thermal control which in turn improved selectivity by suppression of side reactions. Any exothermic runaway reactions were dissipated efficiently thus minimising safety risks when compared to the batch counterpart. The microreactor's large surface area-to-volume ratio design successfully competes with large scale batch reactors with an excellent productivity of 13 kg per day for compound **1.2**.²³ Kappe in 2010, used an X-Cube from ThalesNano which enabled high temperature/pressure reactions to take place in continuous flow via a stainless steel coil reactor. This design facilitated the synthesis of 2-methyl benzimidazole **1.4** from *o*-phenylenediamine **1.3** in neat acetic acid. At 270 °C and 130 bar, 94% of the benzimidazole was synthesised which was comparably better than the microwave process they were exploring. The main limitation of this transformation in batch microwave was the poor thermal control of a large reaction volume and therefore the flow design brought an excellent alternative to scale and heat this reaction safely (Scheme 1).²⁴

Gaseous reagents

The use of gaseous reagents in chemistry has benefits such as good atom economy and can be a readily available feedstock. However, handling gases in the lab can be difficult and potentially dangerous if the gas is flammable or explosive and these risks are significantly intensified by scale of reaction.²⁵ Chapter 2 further describes examples of how different reactor designs effectively facilitates the integration of gas into flow systems.

Catalyst bed reactors/flow cartridges

Polymer supported reagents and/or scavenger resins can be used in flow as useful heterogeneous tools in continuous synthesis. Isolating the solid reagents within a glass flow column enables reactants to interact with the solid support and then continue to be pumped away from the support minimising the need for purification. It is especially beneficial to use solid supported columns for heterogeneous catalysis, where two reagents subjected to the catalyst, react and then subsequently elute from the outlet of the column without the catalyst (Figure 3).²⁶

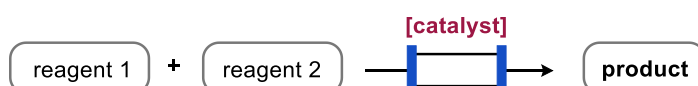
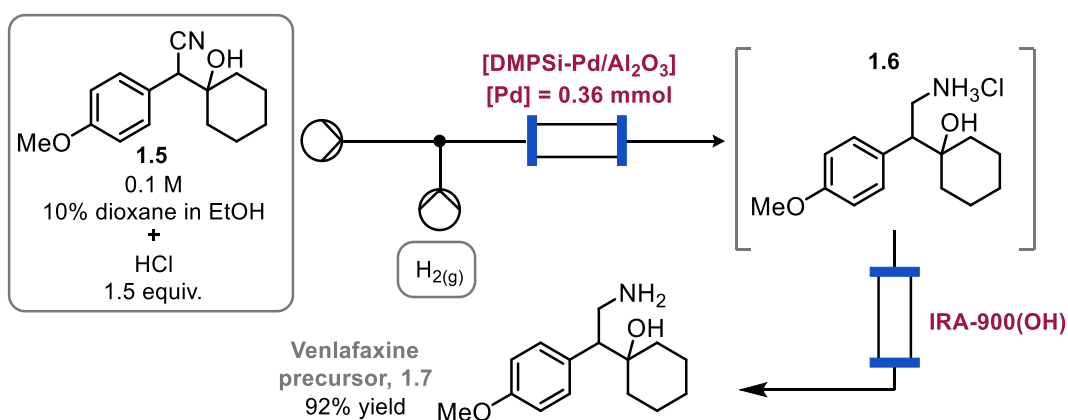


Figure 3 – Use of heterogeneous catalyst to yield pure product in continuous flow

Hydrogenations in flow have become very prevalent due to its abundance in both academia and industry and are an excellent example of a useful reactor design to enable sometimes difficult-to-handle reductions. In 2017, Kobayashi and co-workers demonstrated the use of silica supported palladium catalysis to selectively hydrogenate nitriles to primary amines (Scheme 2).

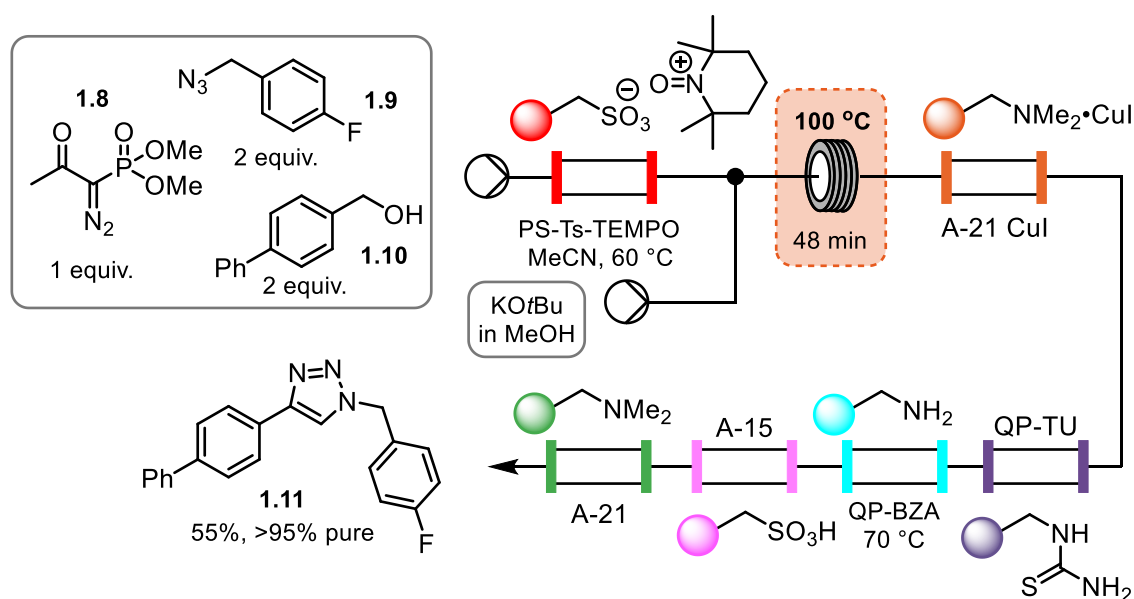


Scheme 2 – Use of immobilised palladium catalysis to reduce the nitrile to a primary amine in flow

Using a poly(dimethylsilane)Pd/Al₂O₃ solid catalyst, the authors could immobilise the catalyst within a flow cartridge. This allowed a Venlafaxine (anti-depressant) precursor **1.7** to be synthesised in flow. Initially, the nitrile **1.5** was pre-mixed with HCl and with the integration of hydrogen gas, via a mass flow controller, the nitrile was reduced over palladium to give the ammonium chloride intermediate **1.6**. Notably they utilised a second cartridge filled with an ion-exchange resin (IRA-900(OH)) which acts as a solid base and can mop up excess protons. This afforded the neutral primary amine compound **1.7** which was later dimethylated in batch to afford Venlafaxine in a 95% average yield over

the two processes. They tested the durability of the [Pd] cartridge over 300 h and found trace amount of leaching and no drop off of reactivity.²⁷ This process has highlighted that solid support cartridges can also be used for in-line purification processes. This is another excellent way a flow reactor can integrate purification into the continuous process thus minimising the work required for the organic chemist after reaction.

In 2009, Ley and co-workers exhibited an innovative flow system that demonstrated the use of solid polymer supported reagents and scavenger materials to facilitate reactions and ensure the quality of the exiting product (Scheme 3).



Scheme 3 – Use of solid support reagents as integral reaction components and in-line purification

This single pass system enabled multiple reaction steps to occur in tandem flow including in-line purification. Initially, the benzyl alcohol **1.10** was oxidised using an immobilised TEMPO oxidant to afford the aldehyde *in situ* at 60 °C. With the addition of KO^tBu in MeOH, the Bestmann-Ohira reagent **1.8** (already present) could react with the newly formed aldehyde to yield the terminal alkyne in a 100 °C reactor coil. Notably, both the 4-fluorobenzyl azide **1.9** and Bestmann-Ohira reagent **1.8** were unaffected by the oxidative conditions and shows the authors had considered the chemical compatibility of this tandem system. In the presence of the solid supported copper catalyst (A-21 CuI) the formed alkyne and available azide **1.9** could readily undergo a click reaction to form the desired triazole **1.11**. The four in-line scavenger flow columns were then used to clean up the reaction. Quadrapure-thiourea (QP-TU) was used to mop up any leached copper from the previously flow column. Quadrapure-benzylamine was heated to 70 °C to react with any unreacted aldehyde via a condensation reaction and therefore removing any residual benzyl alcohol **1.10**. Amberlist-15 (A-15) is an acidic resin that removes

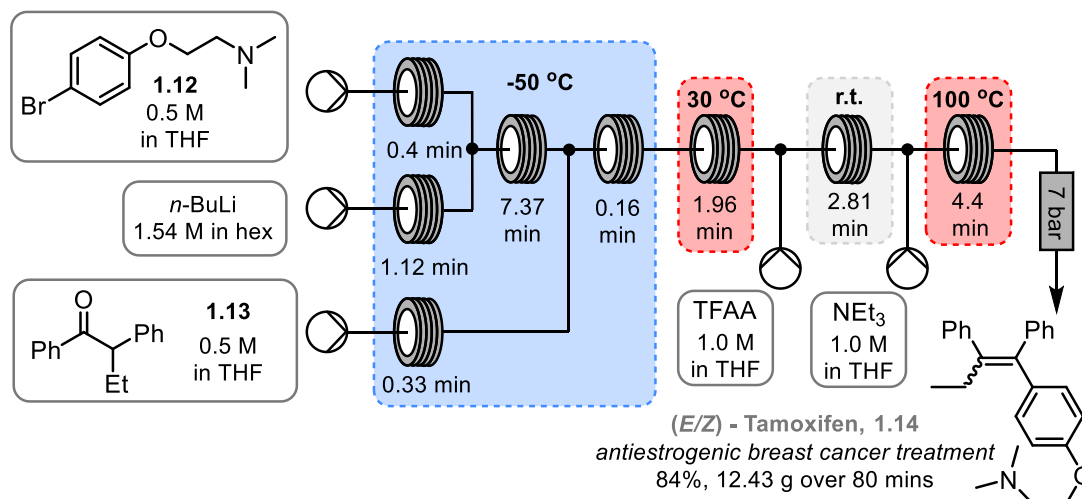
excess base and phosphoric residues coming from the Bestmann-Ohira reagent **1.8**. Finally, the Amberlist-21 (A-21) is a basic resin that removes any remaining acid material. This suite of reactor columns and in-line purification afforded the desired triazole **1.11** in 55% yield and pleasingly, >95% purity. This is another example where the design of this flow system has reduced the work-load for the organic chemist and streamlined the purification process, avoiding unnecessary wastage of workup/purification solvents.²⁸

It is clear from the previous example that flow systems need to increase in complexity to facilitate in-line purification. When introducing multiple reactions in tandem complex flow systems are required, including additional design considerations. This means that the organic chemist must engineer the whole process and relevant compatibility issues rather than focussing solely on the desired synthetic transformation.

1.2.2 Telescoped Systems

The modular nature of flow chemistry enables the easy assembly of complex flow systems. These systems can be efficiently used to facilitate multiple-stage chemistry in one continuous process which can avoid intermediate purification and streamlines chemistry to build complex molecules in one process. The complexity of reactor design most certainly increases when building telescoped flow systems. A common consideration is to be mindful of the increase in flow rate as additional pumps are introduced into the flow. This required much larger tubular reactor volumes to increase required reaction times.

In 2013, Ley and co-workers designed a telescoped flow system that enabled the synthesis of (E/Z) Tamoxifen, an antiestrogenic breast cancer treatment drug (Scheme 4).



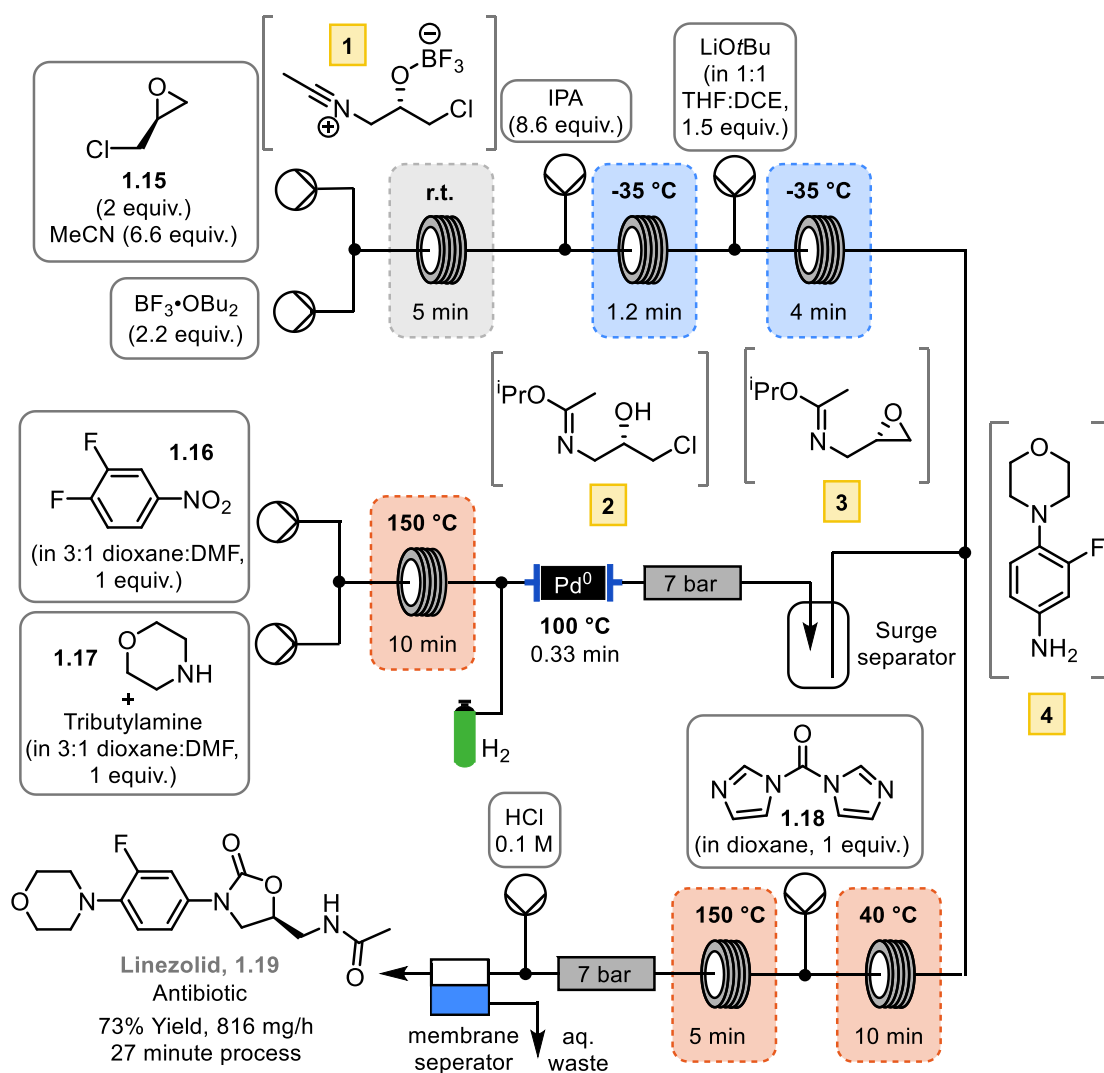
Scheme 4 – Telescoped flow synthesis of (E/Z) – Tamoxifen

The basics of flow chemistry are present in Scheme 2, fundamentally pumps carry various reagents in solvent through tube reactors which enables a reaction to take place. However, additionally this telescoped flow system enabled the synthesis of (E/Z) – Tamoxifen **1.14** in 84% which was scaled to yield 12 g over 80 minutes. This is a prime example of a multi-step synthesis being streamlined into one process and due to the continuous nature of flow chemistry, scale was dependent on time rather than vessel volume. The Vapourtec E-series flow platform has the capacity to pre-cool and maintain temperatures of -50 °C which was utilised for a controlled lithium-halogen exchange of compound **1.12** and subsequent attack of ketone **1.13** in thermally controlled conditions. The modular nature of flow chemistry easily allowed the inception of the reaction stream thus with the addition of TFAA and subsequent Et₃N, the product **1.14** was formed with no intermediate purification required. However, the final reactor volumes had to be 10 mL and 20 mL, respectively, and with the large tubular volumes, the reaction times were still short (<5 min) which raises limitations in applying this system to other examples that may need longer reaction times. Furthermore, the use of organometallic reagents in flow are very useful and managed well in flow, due to the thermal control instilled by the technology. However, pumping these reagents in average HPLC pump is not possible due to the incompatibility in the pump heads. The authors had to use specialised peristaltic pumps to successfully pump the organometallic reagents. These pump heads work by massaging flexible tubing in one direction thus moving the solvent mixture along the tubing but without the mechanical pump heads being wetted by the solvent/reagents.²⁹ The need for specialised equipment in flow chemistry can be a major limitation to developing telescoped flow systems for research. These considerations

demonstrate why the complexity of designing more elaborate flow system require careful planning and innovative enabling technology.

There has been a strong push for developing telescoped flow systems to deliver API's and natural products in succinct flow processes which favourably translate to industrial scale up. For example, in 2015, Jamison and co-workers developed a flow process to synthesise 83% Ibuprofen in 3 minutes with a productivity of 8 g/h.³⁰ Lab-scale flow systems are designed to illustrate the compatibility of the chemistry in an industrial setting whilst also highlighting the benefits of no intermediate purification and tandem reactivity thus saving on environmental and economic cost and once again, the chemist's time.^{18,31-36}

In 2019, Jamison and co-workers designed a seven-step telescoped flow system to synthesise Linezolid, an essential antibiotic. At the time of publication, this was the first example of the highest number of synthetic steps in a continuous flow process with no intermediate purification or solvent exchanges. This demonstrates that flow reactor designs were evolving into more complex processes to achieve succinct and streamline API syntheses (Scheme 5).

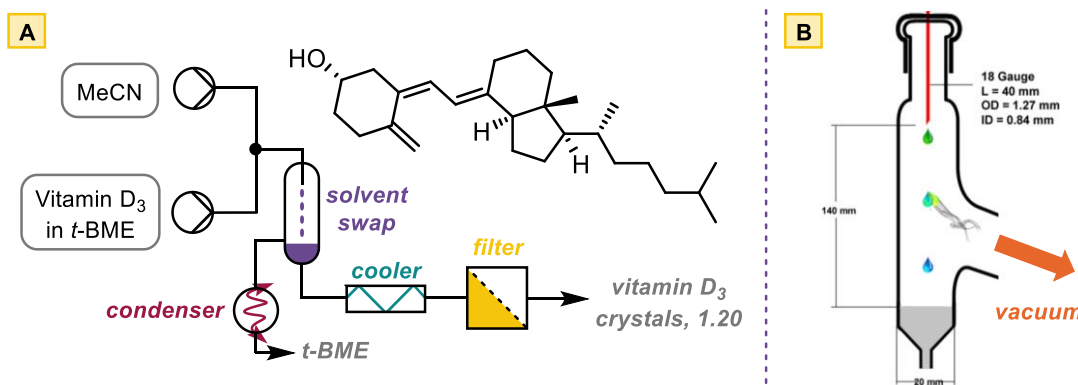


Scheme 5 – Telescoped seven-step flow synthesis of Linezolid

The synthesis of Linezolid **1.19** starts with the commercially available (+)-epichlorohydrin **1.15** undergoing a Ritter-type reaction with acetonitrile for 5 minutes using $\text{BF}_3 \cdot \text{OBU}_2$ as a Lewis acid (intermediate 1, Scheme 5). Addition of isopropyl alcohol, at $-35\text{ }^\circ\text{C}$, formed the soluble boronic ester by-product and furthermore, formed the imidate through attack of the nitrilium ion (intermediate 2, Scheme 5). The epoxide was reformed at $-35\text{ }^\circ\text{C}$ via an excess addition of LiOtBu in 4 minutes (intermediate 3, Scheme 5). The integration of DCE as cosolvent helped to solubilise the lithium chloride salts. Meanwhile, a simultaneous separate synthetic pathway had been initiated. A successful $\text{S}_{\text{N}}\text{Ar}$ reaction was completed using morpholine **1.17** and 1,2-difluoro-4-nitrobenzene **1.16** supported by tributylamine at $150\text{ }^\circ\text{C}$ for 10 minutes. Using a mass flow controller, hydrogen gas was introduced into the flow system and the nitro species was reduced over a palladium flow column at $100\text{ }^\circ\text{C}$ and no dehalogenation was found (intermediate 4, Scheme 5). The hydrogen gas was scrubbed out of the reaction into a surge container by gravity and

the reaction mixture directly pumped back into the flow system. Due to the presence of water in the reaction from the hydrogenation, the imidate was hydrolysed and the newly formed aniline attacked the epoxide intermediate to form an amino alcohol. The final transformation used CDI **1.18** (as a phosgene alternative) to form the oxazolidinone ring at 150 °C for 5 minutes. Upon addition of HCl, an in-line separation was installed to removed aqueous soluble by-products and linezolid **1.19** was collected in an overall yield of 73% in 27 minutes total run time. The use of an in-line separator that can split an organic and aqueous phase is as very useful tool when installing downstream processing to a flow system. There are various separator technologies available, but the two main methods used are: using a semi-permeable material that allows passage of organic solvent but not aqueous (Biotage phase-separator, for example); or using surface tension membrane technology that has pores within a membrane that allow the passage of organic solvents that have a low surface tension than aqueous media (Zaiput continuous separator for example).³⁷ The authors chose to use a Zaiput separator that has a 0.1 µm PTFE membrane. This paper demonstrates, not only an excellent pathway for the synthesis of Linezolid, but also how to manage the chemical compatibility of linking different reactions together in flow. Addition of solvents such as, DCE and DMF, to manage potential solid forming by-products is an innovative way to maintain a durable flow process without running the risk of blockages. It is evident that added design complexity is required to achieve compressed telescoped synthesis as opposed to multiple reactions in sequence in batch, most commonly requiring intermediate workup/purification and/or solvent exchanges.³⁸

The development of flow systems for downstream processes is constantly evolving to integrate purification and isolation of desired compounds into the continuous process. In 2018, Gruber-Wölfler and co-workers designed an innovative and creative way to swap solvents in-line to prepare for the re-crystallisation, and thus purification, of vitamin D₃ **1.20** in a continuous manner (Scheme 6).



Scheme 6 – New technology for solvent swapping in flow (A); Picture taken from literature showing the evaporation of removed solvent (B).

This flow system introduced a stream of MeCN to Vitamin D₃ dissolved in *t*-BME. Their solvent-swap system was glassware kept at 40 °C and 280 mbar of reduced pressure via a vacuum pump. After the solvents were combined in flow, the mixture was dropped from a needle into the vacuum chamber. In the solvent-swap column, the *t*-BME evaporated from the drop (and surrounding splashes) and was condensed and pumped out of the system. The Vitamin D₃ remained dissolved in the higher boiling point MeCN and was collected, cooled for 1 min, and 50% w/w crystals of Vitamin D₃ **1.20** was obtained via filtration.³⁹ This carefully thought-out reactor design had pushed the development of downstream processing into a sophisticated method to swap solvents.

Downstream processing in flow has multiple benefits and research has gone to great lengths to explore the extent of processing compounds in-line.⁴⁰ In 2013, Trout and co-workers created an elaborate flow system that synthesised, purified, and formulated tablets of Aliskiren hemifumarate (direct renin inhibitor) in one continuous process. They integrated crystallisation, drying, powder blending, and tableting via continuous extrusion to create an industrious 2.7 x 10⁶ tablets per year with a plant footprint of 2.4 x 7.3 m². In 2013, this was the first example of end to end manufacturing for a pharmaceutical product and illustrates the power that flow chemistry enables when thoughtful design is executed.⁴¹ An important point to note is that these developments in flow technology have come under scrutiny for being an expensive methodology for problems that do not exist. It is important to recognise that a balance must be applied and that most chemistry functions very well in batch reactions. This was highlighted, in 2013, by Ley and co-workers when they explored the telescoped synthesis of Meclizant. They used innovative flow synthesis where applicable and useful, and utilised efficient batch techniques for the remaining synthesis rather than using technology for the sake of using technology.⁴²

These examples have demonstrated that reactor design needs to increase in complexity to deliver engineering solutions to common flow problems. All the designs, so far, have relied heavily on the flow chemist's problem solving and innovation. The future prospects of flow chemistry have begun to develop toward automation and machine learning through live data acquisition and remote chemical control.

1.2.3 Intelligent data-rich systems

The final section of this introduction will briefly explore the recent developments of flow chemistry and the use of in-line monitoring and automation to streamline continuous

synthesis. To achieve this, the design complexity must increase to support the integration of live data recording/automatic control.

Highly complex automated telescoped systems with in-line monitoring are the front runners of the flow community and have been shown to work impressively to synthesise API compounds with minimal input from the organic chemist. Jensen and co-workers in 2016, published in *Science* detailing their fridge-sized API factory. The system used an automated series of reactor modules that can interchange to effectively synthesise compounds at a push of a button (Figure 4).

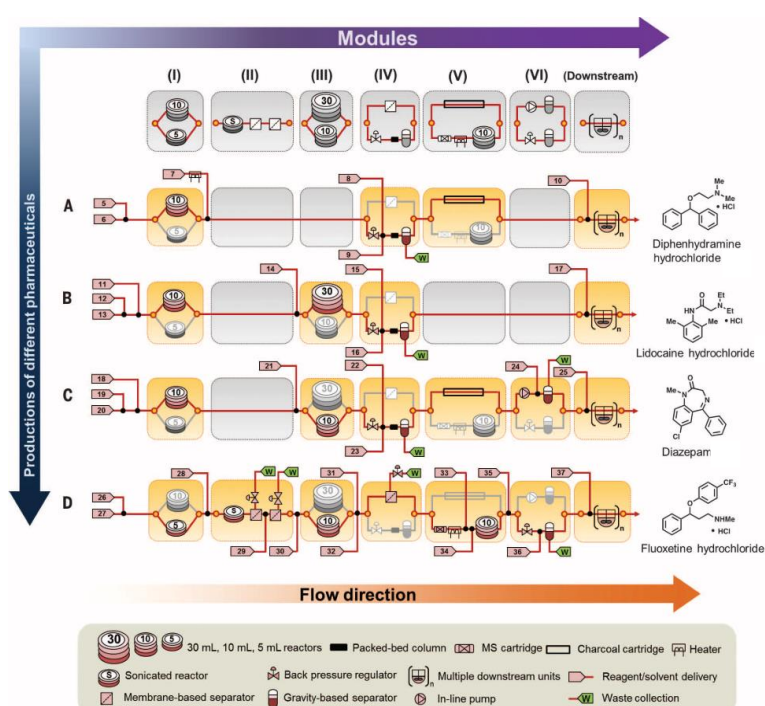


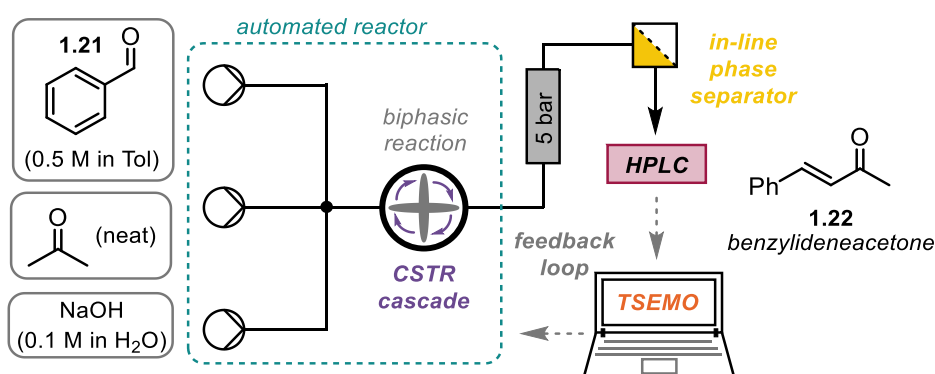
Figure 4 – Figure taken from paper detailing blueprints of automated API factory

The authors had created a multifunctional flow system that allowed the operator to choose which drug they desired to be synthesised and the factory would automatically activate the relevant reaction modules that create the synthetic pathway for the reaction to successfully take place. They used in-line flow-IR monitoring to gauge consumption of reactive intermediates (modules I to VI, Figure 4). The most complex synthetic flow pathway is row **D** which takes DIBAL and 3-chloro-1-phenylpropan-1-one and reduces the ketone in a 10 min reactor which was ultrasonicated to keep the aluminium salts dissolved and extend the longevity of the reactor. The reaction was quenched in-line with HCl for 3.3 minutes and the aqueous and organic phase was separated in flow using a Zaiput surface tension membrane separator twice and the aqueous and gas waste

removed. The 3-chloro-1-phenylpropan-1-ol was then mixed with aqueous MeNH_2 to undergo an $\text{S}_{\text{N}}\text{Ar}$ reaction at $135\text{ }^\circ\text{C}$ for 10 min which was extracted into THF and washed with $\text{NaCl}_{(\text{aq})}$ and subsequently separated. The amino alcohol intermediate was passed through a molecular sieve column to remove any water and pre-heated and combine with the relevant reagents in a $140\text{ }^\circ\text{C}$ coil for 2.6 min to afford the fluoxetine solution. Water was added downstream to prevent KF precipitation and TBME was used to extract the desired API which was subsequently separated through gravity to yield fluoxetine in 43% yield. The API then entered the downstream processing compartment and, with the addition of HCl, lead to the precipitation and recrystallisation of fluoxetine hydrochloride to USP standards. Re-dissolving the fluoxetine hydrochloride could prepare 100-200 doses. The authors envisage a future where their fridge-sized factory could one day be based in a hospital to produce drugs on demand for therapeutic uses. The versatility of this system activates or deactivates flow modules depending on the require synthetic tools needed to synthesise the API.⁴³

It should be noted that this line of research does not aim to kick organic chemists out of the lab; it wants to harness technology to undertake the manual work in a highly repeatable and reliably manner to standardise synthetic methodologies.

To achieve such reactor complexity, monitoring reactions in-line is a vital insight into the progress of reactions and thus illuminating the internal mechanisms of the reaction, in turn, allowing data-lead decisions to drive optimisation. In 2020, Bourne and co-workers optimised a multi-step process with respect to multiple objectives for a Claisen-Schmidt condensation. This used a feedback system based on machine learning methods (TSEMO algorithm) to learn from the data created from the reaction and self-optimize to programmed objectives (Scheme 7).



Scheme 7 – Automatic self-optimising system

This combination of the TSEMO algorithm and an automated flow platform enabled the self-optimisation of a Claisen-Schmidt condensation (of benzaldehyde **1.21** and acetone) to yield benzylideneacetone **1.22**. The TSEMO algorithm was used to optimise multiple objective problems by using the results of the reaction from the HPLC chromatogram and the algorithm used that data to select which parameters to change and perform next. This is repeated until the objective it met and for this reaction the authors were using the algorithm to simultaneously maximise purity, space-time-yield, and reaction mass efficiency. After 109 experiments it found optimal conditions for each objective, however, all three objectives could not be optimised to the same degree. A compromise was found that gave 82.8% purity, 166 kgm⁻³h⁻¹ STY, and a RME of 5.66 which is an approximate equal compromise. The authors noted that due to the multi-step nature of this system, the reaction should be treated as a 'black-box', and you can only see the inputs and output and thus a limitation was found that the data did not illuminate internal workings of the reaction. More analytic tools would be required after each step to precisely know the effects of changing the reaction parameters on each step.⁴⁴ Bourne and co-workers have continuously developed self-optimising flow systems to assist the organic chemist as a useful and time saving synthetic tool. Their reactor designs enable data-rich reactions to illuminate chemical synthesis information that can assist in shortening process development time and increase multi-step reaction efficiency.⁴⁵⁻⁴⁷

This example is demonstrating that a multi-step flow reaction can be optimised without the need of human intervention other than the programming required. Jensen and co-workers have also explored the use of self-optimising flow systems and, for example, have found to successfully optimise a Heck reaction in 19 automated experiments using minimal reagents to then scale their system up 50-fold.⁴⁸ The requirement of computerised programming tools and algorithms shows that these flow systems are far more complex than traditional single-pass flow reactions. In these examples the flow chemist must design the reactor and the synthetic reaction to optimise through traditional methods.

Jensen and co-workers have taken these automated systems a step further where the system can create a synthetic route; design the experiment; synthesise and optimise the reaction in flow; and finally purify and formulate a desired drug ready for use in one contained flow unit (Figure 5).

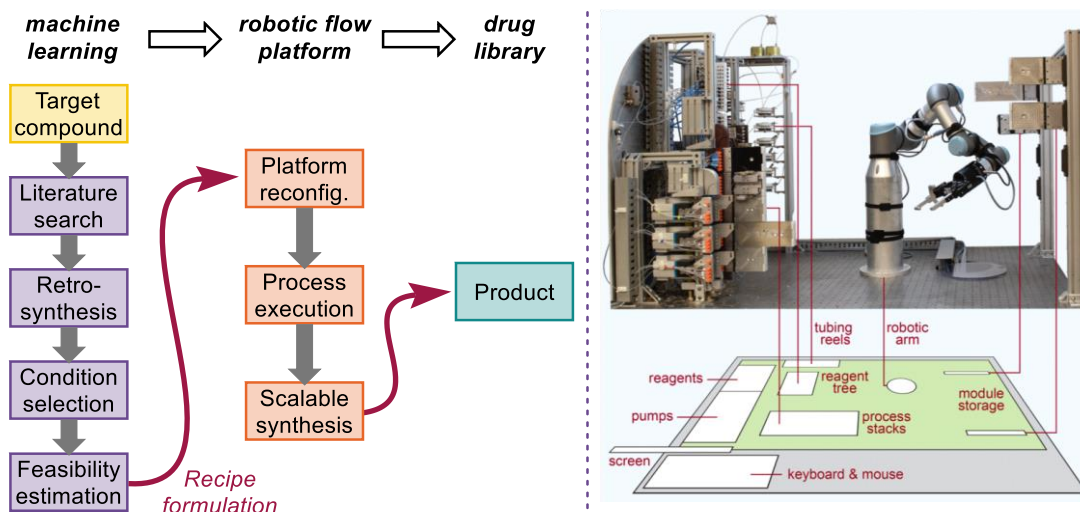


Figure 5 – Workflow of AI system for planning drug synthesis and executing in flow (left); picture taken from literature detailing the automated robotic system for synthesising drug library (right)

There have been great developments in literature exploring automated self-optimising flow systems aided by reaction feed-back algorithms.^{43,49–53} However, this system has integrated computer-aided synthesis planning (CASP) coupled with robotically executed chemical synthesis in flow. The authors demonstrated that the system could make a suite of 15 medicinally relevant compounds. At the inception of process, the AI has access to a database of millions of reactions from Reaxys and the US patent office. It could apply a retrosynthetic analysis on the desired compound and pave a synthetic pathway appropriate to a flow system. After identifying suitable reaction conditions and predicting the economic and chemical feasibility of the reaction, the system formulates a ‘recipe’ file for the desired drug. The robotic arm builds the necessary flow system from a bank of reactor modules and connects the pump inputs and outputs through a fluidic switchboard. This exemplifies the ‘plug and play’ modularity of flow chemistry and how a complex flow system can be constructed easily from various reactor ‘building blocks’. After constructing the required reactor modules, the flow synthesis is performed to yield the desired compound on scale on demand. An important feature of this platform is to create reproduceable flow recipes for common drug syntheses which increases the availability of reaction data into the research community. This is in the aim to relinquish the laborious manual tasks of synthesis to give the organic chemist space for new innovation and ideas.⁵⁴ Leaps towards remote chemistry have been also been explored where a chemist on his laptop in Brazil performed 12 hours of flow reactions in Nottingham, UK through ‘cloud chemistry’.⁵⁵ There is a discussion on whether this technology is an expensive tools that could be done as efficiently as a synthetic chemist

or a technology that could enhance our chemical facilities to aid organic chemist's, creating reproduceable, reliable paths to synthetic targets.

Leroy Cronin has explored removing the organic chemist from the lab altogether by designing a 'chemputer' that can innovate and solve synthetic problems the same as an organic chemist whilst also automatically synthesising the target compound in flow. The aim of this research is to use AI to explore chemical space and therefore discover new reactivity without bias. Using feed-back loops, as discussed previously, robotics can quickly and efficiently, through trial and error, find optimal conditions and potential new chemical reactivity for chemistry. Cronin and co-workers, in 2021, published an automated fume hood that fused batch and flow chemistry including downstream processes such as work up and use of a ro-vap (Figure 6).

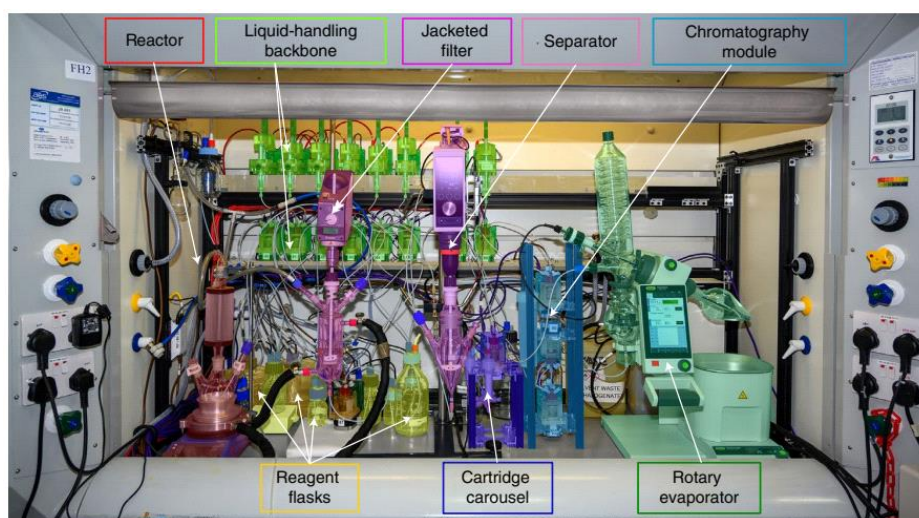


Figure 6 – Picture taken from Cronin and co-workers publication illustrating their automated 'Chemputer'

The 'Chemputer' could synthesise NHS-diazirine in a cheaper manner whilst also stating that the cost of the 'Chemputer' would be covered by two repetitions of the synthesis of NHS-diazirine due to the high value product being synthesised efficiently. This AI system not only explores chemical space to find new reactivity, but it also controls an automated synthetic fume hood which firmly pushes the synthetic chemist out of the lab.⁵⁶⁻⁶⁰

The digitisation of chemistry is an interesting topic of discussion and reactor design plays a vital role in this development. Machine learning and automation stipulates its increase in reproducibility and standardisation of chemical procedures. The examples shown in this introduction demonstrate flow chemistry as a highly versatile enabling technology for synthetic chemistry, but also a seed point for creativity.

1.3 Conclusion

Reactor design has been shown to increase in complexity when more data-rich chemistry is required. By careful considerations, continuous processing can be harnessed to facilitate chemistry that is either unachievable via batch methods or increases the control of variable reaction conditions.

This introduction has described how flow chemistry can implement high thermal control due its high surface area-to-volume ratio and utilise fixed bed reactors to perform heterogenous transformations in single pass systems. These examples required an organic chemist to process and work up/purify the target compound after completion of the reaction. By increasing the complexity of the flow reactor design, these work-up processes can be integrated into the flow systems to leave the laborious tasks of purification up to the flow system. The role of the organic chemist in these scenarios are still fundamental in designing the reactions and optimising the flow systems are still manually performed. The final section of this chapter alludes to the development of self-contained flow systems that perform telescoped reactions, including downstream processing, but with the added addition of self-optimisation. This increase of system complexity in turn reduces the manual workload of the organic chemist. Rather than relying on the scientist's chemical intuition and knowledge to optimise a reaction, an automated algorithm efficiently works through trial and error to arrive at the desire programmed objective.

Nevertheless, the outlook of these evolving technologies seems to be used as an assistive synthetic tool to the organic chemist and not a replacement. The innovation and creativity to design these elaborate reactors are due to the flow chemistry community's drive to solve chemical problems and increase efficiency of synthesis. As one observation, the field has moved rapidly and has become multi-disciplinary and highly complex even within the timeframe of this PhD project. There are indeed several expertise and financial barriers to entering the field at the very front end with robotics and advance machine learning algorithms, it will be exciting to see what emerges from this potentially disruptive technology.

1.4 Thesis outlook

This thesis will explore the development and use of novel reactor designs to facilitate and implement the requirements of a series of synthetic methodology projects. The thesis is split into three research chapters:

- 1) Chapter 2 - Utilisation and generation of acetylene gas in flow and how the continuous system is engineered to successfully meet its target.
- 2) Chapter 3 – This project explores the reactor design for the thermal generation and use of acyl ketenes as a reactive intermediate under flow conditions.
- 3) Chapter 4 – A collaborative project investigates the use of CSTRs to manage precipitation in flow to successfully synthesise the natural product, Civetone.

1.5 References

- 1 P. D. Morse, R. L. Beingessner and T. F. Jamison, *Isr. J. Chem.*, 2017, **57**, 218–227.
- 2 J. C. Pastre, D. L. Browne and S. V. Ley, *Chem. Soc. Rev.*, 2013, **42**, 8849–8869.
- 3 M. B. Plutschack, B. Pieber, K. Gilmore and P. H. Seeberger, *Chem. Rev.*, 2017, **117**, 11796–11893.
- 4 B. Gutmann, D. Cantillo and C. O. Kappe, *Angew. Chemie Int. Ed.*, 2015, **54**, 6688–6728.
- 5 J. Wegner, S. Ceylan and A. Kirschning, *Adv. Synth. Catal.*, 2012, **354**, 17–57.
- 6 I. R. Baxendale, *J. Chem. Technol. Biotechnol.*, 2013, **88**, 519–552.
- 7 T. Noël, Y. Cao and G. Laudadio, *Acc. Chem. Res.*, 2019, **52**, 2858–2869.
- 8 C. Wiles and P. Watts, *Green Chem.*, 2014, **16**, 55–62.
- 9 T. H. Rehm, *Chem. – A Eur. J.*, 2020, **26**, 16952–16974.
- 10 J. Zhang, K. Wang, A. R. Teixeira, K. F. Jensen and G. Luo, *Annu. Rev. Chem. Biomol. Eng.*, 2017, **8**, 285–305.
- 11 N. G. Anderson, *Org. Proc. Res. Dev.*, 2012, **16**, 852–869.
- 12 J. W. Sheeran, K. Campbell, C. P. Breen, G. Hummel, C. Huang, A. Datta, S. H. Boyer, S. J. Hecker, M. M. Bio, Y.-Q. Fang, D. D. Ford and M. G. Russell, *Org. Process Res. Dev.*, 2021, **25**, 522–528.
- 13 Z. Tan, Z. Li, G. Jin and C. Yu, *Org. Process Res. Dev.*, 2019, **23**, 31–37.
- 14 R. L. Hartman, J. P. McMullen and K. F. Jensen, *Angew. Chemie Int. Ed.*, 2011, **50**, 7502–7519.
- 15 Z. Lu, B. S. Bajwa, O. E. Otome, G. B. Hammond and B. Xu, *Green Chem.*, 2019, **21**, 2224–2228.
- 16 C. Huang, X.-Y. Qian and H.-C. Xu, *Angew. Chemie*, 2019, **131**, 6722–6725.
- 17 M. A. Ganiek, M. V. Ivanova, B. Martin and P. Knochel, *Angew. Chemie Int. Ed.*, 2018, **57**, 17249–17253.
- 18 M. Köckinger, C. A. Hone, B. Gutmann, P. Hanselmann, M. Bersier, A. Torvisco

- and C. O. Kappe, *Org. Process Res. Dev.*, 2018, **22**, 1553–1563.
- 19 N. Weidmann, M. Ketels and P. Knochel, *Angew. Chemie Int. Ed.*, 2018, **57**, 10748–10751.
- 20 S. G. Newman and K. F. Jensen, *Green Chem.*, 2013, **15**, 1456–1472.
- 21 D. T. McQuade and P. H. Seeberger, *J. Org. Chem.*, 2013, **78**, 6384–6389.
- 22 F. Benito-López, R. J. M. Egberink, D. N. Reinhoudt and W. Verboom, *Tetrahedron*, 2008, **64**, 10023–10040.
- 23 Y. Chen, Y. Zhao, M. Han, C. Ye, M. Dang and G. Chen, *Green Chem.*, 2013, **15**, 91–94.
- 24 M. Damm, T. N. Glasnov and C. O. Kappe, *Org. Process Res. Dev.*, 2010, **14**, 215–224.
- 25 M. Brzozowski, M. O'Brien, S. V Ley and A. Polyzos, *Acc. Chem. Res.*, 2015, **48**, 349–362.
- 26 W.-J. Yoo, H. Ishitani, Y. Saito, B. Laroche and S. Kobayashi, *J. Org. Chem.*, 2020, **85**, 5132–5145.
- 27 Y. Saito, H. Ishitani, M. Ueno and S. Kobayashi, *ChemistryOpen*, 2017, **6**, 211–215.
- 28 I. R. Baxendale, S. V. Ley, A. C. Mansfield and C. D. Smith, *Angew. Chemie Int. Ed.*, 2009, **48**, 4017–4021.
- 29 P. R. D. Murray, D. L. Browne, J. C. Pastre, C. Butters, D. Guthrie and S. V Ley, *Org. Process Res. Dev.*, 2013, **17**, 1192–1208.
- 30 D. R. Snead and T. F. Jamison, *Angew. Chemie - Int. Ed.*, 2015, **54**, 983–987.
- 31 H. Lin, C. Dai, T. F. Jamison and K. F. Jensen, *Angew. Chemie - Int. Ed.*, 2017, **56**, 8870–8873.
- 32 B. Pieber, T. Glasnov and C. O. Kappe, *Chem. - A Eur. J.*, 2015, **21**, 4368–4376.
- 33 R. E. Ziegler, B. K. Desai, J.-A. Jee, B. F. Gupton, T. D. Roper and T. F. Jamison, *Angew. Chemie Int. Ed.*, 2018, **57**, 7181–7185.
- 34 S. L. Lee, T. F. O'Connor, X. Yang, C. N. Cruz, S. Chatterjee, R. D. Madurawe, C. M. V Moore, L. X. Yu and J. Woodcock, *J. Pharm. Innov.*, 2015, **10**, 191–199.

- 35 M. Baumann and I. R. Baxendale, *Beilstein J. Org. Chem.*, 2015, **11**, 1194–1219.
- 36 R. Porta, M. Benaglia and A. Puglisi, *Org. Process Res. Dev.*, 2016, **20**, 2–25.
- 37 J. Britton and C. L. Raston, *Chem. Soc. Rev.*, 2017, **46**, 1250–1271.
- 38 M. G. Russell and T. F. Jamison, *Angew. Chemie*, 2019, **131**, 7760–7763.
- 39 M. Escribà-Gelonch, V. Hessel, M. C. Maier, T. Noël, M. F. Neira d'Angelo and H. Gruber-Woelfler, *Org. Process Res. Dev.*, 2018, **22**, 178–189.
- 40 I. R. Baxendale, L. Brocken and C. J. Mallia, *Green Process. Synth.*, 2013, **2**, 211–230.
- 41 S. Mascia, P. L. Heider, H. Zhang, R. Lakerveld, B. Benyahia, P. I. Barton, R. D. Braatz, C. L. Cooney, J. M. B. Evans, T. F. Jamison, K. F. Jensen, A. S. Myerson and B. L. Trout, *Angew. Chemie Int. Ed.*, 2013, **52**, 12359–12363.
- 42 C. Battilocchio, B. J. Deadman, N. Nikbin, M. O. Kitching, I. R. Baxendale and S. V. Ley, *Chem. - A Eur. J.*, 2013, **19**, 7917–7930.
- 43 A. Adamo, R. L. Beingessner, M. Behnam, J. Chen, T. F. Jamison, K. F. Jensen, J.-C. M. Monbaliu, A. S. Myerson, E. M. Revalor, D. R. Snead, T. Stelzer, N. Weeranoppanant, S. Y. Wong and P. Zhang, *Science (80-.)*, 2016, **352**, 61–67.
- 44 A. D. Clayton, A. M. Schweidtmann, G. Clemens, J. A. Manson, C. J. Taylor, C. G. Niño, T. W. Chamberlain, N. Kapur, A. J. Blacker, A. A. Lapkin and R. A. Bourne, *Chem. Eng. J.*, 2020, **384**, 123340.
- 45 A. D. Clayton, L. A. Power, W. R. Reynolds, C. Ainsworth, D. R. J. Hose, M. F. Jones, T. W. Chamberlain, A. J. Blacker and R. A. Bourne, *J. Flow Chem.*, 2020, **10**, 199–206.
- 46 C. J. Taylor, M. Booth, J. A. Manson, M. J. Willis, G. Clemens, B. A. Taylor, T. W. Chamberlain and R. A. Bourne, *Chem. Eng. J.*, 2021, **413**, 1385–8947.
- 47 A. M. Schweidtmann, A. D. Clayton, N. Holmes, E. Bradford, R. A. Bourne and A. A. Lapkin, *Chem. Eng. J.*, 2018, **352**, 277–282.
- 48 J. P. McMullen, M. T. Stone, S. L. Buchwald and K. F. Jensen, *Angew. Chemie Int. Ed.*, 2010, **49**, 7076–7080.
- 49 A.-C. Bédard, A. Adamo, K. C. Aroh, M. G. Russell, A. A. Bedermann, J. Torosian, B. Yue, K. F. Jensen and T. F. Jamison, *Science (80-.)*, 2018, **361**, 1220–1225.

- 50 B. J. Reizman and K. F. Jensen, *Acc. Chem. Res.*, 2016, **49**, 1786–1796.
- 51 D. E. Fitzpatrick, C. Battilocchio and S. V. Ley, *Org. Process Res. Dev.*, 2016, **20**, 386–394.
- 52 J.-C. M. Monbaliu, T. Stelzer, E. Revalor, N. Weeranoppanant, K. F. Jensen and A. S. Myerson, *Org. Process Res. Dev.*, 2016, **20**, 1347–1353.
- 53 Z. Amara, E. S. Streng, R. A. Skilton, J. Jin, M. W. George and M. Poliakoff, *European J. Org. Chem.*, 2015, **2015**, 6141–6145.
- 54 C. W. Coley, D. A. Thomas, J. A. M. Lummiss, J. N. Jaworski, C. P. Breen, V. Schultz, T. Hart, J. S. Fishman, L. Rogers, H. Gao, R. W. Hicklin, P. P. Plehiers, J. Byington, J. S. Piotti, W. H. Green, A. J. Hart, T. F. Jamison and K. F. Jensen, *Science (80-.)*, 2019, **365**, eaax1566.
- 55 R. A. Skilton, R. A. Bourne, Z. Amara, R. Horvath, J. Jin, M. J. Scully, E. Streng, S. L. Y. Tang, P. A. Summers, J. Wang, E. Pérez, N. Asfaw, G. L. P. Aydos, J. Dupont, G. Comak, M. W. George and M. Poliakoff, *Nat. Chem.*, 2015, **7**, 1–5.
- 56 S. S. Zaleskiy, P. J. Kitson, P. Frei, A. Bubliauskas and L. Cronin, *Nat. Commun.*, 2019, **10**, 5496.
- 57 P. S. Gromski, J. M. Granda and L. Cronin, *Trends Chem.*, 2020, **2**, 4–12.
- 58 W. Hou, A. Bubliauskas, P. J. Kitson, J.-P. Francoia, H. Powell-Davies, J. M. P. Gutierrez, P. Frei, J. S. Manzano and L. Cronin, *ACS Cent. Sci.*, 2021, **7**, 212–218.
- 59 L. Wilbraham, S. H. M. Mehr and L. Cronin, *Acc. Chem. Res.*, 2021, **54**, 253–262.
- 60 D. Angelone, A. J. S. Hammer, S. Rohrbach, S. Krambeck, J. M. Granda, J. Wolf, S. Zaleskiy, G. Chisholm and L. Cronin, *Nat. Chem.*, 2021, **13**, 63–69.

2 Designing a Reactor to Generate and Use Acetylene Gas

2	Designing a Reactor to Generate and Use Acetylene Gas	25
2.1	Introduction	26
2.1.1	Reactive gases in flow – with a resident gas cylinder.....	26
2.1.2	Reactive gases in flow – without a resident gas cylinder.....	29
2.1.3	Solid gas storage matrix - Calcium carbide.....	30
2.2	Project Aims and Objectives	33
2.3	Results and Discussion	34
2.3.1	Calcium carbide.....	34
2.3.2	Creating the acetylene generator.....	34
2.3.3	Quantifying the acetylene generator	39
2.3.4	Application of the acetylene generating module - Cycloadditions.....	42
2.3.5	Application of the acetylene generating module – Lithium acetylide.....	47
2.4	Conclusions and outlook.....	57
2.5	References	59

2.1 Introduction

The incorporation of gases in flow had not been previously explored in the Browne Group for organic transformations. It was postulated that gases could be formed *in situ* from a solid reagent, rather than installing a gas cylinder into the flow system. Gases are excellent reagents for synthesis due to the atom economy and lower cost as reagent. Installation of gases in flow sometimes require specialist equipment with additional safety precautions for handling highly pressurised flow systems or gas cylinders.^{1,2} There are multiple reactor designs that can incorporate gases into flow systems and this work is focussed on designing a reactor that can integrate gas into a flow system from a solid reagent.

2.1.1 Reactive gases in flow – with a resident gas cylinder

Like many flow reactions reagents are introduced via a pump, however, incorporation of a gas phase into flow system must use a gas cylinder. There are two common methods to incorporate gas into a flow system.

Tube-in-tube reactors

Teflon AF2400 tubing is a semi-permeable tubing that allows the diffusion of the gaseous phase and not the liquid phase (Figure 7).

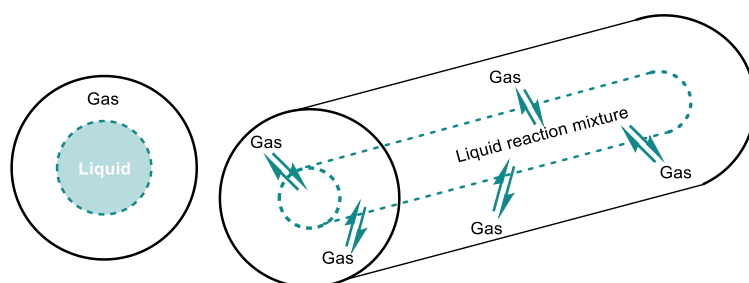
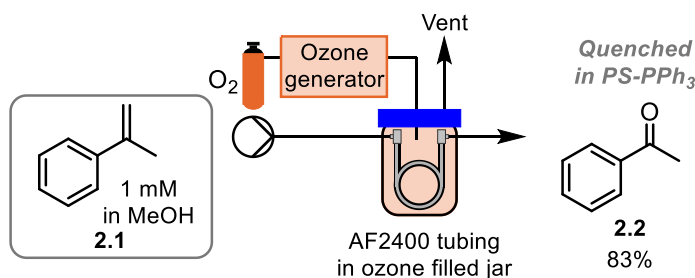


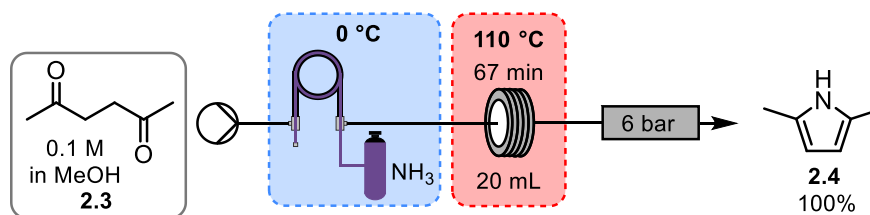
Figure 7 – Cross-section of tube-in-tube reactor (left); illustration of semi-permeable tube inside non-permeable tube (right)

This design of reactor requires a resident gas cylinder to create an atmosphere of gas to surround the semi-permeable tubing. The reaction mixture, normally in organic solvent, can be passed through the AF2400 tubing which is exposed to the surrounding gas. The system can also be switched to have solvent in the outer tube and gas in the inner tube. However, the AF2400 tubing can be expensive, and the installation of a gas cylinder requires higher safety precautions. These limitations have not reduced the area research incorporating gas into organic flow systems. In 2010, Steven V. Ley and co-workers explored the use of the semi-permeable tubing (Scheme 8).³



Scheme 8 – Ozonolysis reaction using a semi-permeable tubing to form acetophenone

Ley's design involved using an ozone generator with a feed stock of oxygen gas. The ozone was pumped into a jar that contained the AF2400 tubing. They successfully synthesized acetophenone, **2.2**, via ozonolysis of α -methyl styrene **2.1** with an hour residence time and a yield of 83%. The reaction was quenched with polymer supported PPh₃ to remove any generated peroxide species for safety reasons. The use of tube-in-tube reactors were heavily explored and utilised gas reagents safely in flow.¹ The Ley group further demonstrated using various gases such as NH₃ for pyrrole synthesis in flow. In this example, the gaseous ammonia was pumped through the central AF2400 tubing and the liquid reagents pump around the outer tubing (Scheme 9).⁴



Scheme 9 – Paal-Knorr pyrrole synthesis using tube-in-tube reactor

Hexan-2,5-dione **2.3** was subjected to 3.5 bar of ammonia gas via a semi-permeable membrane which was subjected to rigorous heating and thus afforded the 2,5-dimethyl pyrrole **2.4**, quantitatively. This is an innovative example illustrating the modular nature of flow chemistry whereby a further reaction coil was required to drive the reaction to completion. This is easily installed after the incorporation of ammonia gas. Both examples presented above have created a homogenised system whereby the incorporated gas is dissolved in the organic solvent. The other common methodology to integrate gaseous reagents into flow is to create a biphasic liquid-gas mixture.

Segmented flow reactors

In segmented flow, alternative phases of gas and liquid are present in the flow tube. Segmented flow can exhibit higher mass transfer between the phases due to vortices created. These toroidal currents in the gas phase allow for efficient mixing and incorporation of gaseous reagent into the reaction liquid media (Figure 8).⁵

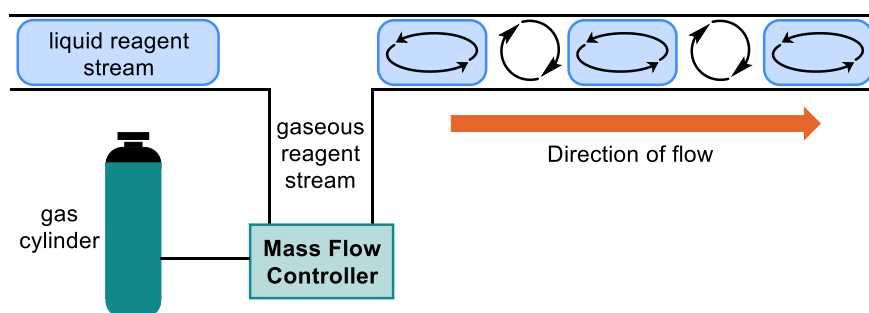
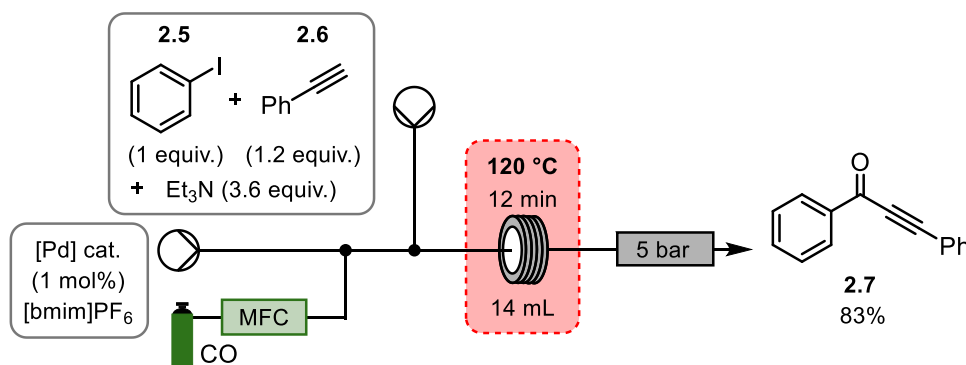


Figure 8 – Segmented flow showing biphasic gas-liquid mixture and internal vortices created

When creating a flow system with a gaseous phase, a Mass Flow Controller (MFC) needs to be used to control the rate of gas addition into the flow system. This allows a (gas) flow rate to be set which can match the liquid flow rate and create the biphasic alternating gas-liquid mixture. The MFC assists in controlling the stoichiometry of the gaseous reagent, however, the MFC can be costly and still requires the presence of gas cylinder as feed stock. Therefore, additional safety precautions will still be required for segmented flow, much the same as tube-in-tube reactors.

Segmented flow has been widely explored to develop a range of organic transformations by installing a gas cylinder, with pressure control, to incorporate various gases into a contained flow system.^{6–8} In 2006, Ryu and co-workers developed a useful carbonylation reaction showing how a MFC can incorporate carbon monoxide gas into a flow system creating segmented flow (Scheme 10).



Scheme 10 – Pd-catalysed carbonylation reaction using a multiphase microflow system

The coupling reaction of iodobenzene **2.5** and phenyl acetylene **2.6** took place at 120 °C in 12 minutes to give the desired compound **2.7** in 83% yield. The palladium in this reaction is dissolved in an ionic liquid to solvate and homogenise the catalyst for the reaction. This example demonstrates how a resident gas cylinder can be controlled to deliver gas into an organic transformation continuously.

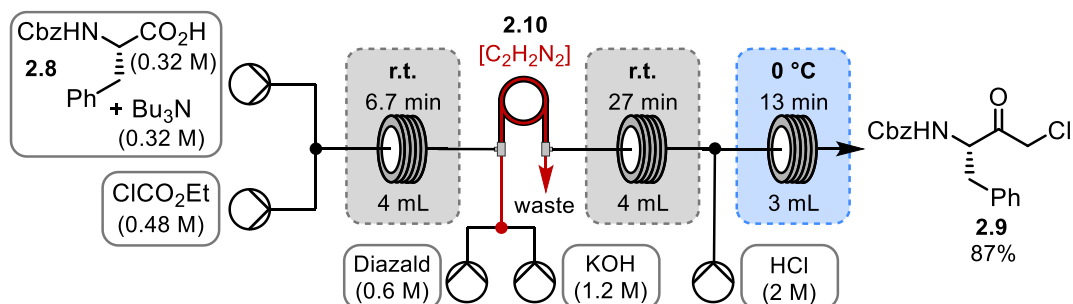
The limitations of both (the tube-in-tube reactor and segmented flow reactor) flow systems are the additional safety precautions required to handle dangerous gas cylinders in the lab.

2.1.2 Reactive gases in flow – without a resident gas cylinder

Reducing the safety risks and need for specialist pressure equipment required when handling gas cylinders in the lab has been a developing area of research. Gases can be liberated from liquid/solid reagents and incorporated into flow systems for organic transformations.

In situ generation of gas from liquids

In this style of system, two reactive liquid reagents are mixed to generate a gas *in situ* which is consumed in the reaction. Tube-in-tube reactors can be used to generate the reactive gas which can permeate through the tubing and be consumed by the reaction.⁹ This is an example of unmasking a reactive intermediate *in situ* which avoids the handling of dangerous reagents and contains the reactivity within the flow reactor. In 2014, Kappe and co-workers explored the generation of diazomethane *in situ* using a tube-in-tube reactor (Scheme 11).¹⁰



Scheme 11 – Synthesis of enantiopure α -chloro ketones using *in situ* generated diazomethane

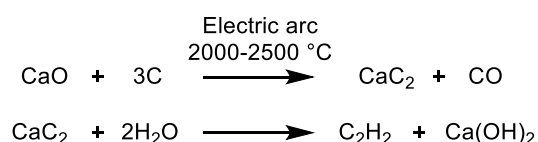
In this example, a dangerous reactive gas, diazomethane **2.10**, was liberated *in situ* from relatively more stable liquid reagents, Diazald and aqueous KOH. This unmasked reactive intermediate passed through the semi-permeable membrane, as a gas, and was incorporated into the reaction stream containing the starting material **2.8** and the reaction components. After a 27 min reaction and in-line acid quench, 87% of enantiopure α -chloro ketone **2.9** was synthesised. Generating a reactive gas without the use of a gas cylinder avoids the dangerous handling of compressed gas in the lab. The liquid reagents are easily handled and safe to use with additional precautions. Tube-in-tube technology has allowed the generation and consumption of diazomethane to occur in a seal contained system which greatly minimises the exposure of dangerous diazomethane to the lab user through clever reactor design.

Solid reagents can also circumvent the need for a gas cylinder. These solid reagents act as a gas storage matrix that can be activated, via solvent, thus liberating the gas from the solid reagent.

2.1.3 Solid gas storage matrix - calcium carbide

Acetylene gas is an excellent reagent which can deliver an alkyne unit to an organic substrate in a highly economical manner and has many uses in organic synthesis.¹¹ Acetylene gas is highly flammable and explosive which requires many additional safety precautions to have a gas cylinder in the lab. Organic transformations in batch glassware with acetylene gas also has limitations due to the nature of the gas collecting in the headspace of the sealed flask requiring long reaction times for passive diffusion to occur into the reaction mixture.¹²

An alternative to a resident acetylene gas cylinder is an inert solid reagent, calcium carbide. Calcium carbide, in 1862 by Wöhler, was found to produce acetylene gas on addition of water. In 1892, Thomas Willson attempted the synthesis of metal calcium in an electric arc furnace, but unfortunately for Mr. Willson, pure crystalline calcium carbide (CaC_2) was synthesised through this method.¹³ Willson's method was later patented in the US due to its commercial viability and its utility as a safe source of stored acetylene gas. Calcium carbide is made by reacting calcium oxide with carbon to form calcium carbide and carbon monoxide. Calcium carbide reacts instantaneously with excess water to produce acetylene gas and calcium hydroxide (Scheme 12).

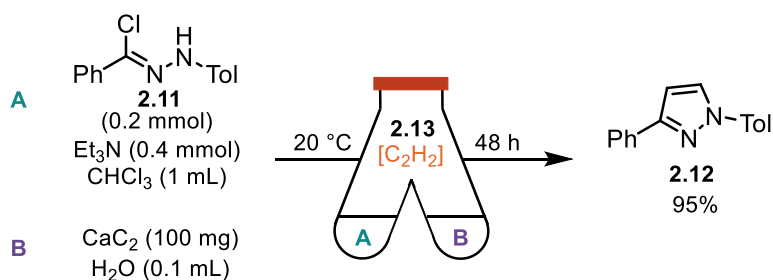


Scheme 12 – Calcium carbide formation (top); Hydrolysis of calcium carbide to acetylene (bottom)

Calcium carbide found many uses throughout history; it played a role in the mining industry as carbide lamp fuel. The bottom cavity of the lamp held rocks of calcium carbide and a reservoir of water above would slowly drip onto the rocks liberating acetylene gas through a tube that could be ignited for underground lighting.¹⁴

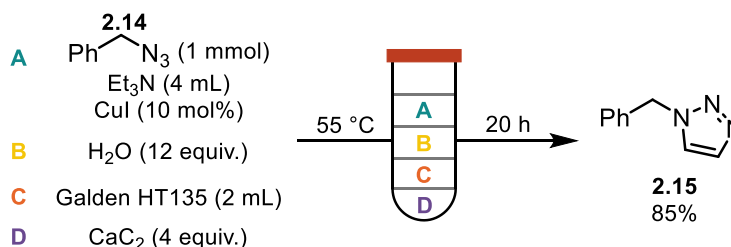
***In situ* generation of acetylene gas from calcium carbide for synthesis**

Calcium carbide has experienced a recent renaissance and has been explored as a reagent for chemical synthesis over the past 10 years.¹⁵⁻²¹ The Ananikov group has utilised calcium carbide as an acetylene generator in batch, where acetylene was used to synthesise pyrazoles via 1,3-dipolar cycloadditions with nitrile imines, generated *in situ* (from 2.11) (Scheme 13).



Scheme 13 – 1,3-dipolar cycloaddition of nitrile imines with acetylene to form pyrazoles

Specialist glassware was required to create an acetylene **2.13** atmosphere via calcium carbide. In one chamber (reaction mixture A, Scheme 13), a solution of chloro imine **2.11** and triethylamine were dissolved in chloroform. In the other chamber (reaction mixture B, Scheme 13), a mixture of water and calcium carbide were mixed. The vessel was sealed, and the acetylene gas (**2.13**) generated filled the headspace of the flask and passively dissolved and reacted with the *in situ* generated nitrile imine to form the desired pyrazole **2.12** in a 95% yield. Due to the presence of the water sensitive nitrile imines, the water required to liberate the acetylene gas (**2.13**) could not be mixed with the organic solvent. Therefore, a 2-chamber flask was required for the transformation which in turn meant that long reaction times were needed for the passive diffusion of acetylene gas to be effectively incorporated into the organic solvent chamber.¹² To deliver acetylene from calcium carbide in organic reactions can be challenging due the undesirable mixing of aqueous and organic solvents and the insolubility of CaC₂ itself. Water is required to liberate acetylene and, although specialise glassware has been shown to work (Scheme 13), others have used a specialist fluoruous solvent to separate the aqueous and organic solvents. Matsubara and co-workers targeted the azide click reaction with acetylene, which used a single glass vessel that had CaC₂ on the bottom layer, then fluoruous solvent (Galden HT135), then a layer of water topped with a layer of organic solvent containing the reagents and substrates (Scheme 14).²²



Scheme 14 – A quadriphasic system to incorporate acetylene gas into an azide click reaction

The quadriphasic solvent system used Galden HT135 fluoruous solvent to separate the water from the calcium carbide initially. After stirring the reaction, the water would pass down through the fluoruous solvent layer and liberate acetylene gas which would slowly

bubble through the top reaction mixture layer and undergo a (3+2)-cycloaddition in the presence of a copper catalyst. This elaborate solvent system allowed the controlled release of acetylene gas into the reaction and after the reaction with benzyl azide **2.14** was complete, two solvent layers (Et₃N and Galden HT135) were left which contained target triazole **2.15** in 85% yield.

Both these papers aim to create systems that safely release acetylene gas *in situ* from calcium carbide, however, they are limited by requiring specialised glassware or a complex, bespoke mixture of solvents to prevent a violent reaction between water and calcium carbide. Additionally, these systems require long reaction times due to creating an acetylene atmosphere in the headspace of the glassware and are therefore restricted by the passive diffusion of acetylene gas into the desired solvent system.

Calcium carbide as a reagent for organic synthesis in batch has been explored and mostly requires special conditions to handle the release of gas or solubility of calcium carbide. Throughout literature, unfavourable conditions such as: use of undesirable solvents such as deep eutectic solvents or hazardous dipolar aprotic solvents like DMSO and DMF; fluoride additives; and long reaction times under harsh conditions are required to unlock the reactivity in this reagent. This is due to calcium carbide's insoluble robust nature and propensity to reactive violently with water releasing acetylene gas in an uncontrolled manner.^{16,19,21,23–33} This posed the question whether a flow reactor design could harness the reactivity of this useful cheap reagent.

2.2 Project Aims and Objectives

The use of calcium carbide as a reagent in flow has not yet been explored which underpins the aim of this project. It was postulated whether calcium carbide could be used as a solid gas-storage matrix that could be activated, via water in flow, to liberate acetylene gas *in situ*. To avoid undesirable long reaction times, flow chemistry has no headspace in the tubing and can therefore create a homogenised reaction mixture of gas and liquid reagents which would increase/improve mass transfer. Using solid calcium carbide, as the acetylene source, would circumvent the use of a resident gas cylinder in the lab and avoid unnecessary additional safety precautions regarding pressurised flammable gases. Flow chemistry is becoming more ubiquitous in organic chemistry labs and therefore more readily accessible than specialised glassware and equipment commonly required. Handling a solid reagent is also more favourable for the lab user than working with gas, thus providing a reduced labour-intensive process to incorporate acetylene gas into a reaction. It was envisaged that calcium carbide could be loaded into a flow cartridge and activated via a water miscible organic solvent thus liberating acetylene gas *in situ* which could be consumed by various reaction conditions (Figure 9).

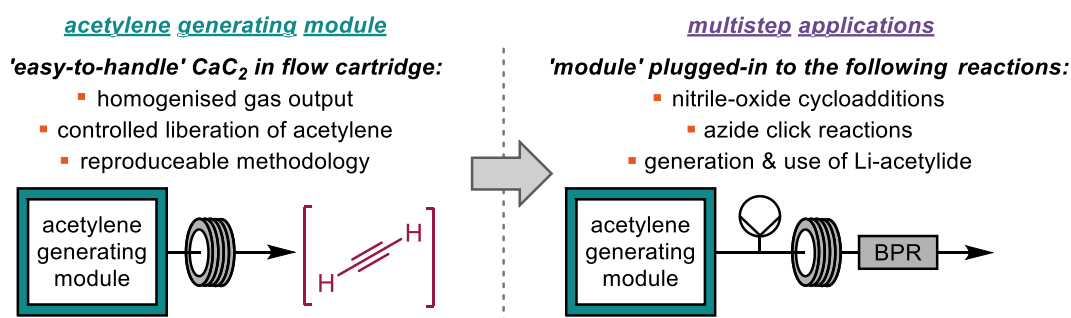


Figure 9 – Envisaged plan to create an acetylene generating module which is plugged into various reactions

Once the acetylene generating module has been established following the criteria (Figure 9), the module could be plugged into various reaction conditions in flow exhibiting a telescoped process. This would demonstrate the successful incorporation of acetylene gas from calcium carbide in a safe contained manner without the need of a resident gas cylinder. This transformation follows the theme on how flow reactor design facilitates organic chemistry that would otherwise not function via standard synthetic methods.

2.3 Results and Discussion

2.3.1 Calcium carbide

Calcium carbide arrived in the lab as large grey chunks which, for an organic flow chemist, was unusable. It was imperative to create/employ a reagent that could be translated to a flow system reliably and safely. As a warning, acetylene gas is extremely flammable and great amounts of care must be taken when working with flammable gases.

2.3.2 Creating the acetylene generator

It was found that on addition of water to the calcium carbide a strong fizz was observed which was assumed to be acetylene gas. Firstly, the CaC_2 in its rock form was placed in an adjustable flow column, any large rocks that did not fit in the column were broken down into smaller pieces (Figure 10).

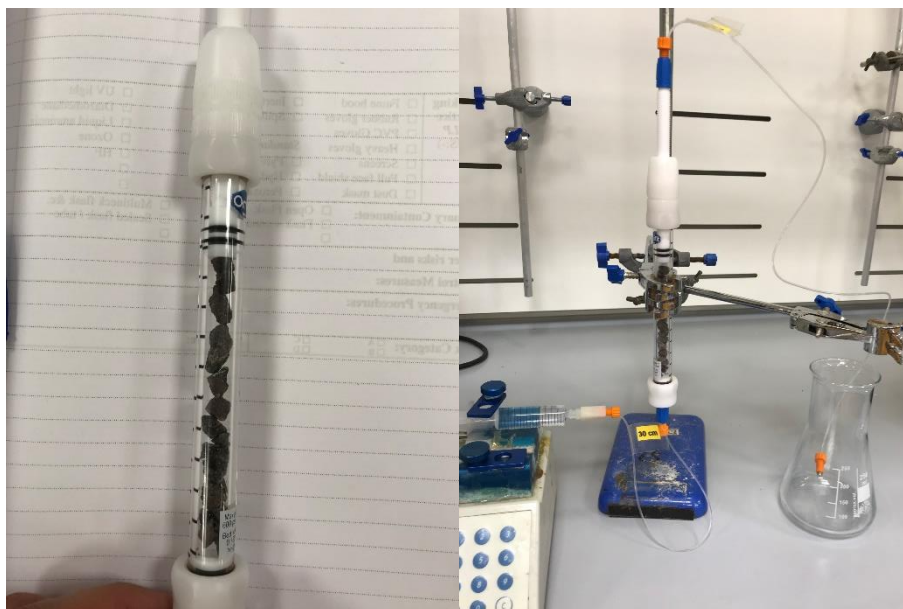
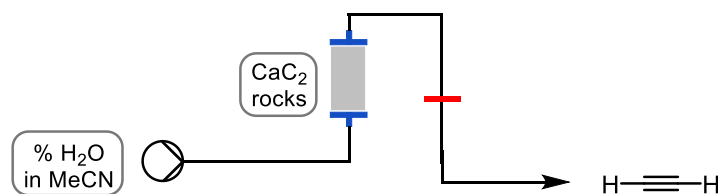


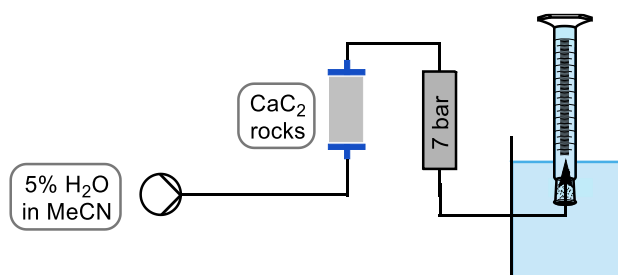
Figure 10 - CaC_2 in rock form stacked in column (left); First flow system to generate acetylene (right)

This was the first attempt to make and harness acetylene gas in a continuous flow. It was found that neat water reacted too violently with the calcium carbide and therefore a percentage of water in miscible acetonitrile was tested to see how much gas was produced. This was a qualitative experiment because the outcome was determined by counting bubbles passing the red line to gauge the appropriate percentage of water needed in the organic solvent (Scheme 15).



Scheme 15 - Initial flow system to generate acetylene from CaC_2

It was found that neat MeCN produced no acetylene; 2% H_2O in MeCN produced 13 sporadic long bubbles across the red line; and 5% H_2O produced >250 bubbles over a 5-minute period. This basic experiment was to find the minimum amount of water required to effectively liberate acetylene gas in a controlled manner over a period of time. It was also important to create a system that released enough acetylene gas to react but not too quickly that the reaction window be too short for an organic transformation to take place. 5% H_2O in MeCN was therefore chosen as the activation solvent that liberates acetylene gas from calcium carbide effectively. It was noted that the bubble formation was non-uniform and produced large slugs of acetylene bubbles in the tubing which caused the flow rate to fluctuate dramatically. The use of a back-pressure regulator would increase the pressure within the tubing thus solvating the gas to create a homogenised mixture of solvent and acetylene gas (Scheme 16).



Scheme 16 - Acetylene generating flow system with BPR addition with gas trap

No outgassing was observed when using the BPR which meant that the flow rate was stable and unfluctuating. A crude water gas trap was used to collect the acetylene gas at the outlet of the flow system, which was simply a water-filled inverted measuring cylinder submerged in a tub of water. This used displacement to quantify the amount of acetylene generated from the calcium carbide. Using the molar volume of a gas equation, the number of moles of acetylene could be calculated due to the known volume of gas collected in the gas trap. The number of moles were converted to a concentration and after various repeats the calculated concentration fluctuated dramatically from 0.083 M to 0.214 M. These inconsistent results were attributed to the various sizes of calcium carbide rocks used, which were of different sizes and shapes and therefore different surface areas. This meant that those rocks with a larger surface area would liberate more acetylene gas. It was noted that the rocks would turn grey/white due to the formation of

an outer layer of Ca(OH)_2 which would in turn conceal the reactive surface. This whitish/grey appearance would occur rather quickly when the calcium carbide was exposed to air due to its reactivity with natural humidity. Three objectives were identified to find a repeatable reliable source of CaC_2 that would solve the inconsistencies mentioned above:

- 1) Uniform particle size of reactive CaC_2 that utilises the whole reagent and avoids clogging of reactive surface.
- 2) A reproduceable process that is operationally simple.
- 3) Relatively stable in air and easy to handle in a lab environment.

The solution was likened to that of a sodium hydride suspension where a reactive reagent is finely coated in oil and thus stable to air. The suspension oil can then be washed off thus exposing the reactive reagent at the desired time. The choice of oil was initially explored by mixing CaC_2 and the different oil sources in a mortar and pestle and observing whether the oil source would dissolve in a desirable organic solvent (Table 1).

Table 1 - Exploring different sources of oil and its dissolution with organic solvent

Entry	CaC_2 (g)	Oil (2 mL)	Observation
1	0.5	tea light wax	no dissolution in MeCN
2	0.5	'oil bath' oil	no dissolution in MeCN
3	0.5	paraffin oil	no dissolution in MeCN; separated from CaC_2
4	0.5	paraffin oil	dissolved in THF

Paraffin oil coated the calcium carbide effectively and with the addition of THF the oil dissolved thus being washed away, which pleasingly is also miscible with water and therefore compatible with the acetylene generator (entry 4, Table 1). Milling via a mortar and pestle is not completely reproduceable to the same degree every time and varies depending on the lab user. Using an electric mixer mill with stainless steel jars and a ball bearing represented a better, more consistent alternative. This allowed parameters to be set and therefore repeated reliably. The ratio of paraffin oil to CaC_2 was explored including different mixer mill conditions (Table 2).

Table 2 – Ratio of paraffin oil to CaC₂ plus milling parameters

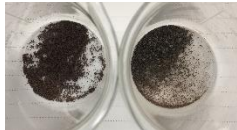
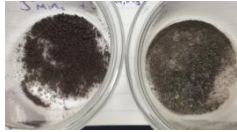
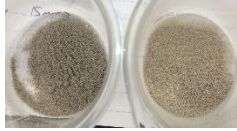
Entry	CaC ₂ (g)	Paraffin oil (mL)	Time (min)	Frequency (Hz)	Observation
1	0.5	0.1	5	5	no change to CaC ₂
2	0.5	0.1	5	10	no change to CaC ₂
3	0.5	0.1	5	15	fine dark powder
4	0.5	0.2	5	15	wet paste
5	0.52	0.15	5	15	wet paste
6	0.51	0.05	5	15	no change to CaC ₂
7	0.51	0.05	10	15	no change to CaC ₂

25 mL stainless steel milling jar, 8 g stainless steel ball

The milling frequency was initially tested, a low frequency was first explored to minimise the aeration of the calcium carbide and in turn minimise the deactivation. However, at a low milling frequency the calcium carbide rocks were intact (entries 1 and 2, Table 2). At 15 Hz, a fine free-flowing powder was found that could be easily handled (entry 3, Table 2). Increasing the amount of paraffin oil was deemed beneficial to increase the preservation of CaC₂, this gave a very wet paste material which was undesirable and, therefore, could not be easily funnelled into a flow column (entries 4 and 5, Table 2). To test that the optimum conditions had been found, lower amounts of paraffin oil were added, with increased milling time, and resulted in the CaC₂ rocks remaining intact (entries 6 and 7, Table 2). These experiments had completed 2 out of 3 of the desired criteria. A reproduceable process that delivered a uniform particle size of calcium carbide had been found. These objectives had been greatly facilitated by the use of the ball mill to create a uniform particle size in a reproduceable manner.

The preservation of reactivity needed to be tested to fulfil all three criteria. A qualitative experiment was set up where 0.5 g CaC₂ was ground in a mortar and pestle with no paraffin oil and 0.5 g CaC₂ was milled with paraffin oil in the mixer mill (entry 3, Table 2 conditions). Both powders were placed in beakers and left exposed to air and observations were taken (Table 3).

Table 3 - Reactivity of CaC_2 suspension

Entry	Time after Milling (h)	CaC_2 Milled suspension	Mortar and Pestle – no oil	Evidence
1	0	Remained dark purple	Loss of colour	
2	1	Remained dark purple	Grey/white	
3	24	Grey – addition of water caused aggressive fizzing	White – addition of water caused no fizzing	
4	168	White – addition of water caused no fizzing	n/a	n/a

Immediately after milling, it was apparent that the CaC_2 ground in the mortar and pestle had lost some colour due to the increased surface area of the smaller particles reacting with moisture in the air without any oil protecting that surface (entry 1, Table 3). After 1 hour, the CaC_2 milled suspension remained the same colour as it did when it came out the milling jar, and the mortar and pestle sample displayed significant discolouration, turning grey/white (entry 2, Table 3). The grey/white complexion was assumed to be Ca(OH)_2 as this is the known by-product of water and CaC_2 . After 24 hours, both samples had turned grey (the suspension was darker) and upon the addition of water, the CaC_2 suspension fizzed aggressively and therefore was deemed very reactive. The mortar and pestle sample caused no fizzing upon the addition of water and was therefore deemed unreactive after 24 hours (entry 3, Table 3). The CaC_2 suspension sample was left for a week to see the extent of its reactivity, unfortunately, upon the addition of water no fizzing was observed (entry 4, Table 3). The pH of the water/milled suspension sample was 10-11 which indicates the presence of a base thus implying Ca(OH)_2 formation. With these results in hand, all three criteria had been met where a reproducible uniform particle size of calcium carbide was formed that remains reactive on exposure to air for a maximum of 24 hours as an easy-to-handle free flowing powder.

To translate this into a flow system, enough CaC_2 suspension must be made to fill a flow column and therefore a mechanochemical scale up had to be explored (Table 4).

Table 4 – Scale up experiments

Entry	CaC ₂ (g)	Paraffin oil (mL)	Time (min)	Frequency (Hz)	Observation
1	1.0	0.2	5	5	no change to CaC ₂
2	1.0	0.2	10	15	no change to CaC ₂
3	1.0	0.2	15	25	fine dark powder
4	3.0	0.6	15	25	no change to CaC ₂
5	3.0	0.6	15	30	no change to CaC ₂
6	3.0	0.6	20	30	no change to CaC ₂
7	3.0	0.6	30	30	fine dark powder

25 mL stainless steel milling jar, 8 g stainless steel ball

Initially, 1 g of CaC₂ was used with 0.2 mL of paraffin oil (keeping the same calcium carbide to oil ratio) was tested at various frequencies and times and found that increasing frequency to 25 Hz for 15 minutes gave the distinctive fine dark powder required (entries 1 to 3, Table 4). To fill a flow column, 3 g of CaC₂ with the addition of 0.6 mL of paraffin oil would be sufficient. It was found that 30 minutes at 30 Hz in the mixer mill produced a fine dark powder suspension (entries 4 to 7, Table 4).

Development of this calcium carbide reagent into a suspension utilised qualitative experiments of observation to create a free-flowing powder that can be transferred into a packed bed reactor to generate acetylene gas in a flow system. Its form and reactivity to water was known, however, quantifying the moles of acetylene gas released from this reagent was still unknown. It was important to find the concentration of acetylene gas in the flow system to design experiments with the correct stoichiometry.

2.3.3 Quantifying the acetylene generator

Initially, it was postulated that use of a water gas trap to titrate the CaC₂ could be used find out the amount of acetylene gas released from the calcium carbide reagent. Calcium carbide was bought from Fisher Scientific (general purpose grade) which contained 72-82% calcium carbide and 12-18% calcium oxide³⁴. The titration method was therefore tested and compared to the reagent composition specifications (Figure 11).

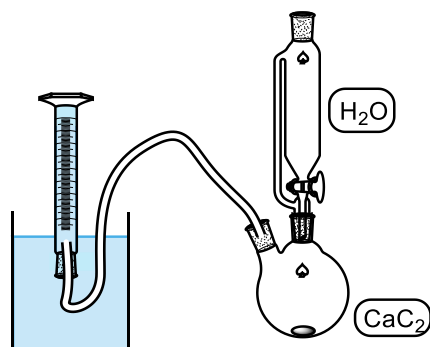
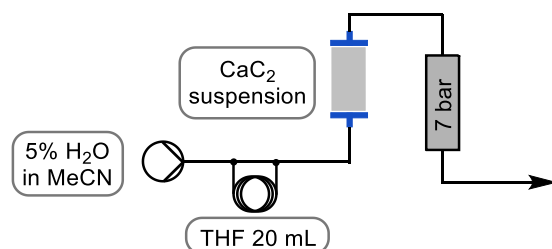


Figure 11 - Acetylene titration method with water gas trap

Using the ideal gas law and the volume of acetylene gas collected in the water trap, it was calculated that 3.02 mmol of CaC_2 produced 2.25 mmol of acetylene gas on addition of water. This confirms the purity of the reagent to be 75% CaC_2 and the rest insoluble impurities. This crude method of acetylene gas collection was taken forward to attempt to calculate the concentration of acetylene gas in a devised flow system.

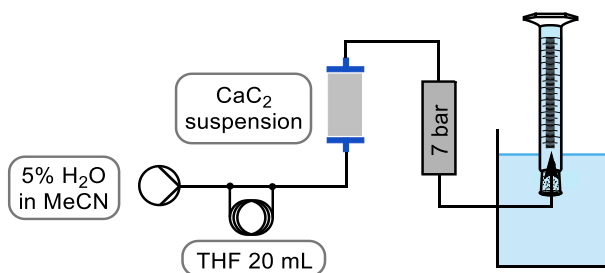
During these experiments, it was noted that the paraffin oil was being pushed out of the column by the MeCN. As with a NaH suspension, the incorporation of a solvent wash was created to remove the paraffin oil and uncover the reactive milled CaC_2 pre-loaded in the flow column (Scheme 17).



Scheme 17 - Installation of THF solvent wash

This methodology pumped dry THF over the milled CaC_2 suspension which dissolved the paraffin oil and removed it from the system to avoid the oil interfering downstream. The solvent wash was then followed by the activating water in MeCN from the now uncovered CaC_2 to produce acetylene gas *in situ*.

The concentration of acetylene liberated *in situ* was calculated by collecting the evolved gas from the outlet in a water gas trap (Scheme 18).



Scheme 18 – Acetylene gas collection method

The volume of acetylene gas was recorded every 10 minutes and using the ideal gas equation the number of moles of acetylene gas per 10 minutes were calculated. Knowing the flow rate of the system (0.2 mL/min), a concentration per 10 minutes was plotted on a concentration over time graph (Figure 12).

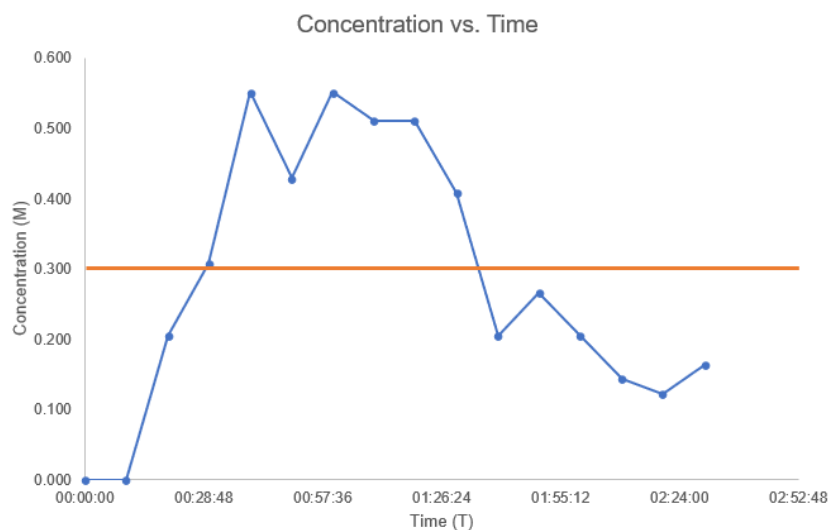


Figure 12 – Concentration over time graph

This data gave an insight into the amount of acetylene gas being evolved from the generator. The orange line indicates that the concentration of acetylene is >0.3 M for 1 hour. This threshold was chosen to keep the concentration of the reaction as high as possible to gain productivity in the flow system. It would be possible to lower the threshold and gain a longer reaction window if necessary. This allowed the stoichiometry of a chemical reaction with acetylene to be planned.

It was observed that the CaC_2 column would visually show the progress of acetylene generation via a colour change (Figure 13).

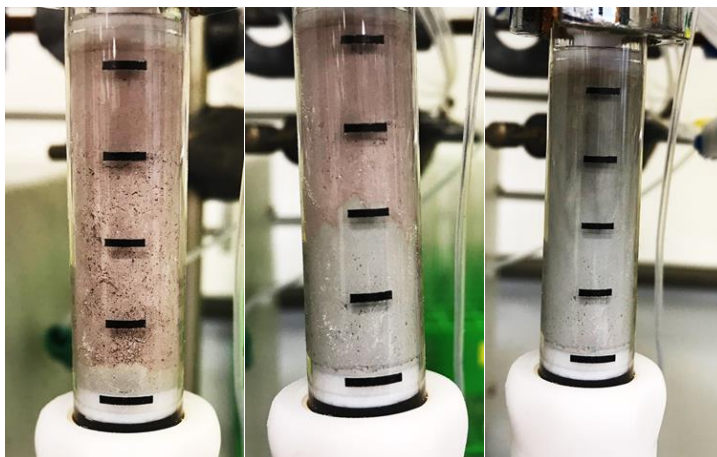
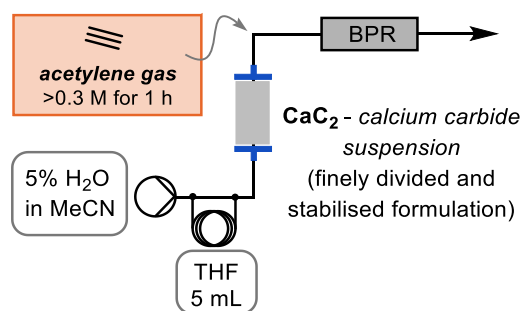


Figure 13 – Visual depletion of CaC_2 column (left to right)

This was a qualitative indication that the CaC_2 suspension (dark purple) was releasing acetylene gas into the flow system and leaving a $\text{Ca(OH)}_2/\text{CaO}$ residue in the column (grey colour).

In summary, an acetylene generating module had been created using a reproducible methodology (Scheme 19).



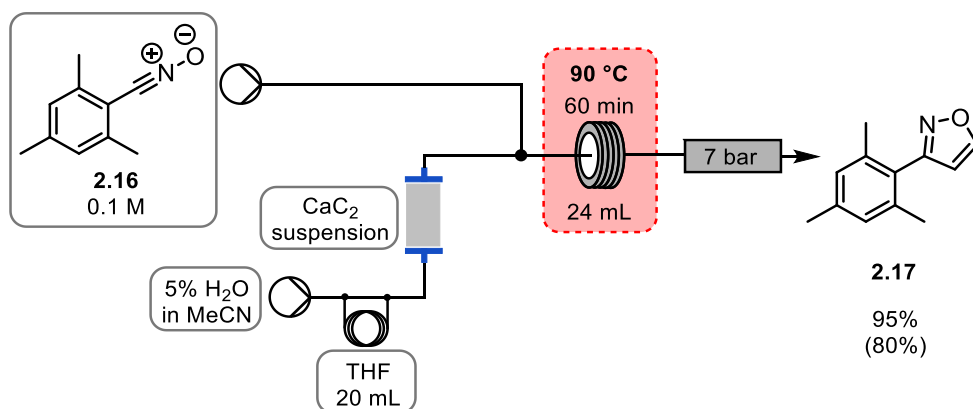
Scheme 19 - Acetylene generating module

The new CaC_2 suspension had a uniform particle size, due to the electronic milling process, and its heightened reactivity to water was masked, by paraffin oil, in an easy-to-handle free-flowing powder. After measuring the amount of acetylene given off, a reactive window was established that produced a concentration of acetylene >0.3 M over a period of 1 hour *in situ*. The addition of a THF loading loop was installed to wash off the paraffin oil from the CaC_2 suspension before it was activated by water.

2.3.4 Application of the acetylene generating module - Cycloadditions

Isoxazole synthesis

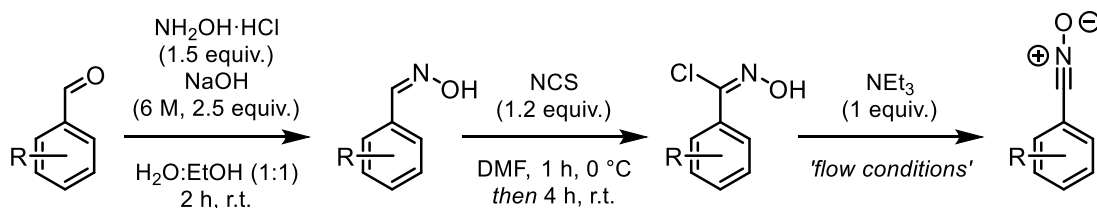
The plug-and-play modular nature of flow chemistry allowed the acetylene generator to be trialed in a 1,3-dipolar cycloaddition reaction. Bench-stable mesityl nitrile oxide **2.16** was introduced downstream to the homogenised acetylene gas in MeCN and heated in a reactor coil over an hour (Scheme 20).



Scheme 20 – Proof of concept – 1,3-dipolar cycloaddition (Flow system 2.1)

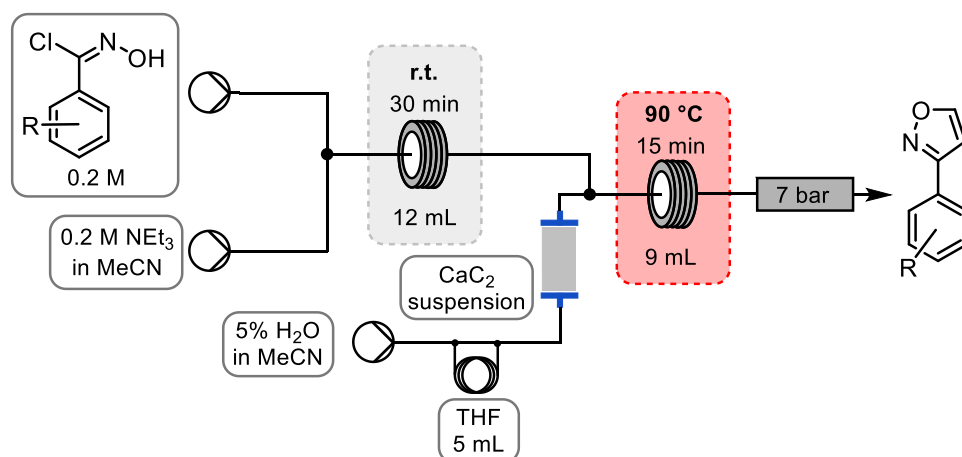
Pleasingly, the cycloaddition worked successfully giving a 95% ^1H NMR yield (80% isolated) of isoxazole **2.17**. This was the first organic reaction demonstrating the acetylene generator in flow, in which the reactive intermediates could be heated and pressurised safely for an hour at 90 °C to drive the reaction to completion. This proof-of-concept example used a nitrile oxide with increased stability due to the mesityl methyl groups inhibiting self-condensation reactions. It was postulated whether the nitrile oxides could be formed *in situ* as a reactive intermediate and consumed by the available acetylene, affording an isoxazole product.

A visiting Master's student, Imke Reuther, explored the further optimisation and expansion of the isoxazole scope. I worked and supervised with Imke and designed all experiments that she did. The flow systems constructure was designed and built by me, allowing Imke to run the experiment. The reaction (in Scheme 20) was optimised and worked successfully at 90 °C for 15 min to give a 97% isolated yield of isoxazole **2.17**. Nitrile oxides are formed via chloro-oximes in the presence of NEt_3 (Scheme 21).³⁵



Scheme 21 – Synthesis of nitrile oxides from aldehyde starting materials

The chloro-oximes were synthesized from purified aldehydes into the corresponding oximes via an imine condensation reaction. The oxime was then chlorinated using NCS, to yield the chloro-oxime. Various chloro-oximes were synthesised and subjected to flow conditions, in the presence of NEt_3 , to afford the reactive nitrile oxide *in situ*. It was planned that the nitrile oxide would be unmasked *in situ* and exposed to the acetylene gas thus quenching the reactivity via a cycloaddition (Scheme 22).



Scheme 22 – Unmasking of nitrile oxide in flow to form isoxazole via cycloaddition with acetylene

The pre-formed chloro-oximes were reacted with NEt_3 for 30 min at room temperature to form the reactive nitrile oxide *in situ*. The acetylene generator was simultaneously run to provide a homogenised acetylene concentration *in situ* whereby it could undergo a 1,3-dipolar cycloaddition at 90 °C for 15 min. The isoxazole scope was then surveyed under the optimised reaction conditions (Figure 14).

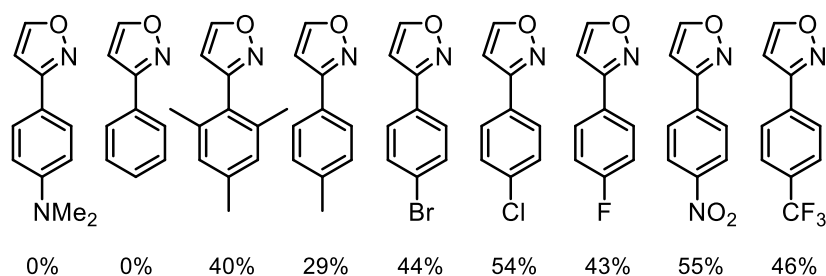


Figure 14 - Isoxazole scope (results provided by Imke Reuther)

A range of chloro-oximes were tested with various electron-donating/withdrawing groups. The yields were modestly ranging from 29% to 55% and it was later found that multiple products were formed during the telescoped flow process. Electron rich substrates reduced the reactivity of the nitrile oxide by donating electrons into the conjugated system and this is reflected in the yields (Figure 14). As previously mentioned, multiple reactions were competing in this transformation and were characterised by mass spectroscopy and ^1H NMR spectroscopy (Figure 15).

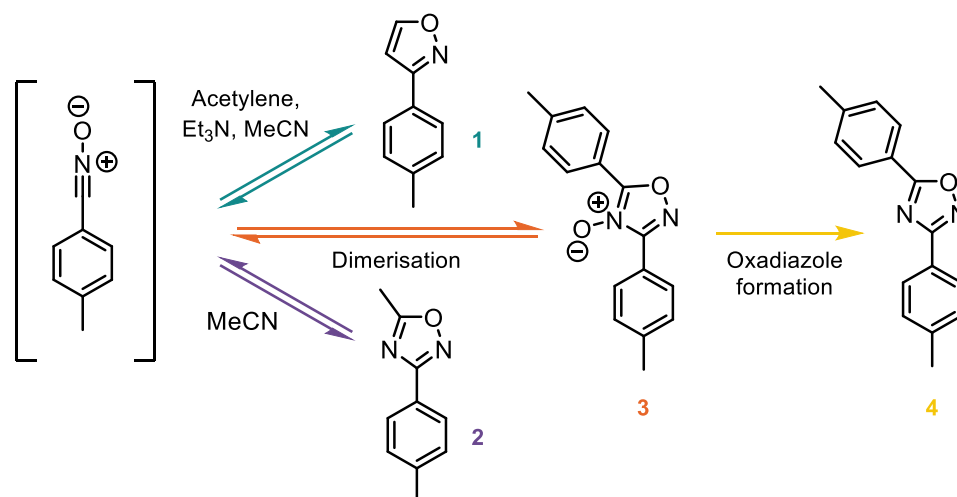


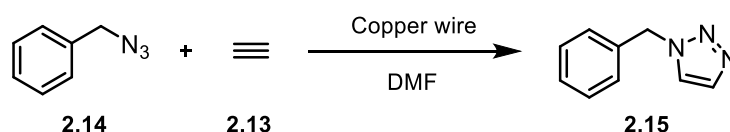
Figure 15 – Different reaction pathways for the nitrile oxide

In the presence of MeCN as solvent, the nitrile oxide could undergo a cycloaddition to give 5-methyl oxadiazole (compound 2, Figure 15). The nitrile oxide can also self-dimerise to give an oxadiazole oxide (compound 3, Figure 15). This can then be irreversibly reacted with another equivalent of nitrile oxide to form the oxadiazole (compound 4, Figure 15).^{36,37} To decrease the dimerization reaction, a reduction in the concentration of nitrile oxide should lower the probability of self-dimerisation due to increasing the excess of reactive acetylene in the reaction. Changing reaction solvent would also removing the formation of the 5-methyl oxadiazole (compound 2, Figure 15), however, this may cause issues with solvent compatibility with respect to the acetylene generating module.

In summary, the acetylene generator was used successfully to incorporate alkyne functionality and synthesise various isoxazoles in a telescoped flow system. The theme of unmasking reactive intermediates *in situ* was further developed by taking chloro-oximes and forming very reactive nitrile oxides *in situ* and quenching this reactivity with another *in situ* generated reactive intermediate, acetylene gas. Due to the adaptability of these flow systems, the reactor design could be readily changed and altered to accommodate problems arising from handling difficult reactive intermediates. The presence of undesirable side-products did not dampen the success of this system because it proved that the reactor design facilitated two reactive intermediates being formed *in situ* and reacting with each other. Furthermore, it demonstrated that the acetylene generator, from calcium carbide, was a viable source of homogenised acetylene gas for organic transformations in flow.

Triazole synthesis – Click chemistry

After exploring the use of the acetylene generating module for cycloadditions with nitrile oxides, the well-established click reaction was tested. It was envisaged that in the presence of metallic copper, benzyl azide **2.14** could react with *in situ* generated acetylene gas **2.13** to form terminal triazoles **2.15** (Scheme 23). Using a copper coil (purpose built) in flow to perform click chemistry has been achieved before by Sach and co-workers to synthesis functionalised triazoles.³⁸ This methodology was adapted to demonstrate the capability of the acetylene generating module by using a copper wire in flow as opposed to a purpose made copper coil as explained in the example above.



Scheme 23 – Reaction profile for formation of a 1,2,3-triazole from benzyl azide and acetylene

To install metallic copper into a pressurised flow system, a Wire-in-Tube (WiT) reactor was built using multiple strands of copper wire. It was postulated that the dissolved acetylene gas would interact with the metallic copper, forming copper acetylide, and therefore undergo the desired click reaction (Figure 16).

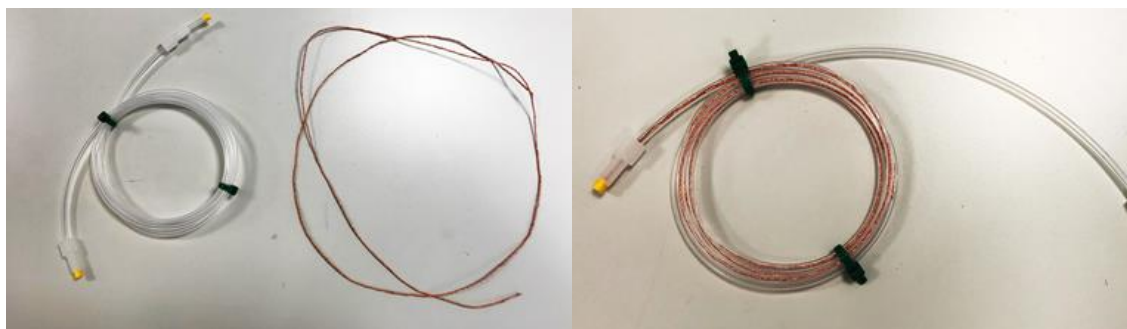
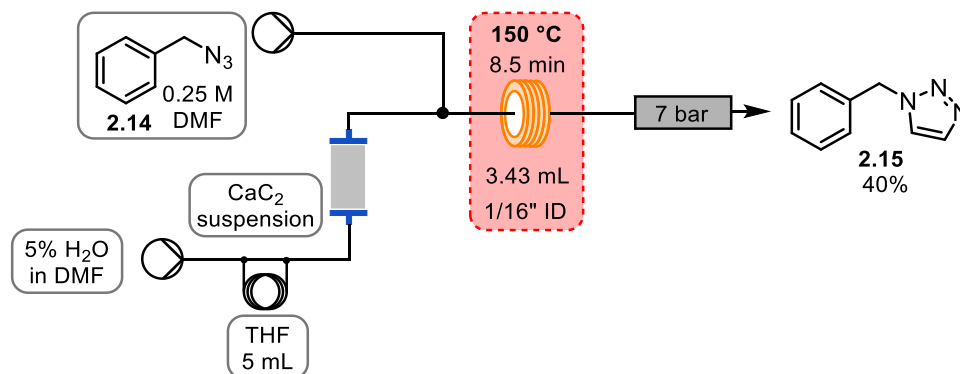


Figure 16 – Pictures showing the construction of the copper WiT reactor

Using wide-bore tubing, copper wire was twisted inside and the internal volume of the reactor coil was measured. After synthesising benzyl azide **2.14** from NaN_3 and benzyl chloride, a flow system was devised incorporating the WiT reactor and the acetylene generating module (Scheme 24). The flow reaction and result were provided by Imke Reuther.



Scheme 24 – Click reaction of benzyl azide in flow incorporating both the WiT reactor and the acetylene generating module, reaction performed by Imke Reuther

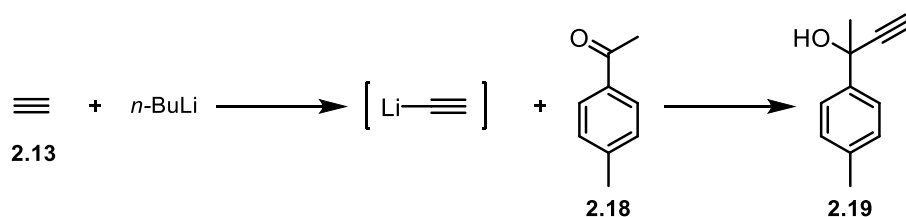
The click reaction with the WiT reactor at 150 °C for 8.5 minutes gave a ^1H NMR yield of 40% for **2.15**. Discolouration of the wire was observed over the course of the reaction, suggesting the reagents were interacting with the copper. This evidence suggests an (direct) interaction between the copper and *in situ* acetylene to deliver the terminal triazole **2.15** via a cycloaddition process.

This is another compelling example of the plug-and-play modality of the acetylene generator where it can incorporate homogenised acetylene gas safely into a pressurised and heated flow system. The *in situ* generated acetylene gas can then be incepted by various reagents via a telescoped flow system. Both the nitrile oxides and azides utilise the acetylene's triple bond functionality by cycloadditions, inspired by the thought of copper acetylide, it was postulated whether acetylene could be deprotonated *in situ* to form a reactive acetylide anion.

Both the isoxazole and triazole forming projects were not pursued further because the results provided show a proof-of-concept that acetylene could be generated *in situ* from solid CaC_2 and manipulated through design of a flow reactor. The engineering developments demonstrate that flow can be used to harness gases without the need of expensive gas handling equipment, and furthermore, organic transformation can be processed continuously in a seal, safe reactor.

2.3.5 Application of the acetylene generating module – Lithium acetylide

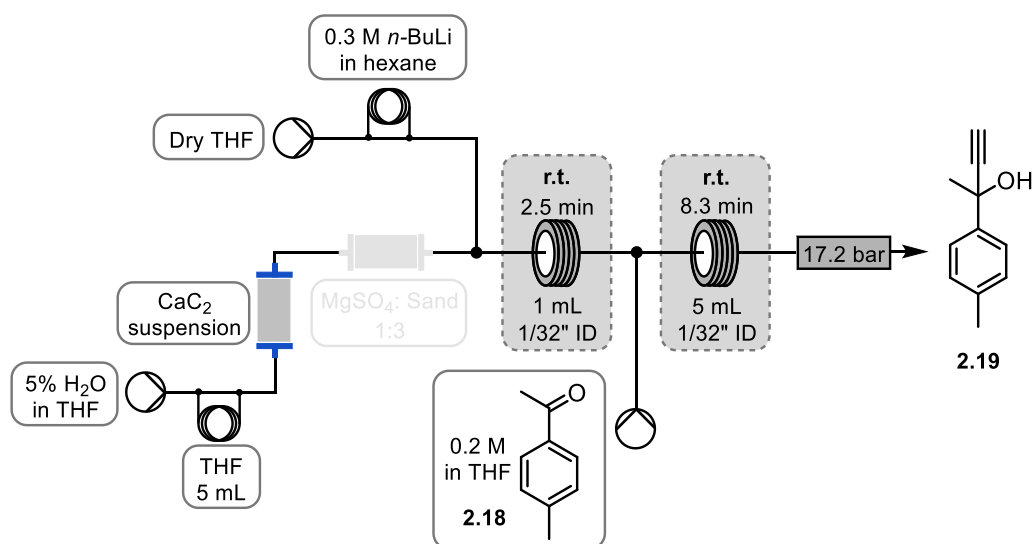
It was reasoned that the acetylene generating module could further be used to deliver a nucleophilic source of an acetylide by deprotonating the acetylene gas, with a suitably strong base, due to its $\text{p}K_{\text{a}}$ of 25-26.³⁹ One such suitable and readily available base considered was *n*-butyl lithium, where it was proposed that the lithium acetylide could be produced *in situ* and quenched with an electrophile, utilising 4-methyl acetophenone as model substrate, yielding a propargyl alcohol (Scheme 25).



Scheme 25 – Reaction profile for generating lithium acetylide and synthesis of a propargyl alcohol

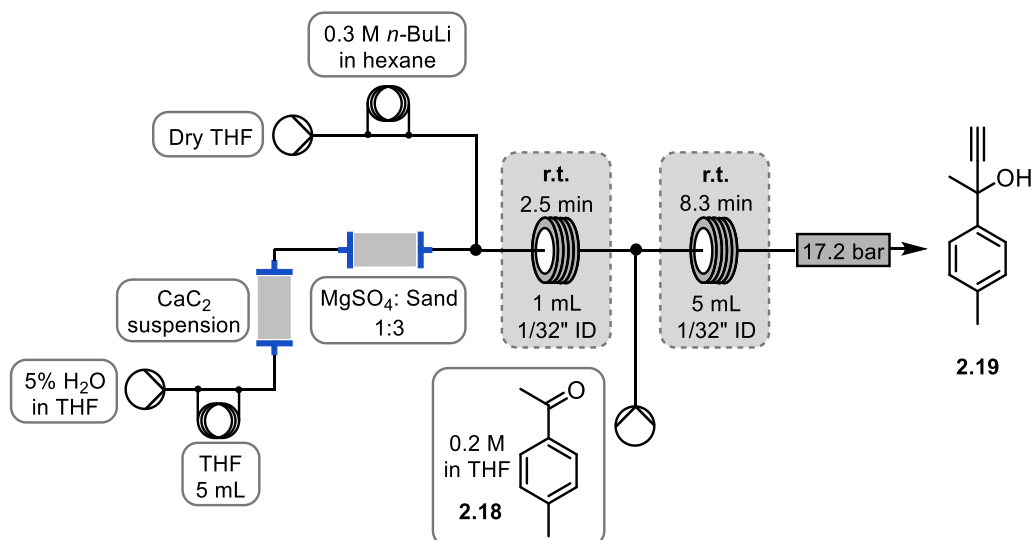
Engineering optimisation to create working flow system

The initial approach to designing the flow system was focussed on making the lithium acetylide *in situ* and subsequently quenching with a carbonyl electrophile to produce the desired propargyl alcohol. Firstly, *n*-BuLi and acetylene **2.13** were reacted together to form lithium acetylide which was intercepted with 4-methyl acetophenone **2.18** to give the desired product **2.19**. The solvent was changed from MeCN to THF to avoid the deprotonation of MeCN by *n*-BuLi. THF is also miscible with water and is therefore compatible with the acetylene generating module (Scheme 26).



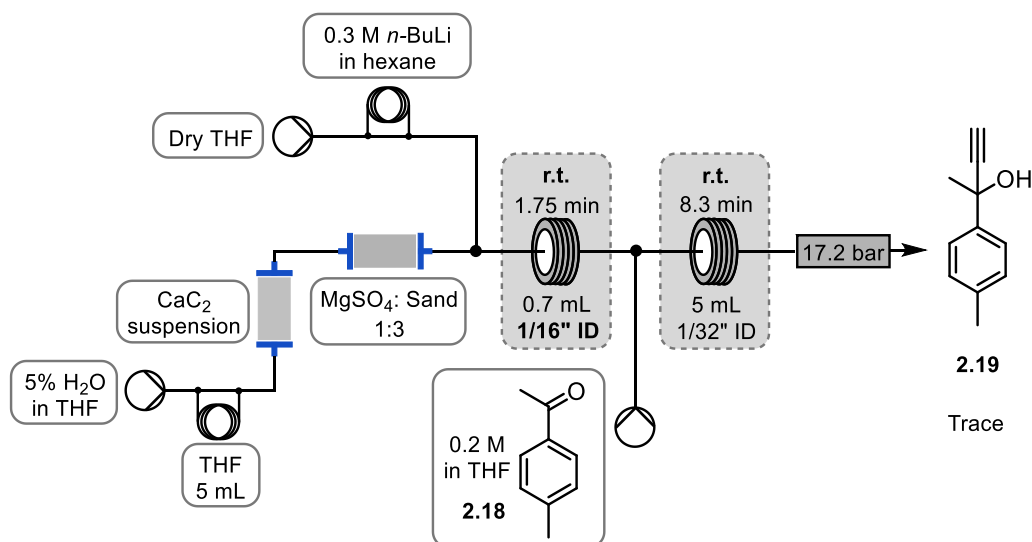
Scheme 26 - Initial flow system (flow system 2.2)

It was found that residual water from the acetylene generating module was quenching the *n*-BuLi and therefore losing its efficacy. A drying column was therefore installed after the acetylene generating module to remove the excess water. A mixture of sand and MgSO₄ (1:3 ratio) was found to be best to remove water and stop clogging. The ratio of sand to MgSO₄ was found to be best at 1:3 to maximise the amount of drying agent while enabling a free-flowing column that would not restrict flow. (Scheme 27).



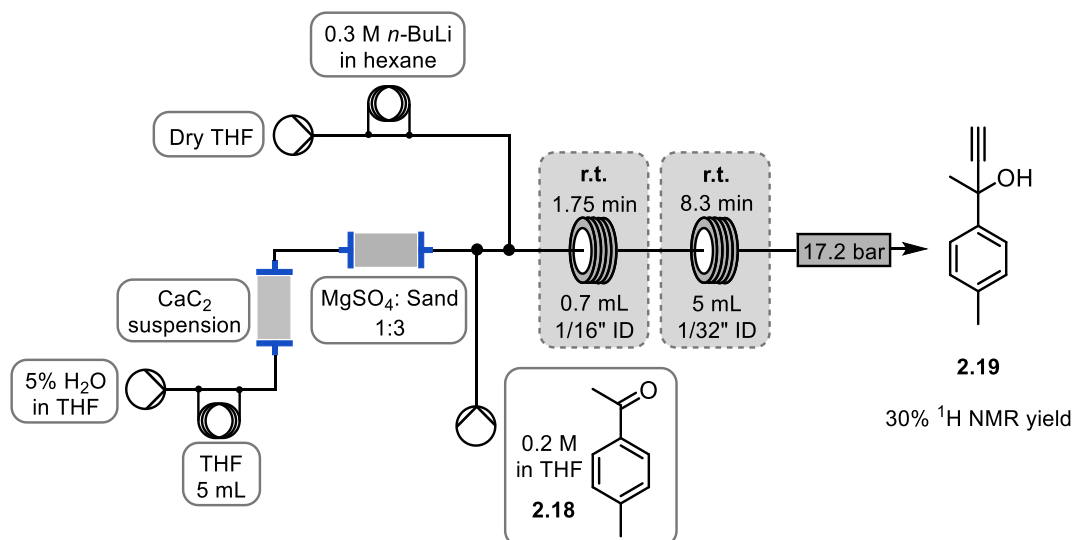
Scheme 27 - Installation of drying column to remove excess water (flow system 2.3)

It was noted that a solid was precipitating out of the THF solvent, assumed to be lithium acetylide, as the observed precipitate disappeared after the addition of 4-methyl acetophenone **2.18**. This implied that the lithium acetylide was reacting with the electrophile and consumed within the reactor coil. The internal diameter (ID) of the reactor coil tubing was increased to a wider bore to help manage the flow of the precipitate formed *in situ* (Scheme 28).



Scheme 28 – Increasing internal diameter of tubing to manage precipitate (flow system 2.4)

The wide bore tubing did however reduce the ability of the lithium acetylide bridging across the tubing and subsequent blocking, which gave the first visual indication that trace amounts of product was being formed. This theory was confirmed using ^1H NMR, via the distinguishable alkyne hydrogen of alcohol **2.19**, with a chemical shift of 2.67 ppm.



Scheme 29 – Introducing the electrophile before the addition of *n*-BuLi (flow system 2.5)

Introduction of the electrophile **2.18** before the addition of *n*-BuLi had the desired effect of delivering **2.19** in 30% ¹H NMR yield. One concern using *n*-BuLi was the potential for butyl nucleophilic addition to the 4-methyl acetophenone **2.18**, however, this was not observed. The wide bore tubing was kept in the system to reduce the risk of any precipitate blockages (Scheme 29). The final reactor was also heated to assist in completing the desired reaction and aiding dissolution of any precipitate formation. The coil was heated to 60 °C and pleasingly gave a yield of **2.19** in 40%, determined by ¹H NMR. Despite the promising results demonstrated, the formation of precipitate, mainly at the Y-piece, was still a problem for this developed flow system and required further development. Tetrabutylammonium bromide (TBAB) was added as a phase-transfer catalyst to help solvate the lithium acetylide precipitate. The addition of TBAB increased the yield of the propargyl alcohol **2.19** to 47% by ¹H NMR. Unfortunately, the system did not perform reliably due to multiple observations of large amounts of precipitate being visibly formed at the Y-piece, causing strain on the flow system. There were numerous instances of pumps failing and tube fittings breaking due to increased pressure caused by blockages.

The nature of the Y-piece directs the flow of two reagents in a collisional manner to mix them and it was postulated whether a mixer could be invented that circumvents this collisional mixing. The Needle-in-Tube mixer (NiT) was created to enable co-directional mixing which takes the formation of precipitate further downstream and away from the mixing junction, minimising risk of blockages. The NiT mixer was made from a cut needle and a Swagelok T-piece (Figure 17).

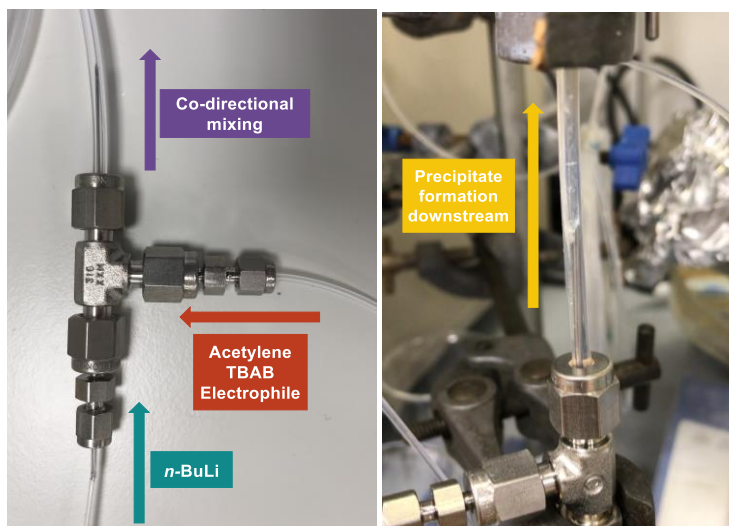
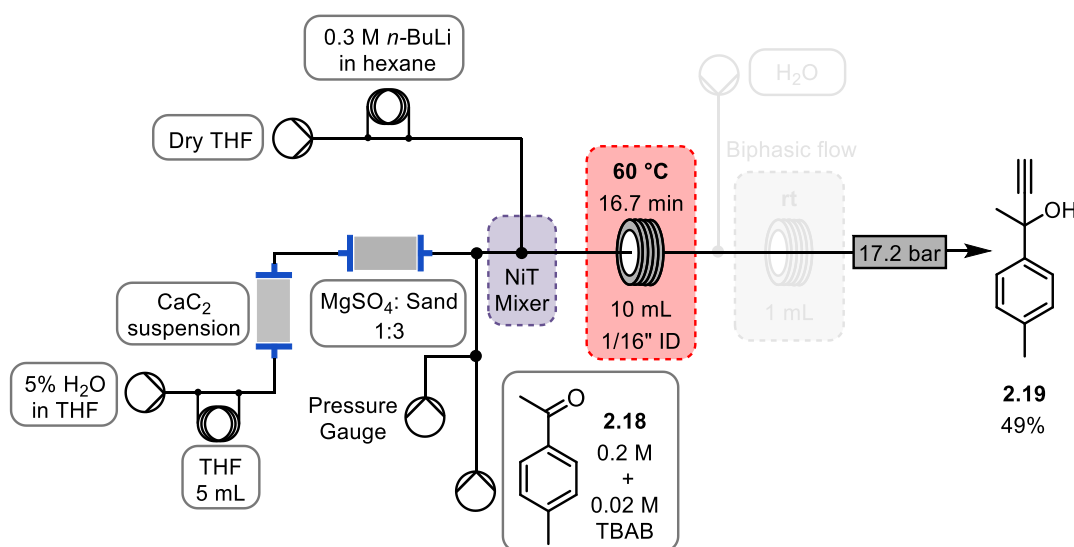


Figure 17 - NiT mixer showing directions of reagent addition (left); white precipitate forming downstream (right)

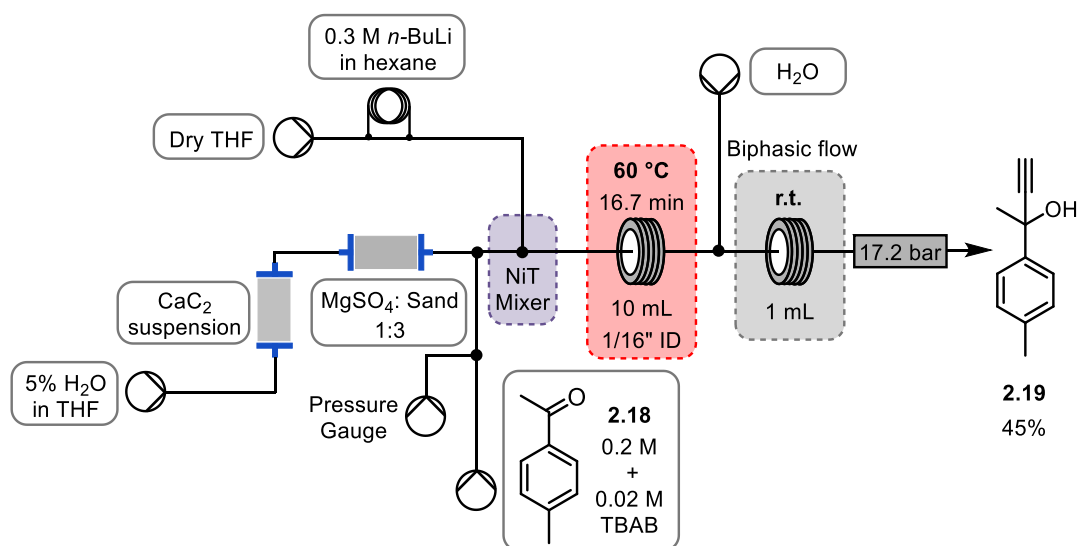
The NiT mixer allowed the introduction of *n*-BuLi into a stream of acetylene to form the required lithium acetylide which can subsequently be consumed by the available electrophile present (Figure 17). With the NiT mixer in hand, the flow system could more reliably manage the precipitate formation by avoiding a build-up of precipitate at the mixing junction. The system now had an integrated wide bore reaction coil to minimise the number of small junctions throughout the flow system thus minimising blockages. It was found to be advantageous to heat the final reactor coil to assist in solvation and resulted in a 49% yield of **2.19** (Scheme 30).



Scheme 30 – Integration of NiT mixer and heated coil (flow system 2.6)

A pressure gauge was installed to monitor the pressure of the system which managed the safety by indicating blockages and therefore pressure build up. It was also found advantageous to add a water quench downstream to dissolve any residual

precipitate/inorganics that could block the back pressure regulator. Once the water stream was added the system became more reliable with no blockages or fluctuations in pressure, which was commonplace beforehand. With the addition of water, a biphasic flow had established which meant that all salts would have been removed from the reaction mixture and excess *n*-BuLi/lithium acetylide quenched safely (Scheme 31).



Scheme 31 – The final engineered flow system that delivered the desired compound reliably (flow system 2.7)

The engineering optimisation process was complete with a final yield of 45% for **2.19**, by ¹H NMR, as this system could be run safely and reliably. This evolution of the above process has shown that reactor design is fundamental to developing a successfully working flow system, especially when handling difficult reagents such as gases and precipitates.

Chemical optimisation of working flow system

After the engineering optimisation had been completed, chemical parameters could be explored to drive the reaction towards completion, targeting high selectivity of the desired propargyl alcohol product.

Table 5 – Temperature and concentration screen

Entry	[2.18] (M)	[<i>n</i> -BuLi] (M)	Temp. (°C)	Time (min)	Additive (10 mol%)	Yield of 2.19
1	0.2	0.5	60	16.7	TBAB	45%
2	0.1	0.5	40	16.7	TBAB	20%
3	0.1	0.5	60	16.7	TBAB	66%
4	0.1	0.5	80	16.7	TBAB	54%

When reducing the concentration of 4-methyl acetophenone **2.18**, the yield increased from 45% to 66% (entries 1 to 3, Table 5). This showed that a higher concentration of the electrophile reduced the yield which implies a greater excess of lithium acetylide is required. A small screen of temperature showed that an optimum temperature of 60 °C gave 66% yield of **2.19** (entry 3, Table 5) as the best result. Further heating of the reaction gave a detrimental effect on the yield, possibly causing side reactions to take place.

Table 6 – *n*-BuLi concentration screen

Entry	[2.18] (M)	[<i>n</i> -BuLi] (M)	Temp. (°C)	Time (min)	Additive (10 mol%)	Yield of 2.19
1	0.1	0.3	60	16.7	TBAB	64%
2	0.1	0.5	60	16.7	TBAB	66%
3	0.1	0.75	60	16.7	TBAB	70%
4	0.1	1	60	16.7	TBAB	-- ^a

^a=reaction blocked due to excess precipitate formation

The concentration of *n*-BuLi was probed and the results showed that increasing the *n*-BuLi concentration, the yield of **2.19** increased to 70% (entries 1 to 3, Table 6). This was an expected result because the more lithium acetylide present in the reaction, the higher the possibility of nucleophilic attack towards 4-methyl acetophenone **2.18**. Increasing the concentration further to 1 M (entry 4, Table 6), failed due to an excess amount of lithium acetylide being produced, resulting in blocking of the NiT mixer.

Table 7 – TBAB removal, time, and 4-methyl acetophenone concentration

Entry	[2.18] (M)	[<i>n</i> -BuLi] (M)	Temp. (°C)	Time (min)	Additive (10 mol%)	Yield of 2.19
1	0.1	0.75	60	16.7	TBAB	70%
2	0.1	0.75	60	16.7	none	78%
3	0.1	0.75	60	25	none	86%
4	0.1	0.75	60	33.3	none	56%
5	0.075	0.75	60	25	none	97% (96%)^a

a = isolated

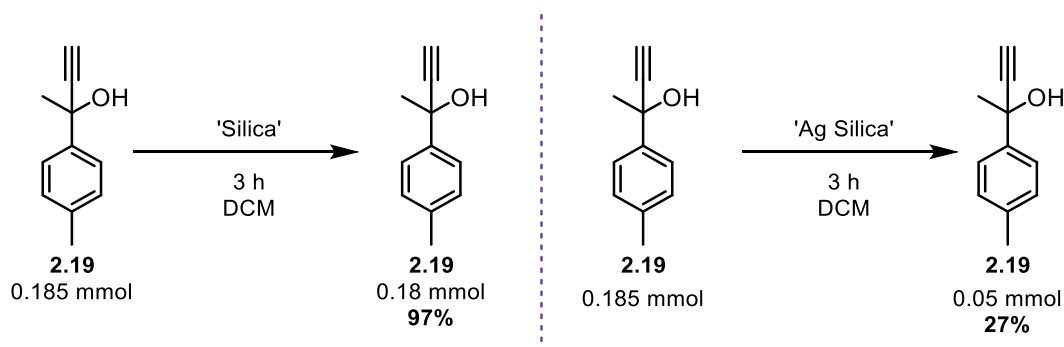
Initially, TBAB was introduced as a phase-transfer catalyst to assist in solvating any insoluble lithium salts. However, upon removing TBAB from the reaction, the yield increased from 70% to 78% (entries 1 to 2, Table 7). Adding the water quench downstream of the reaction alleviated the need of TBAB because any precipitate formed would be dissolved in the biphasic mixture thus removing the risk of a blocked BPR. Increasing the time of reaction by using longer coils showed that the yield of **2.19** could be increased to 86% (entry 3, Table 7), but increasing the reaction time further had a deleterious effect, whereby the yield dropped significantly to 56% (entry 4, Table 7), suggesting instability of the product under prolonged exposure to reaction conditions. The optimal conditions were finally found by reducing the concentration of the 4-methyl acetophenone **2.18** to give 97% yield by ¹H NMR (entry 5, Table 7). This result shows that a greater relative excess of lithium acetylide is necessary for effective nucleophilic addition. Attempted isolation of **2.19** proved incredibly complex, due to both the 4-methyl acetophenone **2.18** and propargyl alcohol **2.19** having identical R_f values across 10 various solvent mixtures tested.

Product isolation and stability tests

It was advised that using a band of silver impregnated silica on column chromatography would assist in the separation of these two compounds.⁴⁰ This was achieved by silica impregnation with silver nitrate, and left in the oven to adsorb onto the silica.

Despite having a high (¹H NMR) yield of the desired product, unreacted starting material was still present due to the collection method of the flow system. To purify the compound, a 1 cm layer of silver silica was incorporated into the column for chromatography. It was observed that upon elution of the crude mixture over the silver-silica band, it changed from off-white to black. Column fractions collected thereafter showed no contained target compound. This would suggest that the propargyl alcohol product decomposed either

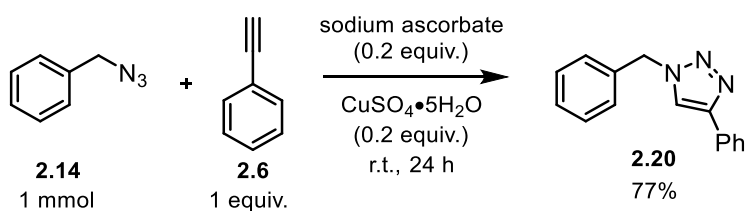
due to the silver silica or the mildly acidic nature of silica itself. A stability test was setup to explore how readily the product decomposes on silver silica versus non-silver silica (Scheme 32).



Scheme 32 – Testing stability of product on both silica and silver impregnated silica

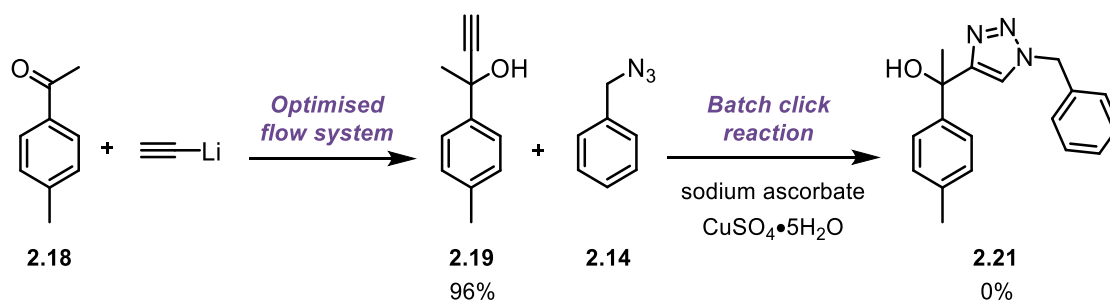
This simple test showed that upon mixing the product with silver impregnated silica there was a 27% recovery of product after 3 hours, therefore 73% degraded in the presence of silver silica. By comparison, almost complete recovery of product was found for the analogous standard silica test. It was clear that the compound was stable on silica and column chromatography was a viable option for isolation. After abandoning the silver silica, uncommon solvent mixtures were explored to isolate this difficult mixture. Pleasingly, an extremely slow cyclohexane and ethyl acetate column managed to isolate the product **2.19** in a 96% isolated yield (entry 5, Table 7).

It was proposed that a post-functionalisation of the propargyl alcohol product might ease the complex isolation process. Click chemistry is an extremely well-known area of transformations and common reagents were used to synthesise the desired triazole (Scheme 33).



Scheme 33 – Click chemistry conditions

The reaction yielded 77% of triazole **2.20** and thus establishing conditions for the click transformation, no attempts were made to further optimise this transformation between benzyl azide **2.14** and phenyl acetylene **2.6**. The tandem 2-step process was tested by flowing the output of the optimised flow system into a collection flask and adding the click reaction reagents which was then left to stir over 2 days (Scheme 34).



Scheme 34 – Tandem lithium acetylide addition and click reaction transformation

The initial flow reaction yielded 96% of **2.19** by ^1H NMR which was carried forward to form the desired triazole **2.21**, and the output subjected to the same click reaction conditions with benzyl azide **2.14** used previously (Scheme 34). Unfortunately, it was found that the reaction did not deliver triazole **2.21**, where the crude reaction mixture contained a complex mixture and a majority of unreacted propargyl alcohol **2.19**.

Unfortunately, after looking at the accessibility and complexity of the lithium acetylide project it was decided that the project cease to be developed. The reaction did yield the desired propargyl alcohol and demonstrated that the reactor design had the ability to generate and deliver acetylene gas safely which was manipulated to form a lithium salt, which could further be consumed *in situ*.

2.4 Conclusions and outlook

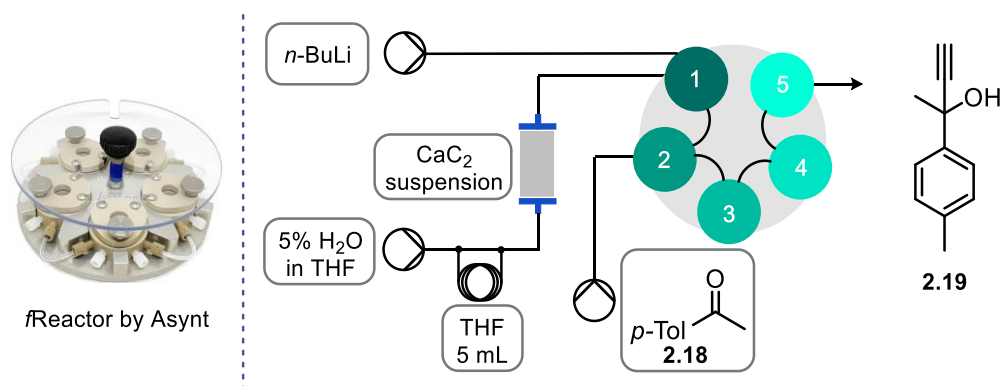
In summary, the project aims had been met: a reproducible, flow compatible acetylene gas source was found and plugged into various reaction conditions in continuous flow. After a rigorous engineering and optimisation, a novel calcium carbide suspension using paraffin oil was created that could be loaded into a flow cartridge and activated via 5% water in miscible organic solvent. This facilitated the generation of acetylene gas from a solid reagent without the need of a resident gas cylinder through the careful planning of reactor design. The acetylene gas generated was homogenised through use of a suitable BPR and an internal concentration obtained. The plug and play modality of the acetylene generating module was demonstrated over three reaction manifolds; initially via a 1,3-dipolar cycloaddition with a stable nitrile oxide to successfully form an isoxazole. This initial work was expanded to explore the generation of unstable nitrile oxides *in situ* and pleasingly an isoxazole scope was produced. Furthermore, click chemistry with benzyl azide were tested with metallic copper wire in an innovative wire-in-tube (WiT) reactor, yielding the target triazole in 40% ¹H NMR yield. Finally, to demonstrate the application of *in situ* generated acetylene, lithium acetylide was formed via deprotonation with *n*-BuLi as base, through a novel mixing design (NiT mixer) which overcame solid precipitation issues. With a functioning system, the lithium acetylide was later consumed by 4-methyl acetophenone successfully to synthesise a propargyl alcohol at 96% isolated yield. Upon reflection, it was felt that in successfully developing the flow system described, the intricacies and design of the reactor module had exceeded the original remit of a user-friendly system. Furthermore, the ability to reproduce the setup by the wider flow chemistry community would be impinged due to its highly bespoke nature, and as such a scope of substrates was not explored.

Overall, three flow systems were shown to use the acetylene generating module successfully and negated the need for a resident gas cylinder of acetylene gas and utilised the cheap robust feedstock, calcium carbide. All reactive intermediates formed were contained safely within the pressurised flow system and avoided dangerous exposure to the flow system operator.

Future proposals

The main limitation with producing lithium acetylide *in situ* was the generation of lithium salt precipitation. This has always been the ‘Achilles heel’ of flow chemistry, however, emerging technologies are being developed and flow systems that can handle precipitates in continuous flow are being innovatively created. The fReactor by Asynt is 5 consecutive continually stirred tank reactors (CSTRs) that have a magnetic stir bar in

each chamber which aid it dealing with slurries/precipitate in flow.⁴¹ This system would be interesting to test on the formation of lithium acetylide from *in situ* generated acetylene gas and *n*-BuLi as described in section 5.3.5 (Scheme 35).



Scheme 35 – *f*Reactor (left); propargyl alcohol synthesis using *f*Reactor and acetylene generating module (right)

The lithium acetylide precipitate formed in the deprotonation could be efficiently moved through the CSTRs and with the addition of electrophilic 4-methyl acetophenone **2.18**, the lithium acetylide precipitate could be consumed without risk of blocking. This would be an interesting example of new technology and reactor design, in flow, overcoming the existing limitations of continuous processing.

With the lessons learnt from harnessing acetylene gas, the concept of using a solid gas-storage matrix to release gas *in situ* can be applied to various examples in flow using the same technique described in this project (Figure 18).

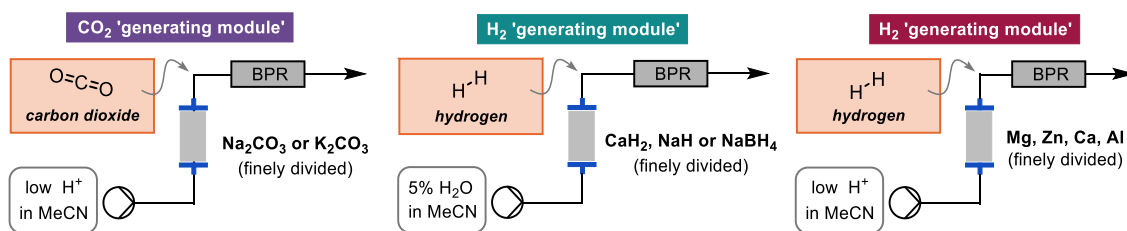


Figure 18 – Carbon dioxide and hydrogen gas generators in flow

Various gases could be formed using flow cartridges filled with solid reagents that liberate gas upon activation via a solvent pump. Carbon dioxide can be generated exposing carbonates to weak acids and thus in the presence of a nucleophile the carbon dioxide can be consumed *in situ*. Another example that could be explored is hydrogen gas, which can be formed either from the combination of water and hydrides, or mild acid and metals. Either generator could be used depending on acid sensitive/water sensitive reactions. These generators would be a useful tool to circumvent the use of

hydrogen/carbon dioxide gas cylinders for common organic transformations, such as, reductions while offering a higher degree of tunability and flexibility.

2.5 References

- 1 M. Brzozowski, M. O'Brien, S. V Ley and A. Polyzos, *Acc. Chem. Res.*, 2015, **48**, 349–362.
- 2 B. Gutmann, D. Cantillo and C. O. Kappe, *Angew. Chemie Int. Ed.*, 2015, **54**, 6688–6728.
- 3 M. O'Brien, I. R. Baxendale and S. V Ley, *Org. Lett.*, 2010, **12**, 1596–1598.
- 4 P. B. Cranwell, M. O'Brien, D. L. Browne, P. Koos, A. Polyzos, M. Peña-López and S. V Ley, *Org. Biomol. Chem.*, 2012, **10**, 5774.
- 5 C. J. Mallia and I. R. Baxendale, *Org. Process Res. Dev.*, 2016, **20**, 327–360.
- 6 M. Köckinger, C. A. Hone, B. Gutmann, P. Hanselmann, M. Bersier, A. Torvisco and C. O. Kappe, *Org. Process Res. Dev.*, 2018, **22**, 1553–1563.
- 7 A. Kouridaki and K. Huvaere, *React. Chem. Eng.*, 2017, **2**, 590–597.
- 8 S. Saaby, K. R. Knudsen, M. Ladlow and S. V Ley, *Chem. Commun.*, 2005, **23**, 2909.
- 9 D. Dallinger and C. O. Kappe, *Nat. Protoc.*, 2017, **12**, 2138–2147.
- 10 V. D. Pinho, B. Gutmann, L. S. M. Miranda, R. O. M. A. de Souza and C. O. Kappe, *J. Org. Chem.*, 2014, **79**, 1555–1562.
- 11 C.-J. Li, D.-L. Chen and C. W. Costello, *Org. Process Res. Dev.*, 1997, **1**, 325–327.
- 12 V. V. Voronin, M. S. Ledovskaya, E. G. Gordeev, K. S. Rodygin and V. P. Ananikov, *J. Org. Chem.*, 2018, **83**, 3819–3828.
- 13 E. Renouf, The Use of Acetylene, shorturl.at/swBJ0, (accessed 20 March 2021).
- 14 A. Sharpe and C. E. Housecroft, *Inorganic chemistry*, 2008.
- 15 D. Yu, Y. N. Sum, A. C. C. Ean, M. P. Chin and Y. Zhang, *Angew. Chemie Int. Ed.*, 2013, **52**, 5125–5128.
- 16 M. Fakharian, A. Keivanloo and M. R. Nabid, *Helv. Chim. Acta*, 2018, **101**, e1800004.

- 17 A. Hosseini, D. Seidel, A. Miska and P. R. Schreiner, *Org. Lett.*, 2015, **17**, 2808–2811.
- 18 R. Matake, Y. Adachi and H. Matsubara, *Green Chem.*, 2016, **18**, 2614–2618.
- 19 R. Fu and Z. Li, *J. Chem. Res.*, 2017, **41**, 341–345.
- 20 Z. Lin, D. Yu, Y. N. Sum and Y. Zhang, *ChemSusChem*, 2012, **5**, 625–628.
- 21 Y. N. Sum, D. Yu and Y. Zhang, *Green Chem.*, 2013, **15**, 2718.
- 22 R. Matake, Y. Niwa and H. Matsubara, *Org. Lett.*, 2015, **17**, 2354–2357.
- 23 A. Hosseini, A. Pilevar, E. Hogan, B. Mogwitz, A. S. Schulze and P. R. Schreiner, *Org. Biomol. Chem.*, 2017, **15**, 6800–6807.
- 24 S. P. Teong, A. Y. H. Chua, S. Deng, X. Li and Y. Zhang, *Green Chem.*, 2017, **19**, 1659–1662.
- 25 R. Fu and Z. Li, *European J. Org. Chem.*, 2017, **2017**, 6648–6651.
- 26 E. Rattanangkool, T. Vilaivan, M. Sukwattanasinitt and S. Wacharasindhu, *European J. Org. Chem.*, 2016, **2016**, 4347–4353.
- 27 M. S. Ledovskaya, K. S. Rodygin and V. P. Ananikov, *Org. Chem. Front.*, 2018, **5**, 226–231.
- 28 K. Rodygin, A. Bogachenkov and V. Ananikov, *Molecules*, 2018, **23**, 648.
- 29 W. E. Van Beek, K. Gadde and K. A. Tehrani, *Chem. - A Eur. J.*, 2018, **24**, 16645–16651.
- 30 X. Ma and Z. Li, *Synlett*, 2021, **32**, 631–635.
- 31 Y. Jiang, C. Kuang and Q. Yang, *Synlett*, 2009, **2009**, 3163–3166.
- 32 K. S. Rodygin, I. Werner and V. P. Ananikov, *ChemSusChem*, 2018, **11**, 292–298.
- 33 G. Werner, K. S. Rodygin, A. A. Kostin, E. G. Gordeev, A. S. Kashin and V. P. Ananikov, *Green Chem.*, 2017, **19**, 3032–3041.
- 34 SDS - Calcium carbide - FisherSci, shorturl.at/rtBV8, (accessed 12 March 2021).
- 35 K.-M. Jiang, U. Luesakul, S.-Y. Zhao, K. An, N. Muangsin, N. Neamati, Y. Jin and J. Lin, *ACS Omega*, 2017, **2**, 3123–3134.
- 36 F. Risitano, G. Grassi, F. Foti and F. Filocamo, *Tetrahedron*, 1997, **53**, 1089–1098.

- 37 J.-S. Poh, C. García-Ruiz, A. Zúñiga, F. Meroni, D. C. Blakemore, D. L. Browne and S. V Ley, *Org. Biomol. Chem.*, 2016, **14**, 5983–5991.
- 38 A. R. Bogdan and N. W. Sach, *Adv. Synth. Catal.*, 2009, **351**, 849–854.
- 39 P. Pässler, W. Hefner, K. Buckl, H. Meinass, A. Meiswinkel, H.-J. Wernicke, G. Ebersberg, R. Müller, J. Bässler, H. Behringer and D. Mayer, in *Ullmann's Encyclopedia of Industrial Chemistry*, Wiley-VCH Verlag GmbH & Co. KGaA, Weinheim, Germany, 2011.
- 40 P. P. Daramwar, P. L. Srivastava, B. Priyadarshini and H. V Thulasiram, *Analyst*, 2012, **137**, 4564.
- 41 Asynt, fReactor summary, shorturl.at/orP02, (accessed 24 March 2021).

3 Designing a Reactor to Thermally Generate and Intercept Acyl Ketenes

3 Designing a Reactor for the Thermal Generation and Interception of Acyl Ketenes.....	62
3.1 Introduction.....	63
3.1.1 Thermal control in flow.....	63
3.1.2 Acyl ketenes	65
3.2.3 Harnessing acyl ketenes in flow.....	68
3.2 Aims and Objectives.....	70
3.3 Results and Discussion	71
3.2.1 Discovery and reactivity of the acyl ketene	71
3.2.2 Exploring various ketene traps.....	73
3.2.3 Post-functionalisation reaction – Biginelli	82
3.4 Conclusions and outlook	93
3.5 References	95

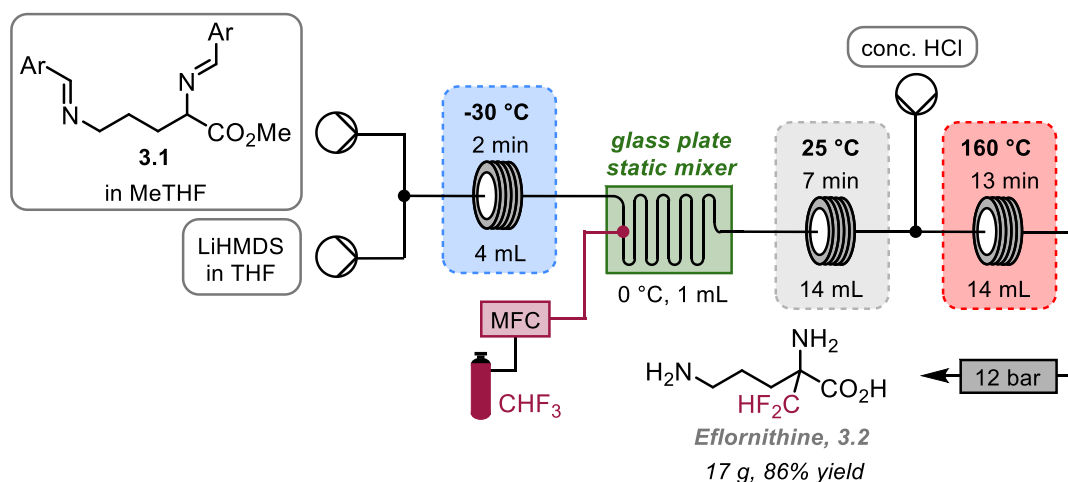
3.1 Introduction

This chapter will explore the use of acyl ketenes in flow and how they can be synthetically utilised. Acyl ketenes are reactive intermediates that can be harnessed in both batch and flow methodologies. This introduction will explore how reactor design of flow systems can facilitate and control this reactivity. The acyl ketene precursor in this chapter is activated through thermal energy, therefore, thermal control in these reactions is imperative. Temperature control in flow chemistry is hailed as a defining benefit due to the high surface area-to-volume ratio and mixing efficiency within tubular reactors. This increases the ability for external heating/cooling to influence the reaction mixture.

3.1.1 Thermal control in flow

Flow chemistry has been used in literature to control highly exothermic reactions and safely contain pressurised systems. With the use of a back-pressure regulator, flow systems can be designed to maintain high pressure within the reactor tubing. Organic solvents, under these high-pressure conditions, can be superheated beyond their boiling point and thus unlock reactivity that cannot be obtained in batch.¹

Flow chemistry allows the integration of various reaction conditions to be installed throughout a flow process. In 2018, Kappe and co-workers reported the synthesis of Eflornithine **3.2** in flow using various reactor temperatures whilst containing highly reactive intermediates (Scheme 36).



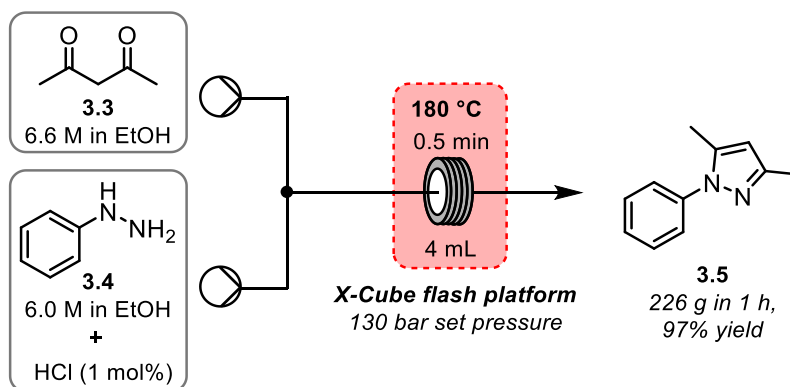
Scheme 36 – Telescoped synthesis of Eflornithine

The authors demonstrated the successful telescoped synthesis and scale up of Eflornithine **3.2** to yield 17 g in 3.5 hours with an 86% yield. Despite the innovative solution to introduce a difluoromethyl source from fluoroform gas, the authors harness flow's ability to control and change temperature effectively and safely. In this example,

the diimine starting material **3.1** is mixed with LiHMDS and cooled to $-30\text{ }^{\circ}\text{C}$ to control any exothermic reactions or overreactions in the deprotonation step. The cool temperature was used to minimise oligomerisation and pre-cool the reagents prior to the addition of fluoroform gas. The gas is introduced via a static glass-plate mixer that must be pressurised to ensure dissolution of the fluoroform gas. The static mixer causes turbulent flow to occur to efficiently mix the reagents and increase heat transfer. The glass plate was cooled to $0\text{ }^{\circ}\text{C}$ to dissipate any exothermic activity and the high surface-area-to-volume ratio of flow chemistry enables tight control of these parameters. The reaction is completed in 7 minutes at $25\text{ }^{\circ}\text{C}$ and subsequently acidified with concentrated HCl. The reaction mixture is then heated to $160\text{ }^{\circ}\text{C}$ liberating the free amines and form the carboxylic acid of Eflornithine **3.2**. Within a total residence time of 23 minutes, the flow system has changed the reaction's temperature effortlessly from $-30\text{ }^{\circ}\text{C}$ to $160\text{ }^{\circ}\text{C}$, under increased pressure to superheat solvents, which would be unmanageable in batch conditions.²

This example exemplifies flow's ability to manage the control of temperature, mixing, and pressure for reactions in a controlled, safe, and continuous manner. Throughout the flow chemistry community, these benefits have been countless exploited to harness reactivity that can be difficult to access, via traditional methods, on scale. Process intensification is a beneficial commodity that flow chemistry can facilitate. Super heating solvents to decrease reaction times is common in flow chemistry due to the ease of adding increased pressure to a flow system via a back-pressure regulator.³⁻¹⁰

Microwave chemistry can also replicate these conditions in sealed vials that are irradiated with microwaves to elicit organic transformations. In 2010, Kappe and co-workers reported a comparison study on the differing technology for a pyrazole formation (Scheme 37).



Scheme 37 – Process intensification example – Pyrazole synthesis

The authors compared the formation of pyrazole **3.5**, from dicarbonyl **3.3** and phenyl hydrazine **3.4**, in both microwave and flow conditions. It was reported that the yields and reaction times were comparably the same except for the space-time-yield (STY). For the flow system, the STY was $15.7 \text{ kgm}^{-3}\text{s}^{-1}$ and the microwave batch process was $0.19 \text{ kgm}^{-3}\text{s}^{-1}$ which is vastly significant with regards to scale. The microwave batch process used ~1 L of reaction mixture to make 468 g whereas the flow system had a reactor volume of 4 mL and could produce 226 g in 1 hour run time thus illustrating the superiority of flow chemistry in this example with respect to scale and safety.¹¹ Process intensification commonly uses higher temperatures and pressures which also have higher safety risks associated with them. However, heating a small volume in a tubular reactor is far safer than a larger bulk solvent solution in batch processing. In 2005, Organ and co-workers demonstrated the integration of an in-line microwave-flow capillary system that facilitated the continuous processing of Suzuki-Miyaura coupling. This highlighted that by coupling the two enabling technologies, the common organic transformation could be streamlined thus increasing the productivity of the required transformations.¹²

The control flow technology can instil over temperature is an important benefit when handling thermally reactive compounds. This chapter explores the use of a thermally activated acyl ketene precursor and, by demonstrating high thermal control via flow chemistry, how the reactive intermediate can be generated safely and chemically manipulated *in situ*.

3.1.2 Acyl ketenes

An intermediate ketene species was first postulated in 1901 by E. Wedekind, however, he unfortunately missed the chance to isolate the ketene.¹³ In 1905, Staudinger reported the isolation, and thus the discovery, of diphenylketene, the first example of a new family of reactive intermediates.¹⁴ Acyl ketenes are a branch of the ketene family and were first reported by Wilsmore and Chick in 1908.¹⁵ Over 100 years have passed exploring the use and generation of ketenes for organic synthesis and is most commonly a reactive intermediate that is generated *in situ* and consumed throughout the transformation.^{16,17} Acyl ketenes contain an acyl functional group α to the ketene functionality which creates an extended conjugated system. This group of chemical compounds are deemed reactive intermediates because the half-life of an acyl ketene in water is $<1 \mu\text{s}$ and isolated acyl ketenes are very uncommon unless highly sterically hindered.^{18–23}

Acyl ketenes can be formed via multiple synthetic strategies using either chemical, thermal, or photochemical activation (Figure 19)

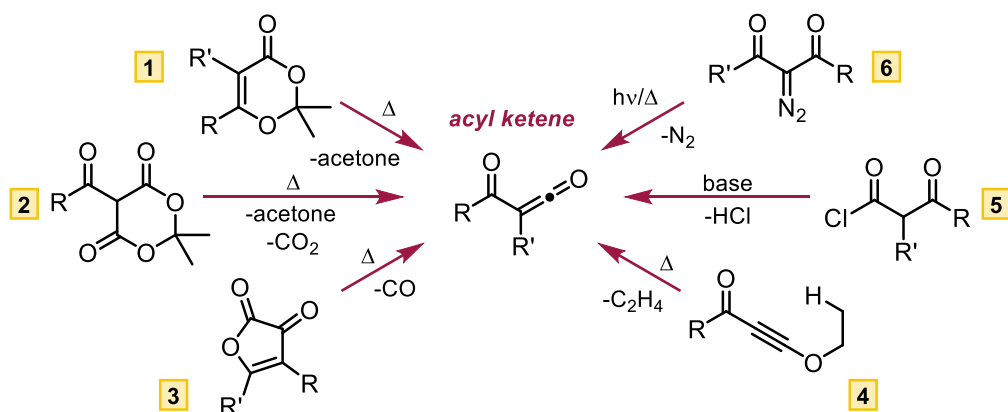
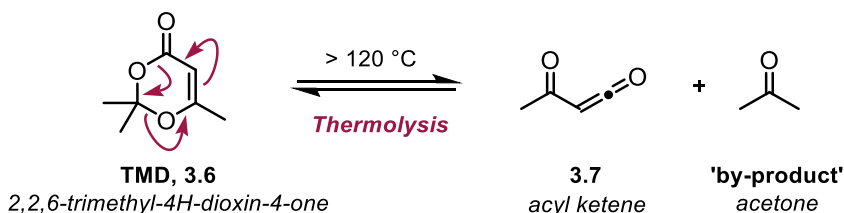


Figure 19 – A variety of synthetic methods to form an acyl ketene via chemical, thermal, or photochemical pathways

Most commonly, thermal or chemical activation is seen throughout literature as the desired methods of acyl ketene formation due to those methods being easily accessible. A range of precursors are available to be activated thus liberating an acyl ketene. Thermal decomposition is a common strategy to generate acyl ketenes, for example, using 1,3-dioxinones (pathway 1 and 2); β -keto esters (pathway 3); and acylated ethoxy alkynes (pathway 4). Each thermolysis example releases a by-product into the reaction which must be considered when designing an organic transformation. Another common method is to use basic conditions on a β -keto acid chloride, via an elimination, to liberate an acyl ketene (pathway 5). Finally, the use of photolysis can also be used to generate an acyl ketene, for example the irradiation of diazo-1,3-dicarbonyls (pathway 6). However, this is less common due to the required photochemical light source technology.^{24–26}

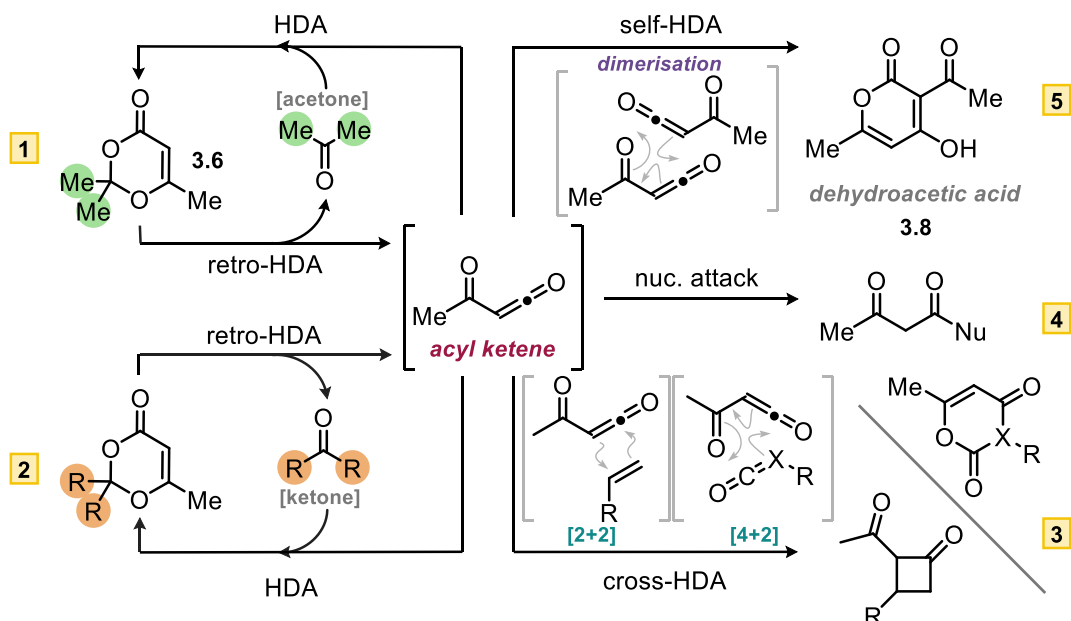
This chapter explores the use of commercially available 2,2,6-trimethyl-4*H*-1,3-dioxin-4-one (TMD, **3.6**) as the acyl ketene precursor that is activated via thermolysis to liberate the acyl ketene **3.7** and acetone by-product (Scheme 38).²⁷



Scheme 38 – Thermolysis of TMD liberates the desired acyl ketene and acetone by-product

TMD, **3.6**, undergoes a thermal decomposition when heated over 120 °C to afford acyl ketene **3.7** and an acetone by-product. Most commonly, high boiling point solvents are used in batch to induce the retro-hetero Diels-Alder process, liberating the reactive acyl

ketene. TMD **3.6** has various possible reaction pathways when decomposed thermally (Scheme 39).²⁸

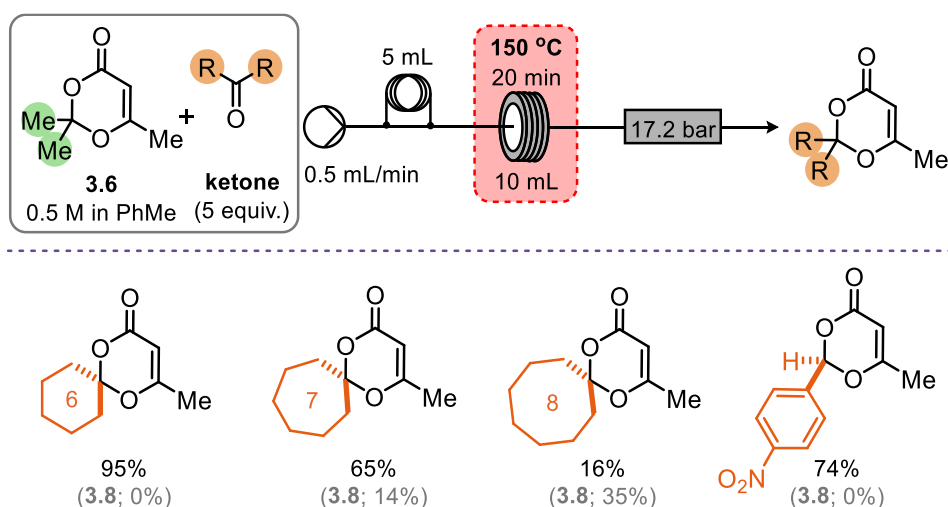


Scheme 39 – Reaction pathways of an acyl ketene

As previously discussed, TMD **3.6** thermally decomposes to afford an acyl ketene. Most commonly, when the acetone by-product is formed, it is boiled out of the system and cannot react with the acyl ketene. However, in a sealed system, such as microwave or flow, a concentration of acetone will be present in the reaction and thus an equilibrium is established which allows a hetero-Diels-Alder (HDA) reaction to take place with acetone and the acyl ketene.²⁹ This can either reform the TMD **3.6** (pathway 1, Scheme 39) or with the introduction of a new ketone, can form a modified acyl ketene precursor (pathway 2, Scheme 39).³⁰ [4+2] and [2+2] cycloadditions are also possible and can form various HDA products (pathway 3, Scheme 39).³¹ [2+2] cycloadditions are thermally allowed due to the orthogonally p-type orbitals that can twist to give favourable overlap thus allowing a commonly disallowed transformation via thermal conditions.^{32,33} In the presence of a nucleophile, the formation of a β-keto species is readily formed due to the highly electrophilic nature of the acyl ketene. Alcohol and amine nucleophiles afford the corresponding β-keto esters and β-keto amides, respectively (pathway 4, Scheme 39). In the absence of a nucleophile the acyl ketene self-dimerises to form dehydroacetic acid **3.8** (pathway 5, Scheme 39).³⁰ TMD **3.6** is a highly versatile reagent that has been modified and used as a synthetic tool towards a range of API's and synthetic targets.^{34–}

3.2.3 Harnessing acyl ketenes in flow

Due to the reactive nature of the acyl ketene **3.7**, flow chemistry has been developed to explore the uses of this interesting reagent in a controlled, safe, and continuous manner. Due to the high temperatures required to thermally decompose TMD **3.6**, flow systems require sealing under high pressure to enable the superheating of solvents to access such temperatures. Within a sealed reactor, the acetone by-product cannot evolve from the reaction and an equilibrium is established with the acyl ketene (as previously discussed in Scheme 39). In 2019, our research group hijacked this equilibrium in flow to modify the TMD **3.6** precursor via addition of various ketones (Scheme 40).

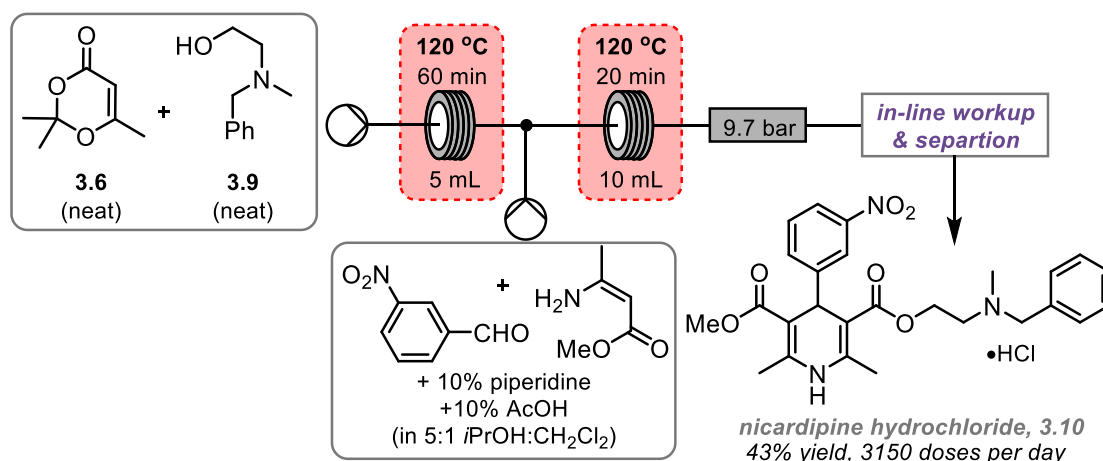


Scheme 40 – Hijacking the equilibrium to afford various acyl ketene precursors

This is an excellent example demonstrating how changing the reactor design gains access to new reactivity. In batch conditions, heating this reagent to afford the acyl ketene would normally involve the removal of acetone via boiling. However, when translating this system to flow, we found that the formation of the acyl ketene is reversible thus open to interception. By introducing various ketones, a range of acyl ketene precursors could be synthesised in moderate to good yields. Formation of the dehydroacetic acid dimer product **3.8** was a competing reaction and is shown in grey. These new acyl ketene precursors were tested with a nucleophilic ketene trap at various temperatures to test whether the new precursor could be activated at a lower temperature, with respect to TMD **3.6**. We found that the 8-membered derived acyl ketene precursor could thermally decompose to form 90% β -keto ester product at 100 °C, which was assumed to be due to the added ring strain induced from the 8-membered ring.³⁰

The use of flow chemistry for acyl ketene formation using TMD **3.6** comes with additional considerations when designing a flow reactor. As previously discussed, a sealed system

prevents the loss of the acetone by-product and when setting up a reaction one must consider how acetone may influence the reactivity of the desired reaction. In 2018, Jensen and co-workers developed a continuous flow platform for the synthesis of pharmaceuticals. In the synthesis of nicardipine hydrochloride **3.10**, the use of TMD **3.6** was employed to afford the *in situ* formation of acyl ketene **3.7** and subsequently make their desired β -keto ester intermediate as part of their telescoped continuous synthesis (Scheme 41).



Scheme 41 – Telescoped flow synthesis using TMD **3.6** as starting material via acyl ketene intermediate for nicardipine hydrochloride **3.10**

The authors used TMD **3.6**, as an acyl ketene precursor, and a substituted alcohol **3.9**, as a ketene trap in neat conditions. Under high temperature and pressure, the acyl ketene was formed *in situ* and quenched via the nucleophilic attack of the alcohol **3.9** to afford a β -keto ester intermediate. With the introduction of Hantzsch dihydropyridine components and conditions, the β -keto ester intermediate was subsequently reacted in a multi-component reaction. Two in-line work-up and membrane separation processes were installed downstream to afford nicardipine hydrochloride in 43% which could provide 3150 doses of the drug in a day. This example has shown that the acyl ketene product was benign in the subsequent reactions and the chemical compatibility had been considered when designing this reactor.³⁷

Flow chemistry can facilitate the safe handling and thermal control required for chemically manipulating acyl ketenes as reactive intermediates. The ability to pressurise flow systems easily allows the superheating of a range of organic solvents to reach temperatures required for the thermal decomposition of TMD **3.6**, otherwise unobtainable under batch conditions.

3.2 Aims and Objectives

After exploring the use of *in situ* generated acetylene gas in flow, it was postulated whether the gaseous reactive intermediate could be reacted with another *in situ* generated acyl ketene reactive intermediate. Liberating these reactive intermediates together in flow was deemed an interesting reactor design experiment in the hope that they would quench their reactivity via a cycloaddition. The initial exploration was to test whether high temperature and pressure conditions could safely combine very reactive species that could not be facilitated under batch conditions.

Further to this, the TMD **3.6** is an interesting reagent, and this chapter explores and develops its reactivity under continuous processing with a focus to create a productive system of desired compounds that could be further functionalised. By utilising flow chemistry, the secondary aim of this project was to demonstrate and explore acyl ketene generation in flow to scale synthetically useful chemical feedstocks.

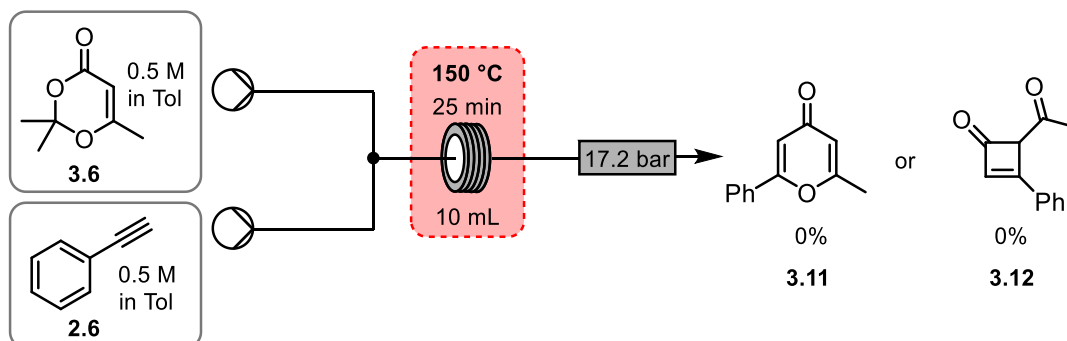
3.3 Results and Discussion

3.2.1 Discovery and reactivity of the acyl ketene

[4+2] and [2+2] Cycloadditions

To test whether acetylene gas and an acyl ketene would react together to form either a pyrone **3.11** or cyclobutenone **3.12**, phenyl acetylene **2.6** was first tested. Phenyl acetylene **2.6** is an easy-to-handle alternative before attempting a vastly more complex flow system to generate acetylene gas from calcium carbide (Chapter 2).

Temperatures >120 °C were known to thermally decompose TMD **3.6** into acyl ketene **3.7** which can undergo two different cycloadditions: a [4+2] cycloaddition or a [2+2] cycloaddition. It was envisaged that TMD, **3.6**, would thermally decompose to form the acyl ketene *in situ* and react with phenyl acetylene. The acyl ketene could either form a γ -pyrone (**3.11**, Scheme 42), via a [4+2] cycloaddition, or, due to the orthogonal π -orbitals, a thermally allowed [2+2] cycloaddition affording cyclobutenone **3.12**. This reactivity has been explored in literature, however, alkyne reactivity has not.^{32,33} The reaction was established in toluene with a BPR to keep the reaction under high pressure thus allowing the solvent to be super-heated to the required temperature for thermal decomposition (Scheme 42).



Scheme 42 – Initial design to synthesise either a γ -pyrone or cyclobutenone in flow

Unfortunately, the reaction did not yield **3.11** and/or **3.12** which could be due to the short reaction time or improper ratio of reagents. After purifying the reaction mixture, 13% TMD **3.6** was recovered and coupled with GC-MS analysis and confirmed by ^1H NMR, 30% was found to be the self-hetero Diels-Alder product, dehydroacetic acid **3.8** (Figure 20).

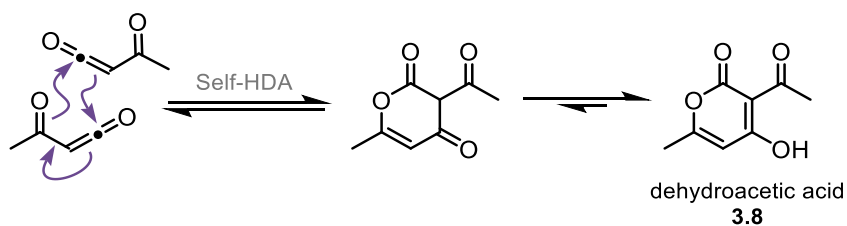
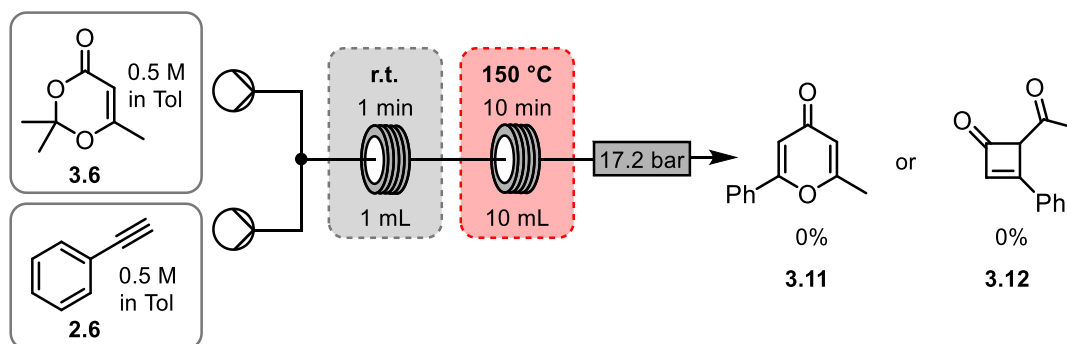


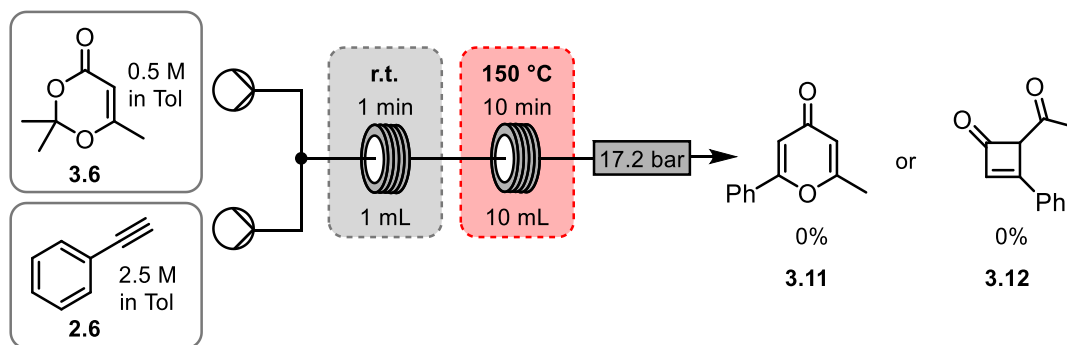
Figure 20 – Illustration of the self-hetero-Diels-Alder to form the dimerised dehydroacetic acid

With the presence of the dimerised product **3.8** found, it implied that the *in situ* generated acyl ketene is very reactive and readily reacts with itself. At a total flow rate of 0.4 mL/min, the flow was laminar and therefore the mass transfer between the two reagents is passive leading to poor mixing. A pre-mixing coil was tested to ensure the reagents were fully mixed before entering the hot coil to reduce the self-HDA (Scheme 43).



Scheme 43 – Installation of pre-mixing coil

The design of this reactor yielded no desirable products and the GC-MS showed the reaction profile to contain 4 products: acetone, phenyl acetylene **2.6**, TMD **3.6**, and dehydroacetic acid **3.8**. It was certain that the acyl ketene was being formed *in situ* due to the presence of both: acetone, the by-product of thermal decomposition, and the dimer **3.8**. Increasing the concentration of phenyl acetylene increases the probability of the acyl ketene interacting with the alkyne as opposed to itself (Scheme 44).



Scheme 44 – Changing equivalence of phenyl acetylene

Incorporating 5 equivalents of phenyl acetylene **2.6** had no effect on the reaction profile and showed the same 4 products as the previous example (Scheme 44). Increasing the equivalents of phenyl acetylene to 10 equivalents (10 M, **2.6**) also gave no appreciable difference in the reaction outcome. Different dienophiles were tested to evaluate whether more electron rich systems would interact with the acyl ketene more favourably. Formation of a cyclobutenone ring seemed highly ambitious due to the increased ring strain of 3 sp^2 centres out of the 4 centres available. Therefore, different substrates were considered that would synthesise either stable 6-membered ring systems or less strained cyclobutanone rings via a [4+2] cycloaddition or a [2+2] cycloaddition, respectively (Figure 21).

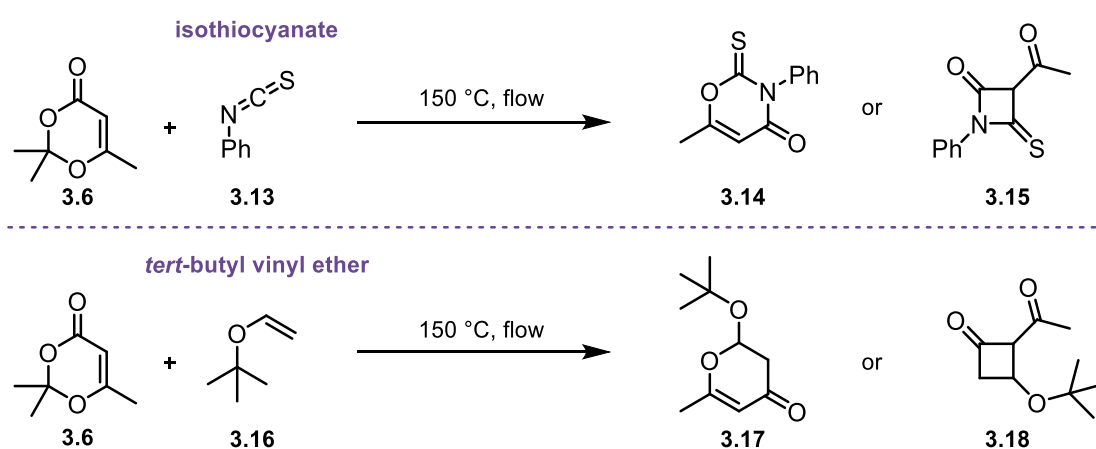


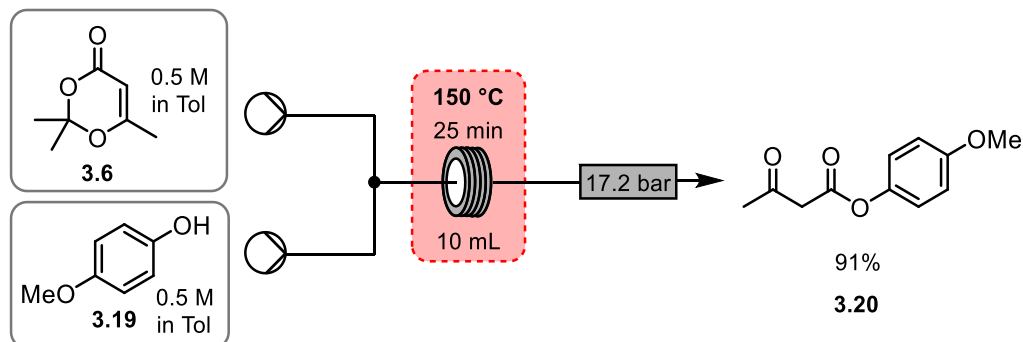
Figure 21 – Predicted products formed from varying substrates process in heated flow system

Both the reactions (Figure 21) did not yield the desired products, it is known that isocyanates can react with ketenes to form 1,3-oxazin-2,4-diones and therefore it was postulated that a similar reactivity would occur with isothiocyanate **3.13** affording the 6-membered product **3.14**.^{30,38,39} The 4-membered ring product **3.15** is unlikely to form, via a [2+2] cycloaddition, over the 6-membered ring due to the ring strain present in the 4-membered product. Interestingly, the *tert*-butyl vinyl ether **3.16** or similar has been used to form γ -pyrones **3.17** and cyclobutanone ring **3.18** before and was expected to work in the [4+2]/[2+2] cycloaddition.^{40,41} However at high temperatures, it was evident from the GC-MS that the *tert*-butyl vinyl ether **3.16** decomposed to form *tert*-butoxide *in situ* which trapped the acyl ketene forming the *tert*-butyl β -keto ester via nucleophilic attack.

3.2.2 Exploring various ketene traps

After the unsuccessful exploration of cycloaddition reactions with acyl ketene **3.7**, trapping the acyl ketene with various nucleophiles were tested. The formation of β -keto esters are known in the literature and can be carried out in large scale reactions (e.g. ~50 mmol) to yield synthetically useful β -keto ester products.²⁷ To translate these

conditions to a flow process a system was designed that would generate and then consume the acyl ketene *in situ* (Scheme 45).



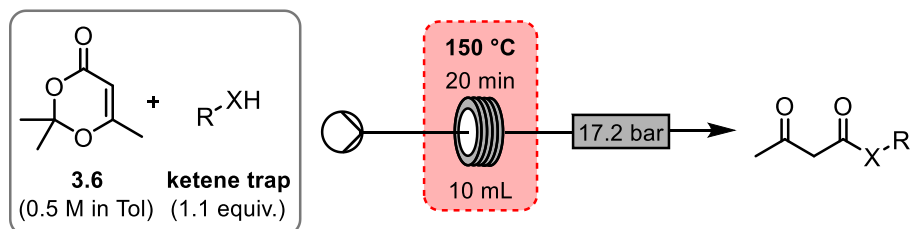
Scheme 45 – Synthesis of a β -keto ester from an acyl ketene precursor and *p*-methoxy phenol

These initial results demonstrated the formation of the β -keto ester **3.20** from *p*-methoxy phenol **3.19** and acyl ketene precursor **3.6**. Pleasingly, the hot coil decomposed TMD **3.6** into the acyl ketene *in situ* which was trapped with nucleophilic *p*-methoxy phenol. This shows that dominant reactivity, under these conditions, is preferably nucleophilic attack of the acyl ketene than a cycloaddition tested previously. A control reaction was explored, and the above reaction (Scheme 45) was repeated at 90 °C and gave 0% β -keto ester product. This shows that the β -keto ester is accessed through an acyl ketene intermediate via thermal decomposition of TMD **3.6** and temperatures below 100 °C cannot thermally decompose TMD **3.6**.

A visiting international PhD student, Renan Galaverna, worked closely on this project also and continued to explore various β -keto esters/amide/thioesters depicted in the following section. I initially designed, built, and ran the previous experiments and Renan used the system I created to further explore the β -keto compounds.

β -keto compound formation

The ketene trap and TMD **3.6** could be pre-mixed before being processed in the flow system due to the 150 °C activation temperature required (Scheme 46).



Scheme 46 – Design of flow system to facilitate ketene trap reactions forming β -keto compounds

The transformation took 20 min at 150 °C to afford excellent yielding β -keto compounds (Figure 22).

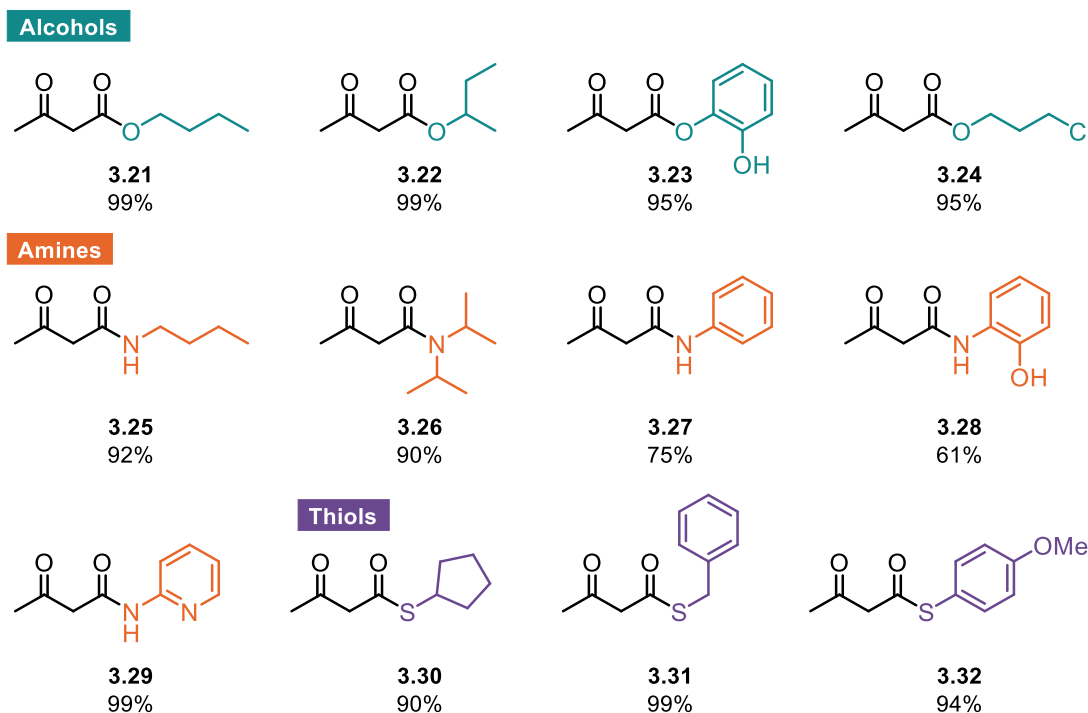


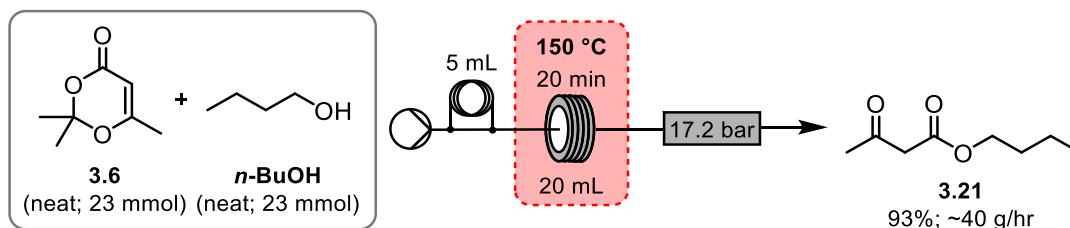
Figure 22 – Various ketene traps tested – results provided by Renan Galaverna

All primary, secondary, and aromatic alcohols gave excellent yields >95% illustrating the extremely electrophilic properties of the acyl ketene. A range of amines were also explored, demonstrating that primary, secondary, and aromatic amines can be used to form β -keto amides. A reduction in yield of 75% occurred for β -keto amide **3.27** which is most likely due to the reduction in the nucleophilicity of aniline due to the nitrogen's lone pair of electrons being conjugated into the aromatic system. A 61% yield was found for β -keto amide **3.28**, which showed preference for the formation of the amide rather than the ester using the phenolic alcohol group. The thiols also exhibited the same reactivity as the alcohols did thus demonstrating the versatile range of β -keto compounds which can be made using this flow process. β -Keto ester **3.21** was also scaled up and ran continuously for 160 minutes to yield 12.6 g of β -keto ester **3.21** at 98% purity after a short silica plug. This scaled up reaction spurred on the exploration of neat conditions thus utilising the continuous nature of flow chemistry and the experimental ease of scaling up the reaction. Under the current conditions for the scale up reaction, the productivity was 4.7 g/hr.

Increasing the productivity and expansion of β -keto ester scope

Both TMD **3.6** and alcohols are mostly liquids, and it was therefore explored whether this reaction could be processed neat which would greatly increase the productivity of the flow reaction. All β -keto esters formed (Figure 22) were also found to be liquid and therefore the risk of solid blockages in the flow tubing was minimised. To examine neat

conditions, the previous flow system was used and a 5 mL sample loop was loaded with a 1:1 molar ratio of TMD **3.6** and *n*-butanol. This neat reagent mixture was carried through the flow system using THF and an aliquot of the reaction mixture slug was collected and purified (Scheme 47).



Scheme 47 – Flow system using neat reagent conditions to yield β -keto ester **3.21** (Flow System 3.1)

The reaction successful yielded **3.21** in 93% which corresponds to ~40 g/hr productivity which is approximately ten times the productivity of the previous β -keto ester scope (4.7 g/hr, Figure 22). Unfortunately, when expanding the scope of this neat process the *tert*-butyl alcohol example decomposed in the hot coil to produce vast quantities of gas, presumably butene gas. Solid depositions were also found to block the BPR and it was decided to add solvent to the reagent to avoid these safety risks. It was found that a concentration of 2.5 M in THF worked effectively to increase productivity whilst avoiding a blocking risk. Various alcohol ketene traps were explored at this new concentration with a focus on productivity (Figure 23).

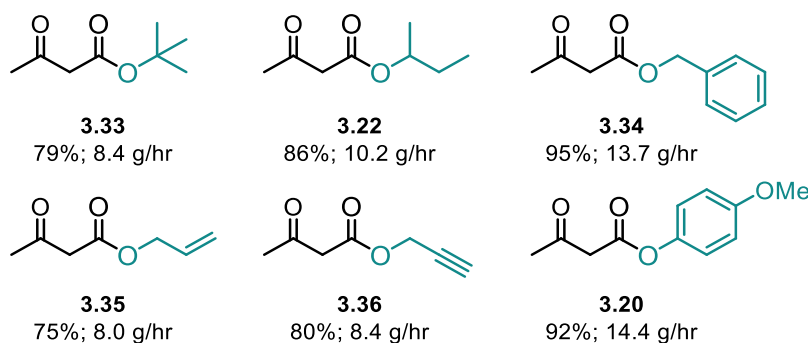


Figure 23 – Increasing the productivity for β -keto ester synthesis in flow

The average productivity of the scope was 10.5 g/hr which is over twice as productive as the scale up reaction originally explored by Dr Galaverna *et al* (4.7 g/hr).³⁰ β -Keto esters are useful feedstocks for various reactions and therefore, both **3.35** and **3.36** were designed to have synthetically useful chemical handles which is discussed further in section 3.2.3, post functionalisation reaction - Biginelli.

In summary, a standard procedure to synthesise β -keto esters successful in flow was created. High yield and productivity were accomplished whilst generating a reactive

intermediate, acyl ketene, *in situ* which was trapped safely under high temperature and pressure using common nucleophilic sources.

Coumarin formation

Exploring the generation of the acyl ketene **3.7** and its reactivity, it was found to react pleasingly with 4-methyl salicylaldehyde **3.37** to yield 3-acetyl substituted coumarins. The reaction was found to succeed with triethyl amine as supporting base (Figure 24).

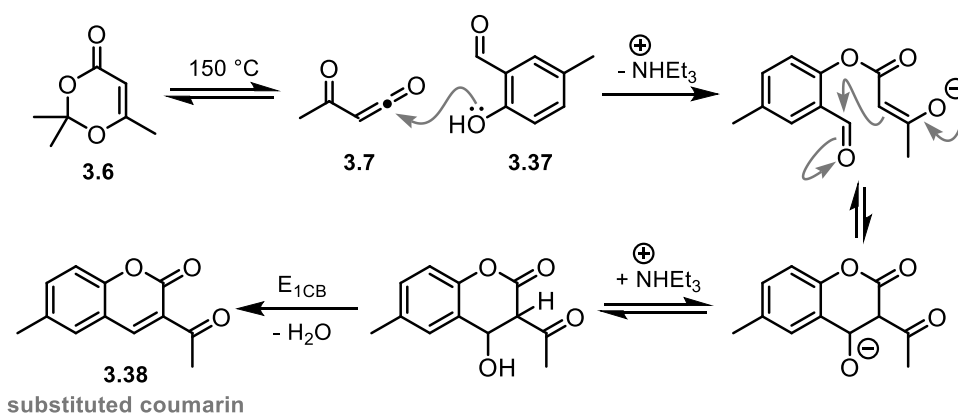
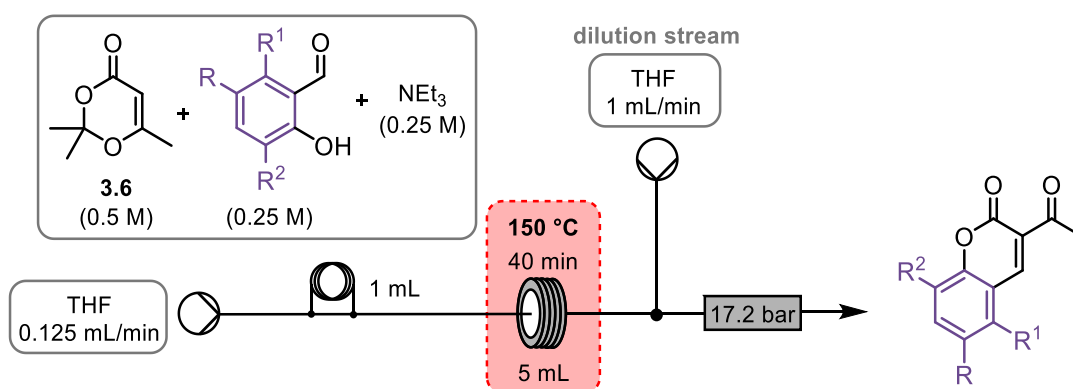


Figure 24 – Proposed mechanism for formation of coumarin from acyl ketene and salicylaldehyde

Initially, the TMD **3.6** decomposes to form the acyl ketene **3.7** at 150 °C which is attacked by the phenol of 4-methyl salicylaldehyde **3.37** to form an enolate intermediate. The C-2 enolate condenses onto the aldehyde to form a 6 membered ring which, after an E_{1CB} , forms the 3-acetyl coumarin compound **3.38**. The flow system was adapted to facilitate successful synthesis of various coumarin species (Scheme 48).



Scheme 48 – Flow system for the synthesis of substituted 3-acetyl coumarins

TMD **3.6**, substituted salicylaldehyde, and NEt_3 were premixed in a loading loop and pumped into the hot reactor coil. The coumarin products were found to be rather insoluble and a dilution stream of THF was installed to prevent precipitation blocking the BPR and tubing. Renan Galaverna explored the various substituted salicylaldehydes and their corresponding coumarins using the new flow conditions (Figure 25).

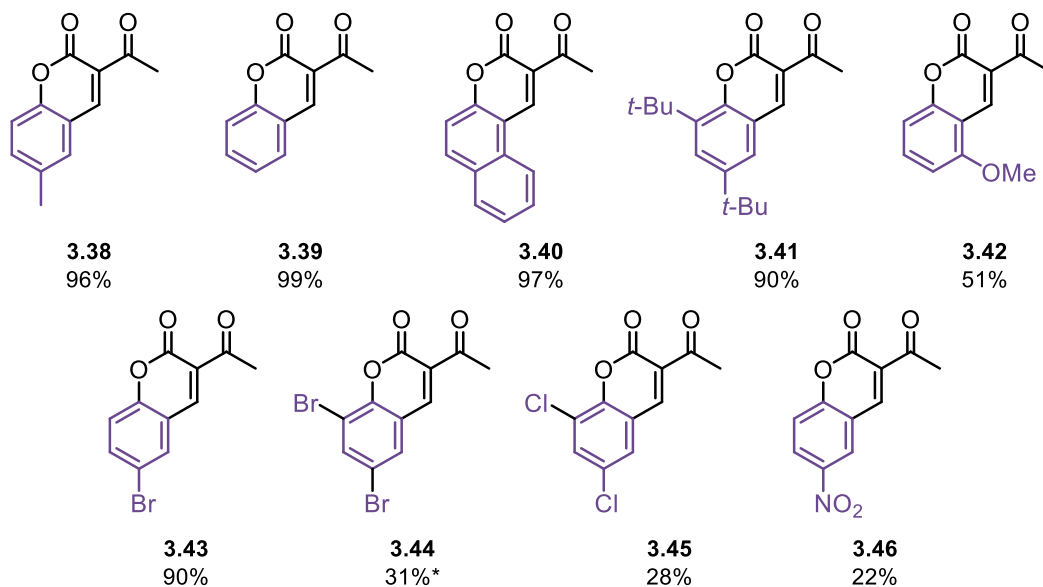


Figure 25 – Varying the salicylaldehyde component to synthesise substituted coumarins – compounds were synthesised by Renan Galaverna; *Reaction ran at 0.125 M due to insolubility of coumarin

Varying the electronics and sterics of the salicylaldehyde explored the scope of the coumarin reaction using the designed flow system. Using electronic rich/neutral salicylaldehydes (**3.38/3.39/3.40**) gave excellent yields >96%. The steric encumbrance of the *ortho*-*t*-Butyl group on **3.41** did not have a high detrimental effect on the yield and successfully yielded 90% of the desired coumarin. A reduced yield of 51% for **3.42** was observed, possibly due to the electron donating properties of the *ortho*-methoxy group reducing the electrophilicity of the aldehyde thus negatively impacting the secondary condensation reaction to form the coumarin. Halogenating the coumarin was explored as an interesting substrate that could be further derivatised as a coupling partner via metal coupling reactions. The *para*-bromo example worked successfully, yielding 90% **3.43**, however, the dibromo substrate **3.44** initially failed due to the solubility of the coumarin forming a precipitate in the flow tubing. It was necessary to dilute the reaction to 0.125 M to avoid any blockages in the reaction. A modest yield of 31% was found for **3.44** which can be attributed to the solubility of the reagent in THF or the electron withdrawing effect reducing the reactivity of the salicylaldehyde. A similar yield of 28% for **3.45** was found for the dichloro-substrate. The *para*-nitro coumarin **3.46** showed a low yield of 22%, mostly likely due to the electron withdrawing effect reducing the nucleophilicity of the phenolic alcohol for the initial nucleophilic attack of the acyl ketene.

γ -Functionalised acyl ketene precursors

The acyl ketene precursor was pre-functionalised before the coumarin transformation with 4-methyl salicylaldehyde **3.37**. The pre-functionalised (at the γ -position) dioxinone would afford coumarins with extended conjugation and functionalisation. Interestingly, by

altering TMD **3.6**, it probes into whether the acyl ketene can form successfully whilst being functionalised with varying electronics (Figure 26).

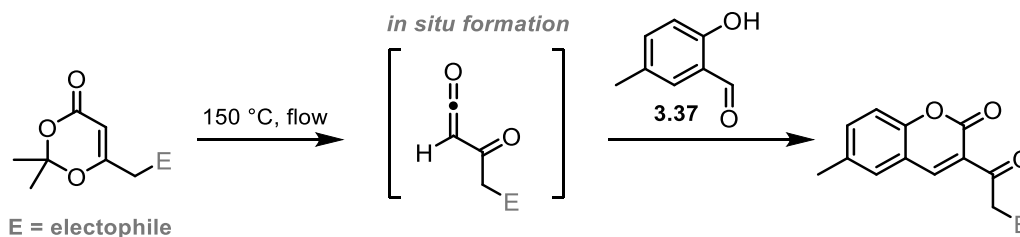
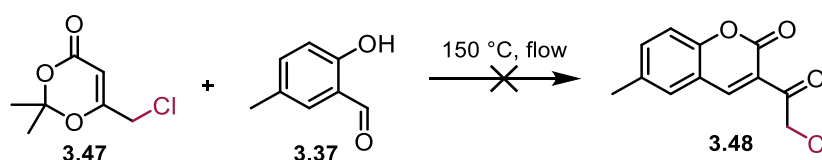


Figure 26 – Functionalisation of acyl ketene precursor affording derivatised coumarins

To synthesise the pre-functionalised dioxinones, a γ -deprotonation of TMD **3.6** occurs using LDA at $-78\text{ }^{\circ}\text{C}$ and combining with an electrophile affords the desired γ -functionalised dioxinones. Initially, electrophilic sources of halogens were explored and yielded compound **3.47** successfully, unfortunately using electrophilic bromine and fluorine did not yield the desired dioxinones (Scheme 49).



Scheme 49 – Attempted reactions to synthesise halogenated coumarin derivatives

The chloro-dioxinone **3.47** was tested and found to solely return 4-methyl salicylaldehyde **3.37** starting material and no trace of dioxinone by-products were found. The introduction of a halogen species into the acyl ketene intermediate, clearly destabilised the acyl ketene intermediate to readily decompose upon heating. In 2005, Katritzky and co-workers formed similar γ -functionalised dioxinone and, under thermal conditions, they reported the formation of 4-hydroxy-6-substituted-2-pyrones via an intramolecular cyclisation.⁴² However, these compounds were not found throughout purification of this system.

Acid chlorides were tested as electrophiles for synthesising the γ -functionalised acyl ketene precursors. Benzoyl chloride worked successfully as the electrophile and pleasingly worked in the coumarin flow synthesis reaction. When comparing the two newly made acyl ketene intermediates, it became clear that the addition of a chloro-dioxinone **3.47** species destabilises the acyl ketene whereas the benzoyl-dioxinone **3.49** stabilises the acyl ketene through additional conjugation/resonance (Figure 27).

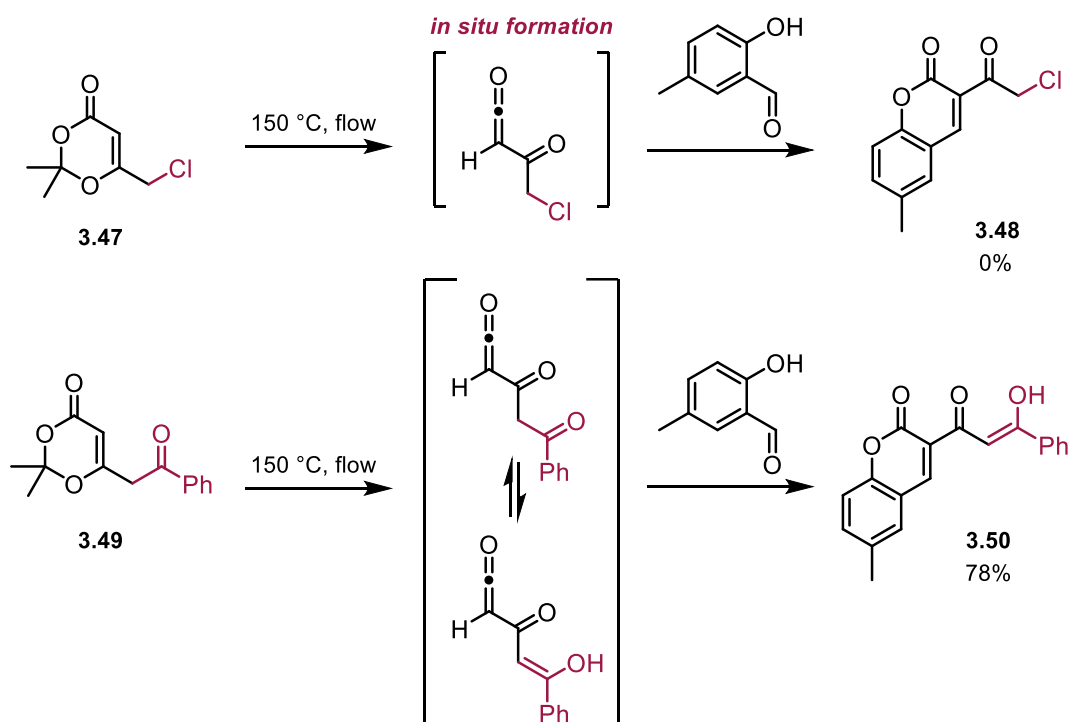
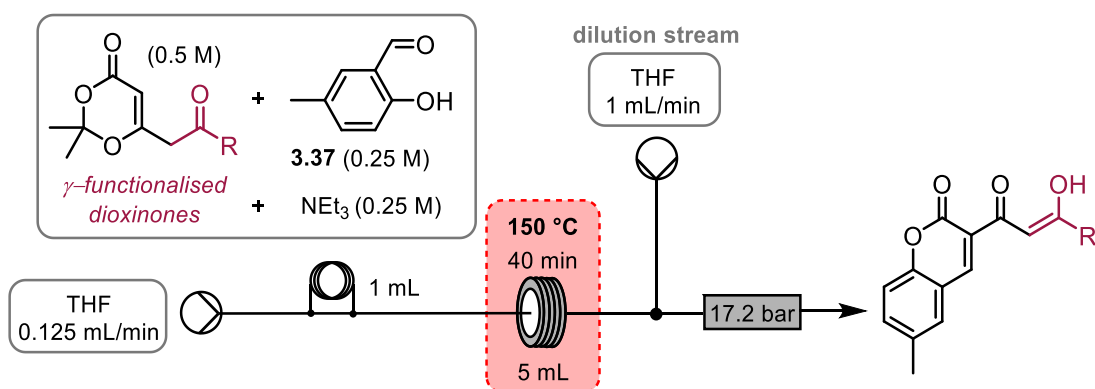


Figure 27 – Comparison between chloro acyl ketene and benzoyl acyl ketene

The increased conjugation in the acyl ketene possibly stabilises its reactivity and allows the coumarin transformation to occur successfully. This reaction was demonstrated using benzoyl dioxinone **3.49** to pleasingly yield coumarin **3.50** in 78% yield. Using a flow system that enabled high temperatures, suitable for acyl ketene formation, a scope of coumarins with extended conjugation was explored (Scheme 50).



Scheme 50 – Flow system for the synthesis of coumarins with extended conjugation (Flow System 3.2)

A novel range of coumarin structures were synthesised which used various acid chlorides as the initial electrophile for the γ -functionalisation of TMD **3.6** (Figure 28). The γ -functionalised dioxinones were prepared and purified prior to the coumarin flow reaction.

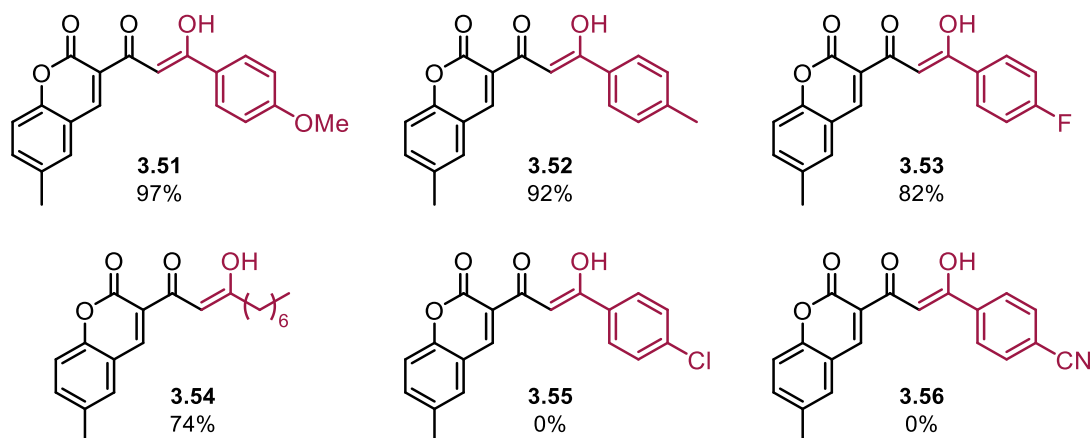


Figure 28 – Scope of coumarin reaction by varying the dioxinone component

The γ -functionalised dioxinones were heated in flow with 4-methyl salicylaldehyde **3.37** to successfully afford novel extended aromatic coumarin compounds. Electron rich aryl groups performed best, with *para*-methoxy **3.51** yielding 97%. Both **3.52** and **3.53** also gave excellent yields of 92% and 82%, respectively. An alkyl substrate was shown to successfully yield 74% of the desired coumarin product **3.54**. Unfortunately, both **3.55** and **3.56** did not yield any coumarin product for the substrates that have electron withdrawing groups. It was noted that a common by-product was being formed where the acetone in the reaction reacts with the γ -functionalised dioxinones via nucleophilic attack of the tautomeric enol of acetone to form a 1,3-dicarbonyl species (Figure 29).

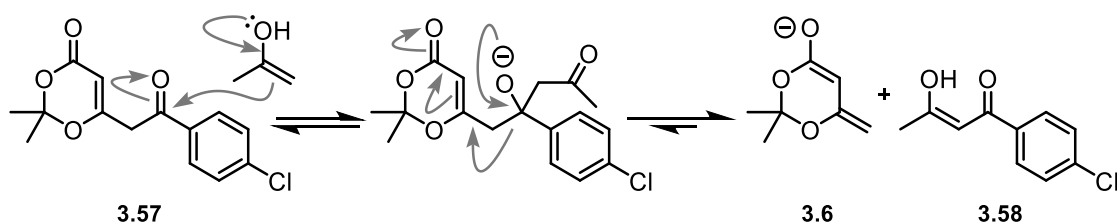


Figure 29 – Proposed mechanism for the formation of 1,3-dicarbonyls

At 150 °C, dioxinone **3.57** breaks down to form the modified acyl ketene and acetone, instead of boiling off in batch, the acetone is trapped in the flow tubing and can therefore interact with the substrates. The trapping of acetone in this transformation is a limitation to flow technology as gaseous by-products cannot escape the reaction coil. It was therefore found that **3.57** was attacked by acetone to form 1,3-dicarbonyl **3.58**. A competitive reaction was established between the acyl ketene formation and subsequent coumarin synthesis and the nucleophilic attack of acetone onto **3.57**. Preference of reaction was determined by the electron withdrawing properties of the *para*-functional group of the aryl ring. This was postulated that an increase in electron withdrawing density from the aryl ring increased the electrophilic properties of the carbonyl thus making it subject to nucleophilic attack. The dioxinone **3.57** was in excess with respect

to the salicylaldehyde **3.37** which meant that with high yielding coumarin reactions (compound **3.51**, Figure 28) 38% of the corresponding 1,3-dicarbonyl **3.60** was obtained, however, the 1,3-dicarbonyl **3.58** for compound **3.57** was found to yield 77% and 0% coumarin **3.55** (Figure 30).

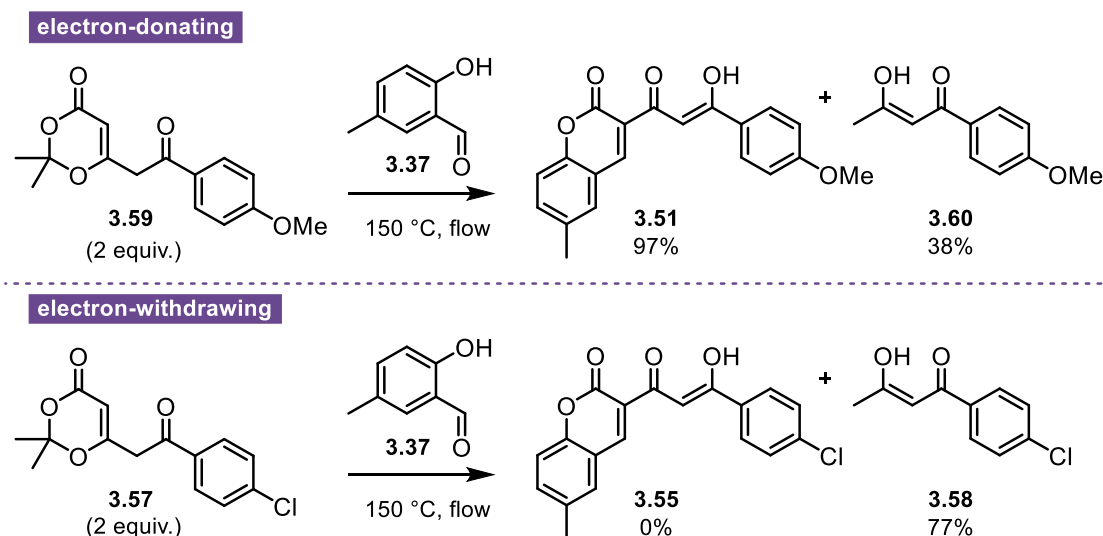


Figure 30 – Proposed mechanism for the formation of 1,3-dicarbonyls

Keeping the reaction conditions the same, there is a switch in reactivity which is clearly determined by the changing substrate. Throughout the coumarin scope the yield of 1,3-dicarbonyl did vary and was always present due to the γ -functionalised dioxinones being in excess to the salicylaldehyde. Perhaps unwisely, the design of this flow reactor facilitates the trapping of acetone into the superheated solvent mixture rather than boiling off in a batch reactor.

In summary, the exploration of the TMD reagent **3.6** in flow was developed and demonstrated its versatile nature as a feedstock for formation of β -keto esters/amides. This reactivity can be extended to synthesise coumarins, if using salicylaldehyde as the ketene trap. It was observed that the coumarin scope could be extended by functionalising TMD **3.6** via γ -deprotonation and subsequent C4-enolate attack of an acid chloride. These functionalised acyl ketene precursors showed alternating reactivity depending on the electron-withdrawing properties of *para*-functional groups on the aryl ring. Electron withdrawing groups preferred formation of a diketone species and electron donating groups favoured coumarin formation in identical reaction conditions.

3.2.3 Post-functionalisation reaction – Biginelli

A short introduction to the Biginelli reaction

The focus of the project turned to the exploration of β -keto esters as a useful feedstock for the multi-component reaction, the Biginelli reaction. β -Keto esters also have various

uses for other synthetic methodologies, such as, pyrazole/pyridine/heterocyclic synthesis.^{43,44} Knowing that the β -keto esters could be synthesised, in some cases, neat and at high yield in the above optimised configuration, it was postulated whether this flow system could be paired with microwave technology. This would create a tandem process that synthesises a feedstock reagent in flow and after subsequent distribution of the β -keto ester in multiple microwave vials (with the addition of other Biginelli reagents) create a compound library, utilising the automated robotic function of the microwave reactor (Figure 31).

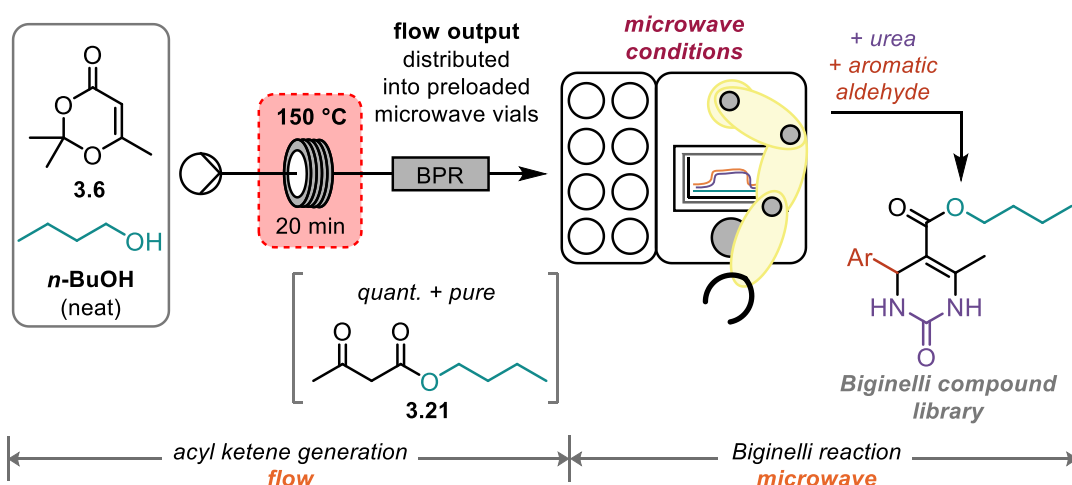


Figure 31 – Tandem flow-microwave synthesis of β -keto ester and subsequent Biginelli reaction

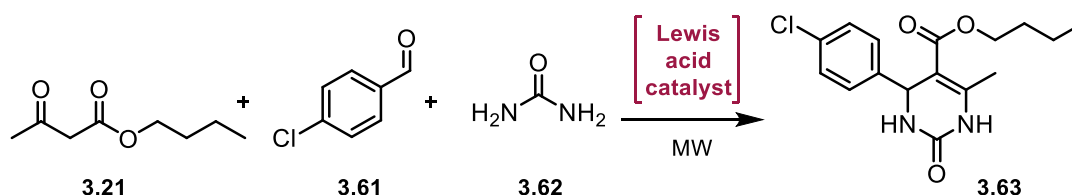
It was postulated whether the output of the optimised β -keto ester flow system could be coupled with microwave technology in a tandem sequence. The neat pure β -keto ester product would be pumped and distributed over various microwave vials with corresponding Biginelli reaction components.

The Biginelli reaction is a multi-component reaction that requires a β -keto ester, urea/thiourea, and an aldehyde species in the presence of a Lewis acid and/or a Brønsted acid. The Biginelli chemical motif can be found in pharmaceutical drugs as it has been used as a calcium channel blocker, useful against hypertension.⁴⁵ Various Lewis/Brønsted acids have been explored to assist the multicomponent reaction that most commonly takes place in an alcoholic solvent. More recently, microwave chemistry has been utilised to explore solvent-free synthesis of Biginelli compounds at reduced reaction times thus increasing the productivity.^{46–53}

Creating neat conditions, with a tailored catalyst system, for the tandem synthesis of a library of Biginelli compounds was the primary aim of this section of post-functionalising the β -keto ester feedstock, previously synthesised by the acyl ketene flow system.

Optimisation of Biginelli reaction

The formation of dihydropyrimidinones (DHPMs) or Biginelli compounds in the microwave is a known area of chemistry, however, microwave conditions for our tandem flow-microwave process had yet to be found and with various conditions in the literature giving fluctuating yields, an optimisation for our system was deemed necessary (Scheme 51).⁵¹ Reaction conditions were also not known in the literature for the β -keto esters synthesised in the previous section.



Scheme 51 – Biginelli reaction profile to synthesise dihydropyrimidinones

The Biginelli transformation to be optimised was initially tested with known conditions using $\text{FeCl}_3 \cdot 6\text{H}_2\text{O}$ (10 mol%) as a Lewis acid and acetic acid (4 equiv.) as a Brønsted acid. There have been reports on using different solvents or solvent-free synthesis and these varying conditions were tested (Table 8).

Table 8 - Initial tests on solvent and concentration

Entry	3.21 (equiv.)	3.61 (equiv.)	3.62 (equiv.)	Temp. (°C)	Time (min)	Solvent	3.63 yield ^a
1	1.0	1.0	1.5	120	10	EtOH (1 M)	42%
2	1.0	1.0	1.5	120	10	MeCN (1 M)	43%
3	1.0	1.0	1.5	120	10	MeCN (0.5 M)	32%
4	1.0	1.0	1.5	120	10	Neat	65%

Reaction conditions: $\text{FeCl}_3 \cdot 6\text{H}_2\text{O}$ (10 mol%), AcOH (4 equiv.); a = yield determined by internal ^1H NMR standard

After a small screen of common solvents for this transformation it was found that neat conditions were the most favourable. This multi-component reaction requires all three substrates to come together and therefore it is predictable that the most concentrated conditions would give the best probability of all substrates coming together hence why neat conditions worked best at 65% (entry 4, Table 8). Neat conditions were kept throughout the optimisation. Temperature, time, and catalyst loading was explored next to increase the yield (Table 9).

Table 9 - Temperature, time, and catalyst loading screen

Entry	3.21 (equiv.)	3.61 (equiv.)	3.62 (equiv.)	Catalyst (mol%)	Temp. (°C)	Time (min)	3.63 yield ^a
1	1.0	1.0	1.5	FeCl₃•6H₂O (10)	120	10	65%
2	1.0	1.0	1.5	FeCl ₃ •6H ₂ O (10)	100	10	58%
3	1.0	1.0	1.5	FeCl ₃ •6H ₂ O (10)	150	10	42%
4	1.0	1.0	1.5	FeCl ₃ •6H ₂ O (10)	120	20	65%
5	1.0	1.0	1.5	FeCl ₃ •6H ₂ O (15)	120	10	64%
6	1.0	1.0	1.5	FeCl ₃ •6H ₂ O (20)	120	10	64%

Reaction conditions: neat; AcOH (4 equiv.); a = yield determined by internal ¹H NMR standard

Reducing and increasing the temperature of the reaction both had a detrimental effect on the yield (entries 2 and 3, Table 9). Increasing the temperature to 150 °C would cause the β -keto ester **3.21** to boil thus increasing the concentration of the ester in the headspace of the reaction vial. Doubling the reaction time to 20 min gave no appreciable change to the yield (entry 4, Table 9). Furthermore, increasing the catalyst loading gave no significant change to the yield also (entries 5 and 6, Table 9). The stoichiometry of the reaction was next explored to see if an excess of β -keto ester **3.21** would drive this reaction to completion (Table 10).

Table 10 – Equivalence of β -keto ester tested

Entry	3.21 (equiv.)	3.61 (equiv.)	3.62 (equiv.)	Catalyst (mol%)	Temp. (°C)	Time (min)	3.63 yield ^a
1	1.0	1.0	1.5	FeCl ₃ •6H ₂ O (10)	120	10	65%
2	1.5	1.0	1.5	FeCl₃•6H₂O (10)	120	10	80%
3	1.75	1.0	1.5	FeCl ₃ •6H ₂ O (10)	120	10	70%
4	1.25	1.0	1.5	FeCl ₃ •6H ₂ O (10)	120	10	73%

Reaction conditions: neat; AcOH (4 equiv.); a = yield determined by internal ¹H NMR standard

Increasing the equivalents of β -keto ester **3.21** available to 1.5 equiv. pleasingly gave 80% yield by ¹H NMR. The mechanism of this reaction shows the reaction is in equilibrium and therefore the addition of more β -keto ester **3.21** to the reaction has driven the equilibrium to favour the desired product **3.63** (entry 2, Table 10). Changing the excess of β -keto ester **3.21** showed a slight increase in yield from 1 equiv. (entries 3 and 4, Table 10). The role of additive in this reaction is to act as a proton shuttle for activating the β -keto ester **3.21** for nucleophilic attack and aiding the E_{1CB} final condensation. It was important to probe the parameters of the additive and test whether changing the equivalents of acetic acid would affect the reaction (Table 11).

Table 11 – Additive equivalence and screen

Entry	3.21 (equiv.)	3.61 (equiv.)	3.62 (equiv.)	Catalyst (mol%)	Additive	3.63 yield ^a
1	1.5	1.0	1.5	FeCl ₃ ·6H ₂ O (10)	none	31%
2	1.5	1.0	1.5	FeCl ₃ ·6H ₂ O (10)	AcOH (2 equiv.)	74%
3	1.5	1.0	1.5	FeCl₃·6H₂O (10)	AcOH (4 equiv.)	80%
4	1.5	1.0	1.5	FeCl ₃ ·6H ₂ O (10)	AcOH (8 equiv.)	64%
5	1.5	1.0	1.5	-	AcOH (4 equiv.)	58%
6	1.5	1.0	1.5	FeCl ₃ ·6H ₂ O (10)	AcOH (4 equiv.) + MgSO ₄ (2 mmol)	60%
7	1.5	1.0	1.5	FeCl ₃ ·6H ₂ O (10)	AcOH (4 equiv.) + MgSO ₄ (0.3 mmol)	72%
8	1.5	1.0	1.5	FeCl ₃ ·6H ₂ O (10)	conc. HCl (4 equiv.)	10%

Reaction conditions: neat; 120 °C; 10 min; a = yield determined by internal ¹H NMR standard

Removing acetic acid from the reaction had a detrimental effect on the yield resulting in a 31% yield (entry 1, Table 11). This demonstrated that the Brønsted acid played a vital role in both further activating the ketone of the β-keto ester **3.21** and the final elimination. Both 2 and 4 equivalents of acetic acid showed good yields with 4 equivalents being optimal (entries 2 and 3, Table 11). Acetic acid could also play a role as a solvent for this reaction and therefore reducing the equivalents could be viewed as increasing the concentration of the reaction which should be beneficial, however, reduction to 2 equivalents did not improve the yield. Interestingly, 8 equivalents of acetic acid reduced the yield significantly to 64% which could be due to the vast amounts of acid diluting the reaction mixture and therefore reducing the probability of all three components reacting (entry 4, Table 11). A control experiment was tested by removing the catalyst from the reaction to illustrate the necessity of the catalyst; with only acetic acid (4 equiv.) the reaction yielded 58% showing that the Lewis acid is required to further activate β-keto ester **3.21** and subsequent imine (entry 5, Table 11). The final stage of the mechanism requires the removal of water, via a conjugated-base elimination, and it was postulated that adding magnesium sulfate as a drying agent would drive the reaction to completion. This decision was based on Le Chatelier's principle of removing the water by-product from the reaction would push the equilibrium to favour product formation. Unfortunately, adding MgSO₄ (2 equiv.) gave a reduced yield of 60% (entry 6, Table 11). This could be attributed to the filling of the reaction vial, with no solvent present and a large amount of magnesium sulfate, the reaction mixture was not homogenous and therefore resulting in very poor mixing. Despite reducing the equivalents of MgSO₄ the yield remained at 72%

and the use of drying agents was not explored further (entry 7, Table 11). Finally, the original synthesis used HCl as the acid additive, therefore, HCl was tested and with this system it gave a detrimental yield of 10% (entry 8, Table 11).⁴⁵ This could be due to the stronger acid hydrolysing β -keto ester **3.21** thus inhibiting the reaction. Owing to the vast range of literature describing various successful Lewis acid catalysts, a catalyst screen was explored (Table 12).

Table 12 – Lewis acid catalyst screen

Entry	3.21 (equiv.)	3.61 (equiv.)	3.62 (equiv.)	Catalyst (10 mol%)	Additive	3.63 yield ^a
1	1.5	1.0	1.5	FeCl₃•6H₂O	AcOH (4 equiv.)	80%
2	1.5	1.0	1.5	NBS	AcOH (4 equiv.)	64%
3	1.5	1.0	1.5	TMSOTf	AcOH (4 equiv.)	67%
4	1.5	1.0	1.5	[bmim][BF ₄]	AcOH (4 equiv.)	60%
5	1.5	1.0	1.5	ZnCl ₂	AcOH (4 equiv.)	57%
6	1.5	1.0	1.5	InCl ₃	AcOH (4 equiv.)	71%
7	1.5	1.0	1.5	CuCl ₂	AcOH (4 equiv.)	71%
8	1.5	1.0	1.5	CuCl	AcOH (4 equiv.)	64%
9	1.5	1.0	1.5	Cu(OAc) ₂	AcOH (4 equiv.)	73%
10	1.5	1.0	1.5	Cu(OTf) ₂	AcOH (4 equiv.)	75%
11	1.5	1.0	1.5	Sc(OTf) ₃	AcOH (4 equiv.)	70%
12	1.5	1.0	1.5	Pyridinium triflate	AcOH (4 equiv.)	69%

Reaction conditions: neat; 120 °C; 10 min; a = yield determined by internal ¹H NMR standard

Various common Lewis acids were tested and found that FeCl₃•6H₂O gave a significant yield due to the iron (III) complex acting as an efficient Lewis acid as explored by Lu and co-workers (entry 1, Table 12).⁴⁸ Karimi and co-workers found that NBS worked as a neutral catalyst that is cheap and safe and catalysed their system successfully; in this system it yielded 64%, inferior to other compared catalysts (entry 2, Table 12).⁵⁴ Ganem and co-workers exhibited that TMSOTf worked well as an *in situ* generated Lewis acid for the Passerini multicomponent reaction. This catalyst was applied to our system and gave a 67% yield which was also inferior to the other catalysts (entry 3, Table 12). The use of an ionic liquid, [bmim][BF₄], was explored due to its emergence as an organocatalyst and an excellent media for microwave reactions as demonstrated by Chakraborti and co-workers.⁵⁵ When applied to the our transformation the ionic liquid gave a moderate yield of 60% which is significantly lower than FeCl₃•6H₂O (entry 4, Table 12). Common Lewis acids were also trialled (ZnCl₂, InCl₃, CuCl₂, CuCl, Cu(OAc)₂,

Cu(OTf)₂, and Sc(OTf)₃) and exhibited various success ranging from 57% with ZnCl₂ to 75% with Cu(OTf)₂. These catalysts presented lower yields than the iron (III) complex for the Biginelli reaction (entries 5 to 11, Table 12). Finally, a pyridinium triflate was used in the reaction and surprisingly showed a modest yield of 69% which is interesting as there is little research in the Lewis acidic ability of pyridinium triflates. There is little discussion on the role of pyridine salts/ammonium salts as catalysts for the Biginelli reaction and how it works as a catalyst.⁵⁶ Ganesan and co-workers use flexible dimeric pyridinium salts to successfully synthesise Biginelli compounds and liken their catalysts to the role ionic liquids play.⁵⁷ Kwak and co-workers used piperidinium triflates to catalyse the Biginelli reaction and proposed that the charged ammonium centre was coordinating to the ketone to activate it by a Lewis acid mechanism.⁵⁸ The various theories discussed meant that the exact role was unknown and was most likely a combination of all factors. It was also proposed, in our system, that the pyridinium triflate was acting as a proton shuttle working both as an acid and then a base. Pyridium triflates were therefore further explored to test whether these catalysts could drive the reaction to completion without the need of Brønsted acid additive (Table 13).

Table 13 – Triflate salt screen

Entry	3.21 (equiv.)	3.61 (equiv.)	3.62 (equiv.)	Catalyst (10 mol%)	Additive	3.63 yield ^a (isolated)
1	1.5	1.0	1.5	Pyridinium triflate	-	73% (76%)
2	1.5	1.0	1.5	Lutidinium triflate	-	66%
3	1.5	1.0	1.5	Collidinium triflate	-	72%

Reaction conditions: neat; 120 °C; 10 min; a = yield determined by internal ¹H NMR standard

Screening the readily available pyridine analogues found that pyridinium triflate gave the highest yield with an isolated yield of 76% (entry 1, Table 13). Both lutidinium and collidinium triflate gave lower yields which could be attributed to the steric hindrance from the ortho 2,6-dimethyl groups (entries 2 and 3, Table 13). It was important to explore some control reactions to find clarity on the reaction catalysts and the role they play in the reaction profile (Table 14).

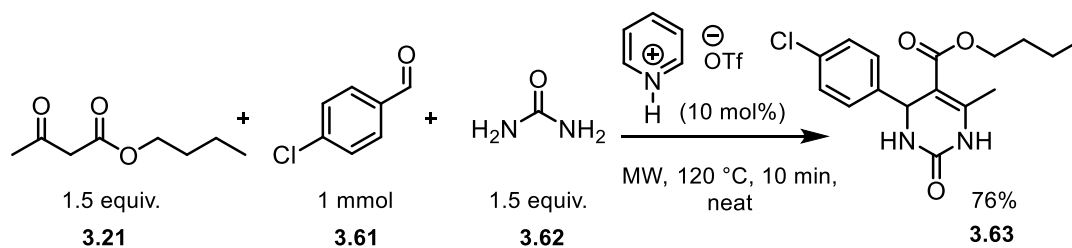
Table 14 – Control reactions

Entry	3.21 (equiv.)	3.61 (equiv.)	3.62 (equiv.)	Catalyst (mol%)	Additive (10 mol%)	3.63 yield ^a
1	1.5	1.0	1.5	-	-	9%
2	1.5	1.0	1.5	FeCl ₃ •6H ₂ O (10)	Pyridinium triflate	51%
3	1.5	1.0	1.5	Pyridine (10)	-	15%
4	1.5	1.0	1.5	Triflic acid (10)	-	53%
5	1.5	1.0	1.5	Pyridinium triflate (1)	-	43%

Reaction conditions: neat; 120 °C; 10 min; a = yield determined by internal ¹H NMR standard

The role of a Lewis acid and/or Brønsted acid in the Biginelli is vital for these reaction conditions, the absence of these reagents caused a poor product yield of 9% (entry 1, Table 14). It was investigated whether the pyridinium triflate was acting solely as an effective Brønsted acid and, with the catalytic activity of FeCl₃•6H₂O, gave a moderate yield of 51% of the desired product (entry 2, Table 14). It was postulated that the basic activity of pyridine could be beneficial to the final elimination mechanistic step and therefore pyridine (10 mol%) was tested and gave a heightened yield of 15% when compared to entry 1, 9% indicating that the pyridine has a mild influence in the reaction profile (entry 3, Table 14). The same principle was applied to triflic acid to examine whether its Brønsted acid ability was solely responsible for the high product yield, however, the yield was 53% which implies that the combination of pyridine and triflic acid, pyridinium triflate, has a stronger productive influence in the reaction than the separate moieties (entry 4, Table 14). This data supports the theory that the pyridinium triflate is acting as a proton shuffle/buffer like system that assists in activating the carbonyls/imines, either through a Brønsted or Lewis acid mechanism or both, and can also act as a base in driving the elimination step to completion. A 1 mol% catalytic system was also tested to see if the reagent could work at lower loading, unfortunately, the yield was 43% which was not optimal (entry 5, Table 14).

After the optimisation, the pyridinium triflate was chosen as the superior catalytic system due to their interesting role as both a catalyst and ionic species which has a higher dielectric value thus beneficial to microwave reactions and removing the need for acetic acid (4 equiv.) (Scheme 52).



Scheme 52 – Optimised reaction conditions for Biginelli microwave reaction

Biginelli compound library synthesis – the aldehyde component

With the optimised conditions in hand (Scheme 52) the tandem flow-microwave system could be tested to explore a varied range of compounds. Initially, a scope of various aldehydes with differing electronics were tested (Figure 32). A visiting international student, Yaoyu Ding, assisted in the synthesis of the Biginelli compound library. Yaoyu was under very strict daily supervision and each experiment was designed and vetted by myself to ensure excellent data integrity was maintained.

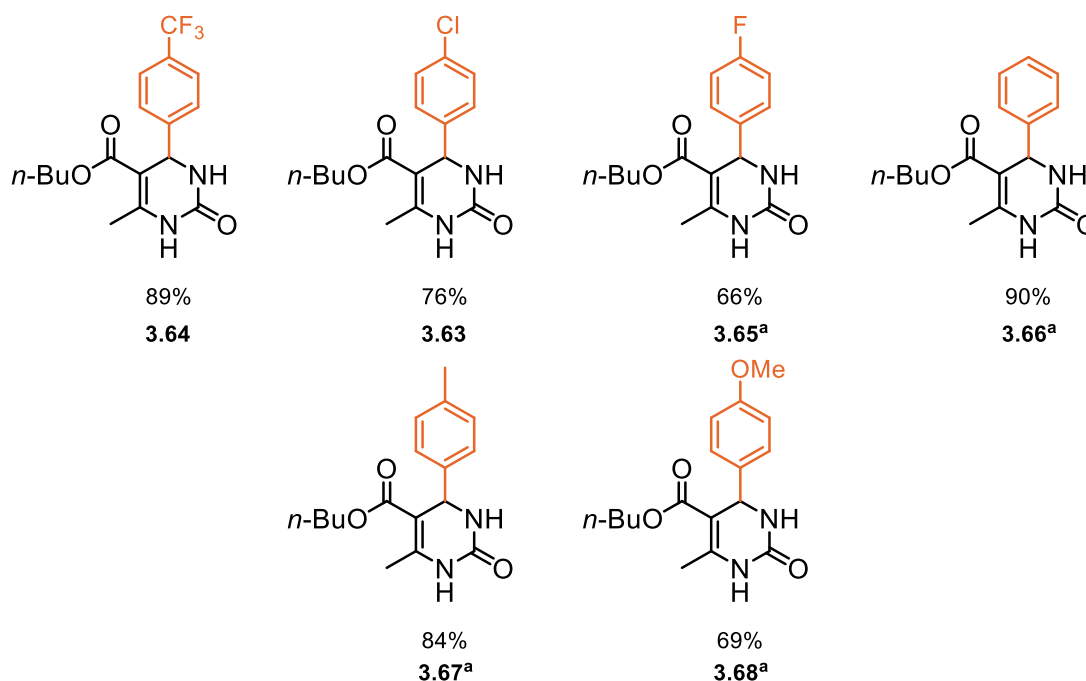


Figure 32 – Scope of various aldehydes used to form Biginelli compound library, a = compounds made by Yaoyu Ding

A range of purified aldehydes were tested and it was found that varying isolated yields of novel and known Biginelli compounds were synthesised. There are no significant trends seen throughout this set of substrates when varying the electronics. One would assume that a more electron withdrawing substituent would have a more reactive aldehyde due to the mesomeric effect. For example, DHPM **3.64** gave an excellent yield of 89% unsurprisingly due to the strongly electron withdrawing 4-trifluoromethyl

substituent further activating the aldehyde, however, DHPM **3.66** also gave an excellent yield of 90% with a relatively neutral aldehyde (benzaldehyde) and performed better than more electron withdrawn aldehydes. This data implies that the rate determining step of this reaction may not necessarily be the initial condensation of the aldehyde and the urea to form the intermediate imine. However, in the past 30 years the mechanism of this system has been thoroughly discussed with the most recently exploration deemed the initial aldehyde condensation with urea to be the rate-determining step.⁴⁷

Biginelli compound library synthesis – the β -keto ester component

Using the β -keto esters formed in section 3.2.2, a library of Biginelli compounds were developed further. Rather than maintain the same aldehyde throughout this scope, the aldehyde component was also varied to mirror the previous scope. This was to demonstrate the variety of compounds possible to synthesis easily via the flow-microwave tandem process (Figure 33).

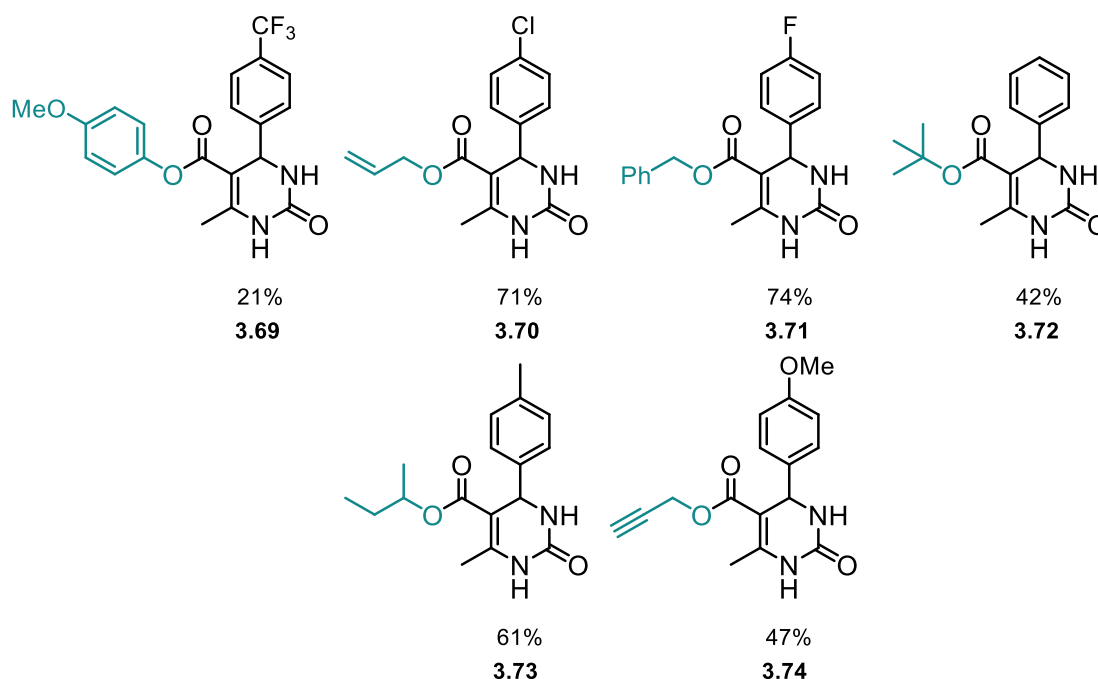


Figure 33 – Scope of various β -keto esters used to develop Biginelli compound library

The scope had a varying degree of success, installing two aromatic components onto Biginelli compound **3.69** gave a surprisingly low yield of 21%. Including an electron withdrawn aldehyde and an electron rich β -keto ester was thought to aid the reaction by increasing the reactivity of the aldehyde for the condensation reaction whilst also increasing the nucleophilicity of the β -keto ester. Unfortunately, this did not have the desired effect and could either be due to the steric repulsion of the two planar aromatic rings or the electron rich β -keto ester slowing down the final elimination step. Pleasingly,

both the allylic β -keto ester and benzyl β -keto ester Biginelli compounds **3.70** and **3.71** gave excellent yields of 71% and 74%, respectively. When comparing compound **3.66** (Figure 32) and compound **3.72** (Figure 33) the yield dropped significantly from 90% to 42% when changing the β -keto ester to the *tert*-Butyl β -keto ester. In this example the electronics have not changed significantly, however, it is possible the primary *n*-butyl chain is more stable than the tertiary *tert*-butyl chain which could decompose more readily, however, no decomposition products were noticeably observed. The *sec*-butyl and propargyl β -keto ester gave modest yields of Biginelli compounds **3.73** and **3.74** in 61% and 47%, respectively.

Biginelli compounds are known to have biological activity, for example, as calcium channel blockers, and it was postulated whether the compounds synthesised in this library could be biologically active. It was pleasing to demonstrate that a selection of these compounds could be made with synthetic handles, ready for further functionalisation. The terminal alkyne of compound **3.74** is a useful handle that could be further reacted via click chemistry to form a triazole tether onto the Biginelli compound. Post-functionalisation can also be applied to the allylic β -keto ester Biginelli compound **3.70** that could be reacted in various reactions such as: metathesis, bromination, and cyclopropanation to name a few.

It is common to interchange the urea component with thiourea when creating a library of Biginelli compounds.⁵⁹ A thiourea scope was explored mirroring the scope in Figure 33, sadly, no Biginelli products could be obtained and a distinct thiol odour was present after the completion of each reaction. This could imply that the thiourea is forming thiols from the β -keto ester component or aldehyde component with possible decomposition products and therefore quenching the reaction.

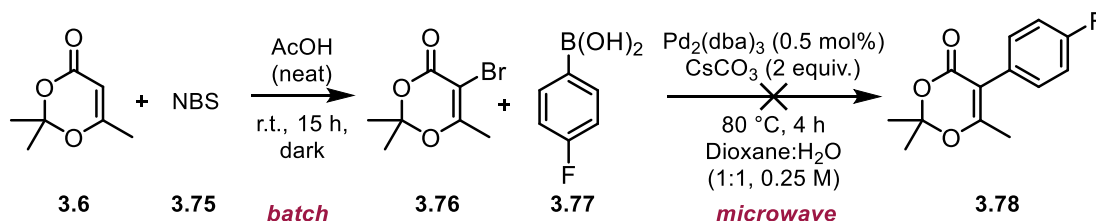
3.4 Conclusions and outlook

This chapter explores a broad scope of acyl ketene reactivity and how it can be contained and manipulated via flow chemistry. To summarise, a range of β -keto esters have been synthesised with the aim to increase productivity by using high concentration reactions. Additional reactivity was found by reacting TMD **3.6** with 4-methyl salicylaldehyde **3.37** to form coumarins in flow. Various coumarins have been synthesised by γ -functionalising the TMD acyl ketene precursor **3.6** to yield novel coumarin species with extended conjugation. To create a tandem flow-microwave system, a range of Biginelli products have been optimised and synthesised using a simple pyridinium triflate catalyst from the β -keto ester feedstocks created by the acyl ketene flow system.

The design of this reactor has facilitated the *in situ* generation of an acyl ketene via thermolysis of TMD **3.6**. The liberated acyl ketene has been safely contained in a sealed flow system and intercepted to explore additional reactivity. The continuous function of flow has enabled scalable reactions to proceed without increasing the safety risks.

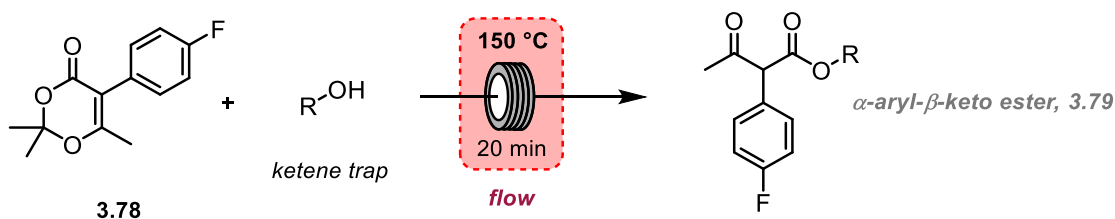
Future proposal and initial findings

It was postulated that α -aryl β -keto esters could be synthesised by pre-functionalising the acyl ketene precursor **3.6** at the α -position with NBS **3.75** (Scheme 53).



Scheme 53 – proposed synthetic plan to α -functionalise dioxinone **3.76**

This α -bromo dioxinone **3.76** can be coupled with an aryl boronic acid **3.77**, via a Suzuki coupling, to furnish the α -aryl substituted dioxinone **3.78** in the microwave. The α -aryl functionalised dioxinone **3.78** could be subjected to the previously established acyl ketene generating conditions, in flow, in the presence of an alcoholic ketene trap (Scheme 54).



Scheme 54 – Flow system design to synthesise α -aryl- β -keto esters

With the application of heat, the newly α -functionalised dioxinone **3.78** would thermally decompose to form the functionalised acyl ketene *in situ* and after nucleophilic attack from the alcoholic ketene trap, the flow system should afford α -aryl- β -keto ester **3.79**. This would be an interesting transformation with respect to installing an aryl functional group in a traditionally nucleophilic position of a dicarbonyl. Synthesising these compounds have been explored before in literature and either use classical palladium coupling chemistry or use specialist reagents such as hypervalent diaryliodonium salts or Cu-MOF-74.^{60–62} This reaction was in the early stages of development due to the inability to successfully couple the palladium Suzuki components. This chemical exploration would push the scope of reactivity available to the acyl ketene precursor **3.6** whilst maintaining the safety of generating an acyl ketene in a continuous manner.

3.5 References

- 1 B. Gutmann, D. Cantillo and C. O. Kappe, *Angew. Chemie Int. Ed.*, 2015, **54**, 6688–6728.
- 2 M. Köckinger, C. A. Hone, B. Gutmann, P. Hanselmann, M. Bersier, A. Torvisco and C. O. Kappe, *Org. Process Res. Dev.*, 2018, **22**, 1553–1563.
- 3 M. Escribà-Gelonch, T. Noël and V. Hessel, *Org. Process Res. Dev.*, 2018, **22**, 147–155.
- 4 D. Znidar, C. A. Hone, P. Inglesby, A. Boyd and C. O. Kappe, *Org. Process Res. Dev.*, 2017, **21**, 878–884.
- 5 F. Benito-López, R. J. M. Egberink, D. N. Reinhoudt and W. Verboom, *Tetrahedron*, 2008, **64**, 10023–10040.
- 6 C. B. Kelly, C. (Xiang) Lee and N. E. Leadbeater, *Tetrahedron Lett.*, 2011, **52**, 263–265.
- 7 I. R. Baxendale, L. Brocken and C. J. Mallia, *Green Process. Synth.*, 2013, **2**, 211–230.
- 8 P. D. Morse, R. L. Beingessner and T. F. Jamison, *Isr. J. Chem.*, 2017, **57**, 218–227.
- 9 K. D. Nagy, B. Shen, T. F. Jamison and K. F. Jensen, *Org. Process Res. Dev.*, 2012, **16**, 976–981.
- 10 S. Karlsson, C. Cook, H. Emtenäs, K. Fan, P. Gillespie and M. Mohamed, *Org. Process Res. Dev.*, 2017, **21**, 1668–1674.
- 11 M. Damm, T. N. Glasnov and C. O. Kappe, *Org. Process Res. Dev.*, 2010, **14**, 215–224.
- 12 E. Comer and M. G. Organ, *J. Am. Chem. Soc.*, 2005, **127**, 8160–8167.
- 13 E. Wedekind, *Berichte der Dtsch. Chem. Gesellschaft*, 1901, **34**, 2070–2077.
- 14 H. Staudinger, *Berichte der Dtsch. Chem. Gesellschaft*, 1905, **38**, 1735–1739.
- 15 F. Chick and N. T. M. Wilsmore, *J. Chem. Soc., Trans.*, 1908, **93**, 946–950.
- 16 T. T. Tidwell, *Angew. Chemie Int. Ed.*, 2005, **44**, 5778–5785.
- 17 A. D. Allen and T. T. Tidwell, *Chem. Rev.*, 2013, **113**, 7287–7342.

- 18 Y. Chiang, H.-X. Guo, A. J. Kresge and O. S. Tee, *J. Am. Chem. Soc.*, 1996, **118**, 3386–3391.
- 19 A. E. May and T. R. Hoye, *J. Org. Chem.*, 2010, **75**, 6054–6056.
- 20 C. O. Kappe, R. A. Evans, C. H. L. Kennard and C. Wentrup, *J. Am. Chem. Soc.*, 1991, **113**, 4234–4237.
- 21 C. O. Kappe, G. Färber, C. Wentrup and G. Kollenz, *Tetrahedron Lett.*, 1992, **33**, 4553–4556.
- 22 R. N. Serdyuk, A. Y. Sizov and A. F. Ermolov, *Russ. Chem. Bull.*, 2003, **52**, 1857–1858.
- 23 R. Leung-Toung and C. Wentrup, *J. Org. Chem.*, 1992, **57**, 4850–4858.
- 24 K. P. Reber, S. D. Tilley and E. J. Sorensen, *Chem. Soc. Rev.*, 2009, **38**, 3022.
- 25 M. Sato, H. Ogasawara and T. Kato, *Chem. Pharm. Bull.*, 1983, **31**, 1896–1901.
- 26 Y. Sugita, J.-I. Sakaki, M. Sato and C. Kaneko, *J. Chem. Soc., Perkin Trans. 1*, 1992, 2855–2861.
- 27 R. J. Clemens and J. A. Hyatt, *J. Org. Chem.*, 1985, **50**, 2431–2435.
- 28 V. Sridharan, M. Ruiz and J. Menéndez, *Synthesis (Stuttg.)*, 2010, **2010**, 1053–1057.
- 29 I. R. Gudipati, D. V. Sadasivam and D. M. Birney, *Green Chem.*, 2008, **10**, 275–277.
- 30 R. Galaverna, T. McBride, J. C. Pastre and D. L. Browne, *React. Chem. Eng.*, 2019, **4**, 1559–1564.
- 31 R. S. Coleman and J. R. Fraser, *J. Org. Chem.*, 1993, **58**, 385–392.
- 32 R. Montaigne and L. Ghosez, *Angew. Chemie Int. Ed.*, 1968, **7**, 221–221.
- 33 R. Huisgen, L. Feiler and G. Binsch, *Angew. Chemie Int. Ed.*, 1964, **3**, 753–754.
- 34 N. Pemberton, L. Jakobsson and F. Almqvist, *Org. Lett.*, 2006, **8**, 935–938.
- 35 A. Zakaszewska, E. Najda and S. Makowiec, *New J. Chem.*, 2016, **40**, 6546–6549.
- 36 N. Pemberton, H. Emtenäs, D. Boström, P. J. Domaille, W. A. Greenberg, M. D. Levin, Z. Zhu and F. Almqvist, *Org. Lett.*, 2005, **7**, 1019–1021.

- 37 P. Zhang, N. Weeranoppanant, D. A. Thomas, K. Tahara, T. Stelzer, M. G. Russell, M. O'Mahony, A. S. Myerson, H. Lin, L. P. Kelly, K. F. Jensen, T. F. Jamison, C. Dai, Y. Cui, N. Briggs, R. L. Beingessner and A. Adamo, *Chem. – A Eur. J.*, 2018, **24**, 2776–2784.
- 38 Y. Song, H. I. De Silva, W. P. Henry, G. Ye, S. Chatterjee and C. U. Pittman, *Tetrahedron Lett.*, 2011, **52**, 4507–4511.
- 39 R. D. Little and W. A. Russu, *J. Org. Chem.*, 2000, **65**, 8096–8099.
- 40 X.-X. Li, L.-L. Zhu, W. Zhou and Z. Chen, *Org. Lett.*, 2012, **14**, 436–439.
- 41 P. Jiao, D. Nakashima and H. Yamamoto, *Angew. Chemie Int. Ed.*, 2008, **47**, 2411–2413.
- 42 A. R. Katritzky, Z. Wang, M. Wang, C. D. Hall and K. Suzuki, *J. Org. Chem.*, 2005, **70**, 4854–4856.
- 43 S. Benetti, R. Romagnoli, C. De Risi, G. Spalluto and V. Zanirato, *Chem. Rev.*, 1995, **95**, 1065–1114.
- 44 C. Simon, T. Constantieux and J. Rodriguez, *European J. Org. Chem.*, 2004, **2004**, 4957–4980.
- 45 C. Oliver Kappe, *Tetrahedron*, 1993, **49**, 6937–6963.
- 46 K. P. Beena, R. Suresh, A. Rajasekaran and P. K. Manna, *J. Pharm. Sci. Res.*, 2016, **8**, 741–746.
- 47 C. O. Kappe, *J. Org. Chem.*, 1997, **62**, 7201–7204.
- 48 J. Lu and H. Ma, *Synlett*, 2000, **2000**, 63–64.
- 49 C. O. Kappe, *Acc. Chem. Res.*, 2000, **33**, 879–888.
- 50 C. O. Kappe, *Chem. Rec.*, 2019, **19**, 15–39.
- 51 J. Lu and Y. Bai, *Synthesis (Stuttg.)*, 2002, **2002**, 466–470.
- 52 E. Ruijter, R. Scheffelaar and R. V. A. Orru, *Angew. Chemie Int. Ed.*, 2011, **50**, 6234–6246.
- 53 F. S. Falsone and C. O. Kappe, *Arkivoc*, 2001, **2001**, 122–134.
- 54 H. Hazarkhani and B. Karimi, *Synthesis (Stuttg.)*, 2004, **2004**, 1239–1242.
- 55 S. Roy, P. Jadhavar, K. Seth, K. Sharma and A. Chakraborti, *Synthesis (Stuttg.)*,

2011, **2011**, 2261–2267.

- 56 A. Shaabani, A. Bazgir and F. Teimouri, *Tetrahedron Lett.*, 2003, **44**, 857–859.
- 57 C. Manikandan and K. Ganesan, *Synlett*, 2016, **27**, 1527–1530.
- 58 C. Ramalingan, S.-J. Park, I.-S. Lee and Y.-W. Kwak, *Tetrahedron*, 2010, **66**, 2987–2994.
- 59 A. Stadler and C. O. Kappe, *J. Comb. Chem.*, 2001, **3**, 624–630.
- 60 J. G. Zeevaart, C. J. Parkinson and C. B. de Koning, *Tetrahedron Lett.*, 2004, **45**, 4261–4264.
- 61 A. Monastyrskiy, N. K. Namelikonda and R. Manetsch, *J. Org. Chem.*, 2015, **80**, 2513–2520.
- 62 P. Leo, G. Orcajo, D. Briones, F. Martínez and G. Calleja, *Catal. Today*, 2020, **345**, 251–257.

4 Designing a Reactor for the Continuous Production of Civetone

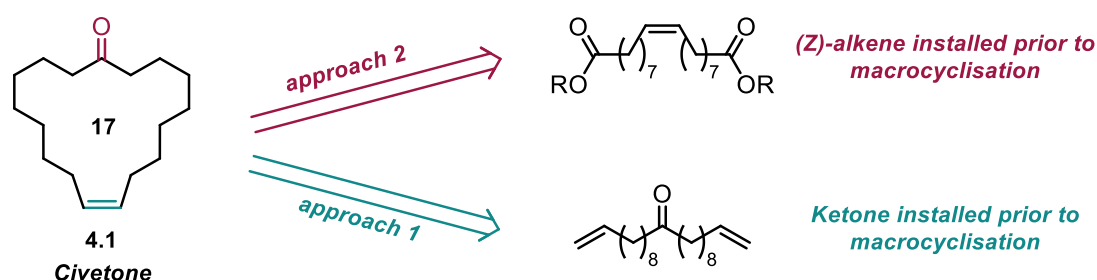
4	Designing a Reactor for the Continuous Production of Civetone.....	99
4.1	Introduction	100
4.1.1	Civetone	100
4.1.2	Designing flow reactors to facilitate the metathesis reaction	106
4.1.3	Designing flow reactors to facilitate solid forming reactions	108
4.2	Background and Aims of Project	110
4.3	Results and Discussion	112
4.3.1	Dieckmann cyclisation – batch conditions.....	112
4.3.2	Designing a flow reactor for the Dieckmann cyclisation	113
4.3.3	Chemical optimisation in the <i>r</i> Reactor.....	119
4.4	Conclusions and outlook.....	124
4.5	References	126

4.1 Introduction

The aim of this project was to develop a synthetic strategy for a continuous process affording the natural product, (*Z*)-Civetone, **4.1**. To create a continuous process, reactor design needs to be considered to facilitate and overcome common problems encountered when synthesising Civetone and converting from batch methods to flow.

4.1.1 Civetone

Civetone is extracted from the Civet cat and its intense musky odour is desirable for the perfume industry.¹ Civetone is still farmed from the Civet cat, however, syntheses of this natural product have been reported in the literature.²⁻⁴ The compound is a symmetrical 17-membered macrocycle with a (*Z*)-alkene and a ketone. There are two main synthetic disconnections to form the macrocycle in literature (Scheme 55).

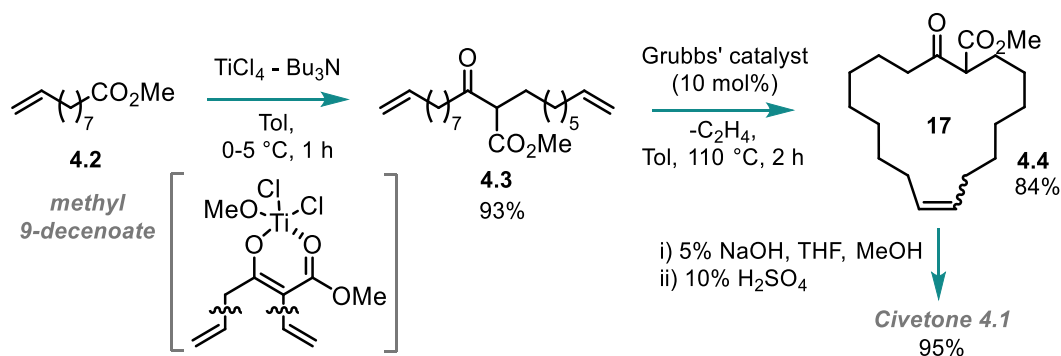


Scheme 55 – Two common methods to form macrocyclic Civetone

Common synthetic strategies either pre-form the (*Z*)-alkene to install the stereochemistry and subsequently cyclise via a condensation method to afford a cyclic intermediate (approach 2, Scheme 55). The intermediate normally undergoes saponification and decarboxylation to afford Civetone **4.1**. The other synthetic approach pre-forms the ketone functionality and subjects the compound to ring-closing metathesis conditions to yield Civetone **4.1** (approach 1, Scheme 55). The RCM reaction, using common metathesis conditions, will not yield the pure (*Z*)-isomer, however, research into specialised catalysts have been found to do this transformation stereoselectively and will be discussed later in this chapter.

Approach 1 – non-stereoselective Civetone synthesis via metathesis macrocyclisation

In 2000, Tanabe and co-workers demonstrated the use of a Ti-Claisen condensation followed by an intramolecular olefin metathesis reaction exemplifying ‘approach 1’ (synthesis of alkene moiety in macrocyclisation, Scheme 55) to afford Civetone **4.1** (Scheme 56).



Scheme 56 – Synthetic strategy for the synthesis of Civetone 4.1 in 3 steps.

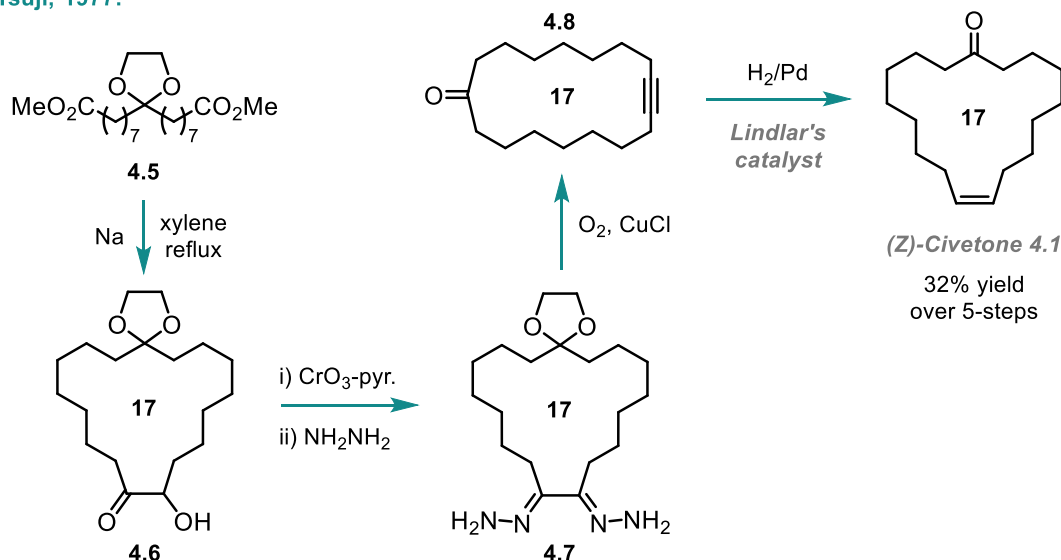
Using methyl 9-decenoate **4.2**, as starting material, the authors demonstrated a Ti-Claisen condensation in the presence of a base to yield 93% of the β -keto ester **4.3** through a titanium stabilised enolate. This step installs the ketone required for the synthesis of Civetone **4.1** which is subsequently subjected to metathesis conditions to close the ring following approach 1 (Scheme 55) to form the desired alkene moiety. The metathesis reaction uses the 1st generation Grubbs' catalyst at 10 mol% to close the macrocyclic ring and exude ethylene gas, yielding 84% cyclic β -keto ester **4.4**. The cyclic β -keto ester **4.4** is then saponified and decarboxylated to give Civetone **4.1** in 95% yield. Over the 3 steps, the average isolated yield was 74% and the authors demonstrated a one-pot process with no intermediate purification but reported a significantly lower yield of 48%. Their olefin metathesis reaction is not stereoselective and it is therefore assumed that the (*Z/E*)-alkene ratio is 1:1. It is known in the literature that a Dieckmann cyclisation using a base can also be employed to couple two ester moieties followed by a RCM metathesis reaction.⁴ This has also been explored by Mol and co-workers in 1991 where they could synthesis Civetone **4.1** in 3 steps from (*Z*)-methyl-9-octadecenoate through a ring-closing metathesis reaction using $\text{Re}_2\text{O}_7/\text{SiO}_2.\text{Al}_2\text{O}_3$ catalyst to yield Civetone in a 1:1 (*E/Z*)-ratio.¹ In 2019, Mauduit and co-workers have explored the use of new ruthenium catalyst to facilitate the RCM towards the synthesis of (*Z*)-Civetone. They achieved a 99% selectivity towards macrocyclisation over oligomerisation and a (*E/Z*) ratio of 7:3 and yield of 52% for Civetone. This reaction was performed with a high substrate dilution (0.01 M) and 1 mol% [Ru] loading. High dilutions are commonly required for macrocyclisation due to the entropic penalty issued for closing larger rings when compared to intermolecular oligomerisation.⁵

Approach 1 – Stereoselective Civetone synthesis via metathesis macrocyclisation and classical synthetic transformations

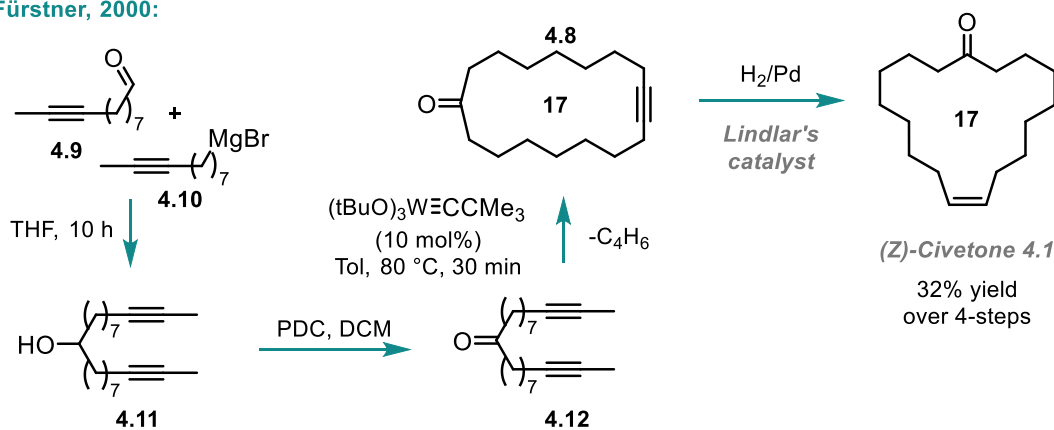
Using approach 1 (Scheme 55) to create the (*Z*)-Civetone macrocycle is difficult due to the high dilution required and the ring-closing metathesis reaction not being selective

towards forming the (*Z*)-alkene. It seems that, via this synthetic approach, it is not feasible to synthesise the macrocycle of (*Z*)-Civetone using stereoselective metathesis conditions to form the (*Z*)-alkene. Non-direct methods to form the (*Z*)-alkene have been explored by installation of an alkyne moiety via metathesis and classical transformations (Scheme 57).

Tsuji, 1977:



Fürstner, 2000:

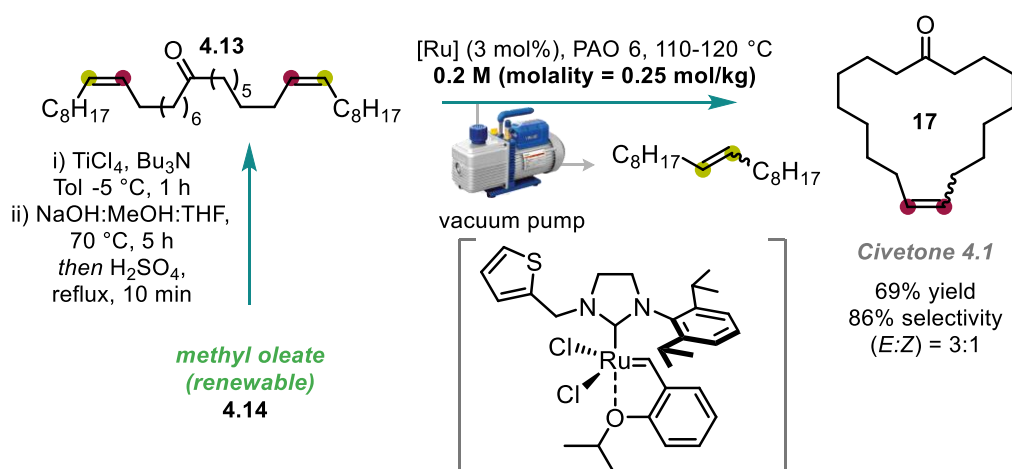


Scheme 57 – Use of alkyne chemistry to synthesis (*Z*)-Civetone

The (*Z*)-alkene in Civetone can be installed by reducing an alkyne using Lindlar's catalyst to facially reduce the alkyne to a (*Z*)-alkene. This methodology has been used in 1977 and 2000 to achieve the stereoselective synthesis of (*Z*)-Civetone. Tsuji and co-workers used classical methods and initiated their synthesis with a ketal protected dimethyl civetonedicarboxylate 4.5 derived from a butadiene telomer. The ketal was subjected to metal sodium which cyclised the dicarboxylate affording the 17-membered macrocyclic α-hydroxy ketone 4.6. After a Collins oxidation, both ketones were converted to hydrazones using 80% hydrazine in refluxing *n*-propanol for 12 hours affording compound 4.7. The dihydrazone 4.7 was converted to the alkyne 4.8 by a copper

catalysed oxidation in pyridine and the intermediate was deprotected with addition of hydrochloric acid to liberate the latent ketone. Finally, Lindlar's catalyst was used to afford (*Z*)-Civetone **4.1** in an overall yield of 32% over 5 synthetic steps.⁶ Fürstner used a similar method but incorporated an alkyne metathesis step to streamline the process. After coupling the two alkynes (**4.9** and **4.10**) via a Grignard addition, the secondary alcohol **4.11** was oxidised using PDC to afford the ketone **4.12** in a 91% yield. A tungsten alkylidyne complex was used as a catalyst for the alkyne cross metathesis reaction affording the penultimate product **4.8** in 65% in 30 min. (*Z*)-Civetone **4.1** was formed also using Lindlar's catalyst to install the (*Z*)-alkene moiety.⁷

Both these syntheses follow approach 1 (Scheme 55) to assemble the macrocyclic ring by forming the alkene. It seems that using metathesis to close the macrocyclic ring of Civetone in a stereoselective manner is difficult and requires high dilution which greatly decreases the productivity of the reaction. Therefore, an alternative batch method has been explored by Grela and co-workers reported in 2018. The authors employ a vacuum to their batch reaction to extract the metathesis by-product and drive the reaction forward for the macrocyclisation at higher concentrations, in turn, increasing the productivity of the reaction (Scheme 58).



Scheme 58 – Synthesis of Civetone under reduced pressure to drive metathesis reaction

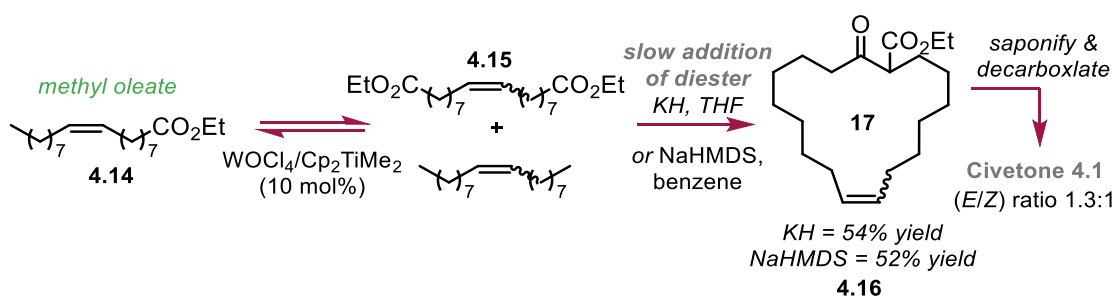
By removing the metathesis by-product, via reduced pressure, Civetone could be synthesised in 69% yield and a high selectivity towards the cyclised product. They could increase the concentration of this reaction to 0.2 M which is relatively high for a macrocyclisation. They used 'renewable' methyl oleate **4.14** as starting material (derived from oleic acid) and after a Ti-Claisen condensation reaction and subsequent saponification and decarboxylation they had prepared the Civetone precursor **4.13**. Using PAO (poly- α -olefin synthetic oil) as a diluent they successfully synthesised Civetone **4.1**. However, their (*E/Z*) ratio was 3:1 which meant that their catalyst system

only made 25% (*Z*)-Civetone **4.1**. The authors have demonstrated that the application of a vacuum to a metathesis reaction drives the desirable transformation by removing the un-wanted by-products thus shifting the equilibrium.⁸

Approach 2 – Civetone synthesis via macrocyclic condensation transformations

As previously discussed, the macrocyclisation of Civetone via alkene formation has many limitations due to managing the metathesis equilibrium and (*E/Z*) selectivity. The alternative approach to synthesise the 17-membered macrocycle is to pre-form the alkene and close the ring via a condensation to afford the ketone (approach 2, Scheme 55).

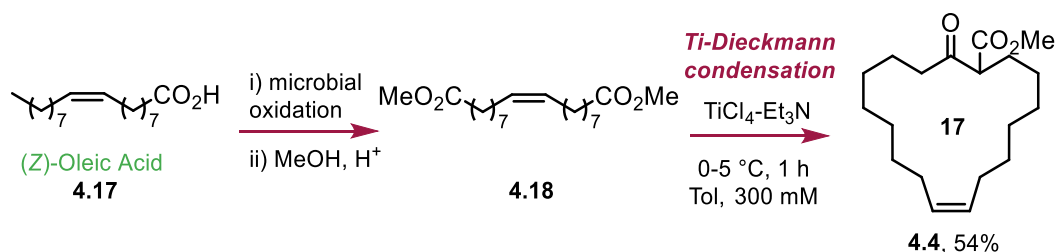
Spencer and co-workers in 1948, synthesised Civetone by installing the alkene bond first then, under high dilution, performed the macrocyclisation via diketenes; they found their diketene methodology superior over the Ziegler method reported in 1943 by Hunsdiecker.⁹ In 1981, Tsuji and co-workers explored the use of the Dieckmann cyclisation to successfully close the Civetone ring (Scheme 59).



Scheme 59 – Using the Dieckmann condensation to facilitate the macrocyclisation of Civetone

In this synthetic strategy, the authors use a tungsten catalyst to convert methyl oleate **4.14** (from oleic acid) into the diester metathesis product via olefin metathesis. The authors commented on the change of (*E/Z*) geometry through the metathesis reaction due to methyl oleate **4.14** starting at 1:10.5 (*E/Z*) and the diester product **4.15** had a ratio of 1.3:1 (*E/Z*). This stereochemistry was carried through to the final product as the macrocyclisation does not affect the alkene geometry. Using potassium hydride as base in THF, a Dieckmann cyclisation was successfully performed to yield the cyclic β -keto ester **4.16**. It is important to note that the diester starting material **4.15** had to be added slowly over the course of the reaction, in high dilution, to prevent oligomerisation and promote macrocyclisation. Sodium hexamethyldisilazane (NaHMDS) was also tried as a base for the cyclisation and a mildly reduced yield of 52% was reported. The cyclic β -keto ester **4.16** was then saponified and decarboxylated to afford Civetone **4.1**, retaining the previous alkene geometry.^{10,11}

Most recently, the Dieckmann condensation reaction has been explored to synthesise Civetone with the added improvement toward synthesising (*Z*)-Civetone. In 2002, Tanabe and co-workers re-designed their synthetic strategy to carry through the (*Z*)-alkene from starting material to (*Z*)-Civetone (Scheme 60).



Scheme 60 – Ti-Dieckmann condensation reaction facilitating the synthesis of (*Z*)-Civetone

A microbial oxidation (*Candida tropicalis*) of (*Z*)-Oleic acid **4.17** and subsequent esterification in acidic methanol formed the dimethyl diester **4.18** with the correct alkene geometry installed. The authors reported the advantages of using TiCl₄, with Et₃N as base, to facilitate a Dieckmann cyclisation compared to the traditional bases used (KH/KHMDS). They suggest the benefits include the use of higher concentrations; lower reaction temperatures; and shorter reaction times. They successfully synthesised the cyclic β-keto ester **4.4** in 54% yield that needed saponification and decarboxylation to afford (*Z*)-Civetone **4.1**. Notably, this reaction only proceeds if the reagents are added dropwise slowly to the reaction mixture and the molar ratio between the reagents are kept balanced.¹² Hagiwara and co-workers, in 2012, use a similar approach by installing the correct (*Z*)-alkene geometry before the macrocyclisation. They reduce an alkyne to the desirable alkene and perform a classical Dieckmann cyclisation with KH in refluxing THF to yield 54% of the macrocyclic β-keto ester which is subsequently converted to (*Z*)-Civetone via saponification and decarboxylation. The reaction must also be in high dilution and slow addition of the diester to the reaction was imperative to its success.³

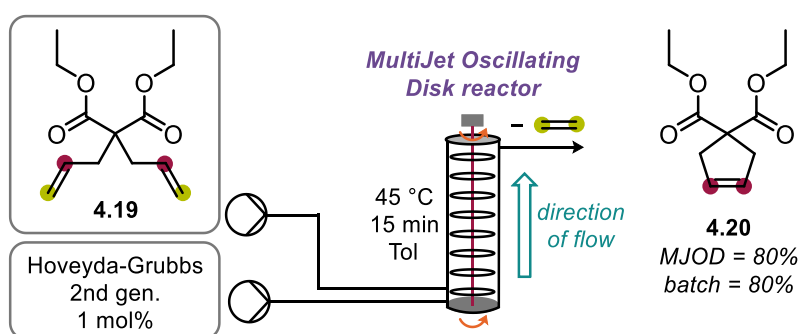
Both synthetic approaches have limitations; approach 1 uses metathesis to form the macrocycle but catalytic systems struggle to gain high (*Z*)-selectivity. The other approach, using basic condensation to form the macrocycle (approach 2, Scheme 55) has drawbacks involving the requirement of slow addition of the diester species for a Dieckmann condensation to stop the more favourable oligomerisation. Both approaches furthermore require high dilution when manipulating macrocycles. Flow chemistry has been explored to determine whether this enabling technique can facilitate the macrocyclisation, via the metathesis reaction and the condensation reaction, more successfully.

In 2019, Collins and co-workers compared batch, flow, and microwave reactors for the ring-closing metathesis reaction. The authors found that flow chemistry produced far lower yields (32%) but a decreased reaction time thus an increase in productivity when compared to batch. The batch conditions took 5 days with high dilution (5 mM) but afforded a higher yield of 57% for the synthesis of macrocyclic musks.¹³ The flow tubing has no headspace to allow the evolution of the ethylene gas by-product which is a strong limitation unless a flow reactor can be designed to allow the removal of ethylene gas.

4.1.2 Designing flow reactors to facilitate the metathesis reaction

As previously discussed, efforts have been made to drive the equilibrium of the metathesis reaction towards product formation. Continuous processes have been developed to enable this transformation successfully.

In 2014, Bjørsvik and co-workers have engineered a MultiJet Oscillating Disk reactor (MJOD) to successfully drive various olefin metathesis reactions (Scheme 61).



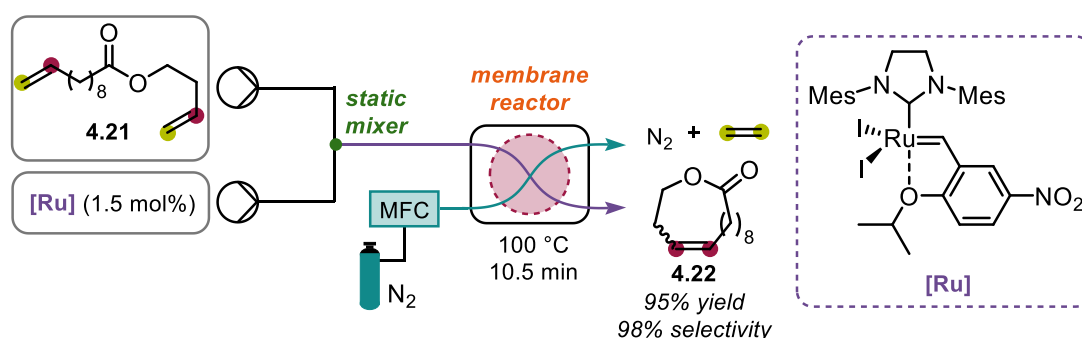
Scheme 61 – A successful ring closing metathesis reaction using a MJOD reactor.

The design of this reactor increases the mass transfer of the reaction by active mixing disks arranged in a column to facilitate metathesis reactions. Diene **4.19** was diluted in toluene and pumped into the MJOD column, simultaneously, a solution of Hoveyda-Grubbs 2nd generation catalyst was also delivered into the MJOD column. After actively mixing the two reagents, the desired cyclopentene product **4.20** was formed in 80% yield. They compared their system with a batch reactor under the same conditions and found the yield to be the same, regardless of the active mixing but argued the benefits of translating a batch protocol into a continuous process. They demonstrated that their MJOD reactor was superior to batch methods for other olefin metathesis reactions, it should be noted that their transformation is the facile ring closing transformation for a 5-membered ring and not a macrocyclisation. The formation of a 5-membered ring is far more favourable than a 17-membered macrocycle (for comparison), however, this example was discussed to demonstrate that unique reactor design was implemented to successfully facilitate a metathesis reaction in a continuous manner. This system is

interesting because the design allows the continuous processing of a metathesis reaction and facilitates any possible precipitate formation with excellent mixing conditions whilst allowing the removal of ethylene gas, unlike other common flow systems.¹⁴

This a common limitation to performing ring-closing metathesis in flow. By trapping the by-product ethylene (gas) in the flow tubing, due to the lack of headspace, does not allow the removal of gas to occur and it commonly remains in the reaction solution. Not removing the ethylene gas, in a pressurised flow system, from the reaction can cause undesirable side products to form and, therefore, does not push the equilibrium towards product formation.

Designing a reactor to facilitate the removal of ethylene gas is an interesting design consideration to enable the metathesis reaction in flow to work effectively. The use of an in-line flow filtration device to assist in successfully isolating desired metathesis products, or removing unwanted by-products, have been explored in literature.^{15–18} In 2020, Jamison and co-workers developed a continuous method using membrane pervaporation to remove ethylene gas from the metathesis reaction (Scheme 62).



Scheme 62 – Using pervaporation to extrude ethylene gas from a macrocyclic ring closing metathesis reaction

The authors found that they could successfully cyclise diene **4.21** using the membrane reactor to afford 95% macrocyclic lactone **4.22** with a 98% selectivity. The bi-phasic streams run parallel, in the membrane reactor, and allow the transfer of gases between streams. Nitrogen gas is used as a benign gas that can elute the unwanted ethylene gas by-product out of the reaction via pervaporation. The authors compared their reactions against a normal tubular flow reactor and found a substantial increase in yield across their various examples with respect to using the membrane reactor. It implies that the removal of ethylene gas drives the equilibrium towards product formation.

This is an excellent example of using metathesis in flow to facilitate a macrocyclisation which is similar to approach 1 (Scheme 55) methodology but in a continuous manner. Reactor design has evolved to allow successful metathesis reactions to take place

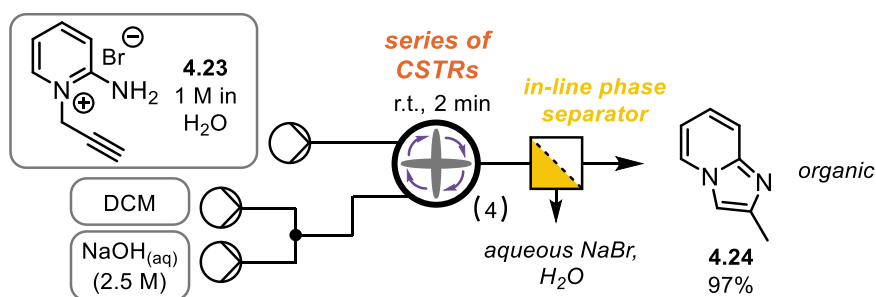
continuously and one could suggest that a macrocyclisation to form Civetone in flow might be possible via the above technology.

4.1.3 Designing flow reactors to facilitate solid forming reactions

Translating approach 2 (Scheme 55) into a flow system has various challenges. Attempting to form a macrocycle via a condensation reaction commonly requires basic conditions under high dilutions/slow dropwise reagent addition. These basic conditions sometimes lead to the formation of precipitates/salts and cause blockages and fouling in a common tubular flow reactor.

Reactor design has evolved to take in these considerations and engineer systems that can handle precipitates in flow via active mixing, bi-phasic solvent systems, and/or continuously stirred tank reactors (CSTRs). Using active mixing in flow highly increases the heat and mass transfer of the reaction and is especially beneficially when adding a reagent dropwise to quickly dissipate the local concentration (to prevent oligomerisation with respect to macrocyclisations).^{19–21} These reactors could be the answer to translating a macrocyclic condensation into flow.

In 2017, Blacker and co-workers developed a series of CSTRs and have demonstrated its use as a ‘plug-and-play’ reactor platform that enables various multi-phasic reactions in a continuous manner.^{22,23} They exemplify their reactor design by demonstrating an electrocyclization with downstream in-line processing to form an imidazopyridine (Scheme 63).



Scheme 63 – Serial array of CSTRs enabling a biphasic electrocyclisation via active mixing

The authors showed they could cyclise *N*-alkynylated 2-aminopyridinium bromides **4.23** over a series of CSTRs, with an in-line workup, to afford 97% imidazopyridine **4.24**. The introduction of a DCM feed meant that upon formation of the desired compound the organic species was immediately extracted into the organic phase that was later separated downstream. This reactor design enables the continuous processing of a bi-phasic mixture in 2 min with heightened mixing thus an increase in heat and mass transfer. Using a membrane phase separator, the aqueous layer, with corresponding salt

by-products, was removed and thus simplified product recovery. Their reactor had a dual purpose of both actively mixing a reaction media whilst simultaneously extracting the desired compound efficiently thus demonstrating the modularity of their design.²⁴

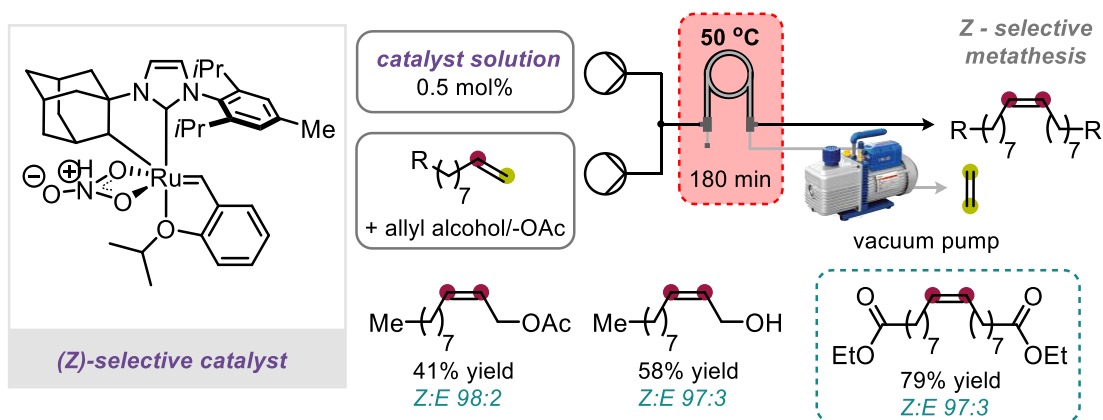
Concluding remarks

Translating the synthesis of Civetone into flow has difficulties for both synthetic approaches (approach 1 and 2, Scheme 55) due to the final macrocyclisation step. Taking inspiration from literature, the design of flow reactors to enable metathesis in flow and/or bi-phasic reactions can be achieved successfully with innovative reaction design considerations and solutions.

4.2 Background and Aims of Project

The primary aim of this was to explore flow reactor design and convert the synthesis of (Z)-Civetone into a continuous process. The main hurdle to explore was to innovative a system that could handle precipitate formation and facilitate a base mediated Dieckmann macrocyclisation in flow.

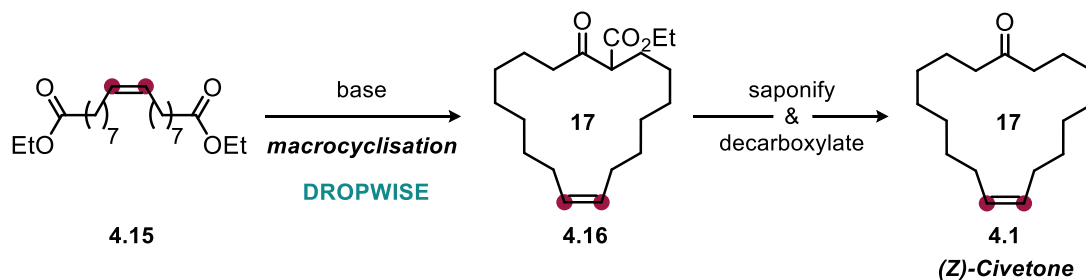
The olefin metathesis reaction is in equilibrium and, to drive this towards product formation, a flow reactor was designed to remove the ethylene gas by-product. To remove the gas, a flow system utilised the benefits of the semi-permeable AF2400 tubing which enabled the passage of gas but not liquid. Construction of a tube-in-tube reactor facilitated the continuous processing of the metathesis reaction, and with an applied vacuum, the tube-in-tube reactor actively drew out and removed the ethylene gas from the reaction. This removal of gas proactively drove the equilibrium of the reaction towards the formation of the desired (Z)-alkene (Scheme 64). The catalyst screening and design of catalyst was done by Idriss Curbet and later developed with our collaborators in the Mauduit group in France, I did not work on the design of the z-selective catalyst. The building of the flow system with the tube-in-tube reactor was design and constructed by Duncan Browne and me. After supervising Idriss on how to run flow experiments, he performed the flow metathesis reaction to afford the desired compound below.



Scheme 64 – Use of a tube-in-tube reactor to drive the completion of the olefin metathesis reaction – results provided by Idriss

After screening various pre-made catalysts, a (Z)-selective catalyst was found to successfully synthesis cross-metathesise products in high Z:E ratio. The desired alkene/mix of alkenes were combined with a solution of the stereoselective catalyst at a flow T-piece and mixed. The metathesis components were heated to 50 °C in a tube-in-tube reactor and, due to the application of a vacuum to the outer tubing, ethylene gas was extracted from the reaction mixture via the semi-permeable membrane. The desired

alkene was synthesised successfully and afforded the diester in 79% and 97:3 *Z*:*E* ratio, highlighted in blue (Scheme 64). Removal of unwanted by-products (or addition of gaseous reagents) in the metathesis reaction via tube-in-tube has been explored before in literature but with reduced selectivity.^{25,26} It was postulated that this (*Z*)-diester could be cyclised and saponified to produce the natural product (*Z*)-Civetone (Scheme 11).



Scheme 65 – Proposed synthetic route to synthesise (*Z*)-Civetone from diester 4.15

Using the Dieckmann cyclisation, the diester 4.15 could undergo a macrocyclisation, in basic conditions, to afford the 17-membered cyclic β -keto ester 4.16. The cyclic β -keto ester can be saponified and decarboxylated to yield (*Z*)-Civetone 4.1, as the alkene geometry is unchanged by the macrocyclisation.

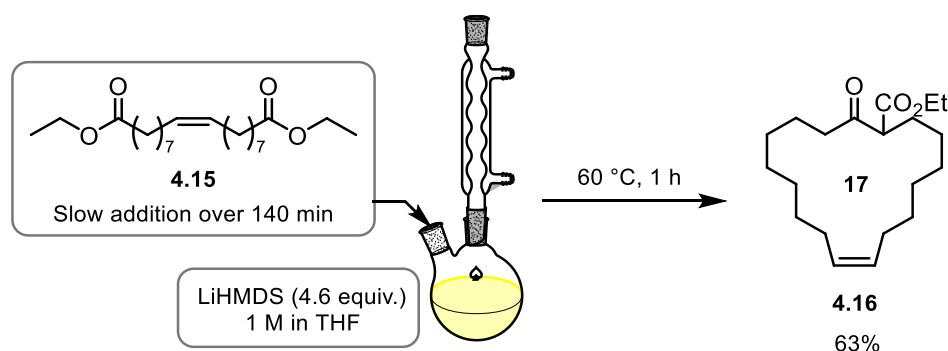
Aims and Objectives

The primary aim of this project was to translate the (*Z*)-diester 4.15 into (*Z*)-Civetone 4.1 via a continuous method. Immediately, the first consideration was that the Dieckmann cyclisation is known to create precipitation and therefore posed the first engineering problem to be solved. As the (*Z*)-alkene had been successfully synthesised, the appropriate synthetic approach to investigate was using a Dieckmann cyclisation to form the macrocycle 4.16 and subsequently, (*Z*)-Civetone 4.1. Translating the Dieckmann cyclisation into flow by exploring different reactor designs was the initial aim, subsequently, this system would ideally be tested on scale and integrated with the previous metathesis in flow system developed by our collaborators.

4.3 Results and Discussion

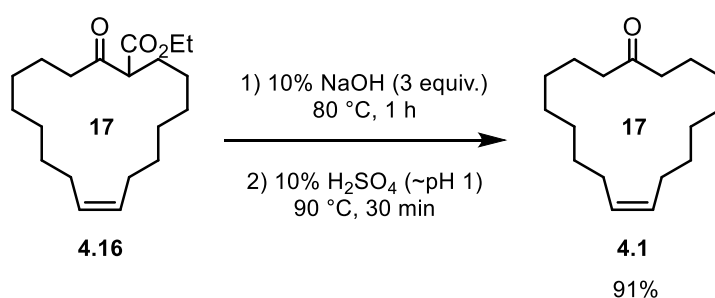
4.3.1 Dieckmann cyclisation – batch conditions

Before transposing the chemistry into a continuous flow system, the Dieckmann cyclisation was first tested in batch with diester **4.15**. It was found in literature that Civetone had been synthesised via a Dieckmann cyclisation using KH/NaH or alcoholic oxide as base.^{3,27} It was postulated that the easy-to-handle base LiHMDS would sufficiently work to facilitate the Dieckmann condensation. KO^tBu was also attempted and was found to unsuccessfully complete the cyclisation (Scheme 66).



Scheme 66 – Initial batch reaction to synthesise Dieckmann condensation product

Slow addition of diester **4.15** (0.646 mmol) into a stirring excess of LiHMDS in THF successfully synthesised the cyclic β -keto ester **4.16** in 63% yield. After isolation of cyclic β -keto ester **4.16**, NaOH was added to saponify the ester group to a carboxylic acid which was later acidified using H₂SO₄ to decarboxylate affording (*Z*)-Civetone **4.1** (Scheme 67).



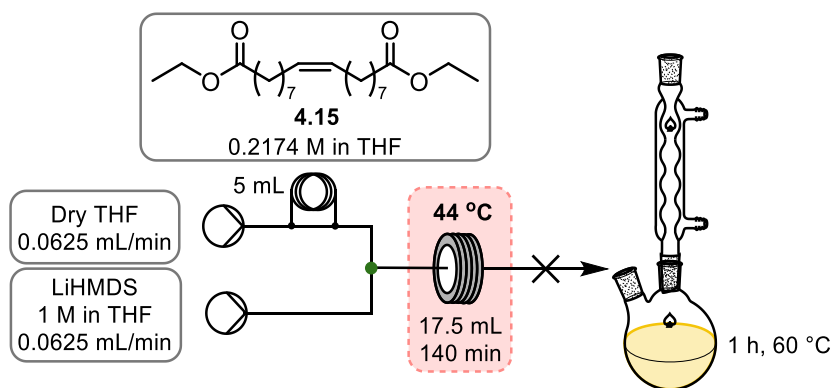
Scheme 67 – Saponification and decarboxylation to afford (*Z*)-Civetone in batch

With the addition of NaOH, the β -keto ester **4.16** was saponified to give an intermediate β -keto acid after 1 hour. Upon acidification using 10% H₂SO₄ to pH 1, (*Z*)-Civetone **4.1** was isolated in a 91% yield after reflux at 90 °C for 30 minutes. This gave an overall average yield of 77% with an intermediate isolation step. This verified that the conditions in Scheme 66 and 67 could be used to afford (*Z*)-Civetone from the diester **4.15**. The slow addition of diester **4.15** is vital for macrocyclisations to avoid oligomerisation rather

than the desired cyclised product. Low concentration conditions are usually required for macrocyclisations to avoid the common oligomerisation limitation. Normally, an intramolecular reaction is far faster than an intermolecular reaction, however, due to the size of the macrocycle, there is an entropic penalty to get the compound into the right conformation for efficient orbital overlap to cyclise the product.⁸ Hence, most commonly in literature, high dilution is employed to reduce the more favourable oligomerisation reaction.

4.3.2 Designing a flow reactor for the Dieckmann cyclisation

Initially, the Dieckmann cyclisation was tested in a normal flow system. The two reagents were introduced separated by two HPLC pumps. Both LiHMDS and diester **4.15** were mixed at a T-piece in flow whilst keeping the equivalence of base the same as the batch reaction (Scheme 68).



Scheme 68 – Using a normal flow T-piece for mixing and tubular coil reactor

Using a regular flow T-piece, the flow reactor blocked immediately after the reagents began to mix. This is due to the relatively high concentration of lithium salts being formed and therefore blocking the T-piece. Rather than lowering the concentration, changing the design of the reactor was explored first to preserve the productivity.

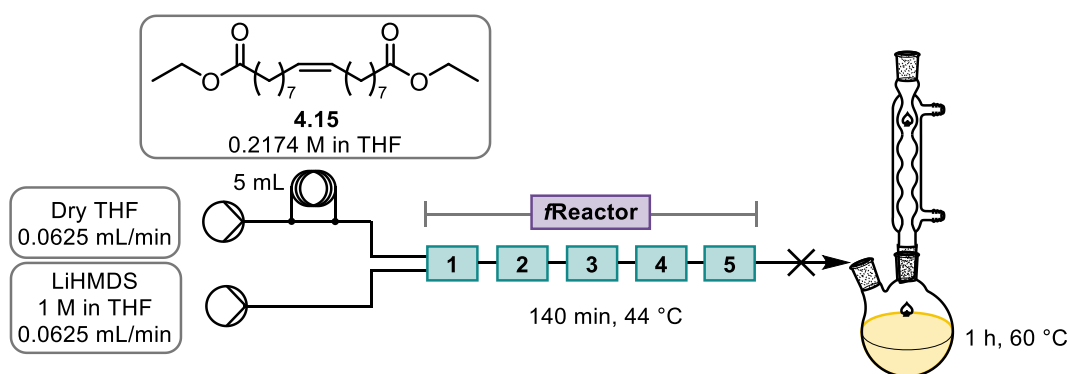
Our research group procured an *f*Reactor from Asynt, originally designed at Leeds University (Figure 34). It is a series of CSTRs that have 4 ports on each mixing unit with a ‘cross’ stir bar inside the chamber. The modular nature of this system allows the user to ‘daisy chain’ link up the CSTR units via wide-bore tubing. It has the capacity for in-line monitoring and the stainless-steel base plate is compatible with a standard hotplate thus able to be heated to a maximum of 60 °C.



*f*Reactor by Asynt

Figure 34 – A series of CSTRs on a stainless-steel base plate

With the *f*Reactor in hand, it was postulated whether the serial array of 5 CSTRs could be used as an active mixer to manage the precipitate formation and prevent blockages from occurring. This was tested by using the *f*Reactor, essentially, as a T-piece to actively mix the two reagents. The concentration was also kept the same to viably compare the reactor differences (Scheme 69).



Scheme 69 – Using the *f*Reactor as an active mixer to handle precipitate formation

This reaction also failed due to a large build-up of precipitate demonstrating that the active CSTR mixing could not handle the lithium salts at that concentration. There were two possible solutions that could be explored to successfully translate the Dieckmann cyclisation into a continuous flow process:

- 1) Lower the concentration of the reaction which would reduce the amount of precipitation formed thus allowing the *f*Reactor to manage the flow process and increase the probability of macrocyclisation over oligomerisation.
- 2) Keep the concentration overall the same but introduce multiple injection points along the reactor to keep the reaction of diester low but preserving the productivity.

Adding multiple injection points along the *f*Reactor also has benefits due to the low concentration promoting macrocyclisation over oligomerisation which is a common problem in macrocyclisations. When deprotonated diester **4.15** with LiHMDS, multiple reaction pathways are possible that give rise to the competition between macrocyclisation and oligomerisation (Figure 35).

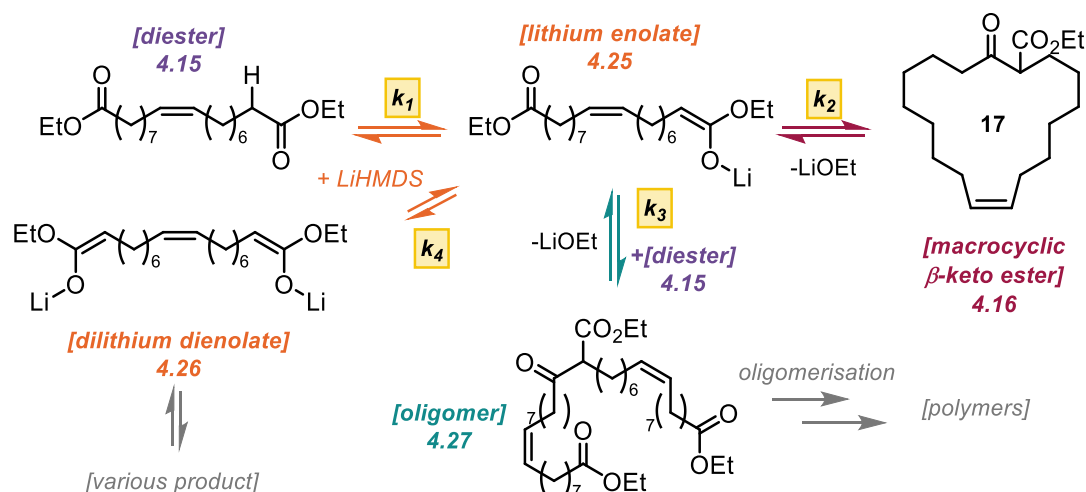


Figure 35 – Mechanism depicting the various pathways possible when deprotonating diester **4.15**.

In the presence of LiHMDS, diester **4.15** can be deprotonated to form lithium enolate **4.25**. The lithium enolate **4.25** can either undergo an intramolecular cyclisation or an intermolecular reaction with another equivalent of diester **4.15**. The Dieckmann cyclisation affords macrocyclic β -keto ester **4.16**, via the self-attack from the lithium enolate **4.25**. However, due to the entropic penalty of the macrocyclisation, the intermolecular reaction between the lithium enolate **4.25** and diester **4.15** can produce the undesirable oligomer **4.27**. Oligomerisation can continue to occur with multiple deprotonations to afford a various array of polymers. If diester **4.15** gets deprotonated twice, it forms the dilithium dienolate species **4.26**. This removes the diester from the reaction as an electrophile and can proceed to react unfavourably into various undesired products. Concentration is important for this reaction because a large [diester] **4.15** would cause $k_3 > k_2$ which affords the oligomer product faster than the formation of the macrocycle **4.16**. If the [diester] **4.15** is too low, the equivalents of LiHMDS will be much higher and in turn will deprotonate diester **4.15** twice, as $k_4 > k_1/k_2/k_3$. The ideal situation is $k_1 k_2 \gg k_3 k_4$, which would form the desired macrocyclic ring **4.16**, however, the mechanistic steps are in equilibrium which means that over time the reaction will find a thermodynamic well unless quenched. The mechanism of this specific transformation has not been elucidated in the literature and is most likely more complex. However, it is a useful tool in the process of designing a flow reactor that will facilitate the successful formation of the desired product.

It was postulated how a flow system could be designed to minimise the concentration to avoid oligomerisation and vast amounts of precipitation whilst maintain a reasonable productivity when translating the Dieckmann cyclisation into flow.

Taking the diester **4.15** from the metathesis in flow system, it was thought that the use of the *r*Reactor could facilitate a ‘dropwise’ approach. This could be installed by introducing the diester **4.15** into the series of CSTRs via multiple injection points. The active mixing in the serial array of CSTRs would quickly dissipate the local concentration of the diester **4.15** upon addition to the reaction and facilitate the processing of a bi-phasic reaction mixture (solid-liquid). This would help to circumvent the competing oligomerisation reaction and use the reactor’s design to proactively enable the macrocyclisation towards the formation of (*Z*)-Civetone **4.1**, whilst also managing a slurry of precipitating salts in a continuous manner.

In the batch system, the diester **4.15** was added to the reaction slowly over 2 hours to keep the diester **4.15** concentration low which is a common limitation of macrocyclisations. Keeping the concentration of the diester **4.15** low is to reduce the concentration of the reactive intermediate enolate species to drive cyclisation rather than the more favourable oligomerisation (Figure 35). These graphical representations are theoretical concentration profiles for the reaction of LiHMDS ([SM A]) with diester **4.15** ([SM B]) via a lithium enolate intermediate **4.25** ([Int]) to afford the cyclised β -keto ester product **4.16** ([Prod]) in batch (Figure 36).

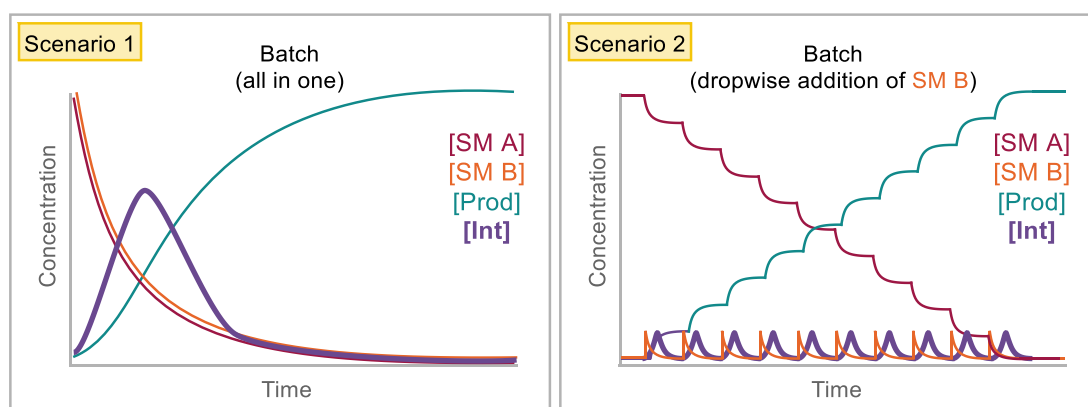


Figure 36 - Graphical description of non-dropwise vs dropwise addition of a reagent to a reaction

At the inception of a reaction with both reagents fully present, the concentration of an intermediate species will increase over time and will be subsequently consumed and converted into the desired product (Scenario 1, Figure 36). With an increased intermediate concentration, the opportunity of the competitive oligomerisation is further increased, therefore, it is essential to keep the reactive intermediate species concentration low. This is achieved via dropwise addition of reagent (Scenario 2, Figure 36). With a high concentration of [SM A] present, the part addition of [SM B] over the course of the reaction keeps the concentration of [Int] low to reduce the chance of

oligomerisation happening. This dropwise addition was successful as described in Scheme 12 affording β -keto ester product **4.16** in 63% yield.

To transpose this dropwise addition reaction profile (Scenario 2, Figure 36) into a flow system becomes more complicated. The time of a flow reaction depends on the length on the tubular reactor, therefore, to simulate a dropwise addition of a reagent, multiple injection points are required along the length of the tubing. The concentration over time reaction profiles for a normal flow system varies depending on which point along the reactor is observed (Figure 37).

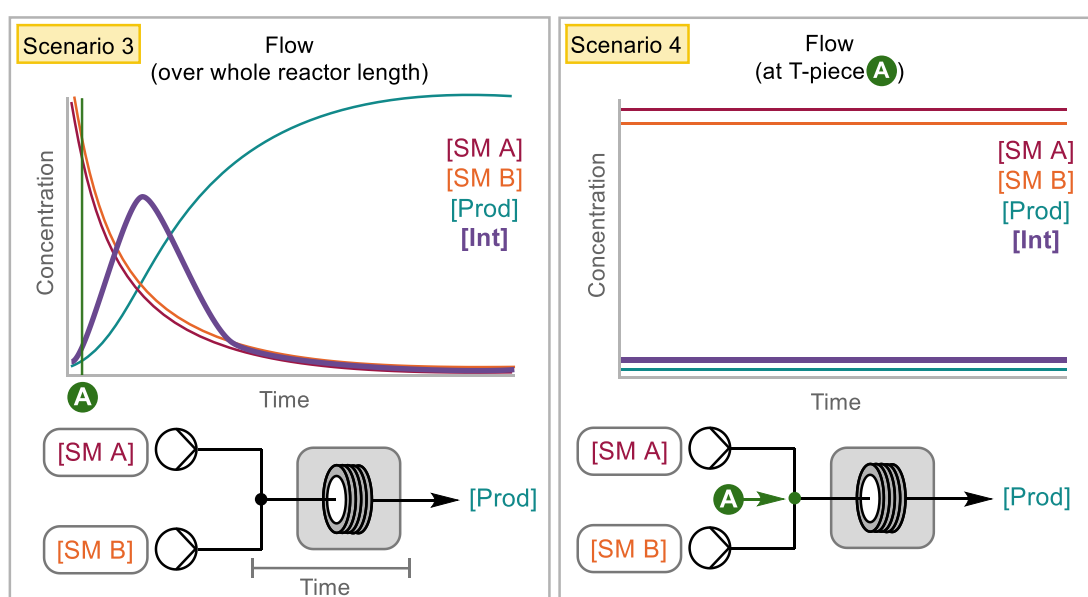


Figure 37 - Graphical description of concentration of reaction components over time in flow

When mixing two streams of reagents in flow, both reagents are mixed at a T-piece equally. Over the length of the reactor, there will be an increase in reactive intermediate concentration. This intermediate concentration will deplete and convert to product arriving at the outlet of the flow system (Scenario 3, Figure 37). If observing the concentration of reagents at T-piece **A**, the concentration of reagents remains constant as there is a continuous stream of reagents being supplied by a pump. (Scenario 4, Figure 37). As previously described, the only way to get 'dropwise' addition of a reagent is to have multiple injection points along a flow reactor in the overall aim to keep the reactive intermediate concentration, **[int]**, as low as possible to avoid oligomerisation (Figure 38).

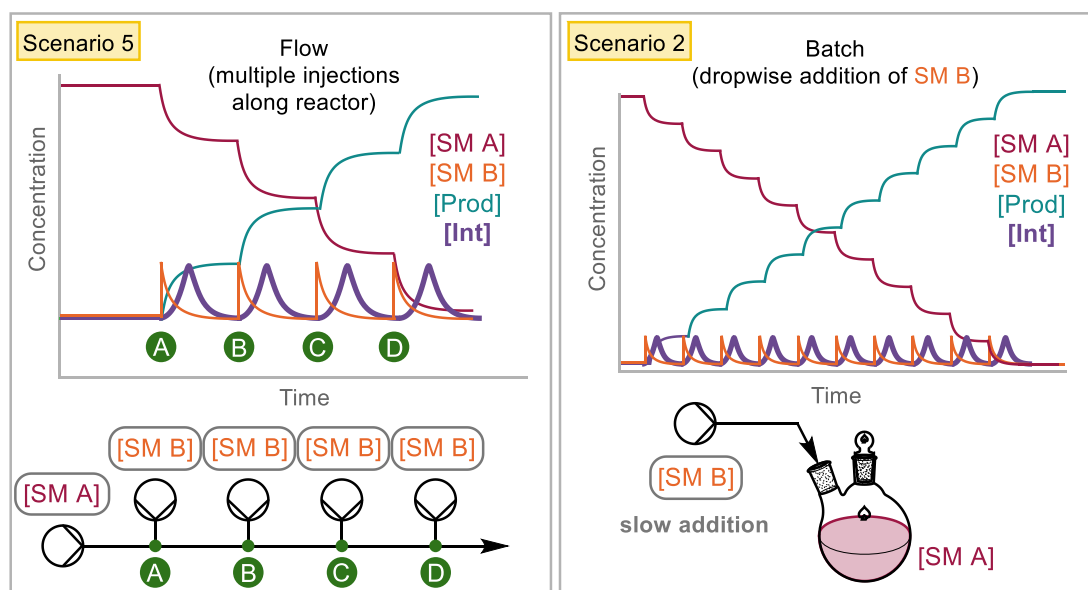
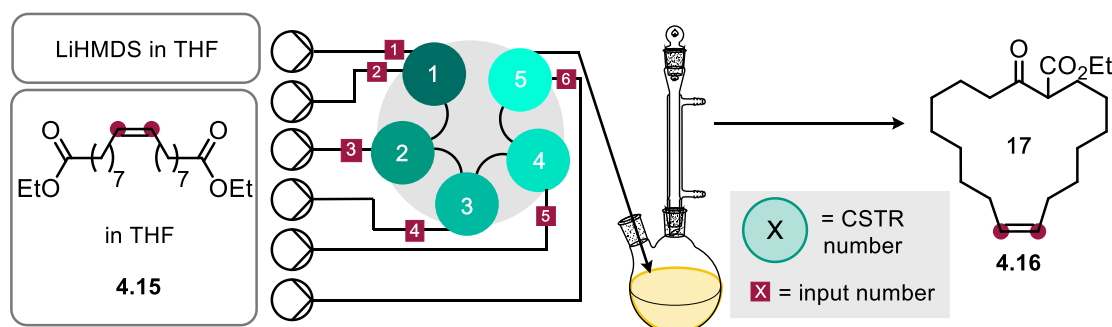


Figure 38 - Graphical description of concentration over time in flow with multiple injection points and a batch 'dropwise addition' comparison

By installing multiple injection points along a flow reactor, a 'dropwise addition' effect can be established (Scenario 5, Figure 38). This keeps the concentration of [Int] relatively low which is the desired outcome as shown in batch also for comparison (Scenario 2, Figure 38).

Distributing diester **4.15** over the length of the reactor, thus minimising the local concentration, creates a pseudo-first order like reaction. The LiHMDS is in great excess throughout the process of the *f*Reactor which enables pseudo-first order kinetics due to the concentration of LiHMDS being relatively unchanged by the end of the reaction with respect to the diester **4.15** concentration. When mixed in batch the bimolecular reaction is second order, however, this reactor design is pushing the kinetics of the system into pseudo-first order via the slow 'dropwise' addition design. Most likely the kinetics of this reaction are more complicated and the above concentration mixing profile were used as a tool to design and hypothesise an effective reactor design that would facilitate a successful Dieckmann cyclisation in flow towards the synthesis of (*Z*)-Civetone **4.1**.

Asynt's *f*Reactor was used as serial array of CSTRs which enables the translation of the batch 'dropwise addition' profile to be applied in flow. The initial design of the reactor utilised all the available ports of the *f*Reactor and diluting the diester **4.15** solution allowed the delivery of the reagent in a 'dropwise' manner with an initial equivalence of 2:1, LiHMDS to diester **4.15** (Scheme 70).



Scheme 70 – Initial flow blueprints for dropwise addition of diester **4.15** to stream of LiHMDS

It was assumed, that after CSTR 1 (and all subsequent CSTRs) that diester **4.15** had been fully consumed and therefore keeping the concentration of diester **4.15** low rather than cumulatively building up as more is added downstream. It was found that the lithium salts produced were causing fouling and precipitation to occur; these precipitates could be LiOEt/LiOH or lithium enolate **4.25**. It was imperative to have all outlet tubing to be wide bore (1/16" ID) to reduce the bridging of the reactive enolate intermediate. The *f*Reactor was set to 1000 rpm to increase the active mixing to its full potential. This assisted the continuous processing of the solid producing reaction which is an excellent design feature of this flow system. With active stirring in place, the flow system continuously ran for the required reaction time without precipitation blocking the reactor.

4.3.3 Chemical optimisation in the *f*Reactor

The total reactor volume of the *f*Reactor is 17.5 mL and each CSTR is 3.5 mL. After all pumps were initiated an entire reactor volume was wasted to allow the system to get to an equilibrium which is a total 'slow addition' time of 140 minutes. The outlet was then collected for 100 min which corresponds to 12.5 mL (0.045 mmol of desired product). The productivity could be change by increasing the flow rate or increasing the concentration of diester **4.15**. The outlet of the *f*Reactor was pumped into a stirring hot RBF which collected the reaction mixture. After 12.5 mL of reaction was collected, the RBF was stirred at reflux for a further 60 min to assure all cyclisation was complete. It should be noted that the final reflux could be performed in flow by using a suitable length reactor coil and heated to the desired temperature. An RBF was used for simplicity that enabled focus onto translating a batch 'dropwise' addition into a flow 'dropwise' addition. It is common when adding a reagent slowly that after the 'dropwise' addition the reaction is stirred and heated for an allotted time to complete the reaction and hence this is mirrored in the flow reactor design.

The first chemical parameter explored was the varying the excess of LiHMDS in the reaction. It was noted in literature that a large excess of base is used to facilitate macrocyclisations which was shortly explored in this chemical optimisation (Table 15).

Table 15 - Exploring base equivalence

Entry	4.15 (equiv.)	LiHMDS (equiv.)	Temp. of fReactor (°C)	Time of final reflux (min)	Temp. of final reflux (°C)	Solvent	4.16 Yield ^a
1	1.0	20	44	60	60	THF	8%
2	1.0	12.5	44	60	60	THF	6%
3	1.0	4.6	44	60	60	THF	46%

^a = yield determined by internal ¹H NMR standard

The equivalence of the reaction was changed by diluting the stock solution of diester **4.15** and keeping the concentration of LiHMDS the same (1 M). It was found that 4.6 equivalents of LiHMDS, the same as the batch conditions, gave the highest yield of β -keto ester **4.16** (entry 3, Table 15). Using both 20 and 12.5 equivalents of LiHMDS as base gave very small amounts of desired product, 8% and 6%, respectively (entries 1 and 2, Table 15). It was noted that a vast amount of precipitate was formed when the base was in great excess which may have affected the mixing and thus the cyclisation, hence a low yield. Collecting the outlet of the reaction into a hot RBF and refluxing for a further hour raised concerns whether the fReactor was assisting the cyclisation or whether the entire reaction was happening in the final hour reflux at a higher temperature. Due to the large difference in yield while changing the base equivalence, it was determined that the reaction is being aided by the fReactor (entries 1 and 2, Table 15). If the reaction were not being facilitated by the fReactor then one would assume that the yield of entries 1 and 2 (Table 15) would be similar to entry 3 (Table 15) due to the same collection flask conditions. Unless the reaction was highly sensitive to varying equivalence of LiHMDS.

The temperature of the 'dropwise' flow addition was explored with a batch 'dropwise' addition comparison (Table 16). The addition time for both batch and flow was 140 minutes. It should be noted that the concentration of the batch reactions were 1.3 x more concentrated but the equivalent of LiHMDS was kept the same.

Table 16 – Temperature screen for both flow and batch conditions

Batch 'dropwise' addition							
Entry	4.15 (equiv.)	LiHMDS (equiv.)	Temp. of addition (°C)	Time of final reflux (min)	Temp. of final reflux (°C)	Solvent	4.16 Yield ^a
1 ^b	1.0	4.6	40	60	60	THF	22%
2 ^b	1.0	4.6	50	60	60	THF	26%
3 ^b	1.0	4.6	60	60	60	THF	(60%)
Flow 'dropwise' addition via fReactor							
Entry	4.15 (equiv.)	LiHMDS (equiv.)	Temp. of addition (°C)	Time of final reflux (min)	Temp. of final reflux (°C)	Solvent	4.16 Yield ^a
4	1.0	4.6	30	60	60	THF	6%
5	1.0	4.6	44	60	60	THF	(60%)
6	1.0	4.6	50	60	60	THF	15%
7	1.0	4.6	70	60	60	THF	0%

a = yield determined by internal ¹H NMR standard; yields in parenthesis are isolated; b = reaction concentration of diester after dropwise addition was 0.05617 M

When adding diester **4.15** slowly over 2 hours in batch into stirring LiHMDS, it was found that 60 °C was the optimal conditions for the cyclisation to take place yielding 60% of β -keto ester **4.16** (entry 3, Table 16). Both 40 °C and 50 °C gave moderately low yields at 22% and 26%, respectively (entries 1 and 2, Table 16). Translating this data over to the fReactor, gave different results. Higher temperatures, 50 °C and 70 °C, gave low yields and the 70 °C reaction blocked the final CSTR due to the loss of THF solvent causing fouling in the outlet of the reactor (entries 6 and 7, Table 16). The 44 °C reaction was found to give a similarly high yield compared to the optimal batch conditions, however, the batch conditions required 60 °C to achieve the same yield (entry 5, Table 16). 30 °C was also tested to see how cold the reaction could go and found the yield dropped off significantly to 6% (entry 4, Table 16). Through ¹H NMR analysis the mass balance of the above reactions found that the remaining material was most commonly the oligomer **4.27**. It was postulated that the higher temperatures used on the fReactor caused THF to boil more readily and therefore increase the local concentration of the reaction which is detrimental for the Dieckmann cyclisation. The removal of THF through boiling also caused the lithium enolate solid to bridge and block the reactor more which in turn causes the process to fail. The use of a BPR to mildly pressurise the fReactor could be installed to superheat the THF solvent and avoid increasing the concentration. However, BPRs create extremely restricted flow and this system processes a reaction mixture that is suspension heavy and thus would most likely block the BPR.

The productivity of this system was still relatively low due to the required low concentration. The productivity of synthesising the cyclic β -keto ester **4.16** was 0.042 g/h which is very low for a flow process, however, further optimisation with concentration and/or flow rate could improve on this.

With the optimal flow conditions established (entry 5, Table 16), the saponification and decarboxylation were explored. This tandem flow-batch system required no intermediate purification, and the saponification reagents were added directly to the collected crude reaction mixture. Using similar conditions to the batch reaction, (*Z*)-Civetone could be isolated (Table 17).

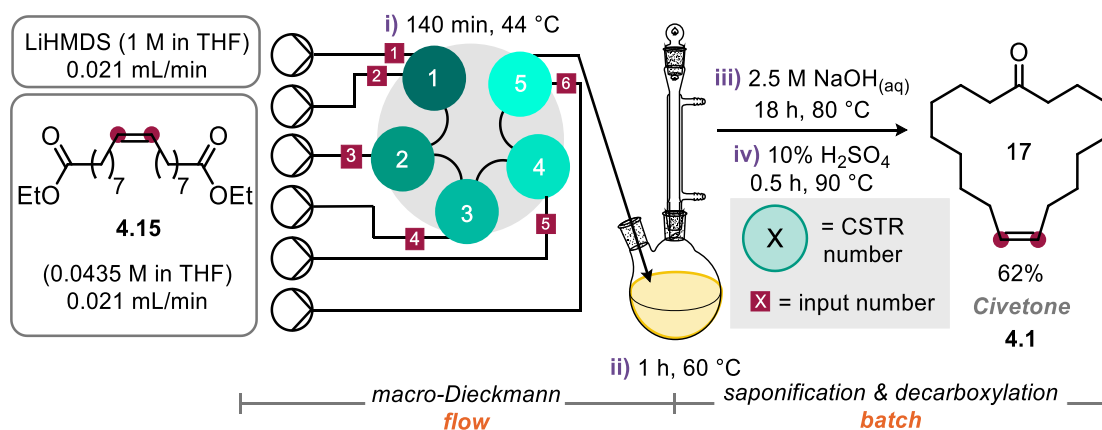
Table 17 - Exploring saponification and decarboxylation conditions

Entry	2.5 M NaOH (equiv.)	Sap. Temp. (°C)	Sap. Time (h)	Decarbox. Temp. (°C)	Decarbox. Time. (min)	Isolated Yield
1	3.0	80	1	90	30	32% Civetone; 21% 4.16
2	3.0	80	18	90	30	62% Civetone

solvent = THF; reaction acidified to pH ~1

The saponification required the available hydroxide anion to attack the ester group on **4.15** to form the carboxylate and upon acidification, the carboxylic acid. Heating the carboxylic acid in the presence of acid (10% H₂SO₄) drove the decarboxylation thus forming (*Z*)-Civetone **4.1** with the removal of CO₂. Initially, the saponification and decarboxylation gave 32% (*Z*)-Civetone **4.1** but 21% of the cyclic β -keto ester **4.16** was also isolated (entry 1, Table 17). This meant the saponification reaction did not go to completion in 1 hour, therefore, the reaction was left overnight for 18 h to drive the reaction to completion. After 18 h, acidification, and subsequent decarboxylation, (*Z*)-Civetone **4.1** was isolated in 62% yield corresponding to 0.07 g of product (entry 2, Table 17).

This was the first time (*Z*)-Civetone had been synthesised via flow methods in a semi-continuous manner. The *Z/E* ratio remained >98/2 throughout the process as the geometry of the alkene was unchanged, however, no *E* product was observed and the isolated (*Z*)-Civetone contained no (visible by ¹H NMR) *E* product or cyclic β -keto ester. As discussed previously, it would be possible to fully process this system continuously by introducing a flow reactor coil downstream from the *f*Reactor. This is an excellent example where reactor design enabled a pseudo-first order system to take place in continuous flow. The slow addition of a reagent via multiple injection points enabled a difficult Dieckmann cyclisation to take place in flow (Scheme 71).



Scheme 71 – Final optimised tandem flow-batch reactor for the synthesis of (Z)-Civetone

Scale up

The longevity and robustness of the *f*Reactor was tested by running the system for an extended period to increase the scale of the reaction. The total collection time was 6 hours which processed a gram of diester **4.15** to yield 0.3 g of Civetone **4.1** in 68% yield. A higher yield of 68% was found when scaling up the reaction, this could be due to more product material being easier to isolate. It was found that the plastic syringes started to swell and leak after 6 hours of running the reactor. This meant that our methodology was robust, up to that point. Moving forward, the use of glass syringes or THF resistant plastic would easily solve this problem. Furthermore, the use of HPLC pumps could be used, however, peristaltic pumps might be superior in handling the corrosive LiHMDS due to the mechanical parts of the pump being non-wetted. The *f*Reactor managed the continual production of lithium salt precipitate without clogging or fouling of the reactor. Due to the increased scale of the reaction, a longer decarboxylation step of 1.5 hours was implemented to assure the complete conversion to (Z)-Civetone **4.1**. The productivity of this scale up was 0.0462 g/h which meant to gain over 1 gram of (Z)-Civetone **4.1** this system would need to run for 23 hours. The productivity could be increased by optimising reaction time/flow rate and/or concentration, however, this is unlikely due to the vast amount of precipitate already produced and increasing the concentration would most likely causes blockages.

4.4 Conclusions and outlook

In summary, exploring reactor design to facilitate the Dieckmann cyclisation in flow towards the synthesis of (*Z*)-Civetone **4.1** has been reported. After attempting to translate the batch chemistry directly to a simple flow system caused an immediate blockage. Subsequently, with the addition of the *f*Reactor as an active mixer without the use of multiple injection points, the continuous process failed again due to the overloading of precipitate in the reaction.

Finally, this chapter has demonstrated the utilisation of the *f*Reactor to mimic a ‘dropwise’ addition of a reagent in flow. This is an excellent example where reactor design has enabled a pseudo-first order reaction via multiple injection points over a series of CSTRs to successfully synthesise (*Z*)-Civetone **4.1** in 62% yield. The tandem flow-batch methodology could be scaled up with a total running time of 6 hours and achieving 0.3 g of (*Z*)-Civetone **4.1** in 68% with a 0.0462 g/h productivity. The use of CSTRs furthermore facilitated the processing of a precipitate forming reaction via active mixing with integrated stirrer bars to prevent blocking or fouling of the reactor.

Outlook

The productivity of the reaction was low for a continuous flow process and a chemical optimisation could be undertaken to explore increasing the concentration of the reaction, however, as previously discussed, this seems an unfavourable option. It is possible to also increase the flow rate thus the amount of reaction mixture dispensed over time. However, due to the batch conditions requiring 2 hours of dropwise addition to yield 62% it is unlikely that a shorter reaction time would improve the yield. It is important to note that the Dieckmann cyclisation is a reversible reaction, and it is therefore possible that over time the cyclic β -keto ester **4.16** could de-cyclise and more favourably oligomerise with neighbouring esters. Currently, the flow system is a semi-flow process due to the coupled downstream batch method to saponify and decarboxylate thus affording (*Z*)-Civetone. The introduction of basic $\text{NaOH}_{(\text{aq})}$ in a continuous manner post cyclisation would be feasible to saponify the product in-line. To fully translate the process into flow, the addition of acid to decarboxylate might raise issues of precipitation via the neutralisation process. However, this should not be an issue due to a bi-phasic mixture being established into the flow process thus circumventing any salt build up in the system. These changes could allow for the continuous synthesis of (*Z*)-Civetone from the (*Z*)-diester **4.15**.

Developing this system further, it would be an interesting feat of engineering to couple the collaborative projects together into a telescoped synthesis of (*Z*)-Civetone **4.16**.

Using the tube-in-tube reactor to synthesise the (*Z*)-diester **4.15** in flow and directly feeding that reaction mixture into the *f*Reactor to undergo the synthesis of (*Z*)-Civetone **4.1**. The modular nature of flow would allow this; however, this concept raises many flags and considerations including solvent and reagent compatibility. Nonetheless, these issues could be circumvented by in-line purification tools such as, membrane filtration and downstream processing.

4.5 References

- 1 M. F. C. Plugge and J. C. Mol, *Synlett*, 1991, **1991**, 507–508.
- 2 H. J. Bestmann and H. Lütke, *Tetrahedron Lett.*, 1984, **25**, 1707–1710.
- 3 H. Hagiwara, T. Adachi, T. Nakamura, T. Hoshi and T. Suzuki, *Nat. Prod. Commun.*, 2012, **7**, 913–915.
- 4 R. Hamasaki, S. Funakoshi, T. Misaki and Y. Tanabe, *Tetrahedron*, 2000, **56**, 7423–7425.
- 5 A. Dumas, S. Colombel-Rouen, I. Curbet, G. Forcher, F. Tripoteau, F. Caijo, P. Queval, M. Rouen, O. Baslé and M. Mauduit, *Catal. Sci. Technol.*, 2019, **9**, 436–443.
- 6 J. Tsuji and T. Mandai, *Tetrahedron Lett.*, 1977, **18**, 3285–3286.
- 7 A. Fürstner and G. Seidel, *J. Organomet. Chem.*, 2000, **606**, 75–78.
- 8 A. Sytniczuk, M. Dąbrowski, Ł. Banach, M. Urban, S. Czarnocka-Śniadała, M. Milewski, A. Kajetanowicz and K. Grela, *J. Am. Chem. Soc.*, 2018, **140**, 8895–8901.
- 9 H. Hunsdiecker, *Berichte der Dtsch. Chem. Gesellschaft*, 1943, **76**, 142–149.
- 10 J. Tsuji and S. Hashiguchi, *J. Organomet. Chem.*, 1981, **218**, 69–80.
- 11 J. Tsuji and S. Hashiguchi, *Tetrahedron Lett.*, 1980, **21**, 2955–2958.
- 12 Y. Tanabe, A. Makita, S. Funakoshi, R. Hamasaki and T. Kawakusu, *Adv. Synth. Catal.*, 2002, **344**, 507–510.
- 13 É. Morin, J. Sosoe, M. Raymond, B. Amorelli, R. M. Boden and S. K. Collins, *Org. Process Res. Dev.*, 2019, **23**, 283–287.
- 14 H.-R. Bjørsvik and L. Liguori, *Org. Process Res. Dev.*, 2014, **18**, 1509–1515.
- 15 D. Ormerod, B. Bongers, W. Porto-Carrero, S. Giegas, G. Vijt, N. Lefevre, D. Lauwers, W. Brusten and A. Buekenhoudt, *RSC Adv.*, 2013, **3**, 21501–21510.
- 16 E. J. O’Neal and K. F. Jensen, *ChemCatChem*, 2014, **6**, 3004–3011.
- 17 M. Rabiller-Baudry, G. Nasser, T. Renouard, D. Delaunay and M. Camus, *Sep. Purif. Technol.*, 2013, **116**, 46–60.
- 18 R. Duque, E. Öchsner, H. Clavier, F. Caijo, S. P. Nolan, M. Mauduit and D. J.

- Cole-Hamilton, *Green Chem.*, 2011, **13**, 1187–1195.
- 19 P. Bianchi, J. D. Williams and C. O. Kappe, *J. Flow Chem.*, 2020, **10**, 475–490.
- 20 V. Hessel, H. Löwe and F. Schönfeld, *Chem. Eng. Sci.*, 2005, **60**, 2479–2501.
- 21 J. R. Bourne, *Org. Process Res. Dev.*, 2003, **7**, 471–508.
- 22 M. R. Chapman, S. C. Cosgrove, N. J. Turner, N. Kapur and A. J. Blacker, *Angew. Chemie Int. Ed.*, 2018, **57**, 10535–10539.
- 23 K. E. Jolley, M. R. Chapman and A. J. Blacker, *Beilstein J. Org. Chem.*, 2018, **14**, 2220–2228.
- 24 M. R. Chapman, M. H. T. Kwan, G. King, K. E. Jolley, M. Hussain, S. Hussain, I. E. Salama, C. González Niño, L. A. Thompson, M. E. Bayana, A. D. Clayton, B. N. Nguyen, N. J. Turner, N. Kapur and A. J. Blacker, *Org. Process Res. Dev.*, 2017, **21**, 1294–1301.
- 25 C. Schotten, D. Plaza, S. Manzini, S. P. Nolan, S. V. Ley, D. L. Browne and A. Lapkin, *ACS Sustain. Chem. Eng.*, 2015, **3**, 1453–1459.
- 26 K. Skowerski, S. J. Czarnocki and P. Knapkiewicz, *ChemSusChem*, 2014, **7**, 536–542.
- 27 J. P. Schaefer and J. J. Bloomfield, in *Organic Reactions*, John Wiley & Sons, Inc., Hoboken, NJ, USA, 2011, pp. 1–203.

5 Experimental

5	Experimental	128
5.1	General Methods.....	129
5.2	Acetylene experimental.....	130
5.3	Acyl ketene experimental.....	136
5.4	Civetone experimental.....	148
5.5	References	152

5.1 General Methods

All chemicals were obtained from commercial sources and were used as supplied, without further purification. Dry solvents were obtained from a Braun MB SPS-800 solvent purification system fitted with the recommended columns. Progress of the reactions was monitored by thin layer chromatography (TLC) using Merck TLC silica gel 60 sheet and visualized with ultraviolet light or potassium permanganate stain or the reaction was monitored using ^1H NMR with an internal standard. Flash column chromatography was performed with Sigma Aldrich silica gel 40-60 Å as the stationary phase and solvents employed were analytical grade. ^1H , ^{13}C , and ^{19}F NMR spectra were recorded on a Bruker AVX500 (500 MHz) and AVX400 (400 MHz) spectrometers at ambient temperature. Chemical shifts (δ) are given in parts per million, referenced to the residual peak of CHCl_3 , $\delta = 7.26$ (^1H NMR) and $\delta = 77.0$ (^{13}C NMR) as internal references. Trifluorotoluene was used as internal standard for ^{19}F NMR and the spectra was reference to the standard peak, $\delta = -63.72$ ppm. Spin-spin coupling constants J are given in Hz and refer to apparent multiplicities rather than true coupling constants. Data are reported as: chemical shift, multiplicity, and integration. The following abbreviations were used to designate chemical shift multiplicities: s = singlet, d = doublet, t = triplet, q = quartet, dd = doublet of doublets, dt = doublet of triplets, dq = doublet of quartets, qt = quartet of triplets, ddd = doublet of doublet of doublets, ddt = doublet of doublet of triplets, app.t = apparent triplet, app.dq = apparent doublet of quartet, and m = multiplet. NMR spectra were processed using MestReNova version 6.0.2-5475 software. Mass spectra data were analysed using Waters LCT Premier TOF Mass spectrometer. Spectra were obtained using electron impact ionisation (EI), chemical ionisation (CI), positive electrospray ionisation (ESI), or atmospheric solids analysis probe (ASAP+). Infrared spectra were recorded on a Shimadzu IR-Affinity-1S FTIR spectrometer. Melting points (m.p.) were measured using a Gallenkamp apparatus and are reported uncorrected. 25 °C means isothermally controlled whereas 'rt' means the reaction is being held at ambient UK temperatures. Where compounds have been previously reported in the literature citing full analytical data, only ^1H NMR data are recorded. However, if a compound has been reported lacking data or is novel, the compound has been fully characterised.

5.2 Acetylene experimental

Flow equipment

The flow setup used both PFA tubing with a 1/32" internal diameter and used wide-bore tubing with a 1/16" internal diameter which was supplied by Polyflon. All flow fittings and connections were purchased from Kinesis (Gripper fitting nuts, Adapters, Omniloc type-p fitting ferrule, Y-Connector (T-piece), Threaded union, 250 psi Back pressure regulator). Pumps used were the SSI Series 1 Stainless Steel HPLC pump and the SSI Series 1 PEEK HPLC pump. The residence coils were made up from the tubing by taking the appropriate length for the desired volume. All pumps were calibrated by pumping solvent into a measuring cylinder, recording the time taken for the desired volume to be dispensed and then adjusting the pump's flow rate to the correct value, if required. Glass columns (150 mm x 10 mm and 6.6 mm x 150 mm) used were supplied by Omnifit. The NiT reactor was assembled using a Swagelok T-Piece with appropriate Swagelok nuts and ferrules.

General procedure for preparation of calcium carbide suspension (GP5.2.1)

Calcium carbide (3 g, 46.8 mmol) and paraffin oil (0.6 mL) was charged into a 25 mL stainless steel milling jar with an 8 g stainless steel ball. The jar was milled in a Retsch MM 400 mixer mill for 30 min at 30 Hz. The suspension was packed into a 150 mm x 10 mm Omnifit column and dry THF was flushed through the column to remove the air and was then ready for use.

General procedure for preparation of MgSO₄ drying column (GP5.2.2)

Magnesium sulfate and sand (1:3) were packed into a 6.6 mm x 150 mm Omnifit column and flushed with anhydrous THF to remove air from the column.

General procedure for titrating *n*-BuLi (GP5.2.3)

3 x 50 mL RBFs with stir bars were dried in the oven overnight. Menthol (0.1563 g, 1 mmol) in dry hexane (5 mL) and 1,10-phenanthroline (0.1 g, 0.55 mmol) were added to each RBF under inert conditions. A recorded amount of *n*-BuLi was added to each stirring RBF and the volume recorded when a permanent colour change was observed. An average titre was calculated over the three reactions and the concentration of *n*-BuLi was found.

General procedure for preparation of silver impregnated silica (GP5.2.4)

Silver nitrate (0.55 g, 3.24 mmol) was dissolved in water (3 mL) and mixed with silica (5 g) in a mortar and pestle for 5 min. The mixture was dried in an oven at 150 °C for 1 h and further dried in a drying pistol with P₂O₅. When loading a flash column, a band of

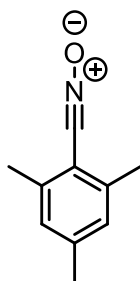
silver impregnated silica was formed on top of the non-silver silica and covered with more non-silver silica.

Calcium carbide titration calculations:

A crude prediction for the amount of acetylene gas liberated from CaC_2 was calculated using the ideal gas equation ($PV = nRT$). CaC_2 (0.1933 g, 3.02 mmol) was loaded into a RBF that was equipped with a gas outlet vent into an inverted water-filled measuring cylinder. Water (25 mL) was added through a septum. 55 mL of gas was recorded therefore it was found that 2.25 mmol of acetylene gas was produced. This corresponded to 75% of CaC_2 added thus confirming the purity of the commercial CaC_2 source (Fisher Sci, c/1000/53, 72-82% calcium carbide, 12-18% calcium oxide).

Starting material synthesis and batch alternatives:

Synthesis of 2,4,6-trimethylbenzyl nitrile oxide (**2.16**)



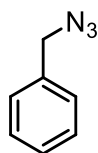
2.16

2,4,6-trimethylbenzaldehyde oxime (2 g, 12.27 mmol) was dissolved in DMF (15 mL) and stirred and cooled to 0 °C. NBS (2.4 g, 13.48 mmol) was dissolved in DMF (13 mL) and added dropwise. Et_3N (1.87 mL, 13.5 mmol) was dissolved in DMF (7 mL) and subsequently added slowly. The reaction was left to warm to room temperature and stirred for an additional 30 min. Iced water (30 mL) was added to form a precipitate and the solution was left at 0 °C for 4 h. The product was collected via filtration, washed with ice cold

water, dried under vacuum, and recrystallised from methanol to yield **2.16** as a white powder (1.81 g, 91%).

^1H NMR (400 MHz, CDCl_3) δ 6.91 (s, 1H), 2.42 (s, 3H), 2.30 (s, 2H) ppm. Characterisation data was in accordance with literature.¹

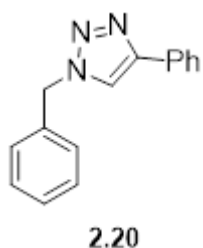
Synthesis of benzyl azide (**2.14**)



2.14

Benzyl chloride (1.15 mL, 10 mmol) was suspended in water (7 mL). NaN_3 (0.6891 g, 10.6 mmol) was added followed by NH_4Cl (1.07 g, 20 mmol) and the reaction was heated to 70 °C for 48 h. After cooling, the reaction mixture was extracted with diethyl ether (25 mL) and dried with MgSO_4 and filtered. The solvent was removed very carefully to yield **2.14** as a colourless oil (1.0766 g, 81%).

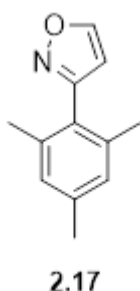
^1H NMR (400 MHz, CDCl_3) δ 7.48 – 7.28 (m, 5H), 4.35 (s, 2H) ppm. ^{13}C NMR (101 MHz, CDCl_3) δ 135.4, 128.9, 128.4, 128.3, 54.9 ppm. HRMS (EI) calc. for $\text{C}_7\text{H}_7\text{N}_3$: 133.0640, found: 133.0643. Characterisation data was in accordance with literature.²

Synthesis of 1-benzyl-4-phenyl-1*H*-1,2,3-triazole (2.20)

Benzyl azide **2.14** (0.13 mL, 1 mmol) and phenyl acetylene (0.11 mL, 1 mmol) were added to a solvent mixture of H₂O:DMSO (1:1, 4 mL). A stock solution of CuSO₄ (0.2 mL, 1 M), and sodium ascorbate (0.0396 g, 0.2 mmol) were sequentially added. The reaction was stirred at rt for 24 h. Water (5 mL) was added, and the reaction left in the fridge overnight for precipitation to occur. The solid precipitate was

filtered and further purified via a short silica plug to yield **2.20** (0.1806 g, 77%).

¹H NMR (400 MHz, CDCl₃) δ 7.79 (s, 2H), 7.66 (s, 1H), 7.49 – 7.28 (m, 8H), 5.58 (s, 2H) ppm. ¹³C NMR (101 MHz, CDCl₃) δ 148.3, 134.7, 130.5, 129.2, 128.8, 128.7, 128.2, 128.1, 125.7, 119.5, 54.3 ppm. Characterisation data was in accordance with literature.³

Synthesis in continuous flow:**Synthesis of 3-mesitylisoazole using flow system 2.1 (2.17)**

GP5.2.1 was followed to prepare the calcium carbide cartridge. Flow system **2.1** was flushed with dry MeCN and the reactor heated to 90 °C. A stock solution of 2,4,6-trimethylbenzyl nitrile oxide (0.1 M, 25 mL) was primed into a HPLC pump. A 5% H₂O in MeCN solvent mixture was primed into another pump and initiated for 6 min at 0.2 mL/min. The nitrile oxide pump was then started at 0.2 mL/min, and the system was left to pump for

1 h. The product was collected for 50 min which equates to 1 mmol of potential product. The flow system was flushed with dry THF followed by dry MeCN. The product was purified via flash column chromatography (20% EtOAc in Hexane) to yield **2.17** as a pale-yellow solid. (0.1485 g, 80%)

¹H NMR (400 MHz, CDCl₃) δ 8.51 (d, *J* = 1.6 Hz, 1H), 6.95 (s, 2H), 6.30 (d, *J* = 1.6 Hz, 1H), 2.33 (s, 3H), 2.12 (s, 6H) ppm. ¹³C NMR (101 MHz, CDCl₃) δ 161.1, 158.3, 138.9, 137.2, 128.4, 125.9, 105.9, 21.1, 20.2 ppm. HRMS (EI) calc. for C₁₂H₁₃NO: 187.0997, found: 187.0993. m.p. 93–96 °C (acetone).

Methodology for flow system 2.2

Using **GP5.2.1**, flow system **2.2** was constructed and all pumps were primed. *n*-BuLi (1.75 M, 1 mL) was diluted in dry hexane (6 mL) and charged into a 5 mL loading loop that had been pre-flushed with N_{2(g)}. A solution of 4-methyl acetophenone (0.2 M) in THF was primed into a pump. A 5% H₂O in THF stock solution was primed into the acetylene generating pump and installed with a loading loop of dry THF (5 mL). The acetylene generating pump was initiated at 0.2 mL/min and left to pump for 25 min, injecting the dry THF loading loop into the flow system. The 4-methyl acetophenone pump was then

started at 0.2 mL/min and the outlet left to waste for 30 min. The *n*-BuLi pump was finally set to 0.2 mL/min, and the loading loop set to inject the *n*-BuLi into the flow system. The outlet was collected for 44 min into an NH₄Cl quench corresponding to 1 mmol of product. No product was observed due to a failing flow system.

Methodology for flow system 2.3

Using **GP5.2.1** and **GP5.2.2** flow system **2.3** was constructed, and all pumps were primed. *n*-BuLi (1.75 M, 1 mL) was diluted in dry hexane (6 mL) and charged into a 5 mL loading loop that had been pre-flushed with N_{2(g)}. A solution of 4-methyl acetophenone (0.2 M) in THF was primed into a pump. A 5% H₂O in THF stock solution was primed into the acetylene generating pump and installed with a loading loop of dry THF (5 mL). The acetylene generating pump was initiated at 0.2 mL/min and left to pump for 25 min, injecting the dry THF loading loop into the flow system. The 4-methyl acetophenone pump was then started at 0.2 mL/min and the outlet left to waste for 30 min. The *n*-BuLi pump was finally set to 0.2 mL/min, and the loading loop set to inject the *n*-BuLi into the flow system. The outlet was collected for 44 min into an NH₄Cl quench corresponding to 1 mmol of product. No product was observed due to a failing flow system.

Methodology for flow system 2.4

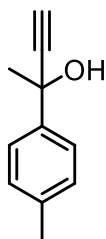
Methodology for flow system **2.4** is the same as flow system **2.3**. However, wide bore tubing (1/16" ID) was used in the construction of the reactor coil. No product was observed due to a failing flow system.

Methodology for flow system 2.5

Using **GP5.2.1** and **GP5.2.2** flow system **2.5** was constructed, and all pumps were primed. *n*-BuLi (1.75 M, 1 mL) was diluted in dry hexane (6 mL) and charged into a 5 mL loading loop that had been pre-flushed with N_{2(g)}. A solution of 4-methyl acetophenone (0.2 M) in THF was primed into a pump. A 5% H₂O in THF stock solution was primed into the acetylene generating pump and installed with a loading loop of dry THF (5 mL). The acetylene generating pump was initiated at 0.2 mL/min and left to pump for 25 min, injecting the dry THF loading loop into the flow system. The 4-methyl acetophenone pump was then started at 0.2 mL/min and the outlet left to waste for 30 min. The *n*-BuLi pump was finally set to 0.2 mL/min, and the loading loop set to inject the *n*-BuLi into the flow system. The outlet was collected for 44 min into an NH₄Cl quench corresponding to 1 mmol of product. The flow system was flushed with dry THF. The collected reaction mixture was extracted with EtOAc (3 × 5 mL) and the organic layer washed with brine (2 × 25 mL). The organic layer was dried with MgSO₄, filtered, and solvent removed. Mesitylene (46 μL) was added as internal standard and ¹H NMR recorded.

Methodology for flow system 2.6

Using **GP5.2.1** and **GP5.2.1** flow system **2.6** was constructed with the installation of the NiT reactor, and all pumps were primed. *n*-BuLi (1.75 M, 1 mL) was diluted in dry hexane (6 mL) and charged into a 5 mL loading loop that had been pre-flushed with N_{2(g)}. A solution of 4-methyl acetophenone (0.2 M) and TBAB (0.02 M) in THF was primed into a pump. A 5% H₂O in THF stock solution was primed into the acetylene generating pump and installed with a loading loop of dry THF (5 mL). The water bath containing the reactor coil was heated to 60 °C. The acetylene generating pump was initiated at 0.2 mL/min and left to pump for 25 min, injecting the dry THF loading loop into the flow system. The 4-methyl acetophenone pump was then started at 0.2 mL/min and the outlet left to waste for 30 min. The *n*-BuLi pump was set to 0.2 mL/min, and the loading loop set to inject the *n*-BuLi into the flow system. The outlet was collected for 44 min into an NH₄Cl quench corresponding to 1 mmol of product. The flow system was flushed with dry THF. The collected reaction mixture was extracted with EtOAc (3 x 25 mL) and the organic layer washed with brine (2 x 25 mL). The organic layer was dried with MgSO₄, filtered, and solvent removed. Mesitylene (46 µL) was added as internal standard and ¹H NMR taken.

Synthesis of 2-tolyl but-3-yn-2-ol (2.19)**2.19**

Using **GP5.2.1** and **GP5.2.2**, flow system **2.7** was constructed with the installation of the NiT reactor and a longer 15 mL reactor coil and all pumps were primed. Titrated (**GP5.2.3**) *n*-BuLi (2.15 M, 2.82 mL) was diluted in dry hexane (5.26 mL) and charged into a 5 mL loading loop that had been pre-flushed with N_{2(g)}. A solution of 4-methyl acetophenone (0.075 M) in THF was primed into a pump. A 5% H₂O in THF stock solution was primed into the acetylene generating pump and installed with a loading loop of dry THF (5 mL). The water bath containing the reactor coil was heated to 60 °C. The acetylene generating pump was initiated at 0.2 mL/min and left to pump for 25 min, injecting the dry THF loading loop into the flow system. The 4-methyl acetophenone pump was then started at 0.2 mL/min and the outlet left to waste for 30 min. The *n*-BuLi pump was set to 0.2 mL/min, and the loading loop set to inject the *n*-BuLi into the flow system. The water dilution pump was set to 0.5 mL/min and initiated. The outlet was collected for 103 min into an NH₄Cl quench corresponding to 0.6367 mmol of product. The flow system was flushed with dry THF. The collected reaction mixture was extracted with EtOAc (3 x 25 mL) and the organic layer washed with brine (2 x 25 mL). The organic layer was dried with MgSO₄, filtered, and solvent removed. The crude product was purified* via flash column chromatography (10% EtOAc in cyclohexane) to afford **2.19** as a colourless semi-solid/oil (0.0979 g, 96%).

*Purification was first attempted using silver impregnated silica which was found to decompose the product. **GP5.2.4** was followed to make the silver silica.

^1H NMR (400 MHz, CDCl_3) δ 7.55 (d, $J = 8.2$ Hz, 2H), 7.18 (d, $J = 7.9$ Hz, 2H), 2.67 (s, 1H), 2.36 (s, 3H), 1.79 (s, 3H) ppm. ^{13}C NMR (101 MHz, CDCl_3) δ 142.3, 137.7, 129.1, 124.9, 87.6, 73.0, 69.8, 33.1, 21.2 ppm. HRMS (EI) calc. for $\text{C}_{11}\text{H}_{12}\text{O}$: 160.0888, found: 160.0887. IR / ν max: 3375, 3291, 2100, 1508, 1368, 1083, 818, 644, 583 cm^{-1}

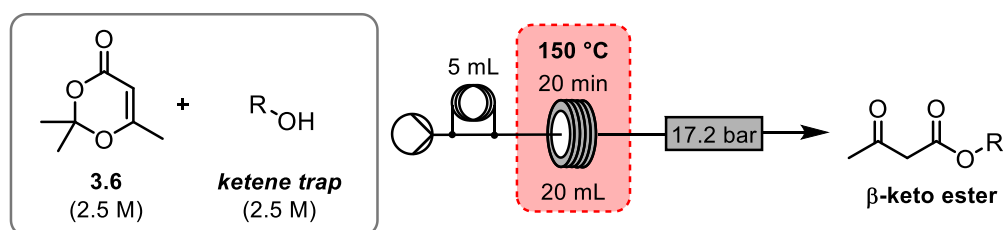
5.3 Acyl ketene experimental

Flow equipment

The flow setup consisted of either stainless steel or PFA tubing of an 0.8 mm ID, one HPLC pump, and a 17.2 bar back-pressure regulator. Residence coils were made from the tubing by taking the appropriate length for the desired volume (i.e. 0.8 mm ID PFA tube, length 20.21 m, volume 10 mL). Sample loop of 1 or 5 mL (PFA) were used to load the reagents. The temperature of the flow residence coil was controlled using a CRD Polar Bear Plus device or an Uniqsis HotCoil. 2,2,6-Trimethyl-4*H*-1,3-dioxin-4-one, **3.6** will be abbreviated to TMD, **3.6**.

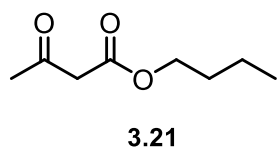
General flow procedure to synthesise β -keto esters from TMD, **3.6** (GP5.3.1)

Using Flow System **3.1**, the flow setup was set to pump THF at 0.5 mL/min and the Uniqsis HotCoil set to 150 °C and left to achieved thermal equilibrium. TMD, **3.6** (1.79 mL, 13.5 mmol) and an alcohol (13.5 mmol) were pre-mixed and diluted in THF (total volume and concentration 5.4 mL and 2.5 M). The pre-mixed reagents were injected into a 5 mL loading loop. The loading loop was set to inject and the system outlet put to waste for 22 min (11 mL). The crude product was collected for 6 min (3 mL) and the system left to waste and flush for 32 min. Purity was calculated via ^1H NMR by adding mesitylene (1 mmol) and β -keto ester (1 mmol) and calculating the integration difference.



Scheme 72 – β -keto ester formation with alcohol ketene trap (Flow System **3.1**)

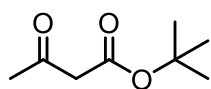
Synthesis of *n*-butyl acetoacetate (**3.21**)



Using **GP5.3.1** but neat conditions for TMD **3.6** (23 mmol, 3 mL) and *n*-butanol (23 mmol, 2.07 mL) as the alcohol. The crude reaction mixture was purified directly via a silica plug (30% EtOAc in hexane) affording butyl acetoacetate **3.21** as a pale-yellow oil

(0.5301 g, 93%, 99.6% purity).

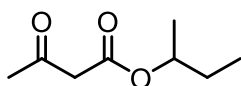
^1H NMR (500 MHz, CDCl_3) δ 4.08 (t, 2H), 3.39 (s, 2H), 2.21 (s, 3H), 1.64 – 1.50 (m, 2H), 1.40 – 1.26 (m, 2H), 0.87 (t, 3H) ppm. ^{13}C NMR (126 MHz, CDCl_3) δ 200.6, 167.2, 65.2, 50.1, 30.5, 30.1, 19.0, 13.6 ppm. HRMS (EI) calc. for $[\text{M}]^+$ $\text{C}_8\text{H}_{14}\text{O}_3$: 158.0943, found: 158.0936. Characterisation data was in accordance with literature.⁴

Synthesis of *t*-butyl acetoacetate (3.33)

3.33

Using **GP5.3.1** and *tert*-butanol as the alcohol, the crude reaction mixture was purified via a silica plug, (20% EtOAc in hexane) to afford *t*-butyl acetoacetate **3.33** as a pale-yellow oil (0.9400 g, 79%).

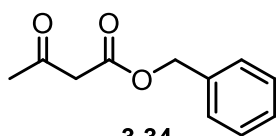
^1H NMR (400 MHz, CDCl_3) δ 3.35 (s, 2H), 2.25 (s, 3H), 1.47 (s, 9H) ppm. ^{13}C NMR (126 MHz, CDCl_3) δ 201.3, 167.0, 82.1, 51.6, 30.1, 28.1 ppm. Characterisation data was in accordance with literature.⁵

Synthesis of *sec*-butyl acetoacetate (3.22)

3.22

Using **GP5.3.1** and *sec*-butanol as the alcohol, the crude reaction mixture was purified via a silica plug (20% EtOAc in hexane) to afford *sec*-butyl acetoacetate **3.22** as a colourless oil (1.0185 g, 86%).

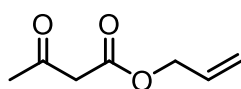
^1H NMR (500 MHz, CDCl_3) δ 4.90 – 4.82 (m, 1H), 3.39 (s, 2H), 2.23 (s, 3H), 1.64 – 1.46 (m, 2H), 1.19 (d, $J = 6.3$ Hz, 3H), 0.87 (t, $J = 7.5$ Hz, 3H) ppm. ^{13}C NMR (126 MHz, CDCl_3) δ 200.8, 166.9, 73.62, 50.5, 30.1, 28.7, 19.4, 9.7 ppm. HRMS (EI) calc. for $[\text{M}]^+$ $\text{C}_8\text{H}_{14}\text{O}_3$: 158.0943, found: 158.0945 Characterisation data was in accordance with literature.⁶

Synthesis of benzyl acetoacetate (3.34)

3.34

Using **GP5.3.1** and benzyl alcohol as the alcohol, the crude reaction mixture was purified via a silica plug (20% EtOAc in hexane) to afford benzyl acetoacetate **3.34** as a colourless oil (1.3697, 95%).

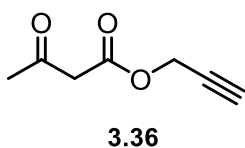
^1H NMR (500 MHz, CDCl_3) δ 7.40 – 7.33 (m, 5H), 5.18 (s, 2H), 3.50 (s, 2H), 2.25 (s, 3H) ppm. ^{13}C NMR (126 MHz, CDCl_3) δ 200.5, 167.1, 135.4, 128.8, 128.6, 128.5, 67.3, 50.2, 30.3 ppm. Characterisation data was in accordance with literature.⁷

Synthesis of allyl acetoacetate (3.35)

3.35

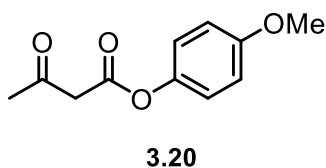
Using **GP5.3.1** and allylic alcohol as the alcohol, the crude reaction mixture was purified via a silica plug (20% EtOAc in hexane) to afford allyl acetoacetate **3.35** as a colourless oil (0.8016 g, 75%).

^1H NMR (500 MHz, CDCl_3) δ 5.91 (ddt, $J = 17.2, 10.4, 5.8$ Hz, 1H), 5.33 (app.dq, $J = 17.2, 1.5$ Hz, 1H), 5.25 (app.dq, $J = 10.4, 1.5$ Hz, 1H), 4.63 (dt, $J = 5.8, 1.5$ Hz, 2H), 3.47 (s, 2H), 2.26 (s, 3H) ppm. ^{13}C NMR (126 MHz, CDCl_3) δ 200.5, 166.9, 131.6, 119.1, 66.1, 50.1, 30.3 ppm. Characterisation data was in accordance with literature.⁸

Synthesis of propargyl acetoacetate (3.36)

Using **GP5.3.1** and propargyl alcohol as the alcohol, the crude reaction mixture was purified via a silica plug (20% EtOAc in hexane) to afford propargyl acetoacetate **3.36** as a colourless oil (0.843 g, 80%).

^1H NMR (500 MHz, CDCl_3) δ 4.74 (d, $J = 2.5$ Hz, 2H), 3.50 (s, 2H), 2.50 (t, $J = 2.5$ Hz, 1H), 2.28 (s, 3H) ppm. ^{13}C NMR (126 MHz, CDCl_3) δ 200.0, 166.4, 77.1, 75.5, 52.9, 49.8, 30.3 ppm. Characterisation data was in accordance with literature.⁷

Synthesis of 4-methoxyphenyl acetoacetate (3.20)

Using **GP5.3.1** and 4-methoxyphenol as the alcohol, the crude reaction mixture was purified via a silica plug (20% EtOAc in hexane) to afford 4-methoxyphenyl acetoacetate **3.20** as a yellow oil (1.4359 g, 92%).

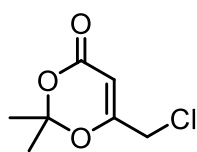
^1H NMR (500 MHz, CDCl_3) δ 7.08 – 6.98 (m, 2H), 6.92 – 6.86 (m, 2H), 3.79 (s, 3H), 3.67 (s, 2H), 2.35 (s, 3H) ppm. ^{13}C NMR (126 MHz, CDCl_3) δ 200.3, 166.3, 157.6, 144.0, 122.3, 114.7, 55.7, 50.1, 30.4 ppm. Characterisation data was in accordance with literature.⁶

Synthesis of acyl ketene precursors via γ -deprotonation

These reactions took place in RBFs fitted with air condensers that were flame dried and kept under nitrogen via vac-nitrogen exchange followed and maintained by a nitrogen filled balloon.

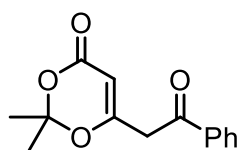
General procedure to synthesis acyl ketene precursors via γ -deprotonation (GP5.3.2)

Isopropyl amine (2.1 mL, 15 mmol) was stirred in THF (40 mL) at -78 °C via a dry ice/acetone bath. *n*-BuLi (7.67 mL, 16.5 mmol, 2.15 M) was added dropwise over 20 min via a syringe pump. A solution of TMD **3.6** (1.73 mL, 13 mmol) in THF (20 mL) was added dropwise over 20 min via a syringe pump. The reaction was stirred at -78 °C for 1.5 h. A solution of the desired electrophile (11 mmol) in THF (10 mL) was added. The reaction was subsequently stirred at -78 °C for 1 h. The reaction was quenched with sat. NH_4Cl (40 mL) and extracted with EtOAc (3 \times 20 mL). The combined organic layers were washed with brine (10 mL) and subsequently dried with MgSO_4 , filtered and solvent removed. The crude oil was purified via flash column chromatography (20% EtOAc in hexane) to afford the pure product.

Synthesis of 6-(chloromethyl)-2,2-dimethyl-4*H*-1,3-dioxin-4-one (3.47)**3.47**

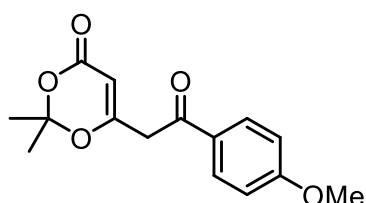
Using **GP5.3.2** and NCS (1.4688 g, 11 mmol) as the electrophile; the product **3.47** was purified as a yellow oil (0.6717 g, 36%).

^1H NMR (500 MHz, CDCl_3) δ 5.53 (t, $J = 0.7$ Hz, 1H), 4.01 (d, $J = 0.7$ Hz, 2H), 1.69 (s, 6H) ppm. ^{13}C NMR (126 MHz, CDCl_3) δ 164.6, 160.5, 107.6, 95.7, 41.1, 24.9 ppm. HRMS (ES) calc. for $[\text{M}+\text{H}]^+$ $\text{C}_7\text{H}_{10}\text{O}_3\text{Cl}$: 177.0318, found: 177.0318. Characterisation data was in accordance with literature.⁹

Synthesis of 2,2-dimethyl-6-(2-oxo-2-phenylethyl)-4*H*-1,3-dioxin-4-one (3.49)**3.49**

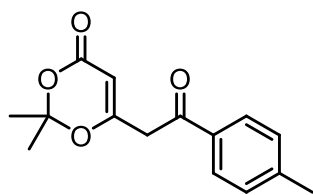
Using **GP5.3.2** and benzoyl chloride (1.28 mL, 11 mmol) as the electrophile; the product **3.49** was purified as a pale-yellow oil (0.6403 g, 24%).

^1H NMR (500 MHz, CDCl_3) δ 8.00 – 7.84 (m, 2H), 7.68 – 7.58 (m, 1H), 7.55 – 7.44 (m, 2H), 5.42 (s, 1H), 3.90 (s, 2H), 1.70 (s, 6H) ppm. ^{13}C NMR (126 MHz, CDCl_3) δ 193.2, 165.3, 160.9, 136.0, 134.2, 129.1, 128.5, 107.5, 97.2, 43.5, 25.1 ppm. HRMS (ES) calc. for $[\text{M}+\text{H}]^+$ $\text{C}_{14}\text{H}_{15}\text{O}_4$: 247.0970, found: 247.0963. Characterisation data was in accordance with literature.¹⁰

Synthesis of 6-(2-(4-methoxyphenyl)-2-oxoethyl)-2,2-dimethyl-4*H*-1,3-dioxin-4-one (3.59)**3.59**

Using **GP5.3.2** and *p*-anisoyl chloride (11 mmol, 1.8765 g) as the electrophile; the product **3.59** was purified as a pale-yellow oil (1.2562 g, 41%).

^1H NMR (500 MHz, CDCl_3) δ 7.91 (d, $J = 8.8$ Hz, 2H), 6.96 (d, $J = 8.8$ Hz, 2H), 5.41 (s, 1H), 3.89 (s, 3H), 3.84 (s, 2H), 1.70 (s, 6H) ppm. ^{13}C NMR (126 MHz, CDCl_3) δ 191.6, 165.6, 164.4, 161.0, 130.9, 129.1, 114.2, 107.4, 97.0, 55.7, 43.2, 25.2 ppm. HRMS (ES) calc. for $[\text{M}+\text{H}]^+$ $\text{C}_{15}\text{H}_{17}\text{O}_5$: 277.1076, found: 277.1067. Characterisation data was in accordance with literature.¹¹

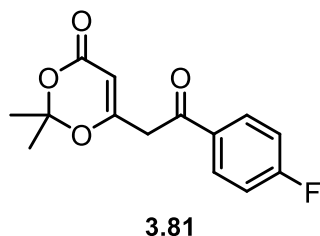
Synthesis of 2,2-dimethyl-6-(2-oxo-2-(*p*-tolyl)ethyl)-4*H*-1,3-dioxin-4-one (3.80)**3.80**

Using **GP5.3.2** and 4-methylbenzoyl chloride (1.45 mL, 11 mmol) as the electrophile; the product **3.80** was purified as a colourless oil (0.7165 g, 25%).

^1H NMR (500 MHz, CDCl_3) δ 7.83 (d, $J = 8.2$ Hz, 2H), 7.29 (d, $J = 8.2$ Hz, 2H), 5.41 (s, 1H), 3.87 (s, 2H), 2.43 (s, 3H), 1.70 (s, 6H) ppm. ^{13}C NMR (126 MHz, CDCl_3) δ 192.8, 165.5, 160.9, 145.2, 133.6, 129.7,

128.6, 107.4, 97.1, 43.4, 25.2, 21.9 ppm. HRMS (ES) calc. for $[M+H]^+$ $C_{15}H_{17}O_4$: 261.1127, found: 261.1132. Characterisation data was in accordance with literature.¹⁰

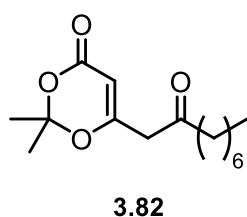
Synthesis of 6-(2-(4-fluorophenyl)-2-oxoethyl)-2,2-dimethyl-4H-1,3-dioxin-4-one (3.81)



Using **GP5.3.2** and 4-fluorobenzoyl chloride (1.3 mL, 11 mmol) as the electrophile; the product **3.81** was purified as a colourless oil (0.5833 g, 20%).

1H NMR (500 MHz, $CDCl_3$) δ 7.97 (dd, $J = 8.7, 5.3$ Hz, 2H), 7.18 (app.t, $J = 8.5$ Hz, 2H), 5.42 (s, 1H), 3.87 (s, 2H), 1.70 (s, 6H). ^{13}C NMR (126 MHz, $CDCl_3$) δ 191.6 (s), 166.4 (d, $J = 256.8$ Hz), 164.9 (s), 160.8 (s), 132.5 (d, $J = 3.0$ Hz), 131.2 (d, $J = 9.5$ Hz), 116.13 (d, $J = 22.0$ Hz), 107.5 (s), 97.2 (s), 43.4 (s), 25.2 (s) ppm. ^{19}F NMR (471 MHz, $CDCl_3$) δ -103.14 ppm. HRMS (ES) calc. for $[M+H]^+$ $C_{14}H_{14}O_4F$: 265.0876, found: 265.0875. Characterisation data was in accordance with literature.¹²

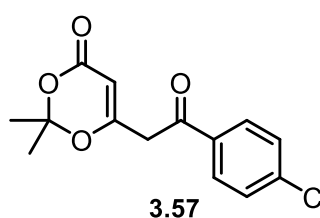
Synthesis of 2,2-dimethyl-6-(2-oxononyl)-4H-1,3-dioxin-4-one (3.82)



Using **GP5.3.2** and octanoyl chloride (1.88 mL, 11 mmol) as the electrophile; the product **3.82** was purified as a colourless oil (0.5664 g, 20%).

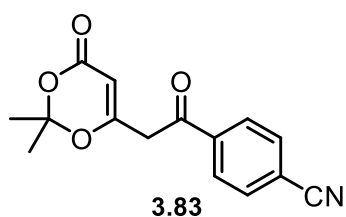
1H NMR (500 MHz, $CDCl_3$) δ 5.33 (s, 1H), 3.31 (s, 2H), 2.49 (t, $J = 7.3$ Hz, 2H), 1.71 (s, 6H), 1.34 – 1.24 (m, 10H), 0.88 (t, $J = 6.8$ Hz, 3H) ppm. ^{13}C NMR (126 MHz, $CDCl_3$) δ 203.5, 168.8, 160.8, 107.3, 94.0, 47.2, 43.3, 31.7, 29.1, 25.2, 23.6, 22.7, 14.2 ppm. HRMS (ES) calc. for $[M+H]^+$ $C_{15}H_{25}O_4$: 269.1753, found: 269.1742. Characterisation data was in accordance with literature.¹⁰

Synthesis of 6-(2-(4-chlorophenyl)-2-oxoethyl)-2,2-dimethyl-4H-1,3-dioxin-4-one (3.57)



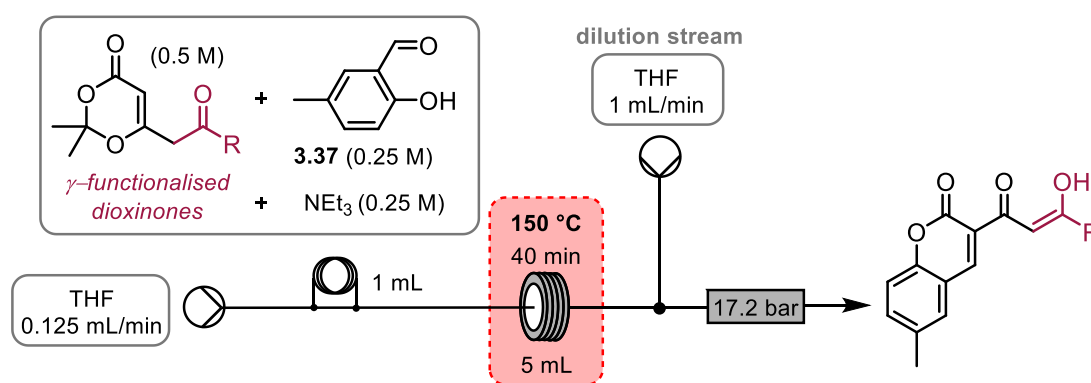
Using **GP5.3.2** and 4-chlorobenzoyl chloride (1.41 mL, 11 mmol) as the electrophile; the product **3.57** was purified as a pale-yellow oil (0.9436 g, 31%).

1H NMR (500 MHz, $CDCl_3$) δ 7.88 (d, $J = 8.7$ Hz, 2H), 7.48 (d, $J = 8.7$ Hz, 2H), 5.42 (s, 1H), 3.87 (s, 2H), 1.71 (s, 6H) ppm. ^{13}C NMR (126 MHz, $CDCl_3$) δ 192.0, 164.8, 160.8, 140.8, 134.3, 129.9, 129.4, 107.5, 97.3, 43.4, 25.2 ppm. HRMS (ES) calc. for $[M+H]^+$ $C_{14}H_{14}O_4Cl$: 281.0581, found: 281.0574. Characterisation data was in accordance with literature.¹⁰

Synthesis of 4-(2-(2,2-dimethyl-4-oxo-4H-1,3-dioxin-6-yl)acetyl)benzotrile (3.83)

Using **GP5.3.2** and 4-cyanobenzoyl chloride (1.8214 g, 11 mmol) as the electrophile; the product **3.83** was purified as a yellow oil (0.1372 g, 5%).

$^1\text{H NMR}$ (400 MHz, CDCl_3) δ 8.03 (d, $J = 7.9$ Hz, 2H), 7.81 (d, $J = 7.9$ Hz, 2H), 5.43 (s, 1H), 3.91 (s, 2H), 1.71 (s, 6H) ppm. $^{13}\text{C NMR}$ (126 MHz, CDCl_3) δ 194.3, 167.0, 139.2, 138.4, 132.1, 129.4, 119.0, 117.3, 112.4, 90.0, 49.0, 24.3 ppm. HRMS (ES) calc. for $[\text{M}+\text{H}]^+$ $\text{C}_{15}\text{H}_{14}\text{O}_4\text{N}$: 272.0923, found: 272.0924. Characterisation data was in accordance with literature.¹³

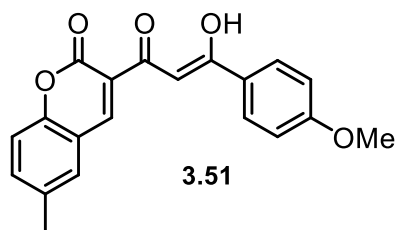
Synthesis of coumarins using Flow System 3.2

Scheme 73 – Flow system for the synthesis of coumarins (Flow System 3.2)

General procedure to synthesise coumarins (GP5.3.3)

γ -Functionalised dioxinone (0.75 mmol, 0.5 M), 4-methyl salicylaldehyde **3.37** (0.375 mmol, 0.25 M) and Et_3N (0.375 mmol, 0.25 M) were mixed and diluted in THF (1.5 mL). Using Flow System **3.2**, both HPLC pumps were set to pump THF at 0.125 mL/min and 1 mL/min, respectively and the Uniqsis HotCoil was set to 150 °C and left for 30 min to reach thermal equilibrium. The solution of reagents was charged into a 1 mL loading loop and the loading loop was set to inject. The outlet of the flow system was collected for 60 min and then left to waste for 30 min to flush the flow system. It should be noted that the T-piece for the dilution stream was placed under the protective heat shield of the Uniqsis Hotcoil to heat the T-piece to aid dissolution of the solid coumarin products. Chromatography silica (2 nuffield spatulas) was added to the collected reaction mixture and the sample dry loaded by removal of THF solvent. The product was purified via flash column chromatography (20% EtOAc in hexane) to afford the coumarin product.

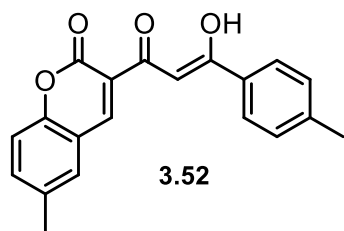
Synthesis of (Z)-3-(3-hydroxy-3-(4-methoxyphenyl)acryloyl)-6-methyl-2H-chromen-2-one (3.51)



Using **GP5.3.3** and **3.59** (0.2072 g, 0.75 mmol) as the γ -functionalised dioxinone; the product **3.51** was purified as a yellow solid (0.0816 g, 97%).

^1H NMR (500 MHz, CDCl_3) δ 8.68 (s, 1H), 8.06 (d, J = 8.9 Hz, 2H), 7.75 (s, 1H), 7.45 (d, J = 6.8 Hz, 2H), 7.29 (s, 1H), 6.99 (d, J = 8.9 Hz, 2H), 3.90 (s, 3H), 2.44 (s, 3H) ppm. ^{13}C NMR (126 MHz, CDCl_3) δ 190.3, 173.4, 163.9, 158.7, 152.8, 145.3, 135.2, 134.9, 132.0, 130.3, 129.3, 128.8, 121.1, 116.5, 114.2, 97.6, 55.7, 20.9 ppm. HRMS (ASAP) calc. for $[\text{M}+\text{H}]^+$ $\text{C}_{20}\text{H}_{17}\text{O}_5$: 337.1076, found: 337.1076. IR ν max: 2926, 1724, 1602, 1570, 1508, 1489, 1411, 1298, 1257, 1168, 1026, 804 cm^{-1} . m.p. 165 – 169 $^\circ\text{C}$.

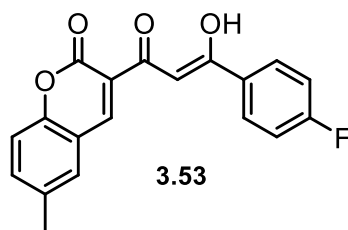
Synthesis of (Z)-3-(3-hydroxy-3-(*p*-tolyl)acryloyl)-6-methyl-2H-chromen-2-one (3.52)



Using **GP5.3.3** and **3.80** (0.1952 g, 0.75 mmol) as the γ -functionalised dioxinone; the product **3.52** was purified as a pale-yellow solid (0.0737 g, 92%).

^1H NMR (500 MHz, CDCl_3) δ 8.68 (s, 1H), 7.96 (d, J = 8.2 Hz, 2H), 7.77 (s, 1H), 7.49 – 7.39 (m, 2H), 7.32 – 7.26 (m, 3H), 2.44 (s, 6H) ppm. ^{13}C NMR (126 MHz, CDCl_3) δ 190.6, 174.6, 158.7, 152.9, 145.6, 144.1, 135.3, 134.9, 133.4, 129.6, 129.4, 128.1, 121.2, 118.6, 116.5, 97.8, 21.9, 20.9 ppm. HRMS (ES) calc. for $[\text{M}+\text{H}]^+$ $\text{C}_{20}\text{H}_{17}\text{O}_4$: 321.1127, found: 321.1127. IR ν max: 1724, 1568, 1516, 1489, 1294, 1197, 993, 970, 808 cm^{-1} . m.p. 179 – 184 $^\circ\text{C}$.

Synthesis of (Z)-3-(3-(4-fluorophenyl)-3-hydroxyacryloyl)-6-methyl-2H-chromen-2-one (3.53)

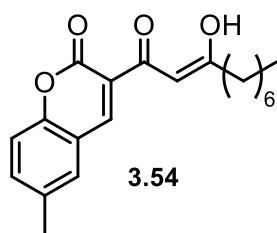


Using **GP5.3.3** and **3.81** (0.1982 g, 0.75 mmol) as the γ -functionalised dioxinone; the product **3.53** was purified as a pale-yellow solid (0.0669 g, 82%).

^1H NMR (500 MHz, CDCl_3) δ 8.72 (s, 1H), 8.11 (dd, J = 8.9, 5.4 Hz, 2H), 7.79 (s, 1H), 7.51 – 7.46 (m, 2H), 7.33 (s, 1H), 7.20 (t, J = 8.6 Hz, 2H), 2.47 (s, 3H) ppm. ^{13}C NMR (126 MHz, CDCl_3) δ 189.5 (s), 174.6 (s), 165.9 (d, J = 254.8 Hz), 158.6 (s), 152.9 (s), 145.8 (s), 135.5 (s), 135.0 (s), 132.4 (d, J = 3.0 Hz), 130.6 (d, J = 9.3 Hz), 129.4 (s), 120.8 (s), 118.5 (s), 116.5 (s), 116.0 (d, J = 21.9 Hz), 97.7 (s), 20.9 (s) ppm. ^{19}F NMR (471 MHz, CDCl_3) δ -105.32 ppm. HRMS (ES)

calc. for $[M+H]^+$ $C_{19}H_{14}O_4F$: 325.0876, found: 325.0870. IR ν max: 1716, 1597, 1570, 1508, 1490, 1294, 1224, 1201, 1159, 1116, 1097, 806 cm^{-1} . m.p. 195 – 199 °C.

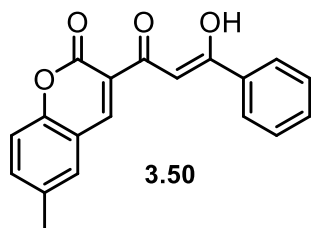
Synthesis of (Z)-3-(3-hydroxydec-2-enyl)-6-methyl-2H-chromen-2-one (3.54)



Using **GP5.3.3** and **3.82** (0.2013 g, 0.75 mmol) as the γ -functionalised dioxinone; the product **3.54** was purified as a white solid (0.0609 g, 74%).

1H NMR (400 MHz, $CDCl_3$) δ 8.60 (s, 1H), 7.46 – 7.40 (m, 2H), 7.27 (s, 1H), 7.02 (s, 1H), 2.50 (t, 2H), 2.43 (s, 3H), 1.39 – 1.23 (m, 10H), 0.88 (t, J = 6.9 Hz, 3H) ppm. ^{13}C NMR (101 MHz, $CDCl_3$) δ 211.1, 192.2, 163.4, 145.5, 135.2, 132.9, 129.3, 124.5, 116.5, 109.3, 101.2, 60.1, 40.9, 31.8, 29.4, 29.2, 25.6, 22.8, 20.9, 14.2 ppm. HRMS (ES) calc. for $[M+H]^+$ $C_{20}H_{25}O_4$: 329.1753, found: 329.1756. IR ν max: 2926, 2846, 1726, 1616, 1571, 1406, 1286, 1136, 1103, 823, 812 cm^{-1} . m.p. 94 – 96 °C.

Synthesis of (Z)-3-(3-hydroxy-3-phenylacryloyl)-6-methyl-2H-chromen-2-one (3.50)



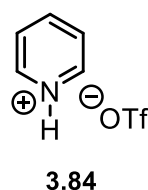
Using **GP5.3.3** and **3.49** (0.1847 g, 0.75 mmol) as the γ -functionalised dioxinone; the product **3.50** was purified as a pale-yellow solid (0.06 g, 78%).

1H NMR (500 MHz, $CDCl_3$) δ 8.70 (s, 1H), 8.08 – 8.05 (m, 2H), 7.80 (s, 1H), 7.61 – 7.56 (m, 1H), 7.53 – 7.48 (m, 2H), 7.47 – 7.43 (m, 2H), 7.29 (d, J = 9.1 Hz, 1H), 2.45 (s, 3H) ppm. ^{13}C NMR (126 MHz, $CDCl_3$) δ 190.4, 175.2, 158.7, 152.9, 145.8, 136.0, 135.4, 134.9, 133.2, 129.4, 128.9, 128.0, 121.1, 118.5, 116.5, 98.0, 20.9 ppm. HRMS (ES) calc. for $[M+H]^+$ $C_{19}H_{15}O_4$: 307.0970, found: 307.0974. IR ν max: 1722, 1568, 1456, 1296, 1203, 1112, 815, 783, 680, 574 cm^{-1} . m.p. 180 – 182 °C.

Synthesis of Biginelli products in the microwave

The multicomponent reaction took place in a 0.5 mL Biotage glass microwave vial equipped with tapered stir bar and a crimped lid which sealed the reaction vessel. A Biotage microwave with robotic sample arm was used for the microwave reactions.

Synthesis of pyridinium triflate (3.84)



Pyridine (0.16 mL, 2 mmol) was added to Et_2O (5 mL) in a stirring 10 mL RBF. Triflic acid (0.18 mL, 2 mmol) was added dropwise to form a precipitate at 25 °C. The reaction was stirred for 10 min and the precipitate was filtered and washed with cold Et_2O and dried under vacuum. The

pyridinium triflate **3.84** was isolated as a white crystalline solid (0.4478 g, 98%).

^1H NMR (500 MHz, DMSO) δ 8.92 (dd, J = 6.5, 1.4 Hz, 2H), 8.59 (td, J = 7.8, 1.4 Hz, 1H), 8.07 (dd, J = 7.8, 6.5 Hz, 2H) ppm. ^{13}C NMR (126 MHz, DMSO) δ 145.96 (s), 142.54 (s), 127.09 (s), 120.68 (q, J = 322.3 Hz) ppm. HRMS (ASAP) calc. for $[\text{M}+\text{H}]^+$ $\text{C}_5\text{H}_6\text{N}$: 80.0500, found: 80.0504. Characterisation data in accordance with literature.¹⁴

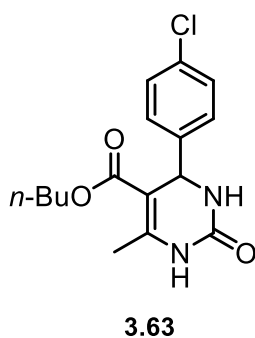
Purification of reactive aldehydes (GP5.3.4)

All aldehydes used in the multicomponent reaction were purified before subjecting to reaction conditions. This was to remove the common carboxylic acid impurity found in the aldehyde reagent bottle. 2" of basic alumina in a Pasteur pipette was clamped and the crude aldehyde was gravity fed through the column and the aldehyde product was immediately used in the reaction.

General procedure to synthesise the Biginelli products (GP5.3.5)

β -keto ester (1.5 mmol), purified aldehyde (1 mmol) (see GP5.3.4), and urea **3.62** (0.0901 g, 1.5 mmol) were loaded into a 0.5 mL microwave vial with stir bar. Pyridium triflate **3.84** (10 mol%, 0.0229 g) was added and the microwave vial sealed with a crimped lid. The reaction conditions set on the microwave were: 120 °C, 10 min, high absorbance. After completion of the reaction the reaction mixture was extracted (and vial rinsed) with EtOAc (25 mL). The organic layer was washed with water (25 mL). The organic layer was dried with MgSO_4 , filtered, and solvent removed. The Biginelli product was purified via flash column chromatography (50% EtOAc in hexane) to afford the pure compound.

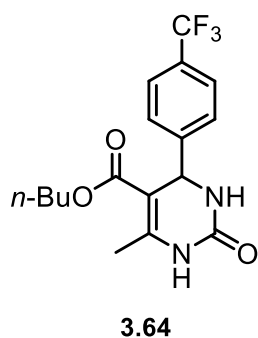
Synthesis of butyl 4-(4-chlorophenyl)-6-methyl-2-oxo-1,2,3,4-tetrahydropyrimidine-5-carboxylate (**3.63**)



Using GP5.3.5 and β -keto ester **3.21** (0.2373 g, 1.5 mmol) and 4-chloro benzaldehyde **3.61** (0.1406 g, 1 mmol) as the variable multicomponent reagents; the product **3.63** was purified as a pale-yellow solid (0.2436 g, 76%).

^1H NMR (300 MHz, CDCl_3) δ 8.78 (s, 1H), 7.18 (d, J = 8.3 Hz, 2H), 7.13 (d, J = 8.7 Hz, 2H), 6.58 (s, 1H), 5.25 (d, J = 2.7 Hz, 1H), 4.00 – 3.85 (m, 2H), 2.22 (s, 3H), 1.49 – 1.36 (m, 2H), 1.20 – 1.09 (m, 2H), 0.78 (t, J = 7.3 Hz, 3H) ppm. ^{13}C NMR (75 MHz, CDCl_3) δ 165.7, 154.1, 146.9, 142.3, 133.7, 128.9, 128.0, 100.9, 64.1, 54.9, 30.7, 19.2, 18.7, 13.7 ppm. HRMS (ES) calc. for $[\text{M}+\text{H}]^+$ $\text{C}_{16}\text{H}_{20}\text{N}_2\text{O}_3\text{Cl}$: 323.1162, found: 323.1162. IR ν max: 3242, 2954, 1674, 1456, 1220, 1080, 773 cm^{-1} . m.p. 135 – 141 °C

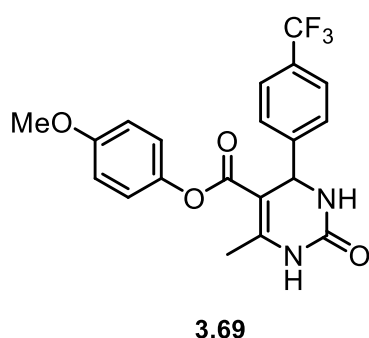
Synthesis of butyl 6-methyl-2-oxo-4-(4-(trifluoromethyl)phenyl)-1,2,3,4-tetrahydropyrimidine-5-carboxylate (3.64)



Using **GP5.3.5** and β -keto ester **3.21** (0.2373 g, 1.5 mmol) and 4-trifluoromethyl benzaldehyde (0.14 mL, 1 mmol) as the variable multicomponent reagents; the product **3.64** was purified as a pale-yellow solid (0.3164 g, 89%).

^1H NMR (500 MHz, CDCl_3) δ 7.59 (d, $J = 8.1$ Hz, 2H), 7.44 (d, $J = 8.1$ Hz, 2H), 5.47 (d, $J = 2.9$ Hz, 1H), 4.04 (qt, $J = 10.9, 6.6$ Hz, 2H), 2.37 (s, 3H), 1.54 – 1.47 (m, 2H), 1.25 – 1.18 (m, 2H), 0.85 (t, $J = 7.4$ Hz, 3H) ppm. ^{13}C NMR (126 MHz, CDCl_3) δ 165.6 (s), 153.4 (s), 147.5 (s), 147.1 (s), 130.4 (q, $J = 32.6$ Hz), 127.1 (s), 125.9 (q, $J = 3.7$ Hz), 124.1 (q, $J = 272.1$ Hz), 100.9 (s), 64.3 (s), 55.5 (s), 30.8 (s), 19.3 (s), 18.9 (s), 13.7 (s) ppm. HRMS (CI) calc. for $[\text{M}+\text{H}]^+$ $\text{C}_{17}\text{H}_{20}\text{N}_2\text{O}_3\text{F}_3$: 357.1421, found: 357.1419. IR ν max: 3236, 3118, 2960, 1707, 1647, 1465, 1425, 1382, 1219, 1163, 1087, 1066, 1016, 775 cm^{-1} . m.p. 115 – 117 $^\circ\text{C}$.

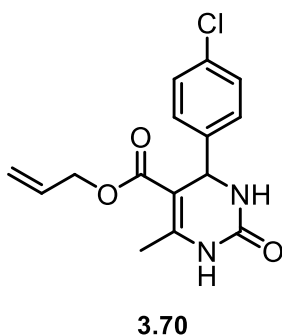
Synthesis of 4-methoxyphenyl 6-methyl-2-oxo-4-(4-(trifluoromethyl)phenyl)-1,2,3,4-tetrahydropyrimidine-5-carboxylate (3.69)



Using **GP5.3.5** and β -keto ester **3.20** (0.3123 g, 1.5 mmol) and 4-trifluoromethyl benzaldehyde (0.14 mL, 1 mmol) as the variable multicomponent reagents; the product **3.69** was purified as a pale-yellow solid (0.0868 g, 21%).

^1H NMR (500 MHz, DMSO) δ 9.59 (d, $J = 1.7$ Hz, 1H), 8.03 (d, $J = 2.1$ Hz, 1H), 7.79 (d, $J = 8.1$ Hz, 2H), 7.57 (d, $J = 8.1$ Hz, 2H), 6.92 (d, $J = 9.3$ Hz, 2H), 6.87 (d, $J = 9.3$ Hz, 2H), 5.43 (d, $J = 3.3$ Hz, 1H), 3.75 (s, 3H), 2.36 (s, 3H) ppm. ^{13}C NMR (126 MHz, DMSO) δ 164.1, 156.7, 151.7, 151.6, 149.2, 143.7, 127.3, 127.2, 125.7, 125.7, 122.7, 114.3, 97.4, 55.4, 53.8, 18.2 ppm. ^{19}F NMR (471 MHz, DMSO) δ -60.81 ppm. HRMS (ES) calc. for $[\text{M}+\text{H}]^+$ $\text{C}_{20}\text{H}_{18}\text{N}_2\text{O}_4\text{F}_3$: 407.1219, found: 407.1216. IR ν max: 1685, 1637, 1504, 1321, 1190, 1163, 1107, 1066, 1016, 835, 761 cm^{-1} . m.p. 96 – 100 $^\circ\text{C}$.

Synthesis of allyl 4-(4-chlorophenyl)-6-methyl-2-oxo-1,2,3,4-tetrahydropyrimidine-5-carboxylate (3.70)

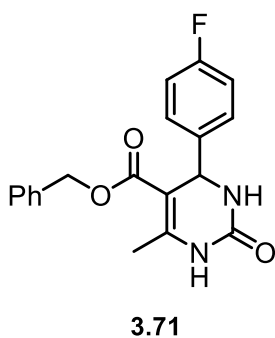


Using **GP5.3.5** and β -keto ester **3.35** (0.2132 g, 1.5 mmol) and 4-chloro benzaldehyde **3.61** (0.1406 g, 1 mmol) as the variable multicomponent reagents; the product **3.70** was purified as a pale-yellow solid (0.2168 g, 71%).

^1H NMR (500 MHz, DMSO) δ 9.33 (d, J = 1.6 Hz, 1H), 7.82 (dd, J = 3.2, 2.1 Hz, 1H), 7.39 (d, J = 8.5 Hz, 2H), 7.24 (d, J = 8.4 Hz, 2H), 5.83 (ddt, J = 17.1, 10.6, 5.2 Hz, 1H), 5.16 (d, J = 3.4 Hz,

1H), 5.12 – 5.05 (m, 2H), 4.48 (ddd, J = 6.6, 3.2, 1.6 Hz, 2H), 2.26 (s, 3H) ppm. ^{13}C NMR (126 MHz, DMSO) δ 164.9, 152.0, 149.6, 143.6, 133.0, 131.9, 128.6, 128.3, 117.2, 98.4, 63.9, 53.4, 18.0 ppm. HRMS (ES) calc. for $[\text{M}+\text{H}]^+$ $\text{C}_{15}\text{H}_{16}\text{N}_2\text{O}_3\text{Cl}$: 307.0849, found: 307.0857. Characterisation data in accordance with literature.¹⁵

Synthesis of benzyl 4-(4-fluorophenyl)-6-methyl-2-oxo-1,2,3,4-tetrahydropyrimidine-5-carboxylate (3.71)

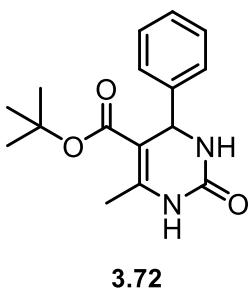


Using **GP5.3.5** and β -keto ester **3.34** (0.2883 g, 1.5 mmol) and 4-fluoro benzaldehyde (0.11 mL, 1 mmol) as the variable multicomponent reagents; the product **3.71** was purified as a pale-yellow solid (0.2526 g, 74%).

^1H NMR (500 MHz, CDCl_3) δ 7.65 (s, 1H), 7.31 – 7.27 (m, 3H), 7.20 (dd, J = 8.7, 5.3 Hz, 2H), 7.16 – 7.11 (m, 2H), 6.94 (t, J = 8.7 Hz, 2H), 5.57 (s, 1H), 5.38 (d, J = 2.8 Hz, 1H), 5.09 (d, J =

12.3 Hz, 1H), 5.01 (d, J = 12.4 Hz, 1H), 2.36 (d, J = 0.6 Hz, 3H) ppm. ^{13}C NMR (126 MHz, CDCl_3) δ 165.3 (s), 162.5 (d, J = 246.7 Hz), 152.7 (s), 147.0 (s), 139.6 (d, J = 3.2 Hz), 136.0 (s), 128.6 (s), 128.5 (d, J = 8.3 Hz), 128.3 (s), 128.3 (s), 115.8 (d, J = 21.5 Hz), 101.2 (s), 66.2 (s), 55.3 (s), 19.1 (s) ppm. HRMS (ES) calc. for $[\text{M}+\text{H}]^+$ $\text{C}_{19}\text{H}_{18}\text{N}_2\text{O}_3\text{F}$: 341.1301, found: 341.1309. Characterisation data in accordance with literature.¹⁶

Synthesis of tert-butyl 6-methyl-2-oxo-4-phenyl-1,2,3,4-tetrahydropyrimidine-5-carboxylate (3.72)

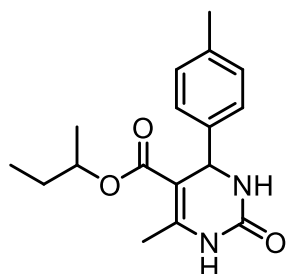


Using **GP5.3.5** and β -keto ester **3.33** (0.2373 g, 1.5 mmol) and benzaldehyde (0.1 mL, 1 mmol) as the variable multicomponent reagents; the product **3.72** was purified as a pale-yellow solid (0.1224 g, 42%).

^1H NMR (500 MHz, CDCl_3) δ 7.33 – 7.29 (m, 5H), 5.45 (s, 1H), 5.35 (dd, J = 2.7, 0.7 Hz, 1H), 2.32 (d, J = 0.7 Hz, 3H), 1.32 (s, 9H). ^{13}C

NMR (126 MHz, CDCl₃) δ 165.0, 152.8, 145.1, 143.8, 128.8, 128.1, 126.8, 102.8, 80.7, 56.4, 28.3, 18.8 ppm. HRMS (ES) calc. for [M+H]⁺ C₁₆H₂₁N₂O₃: 289.1552, found: 289.1551. Characterisation data in accordance with literature.¹⁷

Synthesis of *sec*-butyl 6-methyl-2-oxo-4-(*p*-tolyl)-1,2,3,4-tetrahydropyrimidine-5-carboxylate (**3.73**)

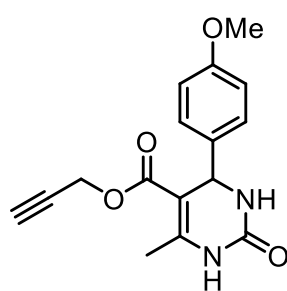


3.73

Using **GP5.3.5** and β -keto ester **3.22** (0.2373 g, 1.5 mmol) and 4-methyl benzaldehyde (0.11 mL, 1 mmol) as the variable multicomponent reagents; the product **3.73** was purified as a pale-yellow solid as a mixture of diastereomers (1:1) (0.1847 g, 61%).

¹H NMR (500 MHz, DMSO) δ 9.15 (s, 1H), 7.68 (d, *J* = 1.3 Hz, 1H), 7.13 – 7.07 (m, 4H), 5.08 (t, *J* = 3.3 Hz, 1H), 4.72 – 4.60 (m, 1H), 2.25 (s, 3H), 2.23 (s, 3H), 1.53 – 1.41 (m, 1H), 1.40 – 1.26 (m, 1H), 1.11 (d, *J* = 6.3 Hz, 1.5H), 0.93 (d, *J* = 6.2 Hz, 1.5H), 0.81 (t, *J* = 7.4 Hz, 1.5H), 0.52 (t, *J* = 7.4 Hz, 1.5H) ppm. ¹³C NMR (126 MHz, DMSO) δ 165.1, 165.0, 152.2, 152.2, 148.4, 148.0, 142.1, 142.0, 136.4, 136.4, 128.9, 128.9, 126.3, 126.3, 99.7, 99.4, 70.7, 70.7, 53.8, 53.7, 28.4, 28.2, 20.7, 19.6, 19.1, 17.8, 9.6, 9.3 ppm. HRMS (ES) calc. for [M+H]⁺ C₁₇H₂₃N₂O₃: 289.1552, found: 289.1551. IR ν max: 3236, 3111, 2970, 1703, 1649, 1458, 1382, 1315, 1284, 1222, 1083, 761, 678, 499 cm⁻¹. m.p. 153 – 155 °C.

Synthesis of prop-2-yn-1-yl 4-(4-methoxyphenyl)-6-methyl-2-oxo-1,2,3,4-tetrahydropyrimidine-5-carboxylate (**3.74**)



3.74

Using **GP5.3.5** and β -keto ester **3.36** (0.2102 g, 1.5 mmol) and 4-methoxy benzaldehyde (0.12 mL, 1 mmol) as the variable multicomponent reagents; the product **3.74** was purified as a pale-yellow solid (0.1416 g, 47%).

¹H NMR (500 MHz, DMSO) δ 9.31 (s, 1H), 7.76 (s, 1H), 7.15 (d, *J* = 8.6 Hz, 2H), 6.87 (d, *J* = 8.6 Hz, 2H), 5.08 (d, *J* = 3.1 Hz, 1H), 4.69 – 4.56 (m, 2H), 3.71 (s, 3H), 3.49 – 3.46 (m, 1H), 2.25 (s, 3H) ppm. ¹³C NMR (126 MHz, DMSO) δ 164.6, 158.6, 152.2, 149.6, 136.8, 127.4, 113.8, 98.7, 78.9, 77.4, 55.1, 53.1, 51.0, 18.0 ppm. HRMS (ES) calc. for [M+H]⁺ C₁₆H₁₇N₂O₄: 301.1188, found: 301.1193. Characterisation data in accordance with literature.¹⁸

5.4 Civetone experimental

Flow equipment

The flow setup consisted of PFA tubing, both 1/32" and 1/16" ID, and used a Chemyx Fusion 100 syringe pump. Outlet of CSTR 5 uses 1/16" ID PFA tubing. All flow fittings and connections were purchased from Kinesis (Gripper fitting nuts, part number: 002103; Adapters, part number: P-618; Omniloc type-p fitting ferrule, part number: 008FT16; Threaded union, part number: P-623). *f*Reactor was purchased from Asynt. It is advised that when conducting the experiment for longer than 6 hours run time, glass syringes or THF resistant syringes should be used to avoid swelling of the plastic barrel. All reaction glassware was flame-dried and back-filled with nitrogen gas.

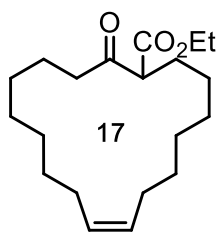
Asynt provided an equation to calculate the internal temperature of the reaction mixture inside the CSTR when setting the hotplate to a desired temperature. To calculate the fluid temperature:

$$\text{Fluid Temperature (}^{\circ}\text{C)} = (0.8 \times \text{hotplate temperature (}^{\circ}\text{C)}) + 4.4$$

Knowing the hotplate temperature and using the above equation the reaction temperature could be calculated and the temperature of the reaction reported throughout this document is the reaction fluid temperature.

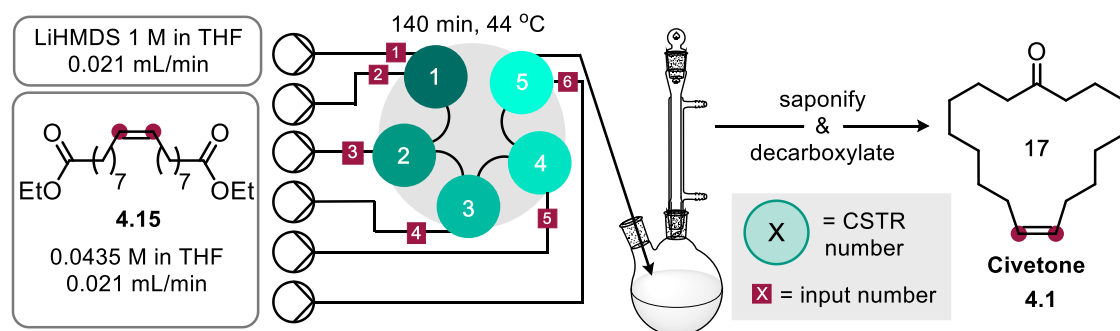
The *f*Reactor CSTRs require the air spaces to be removed when filling the reactor with solvent prior to the reaction. To achieve this, a syringe (filled with dry THF) was connected to the first CSTR input. Using gravity, the *f*Reactor's first CSTR is filled with THF whilst guiding the exiting bubble into the next CSTR chamber leaving the first CSTR chamber filled with THF. This was repeated by rotating the *f*Reactor base plate against gravity until the entire unit was filled with THF and the reactor placed back onto the hotplate. It is important to note that all connections were blocked off with plug fittings and the only outlet was the final outlet tubing of the reactor.

Characterisation of cyclic β -keto ester (4.16)



4.16

^1H NMR (500 MHz, CDCl_3) δ 5.40 – 5.30 (m, 2H), 4.16 (qd, $J = 7.1$, 0.9 Hz, 2H), 3.46 (dd, $J = 9.2$, 5.1 Hz, 1H), 2.52 (t, $J = 6.8$ Hz, 2H), 2.12 – 1.89 (m, 6H), 1.69 – 1.60 (m, 2H), 1.35 – 1.27 (m, 16H), 1.24 (t, $J = 7.1$ Hz, 3H) ppm. ^{13}C NMR (126 MHz, CDCl_3) δ 206.7, 170.0, 125.8, 58.9, 41.6, 29.2, 28.7, 28.6, 28.3, 28.2, 28.1, 27.3, 26.8, 23.6, 14.2 ppm.

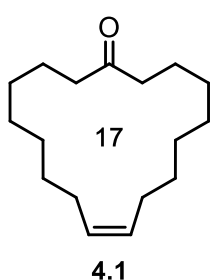
Procedure using fReactor in flow to synthesise Civetone 4.1 (standard scale):

fReactor was purged with THF and all air bubbles removed. A stock solution of diethyl (*Z*)-octadec-9-enedioate, **4.15**, (0.0435 M, 25 mL) was charged into 5 x 5 mL syringes and connected to the inputs 2, 3, 4, 5 and 6, via 1/32" PFA tubing. LiHMDS (1 M in THF, 5 mL) was charged into a 5 mL syringe and connected at input 1. The hotplate temperature and stirring were set to 50 °C (Fluid temperature = 44 °C) and 1000 rpm, respectively. All syringe pumps were set to pump at 0.02083 mL/min and the outlet stream set to waste for 140 min. The outlet stream was collected for 100 min into a stirring two-neck 25 mL RBF with condenser, under nitrogen, at 60 °C which corresponds to 12.5 mL reaction mixture collected ([product] = 0.03625 M, calc. by [stock solution] x (5/6)). After the collection time, the reaction was stirred at 60 °C for 60 min. The reaction was cooled to rt and NaOH_(aq.) (2.5 M, 1.35 mmol, 0.54 mL) was added slowly whilst stirring. The reaction was heated to 80 °C for 18 h. The reaction was cooled to rt and acidified to pH ~1 using 10% H₂SO_{4(aq.)} and then heated to 90 °C for 30 min. The reaction mixture was diluted with H₂O (10 mL) and extracted with Et₂O (3 x 20 mL). The combined organic layers were washed with H₂O (20 mL) then brine (20 mL) and dried using MgSO₄, filtered, and solvent removed carefully. Civetone **4.1** was isolated via flash column chromatography (Et₂O:pentane, 1:9) to yield low-melt colourless crystals (0.0697 g, 62%).

Procedure using f-reactor in flow to synthesise Civetone 4.1 (large scale):

fReactor was purged with THF and all air bubbles removed. A stock solution of diethyl (*Z*)-octadec-9-enedioate, **4.15**, (0.0435 M, 75 mL) was charged into 5 x 15 mL syringes and connected to the inputs 2, 3, 4, 5 and 6, via 1/32" ID PFA tubing. LiHMDS (1 M in THF, 15 mL) was charged into a 15 mL syringe and connected at input 1. The hotplate temperature and stirring were set to 50 °C (Fluid temperature = 44 °C) and 1000 rpm, respectively. All syringe pumps were set to pump at 0.02083 mL/min and the outlet stream set to waste for 140 min. The outlet stream was collected for 360 min into a stirring two-neck 250 mL RBF with condenser, under nitrogen, at 60 °C which

corresponds to 45 mL reaction mixture collected ($[\text{product}] = 0.03625 \text{ M}$, calc. by $[\text{stock solution}] \times (5/6)$). After the collection time, the reaction was stirred at $60 \text{ }^\circ\text{C}$ for 60 min. The reaction was cooled to rt and $\text{NaOH}_{(\text{aq.})}$ (2.5 M, 5 mmol, 2.3 mL) was added slowly whilst stirring. The reaction was heated to $80 \text{ }^\circ\text{C}$ for 18 h. The reaction was cooled to rt and acidified to pH ~ 1 using 10% $\text{H}_2\text{SO}_{4(\text{aq.})}$ and then heated to $90 \text{ }^\circ\text{C}$ for 30 min. The reaction mixture was diluted with H_2O (10 mL) and extracted with Et_2O (3 x 20 mL). The combined organic layers were washed with H_2O (20 mL) then brine (20 mL) and dried using MgSO_4 , filtered, and solvent removed carefully. Civetone, **4.1**, was isolated via flash column chromatography (Et_2O :pentane, 1:9) to yield low-melt colourless crystals (0.2772 g, 68%).



^1H NMR (500 MHz, CDCl_3) δ 5.38 – 5.30 (m, 2H), 2.42 – 2.36 (m, 4H), 2.05 – 1.96 (m, 4H), 1.66 – 1.58 (m, 4H), 1.36 – 1.25 (m, 16H) ppm.
 ^{13}C NMR (126 MHz, CDCl_3) δ 212.72, 130.31, 42.60, 29.18, 28.75, 28.36, 28.29, 26.85, 24.01 ppm. HRMS (EI) calc. for $[\text{M}]^+$ $\text{C}_{17}\text{H}_{30}\text{O}$: 250.2297, found: 250.2297. Characterisation data was in accordance with literature.¹⁹

Pictures of setup – small scale setup



Pictures of setup – Large scale setup with top view of fReactor in action



5.5 References

- 1 O. Altintas, M. Glassner, C. Rodriguez-Emmenegger, A. Welle, V. Trouillet and C. Barner-Kowollik, *Angew. Chemie Int. Ed.*, 2015, **54**, 5777–5783.
- 2 J. Pietruszka and G. Solduga, *European J. Org. Chem.*, 2009, **2009**, 5998–6008.
- 3 I. Jlalila, F. Meganem, J. Herscovici and C. Girard, *Molecules*, 2009, **14**, 528–539.
- 4 H. Yue, H. Yu, S. Liu and C. Xu, *RSC Adv.*, 2016, **6**, 19041–19051.
- 5 Sigma Aldrich, tert-butyl acetoacetate, <https://www.sigmaaldrich.com/spectra/fnmr/FNMR009571.PDF>, (accessed 24 May 2021).
- 6 R. Galaverna, T. McBride, J. C. Pastre and D. L. Browne, *React. Chem. Eng.*, 2019, **4**, 1559–1564.
- 7 S. P. Chavan, R. R. Kale, K. Shivasankar, S. I. Chandake and S. B. Benjamin, *Synthesis (Stuttg.)*, 2003, 2695–2698.
- 8 B. R. Madje, P. T. Patil, S. S. Shindalkar, S. B. Benjamin, M. S. Shingare and M. K. Dongare, *Catal. Commun.*, 2004, **5**, 353–357.
- 9 R. Boeckman, R. Perni, J. Macdonald and A. Thomas, *Org. Synth.*, 1988, **66**, 194.
- 10 A. R. Katritzky, Z. Wang, M. Wang, C. D. Hall and K. Suzuki, *J. Org. Chem.*, 2005, **70**, 4854–4856.
- 11 B. H. Patel, A. M. Mason and A. G. M. Barrett, *Org. Lett.*, 2011, **13**, 5156–5159.
- 12 Z. (Amphi) Fang, G. J. Clarkson and M. Wills, *Tetrahedron Lett.*, 2013, **54**, 6834–6837.
- 13 I. S. Makarov, T. Kuwahara, X. Jusseau, I. Ryu, A. T. Lindhardt and T. Skrydstrup, *J. Am. Chem. Soc.*, 2015, **137**, 14043–14046.
- 14 M. K. Saini, H. S. Korawat, S. K. Verma and A. K. Basak, *Tetrahedron Lett.*, 2020, **61**, 152657.
- 15 B. Desai, D. Dallinger and C. O. Kappe, *Tetrahedron*, 2006, **62**, 4651–4664.
- 16 S. Sepehri, S. Soleymani, R. Zabihollahi, M. R. Aghasadeghi, M. Sadat, L. Saghaie, H. R. Memarian and A. Fassihi, *Chem. Biodivers.*, 2018, **15**, 1700502.
- 17 A. Stadler and C. O. Kappe, *J. Comb. Chem.*, 2001, **3**, 624–630.

- 18 G. B. D. Rao, B. Anjaneyulu and M. P. Kaushik, *RSC Adv.*, 2014, **4**, 43321–43325.
- 19 R. Hamasaki, S. Funakoshi, T. Misaki and Y. Tanabe, *Tetrahedron*, 2000, **56**, 7423–7425.